Design and Development of Pre-Clinical Hip Stem Stability Testing Methods

Clements, Jeremy Peter

Award date:
2006

Awarding institution:
University of Bath

Design and Development of Pre-Clinical Hip Stem Stability Testing Methods

Jeremy Peter Clements

A thesis submitted for the degree of Doctor of Philosophy

University of Bath

Department of Mechanical Engineering

November 2006

Signed

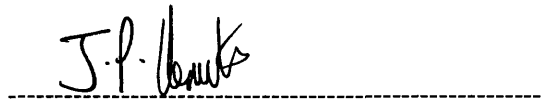

ProQuest LLC
789 East Eisenhower Parkway
P.O. Box 1346
Ann Arbor, MI 48106-1346

Abstract

Total hip replacement (THR) is a very common technique with almost 50,000 operations per year carried out on the NHS alone. Immediate postoperative stability of cementless hip stems is one of the key factors for the long-term success of cementless THR. The ability to discriminate between stable and unstable stems in the laboratory constitutes a desirable tool for the industry, as it would allow the identification of unsuitable stem designs prior to clinical trials. Researchers have developed several different *in vitro* methods to assess stem stability. The testing procedures aim to replicate the physiological loading conditions found in the hip joint, to assess the motion between the hip stem and the host bone in femoral models. These models can be cadaveric or synthetic composite bone. Currently most of these tests are performed with the femur held statically, thus negating any kinematic effect on stability. This might constitute an oversimplification of the clinical environment in which the implant operates and it may lead to underestimating the extent of movement the implant is subjected to *in vivo*. This thesis describes the design and development of a dynamic hip simulator capable of simulating *in vivo* conditions of femoral head loading and femoral kinematics. Initial results suggested that the inclusion of femoral kinematics produces higher levels of bone implant motion. However, further studies showed that the simulator was sensitive to small changes in the set up and suggestions are made as to how these might be avoided.

In addition, the use of composite femora for stability investigations is wide spread, however, their use in this application has yet to be validated. Two case studies are presented investigating the use of Sawbones in hip stem stability studies and the relationship between initial and long-term stability in cadaveric femora. The results from these studies showed that the Sawbones composite femora are suitable for the assessment of micromotion between hip stems and host bone. However, migration results suggested that Sawbones composite femora may produce an underestimate of the stability levels. The second case study researching the relationship between initial stability and long term survival concluded that the SL Plus stem produces high levels of initial stability which is continued in the long-term.

Acknowledgements

During the last three years there have been many people and organisations that have helped me in different ways both inside the Department of Mechanical Engineering and outside in the rest of my life.

Firstly I would like to thank Professor Tony Miles and Dr Sabina Gheduzzi for their supervision, guidance and support throughout this project, which has maintained my motivation and provided many new ideas to explore. I would also like to thank Richard Weston for all his help with the development of testing rigs and the two final year project students, Chris Butt and Alex Jezequel, for their input into the mechanical design of the dynamic simulator. Steve Coombes and the instrumentation department have also provided very good assistance with data capture from the rig.

One of the most enjoyable activities during the last three years has been travelling to conferences in Ixia (Greece), San Francisco and Washington (US) so I am very grateful to additional funding provided by the Royal Academy of Engineering and the Institution of Mechanical Engineers. At the University and in the office I would like to thank my colleagues and friends Hazel, Dan, Simon, Fabian, Iain, Andy and Susie for their help with solving awkward problems and general support.

Outside work I would like to thank my house mate Paints, the players of Claverton Academicals football club, Mechanical Engineering football team, staff of the Ayrlington hotel and my close friends who have all, in some way, provided healthy distractions from work and the frustrations of my rig.

Finally I would like to thank those who really have helped through everything, my family and, most importantly, Marie who have been fantastic and supportive for far longer than the last three years.

Contents

List of Figures

List of Tables

Equations

Definitions

Acetabular component - Implant of monobloc or modular construction intended to be fixed to the prepared biological acetabulum

Abduction – Movement of the limbs toward the lateral plane or away from the body

Adduction - Movement of the limbs toward the medial plane of the body or toward the axial line of the limb

Cancellous bone - Bone that has a lattice-like or spongy structure

Cortical bone - The superficial thin layer of compact bone

Coxa Valga - Alteration of the angle made by the axis of the femoral neck to the axis of the femoral shaft, so that the angle exceeds 125°; the femoral neck is in more of a straight-line relationship to the shaft of the femur

Coxa Vara - alteration of the angle made by the axis of the femoral neck to the axis of the femoral shaft so that the angle is less than 125°; the femoral neck becomes more horizontal

Debridements - A term of French origin for the removal of necrotic, infected or foreign material from a wound

Distal - Situated farthest from point of attachment or origin, as of a limb or bone

DoF – Degree of freedom

Femoral component - Part of a total or partial hip joint replacement which is intended to be attached to the femur

Flexion (of the hip joint) – Movement of the femur forwards with the knee moving in front of the body

Extension (of the hip joint) - Movement of the femur backwards with the knee moving behind the body

Internal rotation (of the hip joint) – Rotation of the femur bringing the toe towards the medial plane of the body

External rotation (of the hip joint) – Rotation of the femur moving the toe away from the medial plane of the body

Lateral – The side of the joint or component that lies away from the median and sagittal plane of a body

LVDT – Linear Variable Differential Transformer

Medial - The side of the joint or component that is nearer to the middle or centre (median) of the body

Micromotion - The recoverable movement of an implant relative to the host bone under cyclic loading, a function of the elasticity of the bone-implant construct

Migration - The unrecoverable movement of an implant with respect to the surrounding bone, it reflects the micro-damage caused by the implant to the host tissue

Osseointegration – The growth action of bone tissue as it integrates with implanted devices or prostheses to be used as replacement parts (e.g. hip)

Osteolysis – The dissolution of bone, applied especially to the removal or loss of the calcium of bone

Partial hip joint replacement (hip hemiarthroplasty) - implant comprising a femoral component whether monobloc or modular intended to replace the femoral articulating surface of the hip joint

Planes of the body

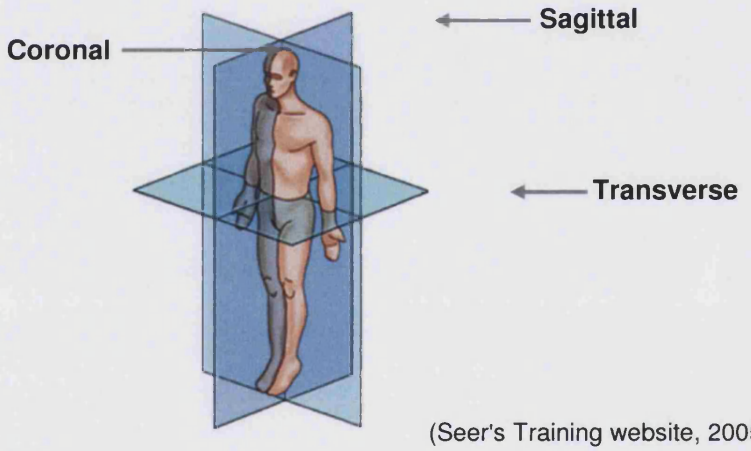

(Seer's Training website, 2005)

Proximal - Situated near the point of attachment or origin, for example the proximal part of a limb

Stress Shielding – the stress protection effect of an implanted device. Due to mismatch of stiffness between implant and bone most of the load is carried by the device and is abnormally transferred to the surrounding bone. This can cause a loss of the bone adjacent to the device as the stress is diverted from the area.

Total hip joint replacement (THR) - implant comprising a femoral component and an acetabular component whether monobloc or modular intended to replace both of the articulating surfaces of the hip joint

Woods metal - a lead based alloy with low melting point used for potting specimens

Chapter 1. Background to total hip replacement and reasons for pre-clinical testing

1.1. *Introduction*

Total hip replacement (THR) surgery is the second most common elective procedure performed through the NHS (Government Statistical Service, 2003). THR is a victim of its own success: the steady improvement of the success rates associated with THR have resulted in an extension of the indication for surgery to a larger number of young and active patients (Berry *et al.,* 2003). Due to the large numbers involved (50,000 in the UK in 2006) even a small percentage failure rate represents a significant burden for society.

Due to high standards of care and legislation, new designs must be proven to work before they can be introduced to clinical trials. To test these implants successfully, the in vivo conditions must be modelled requiring a full understanding of the anatomy and function of the hip joint.

This chapter introduces the anatomy of the healthy hip and highlights the disorders that can constitute indication for total hip replacement surgery. A brief history of THR and common causes for failure are also presented.

1.2. *Anatomy*

The hip joint (Figure 1-1) is one of the largest and most stable joints in the body (Nordin and Frankel, 1980). It is formed where the femur and pelvis meet and consists of a ball and socket joint. It is characterised by a large range of motion and intrinsic stability due to its deep socket and strong ligaments.

The femoral head locates into a depression on the pelvis called the acetabulum (Hanssen, 2003). In normal healthy subjects, both the femoral head and acetabulum are covered with a cartilage layer of varying thickness. The joint is surrounded by synovial fluid and is encapsulated by fibrous tissue. The synovial fluid lubricates the bearing surfaces and, in conjunction with the cartilage that covers them, it allows virtually frictionless movement. The cartilage ensures the

joint performs its main functions of supporting the weight of the upper body during standing and transmitting and distributing the forces experienced during locomotion with minimal wear over a life-time.

The acetabulum is a concave feature of the pelvis and constitutes the socket component of the hip joint (Figure 1-1). It opens forwards, outwards and downwards presenting an opening to receive the femoral head. The acetabulum, without force applied, has a diameter smaller than that of the femoral head but it deforms under load to ensure a congruous fit (Greenwald and Haynes, 1972). The cartilage layer that covers the acetabulum thickens peripherally and laterally (Kempson *et al.*, 1971). The acetabulum deepens on the inferior side of the cavity to create a ridge called the labrum which contains nerve and sensory organs.

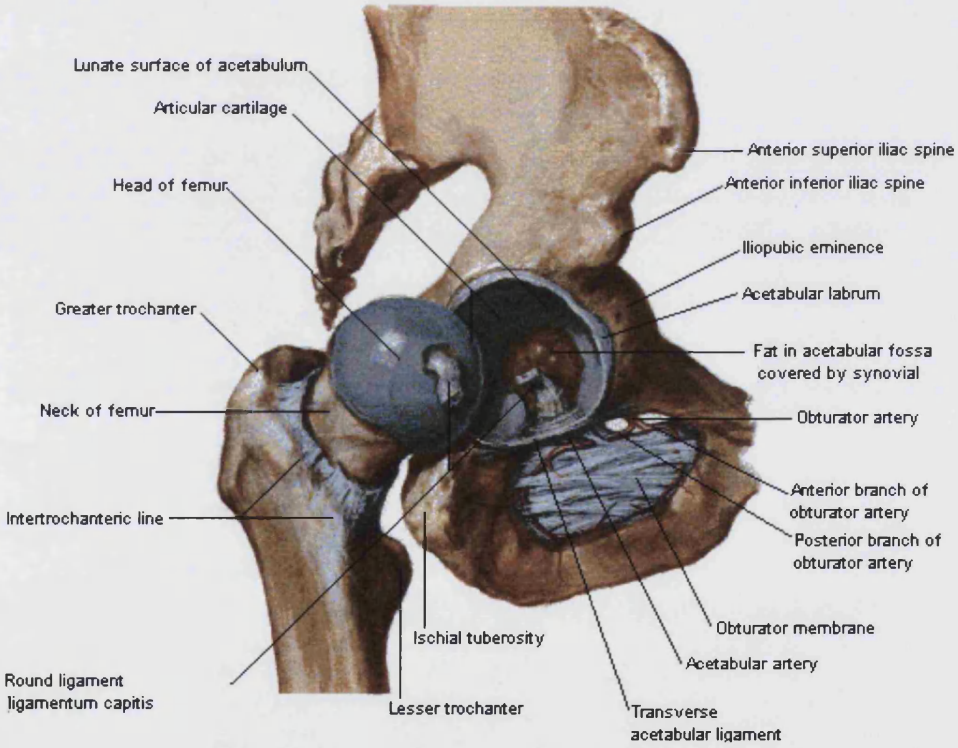

Figure 1-1 - Picture showing the femoral head and acetabulum (Netter, 1997)

The femoral head forms the ball component of the joint and consists of approximately two thirds of a sphere connecting to the main body of the femur via the femoral neck, see Figure 1-1. The articular cartilage thickens on the

medial-central area and thins to the periphery resulting in varying strength and stiffness across the femoral head (Kempson *et al.*, 1971). The femoral neck transmits the forces from the head to the main body of the femur. The angle of the neck to the shaft is typically about 125°. Deviations from the normal neck-shaft angle are known as Coxa Vara if the angle is reduced and Coxa Valga if the angle is increased. These conditions can seriously alter the force distribution across the femoral head and can lead to painful joints (Nordin and Frankel, 1980). These pathologies can be corrected by surgery through removal of excess bone (osteotomy). This normally results in relief of pain for the patient.

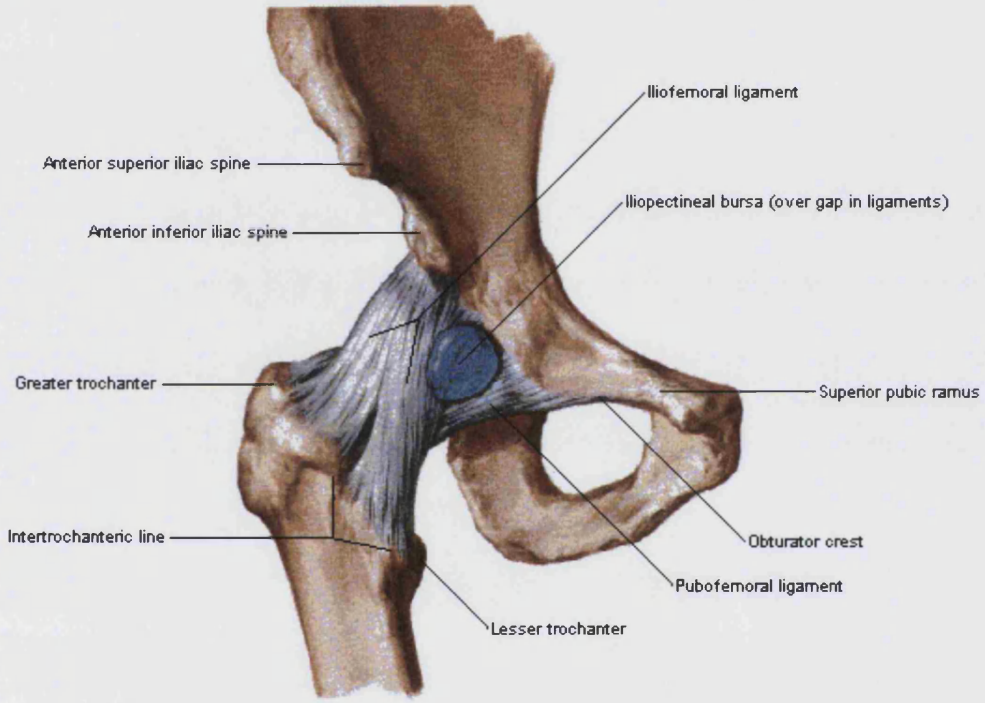

Figure 1-2 - View of the hip Joint
(Netter, 1997)

The hip joint is characterised by a very large range of motion. This allows a great range of different activities, each of which is associated with complex loading patterns. The motion of the joint is constrained by a group of ligaments named according to their attachment. The iliofemoral ligament attaches to the front of the ilium (pelvic bone) and to the femur forming a Y shape (Figure 1-2). The pubofemoral ligament attaches to the pubis and to the greater trochanter (Figure 1-2). The ischiofemoral ligament attaches to the rear of the pelvis and to the anterior femur. The joint is encompassed entirely by the articular capsule

which retains the synovial fluid. Pathologies of the hip often affect the capsule. In particular, in patients with rheumatoid arthritis, the capsule can become less resilient and thicker (Hanssen, 2003).

The femur is the longest bone in the body; it takes the form of a long shaft expanding at both ends. The proximal part of the femur provides attachment sites for the main actuating muscle groups of the hip, originating from the pelvis and inserting at the greater and lesser trochanter. These muscles provide the power to create the motion for varying activities, with different groups controlling different movements. A summary of muscle function is presented in Table 1-1, diagrams of muscle locations are presented in Figure 1-3 and Figure 1-4.

Primary Function	Muscle	Nerve	Secondary Function
Extension	Gluteus Maximus	Inferior Gluteal	External rotation
			Adduction
	Semimembranous	Tibial	Internal rotation
	Semitendious	Tibial	Internal rotation
	Biceps femoris	Tibial	
	Adductor magnus	Tibial	Internal rotation
Flexion	Iliopsoas	Iliopsoas	Adduction, external rotation
	Pectineus	Femoral or obturator	Adduction
	Rectus femoris	Femoral	
	Satorius	Femoral	External rotation
Adbuction	Gluteus medius	Superior gluteal	Internal rotation
	Gluteus minimus	Superior gluteal	Flexion, Internal rotation
	Tensor fascia lata	Superior gluteal	Flexion, internal rotation
Adduction	Adductor brevis	Obturator	Flexion
	Adductor longus	Obturator	Flexion
	Adductor magnus	Obturator	Flexion
	Gracilis	Obturator	Flexion
	Obturator externus	Obturator	External rotation
External rotation	Piriformis	Piriformis	
	Obturator internus	Obturator internus	
	Superior gemellus	Quadratus femoris	
	Inferior gemells		
	Quadratus femoris		

Table 1-1 - Muscles of the hip joint and their functions (Hanssen, 2003)

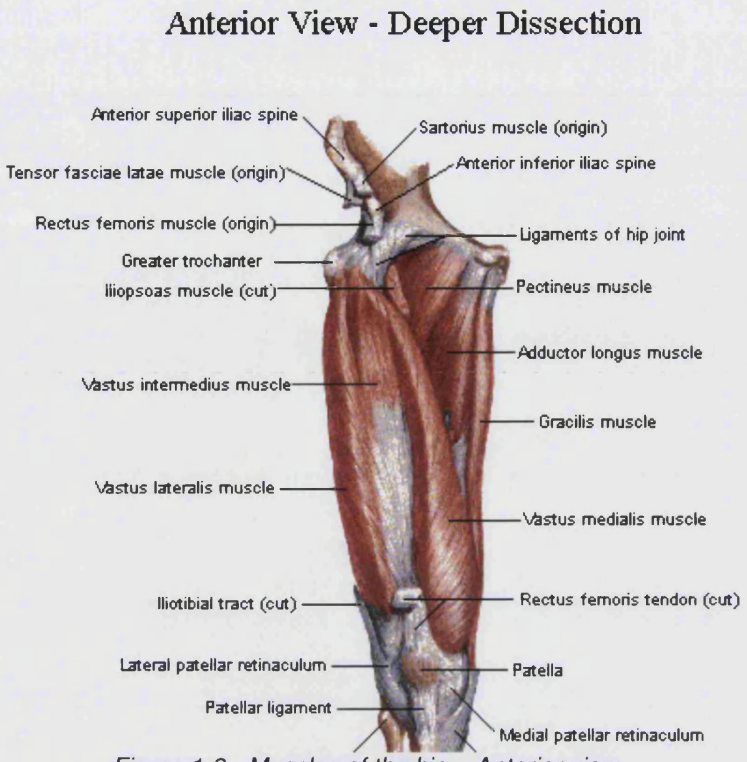

Figure 1-3 - Muscles of the hip – Anterior view
(Netter, 1997)

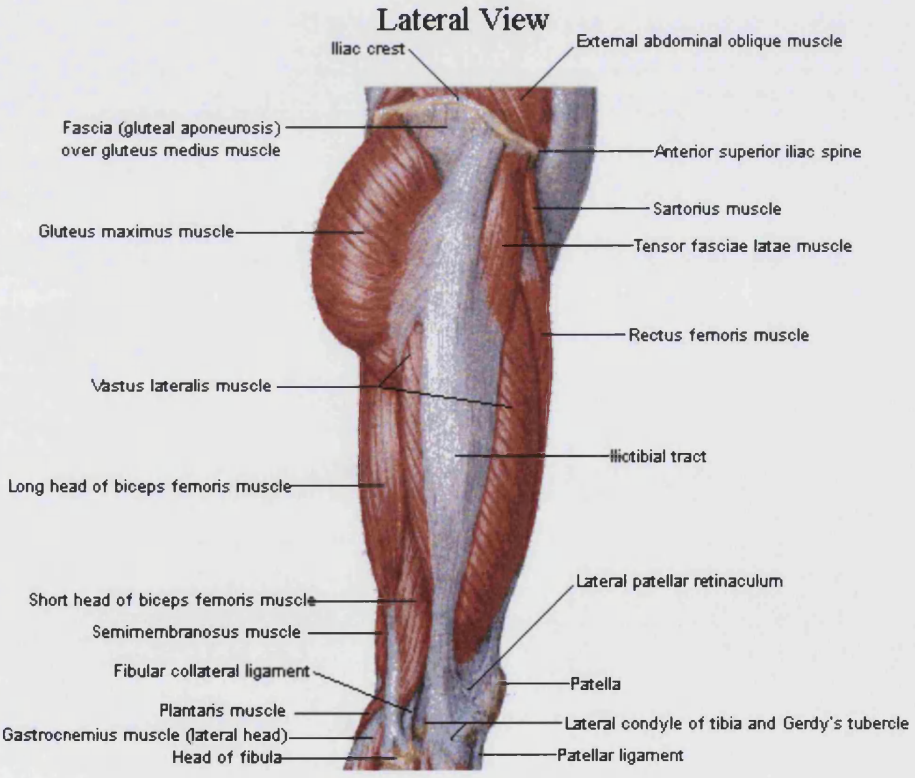

Figure 1-4 - Muscles of the hip – Lateral view
(Netter, 1997)

1.3. *Disorders of the hip and indications for arthopiasty*

The hip joint is one of the most heavily loaded, and frequently used joints of the body and therefore is susceptible to damage and disease. The damage can cause pain and restrict mobility, thereby impairing the quality of life. According to the Swedish Hip Register the most common reason for hip replacement surgery is osteoarthritis accounting for 74.5% THRs performed since 1992 followed by, respectively fracture of the femoral neck, inflammatory arthritis and idiopathic femoral head necrosis (Swedish Orthopaedic Association, 2003). The number of joints replaced is classified according to primary diagnosis in Table 1-2.

Diagnosis	**Total**	**Share**
Primary osteoarthritis	95,555	74.5%
Fracture	14,657	11.4%
Inflammatory arthritis	5,895	4.6%
Idiopathic femoral head necrosis	3,697	2.9%
Childhood disease	2,003	1.6%
Secondary osteoarthritis	1,293	1.0%
Tumour	557	0.4%
Secondary arthritis after trauma	335	0.3%
Missing results	4,347	3.4%
Total	128,339	100%

Table 1-2 - Number of THR and primary diagnosis 1992-2003 (Swedish Orthopaedic Association, 2003)

Osteoarthritis or degenerative joint disease is mainly a hereditary disease (Rothman Insitute, 2005). It results in the degradation of the cartilage layer on the conforming surfaces of joints. As the cartilage thins the joint becomes stiff and painful to move. If the cartilage wears away completely the bones can rub against each other resulting in great pain and loss of mobility. Early treatment is to rest the hip from overuse and only engage in low impact sports like swimming and cycling. For overweight patients, a diet may help to reduce bodyweight and hence loading. In the later stages when the pain becomes unbearable the only solution is to replace both surfaces of the hip with a total hip replacement.

A fracture at the neck of the femur resulting from a fall or blow to the hip can require a prosthetic implant to repair the joint and restore movement. If a fracture does not heal correctly then altered force patterns on the hip may cause accelerated cartilage wear leading to osteoarthritis and the problems mentioned above. Hip fractures are more likely in older women who suffer from osteoporosis, a metabolic disease that weakens the skeleton.

Inflammatory or rheumatoid arthritis (RA) is an autoimmune disease that causes chronic inflammation of joints. Autoimmune diseases are illnesses which occur when the body is mistakenly attacked by its own immune system. RA affects internal organs as well as joints and while the cause of RA is unknown some researchers believe it could be hereditary. In the hip, the joint swells and the fibrous capsule around the joint releases enzymes, which attack and soften the cartilage leading to faster wear of the surfaces (Rothman Insitute, 2005).

Osteonecrosis occurs when part of a bone loses its blood supply and begins to die due to the lack of nutrients. The bone loses strength and will eventually collapse causing severe pain. Excessive alcohol consumption and use of steroids can both lead to osteonecrosis (Rothman Insitute, 2005).

All the diseases and conditions described above cause pain and discomfort to the patient and constitute indications for THR surgery.

1.4. *Brief history of Total Hip Replacement (THR)*

Total hip replacement (THR) is the most common form of joint replacement surgery. The surgical procedure involves the replacement of both sides of the hip joint with an acetabular cup inserted in the pelvis and a femoral component (hip stem) inserted into the femur. The two components are designed to work together to replicate the function and, as far as possible, the structure of the natural hip. The hip stem and acetabular cup function by transferring the loads from the pelvis to the leg and providing low friction articulation between the two adjoining surfaces. THR is now the second most common elective surgical procedure in the UK with about 50,000 operations performed through the NHS each year (Government Statistical Service, 2003). The procedure has achieved very good success rates through incremental developments. THR alleviates

pain, restores normal function and can outlive the patient. Since the first attempts over a century ago the development of THR has been remarkable. THR became a common procedure in the 1960s and its popularity continues, with many innovations, to the present day.

Early techniques to manage pain relief in hips included fusion, nerve division and joint debridements. The goal was to remove arthritic spurs, irregular cartilage and smooth the surfaces of the hip (Utah Hip and Knee Centre, 2005). These procedures achieved limited success and surgeons moved on to trying to replace the surface of the femur. The main problems experienced with early resurfacing of the femoral head were associated with biocompatibility of the materials used. Subsequent attempts were made to find materials that could withstand the high forces in the hip and the aggressive environment of the body without causing infections and other adverse biological reactions. Materials tried were muscle, fat, chromicized pig bladder, gold, magnesium and zinc. The next step in the development of treatment for painful hips was known as "Mold Arthroplasty", pioneered through the 1920s and 30s by Smith-Petersen (Smith-Petersen, 1939) who noticed that a layer of synovium had formed over a piece of glass found in the body of one of his patients. He hypothesised that the formation of a synovium layer could help articulation. The Mold Arthoplasty consisted of a piece of glass modelled into a hollow hemisphere which could fit over the femoral head. Unfortunately, although the material of choice was biocompatible it tended to fracture with catastrophic consequences. The technique was improved by the introduction of a cobalt-chromium alloy known as Vitallium, but only about half of the patients treated this way experienced pain relief and the implants often loosened. In addition, the technique offered no solutions to some of the more varied symptoms seen in arthritic hips and was soon abandoned. However, hip resurfacing has been re-introduced in recent years and early results with modern implants are encouraging (Grigoris *et al.,* 2005; McMinn *et al.,* 1996).

During the 1940s surgeons began experimenting with a technique known as hemi-arthroplasty where the femoral head was removed and replaced by a mechanical component. One breakthrough occurred in 1939 when Bohlamn (Cofield, 1984) fitted a chrome-cobalt ball to a Smith Petersen nail to replace the head of the femur. The Judet brothers (Judet J *et al.,* 1954) experimented with acrylic to replace the femoral head but experienced problems with wear. All

these techniques constitute important steps in the development of hemi-arthroplasty. The acetabulum was left untouched and there was no effective method of securing the femoral component to the host, this led to loosening and eventual failure of the procedure. Further advances in the fixation of implants came with Haboush (Gunston, 1971) who used a "fast setting dental acrylic" to secure the femoral component to the bone. This was the start of cemented hip replacements.

In the 1950s Sir John Charnley began extensive research that revolutionised the design of the hip stems and the materials used. Charnley had many creative and bold ideas about hip surgery including the belief that both sides of the joint should be replaced. His work is commonly recognised as fundamental in facilitating the birth of modern total hip replacement. Charnley's innovations included the introduction of low friction high density polyethylene polymer cups to replace the acetabulum and the popularisation of the use of dental bone cement (polymethylmethacrylate) as a grout to secure the hip stem to the femur. During the 1960s, the innovations introduced by Charnley were further refined and the low friction arthoplasty he devised became very popular. The Charnley low friction arthroplasty forms the basis of modern total hip replacement (Figure 1-5).

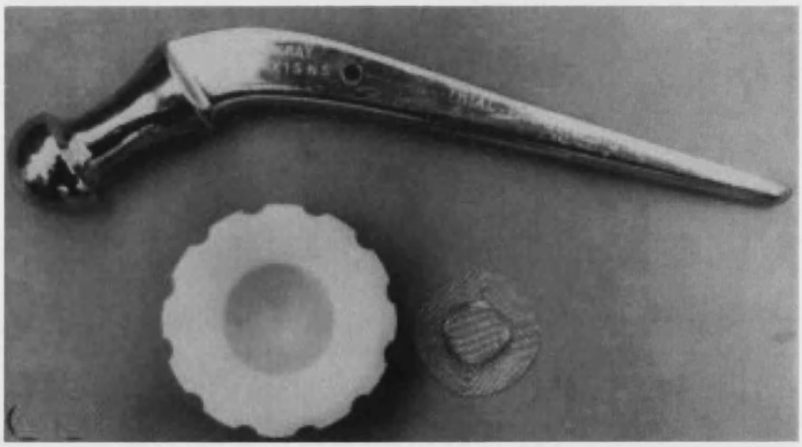

Figure 1-5 - A Charnley Total Hip Replacement
(Centre for the History Science, 2003)

Cemented THR have contributed to revolutionise the way in which osteoarthritis is treated. This has been achieved by offering an alternative to conservative treatment for this delibititating disease. Cemented THR was (and still is)

affected by early and late complications (Utah Hip and Knee Centre, 2005). In the early days problems associated with the use of bone cements were relatively common. Unfavourable material properties (e.g. poor fracture toughness and low tensile or fatigue strength) make cement liable to cracking; this can result in the loosening of the implant inside the cement mantle (Gruen *et al.,* 1979).

The problems associated with the use of cements have resulted in two major technical advances; the first one consists of the introduction of improved cementing techniques consisting of meticulous bone preparation, distal plugging of the femur and pressurisation of the cement to achieve inter-digitation with the host bone (Oh and Harris, 1982). The second one was the drive to achieve alternative methods of fixation.

This new way of thinking can be traced back to the 1970s with the search for a material that would encourage bony ingrowth around the stem. Stems could then be inserted with a press fit and would rely on the biological matrix for support. This technique is based on the assumption that a living bond will create a longer lasting and stronger method of fixation. Several practical ways to encourage bone to grow onto and into the implants were experimented with, these are characterised by different philosophies including coating the stems with hydroxyapatite (HA), a mineral found in bone, and offering a porous surface that bone could grow into. This new method of fixation was introduced in the 1980s and the resulting procedure is known as the cementless (or uncemented) total hip replacement. Uncemented THR presents advantages over cemented arthroplasty. In particular, cementless surgery preserves more original bone as removal of bone is not required to provide space for a cement mantle. This has significant advantages should the patient require a revision operation as the chances of a successful procedure are increased with more original bone remaining. Continuous refinements in materials, implants and operating techniques have contributed to extend the survival of uncemented THR to similar levels to that of cemented THR (Swedish Orthopaedic Association, 2003).

Advances in the operating technique have allowed surgeons to perform total hip replacements through minimal incisions, thus enabling patients to be discharged from the hospital in less than 24 hours from the operation. This short length of stay is mainly due to reduced trauma to surrounding soft tissues (BBC, 2003a).

More recent developments include the design of a 'smart' hip that holds a reservoir of antibiotics that are released when an infection is detected by sensors embedded in the stem (BBC, 2003b).

All new developments aim to optimise at least one aspect of the surgical procedure without compromising other factors included in the success of the surgery. This might be reducing the trauma to the patient, improving the longevity of the implant, reducing surgical costs or enabling 'smart' technologies to counter biological reactions later in the life of the implants. These alterations have the potential to impair the initial postoperative and long-term stability of a hip stem. The new techniques and the increasing numbers of THR per year leads to a large number of designs on the market, which are not all rigorously tested in the same way. Therefore, there is a clear need for a standard bench mark test to simulate the factors leading to postoperative failure and screen out inferior design concepts pre-clinically.

1.5. *Cementless hip replacement*

Since the popularisation of cementless total hip replacement in the 1980s, there have been considerable improvements in performance and survival for this type of implant. The key areas that have contributed to this success are the materials used, the geometry of the design and the coatings applied to the surface.

The materials used to form the stem must not be toxic to the body and can be selected from those stated in the ISO standards. Most commonly used are the cobalt-chromium and titanium alloys which both show clinically satisfactory osseointegration, however, the titanium shows superior clinical results (Kang *et al.,* 1991). In addition, to prevent stress shielding the modulus of elasticity of the material should be approximately equal to that of bone so that the two materials have equal compliance and the load exerted on the femoral head is distributed evenly through the bone. Titanium has a modulus of elasticity about half that of cobalt-chromium but still significantly higher than that of bone (Figure 1-6). Therefore titanium should be preferred; however the strength of titanium can be seriously reduced by surface flaws or imperfections.

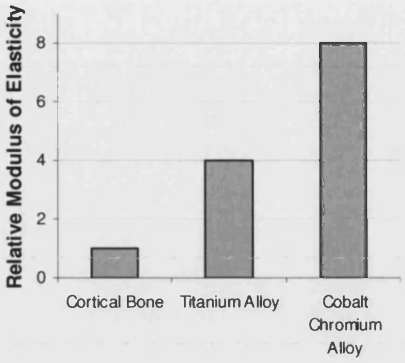

Figure 1-6 - Graph showing relative elastic modulus of stem materials (Berry et al., 2003)

Biological fixation (osseointegration) occurs over several months and requires very stable conditions. Good postoperative stability relies on the geometry of the stem and the fit within the femur. Typically, the shape of the stem is modelled on the internal geometry of the femur to fit anatomically within the cortical bone shell. The geometry of the proximal femur can vary widely from person to person and is affected by metabolic and displastic diseases (Nordin and Frankel, 1980). This can make a generic stem design difficult to define. The geometry of the femur becomes more consistent distally so some designs concentrate on achieving fixation through the cortical bone of the medullary canal (Berry *et al.*, 2003). The "fill" of a stem in the femur is important and is defined as the proportion between the width of the stem to the width of the femur. This property is generally larger for uncemented stems to ensure a tight fit but it presents problems with the stiffness of the stem. To reduce stiffness flutes and slots have been used to achieve a good "fill" without creating a stiff implant.

The stability of an implant has been highlighted as critical to its long-term clinical success and it is important that both translational and rotational stability are considered. Bones can tolerate translational micromotion of about 30-50 microns (Pilliar *et al.*, 1986; Doehring *et al.*, 1999) which is predominately along the axis of the femur in the direction of the highest load. However, subsidence or migration of 2-3mm over the first year can be tolerated without pain. Rotational motion is induced when loads are applied out of plane inducing torque on the stem. Out of plane loads are produced when performing daily living activities such as stair climbing and rising from a chair. The movement

thus induced on the stem can cause severe pain to the patient. Care has to be taken at the stage of stem design to ensure that stabilising features are included in order to minimise discomfort to the patient. A curved design can help to minimise rotational motion in stair climbing (Callaghan *et al.*, 1992). Another alternative technique is used in the SL Plus stem, this utilises a rectangular cross section with a double tapered stem that effectively wedges the stem and prevents rotational motion.

A large difference between most cemented and cementless stems is that cementless stems often do not include a collar (Mandell *et al.,* 2004). If stems use a taper and collar this may prevent the subsidence that can allow the stems to find a stable fit in the medullary canal. However, well seated stems with a collar have been shown to increase stability especially during stair climbing. Some manufacturers give the choice of a collar to the surgeon by offering it in a modular form.

In parallel with the design factors of the stem, the surface texture and chemistry are key factors to achieve stability. A good hip stem will encourage bone to grow onto the surface of the implant to achieve biological incorporation giving maximum strength and support. This can be achieved through several methods using strategic coatings or surface treatments.

The surface coatings may consist of small beads that are sintered onto the implant all over or in discreet areas to achieve a porous texture that bone can grow into. Most stems are now characterised by coatings applied around the whole circumference of the stem as the ingrowth seems to "seal the stem" preventing wear debris from travelling down the stem and causing osteolysis (Goetz D.D *et al.,* 1994; Wood *et al.,* 1995). The extent of surface treatment also raises a debate. In primary THR most surgeons favour a proximally coated stem for a more anatomic stress transfer to the host bone creating a favourable remodelling environment. On the other hand, fully coated stems offer more area for fixation and can lead to more rapid integration at the risk of proximal stress shielding (Engh *et al.,* 1994).

The two main materials used to coat implants are hydroxyapatite (HA) and tricalcium phosphate (TCP) (Berry *et al.,* 2003). HA and TCP are synthetic formulations of minerals naturally found in bone. HA and TCP have been found

to encourage bone growth onto the surface of the implant. HA is widely used and clinical results show good success (Soballe *et al.,* 1993) although the coating can be absorbed by the body after several years. De-lamination of the coating was a problem in the past as it could cause third-body wear around the interface; however thin coatings have been shown to be durable (Bauer *et al.,* 1994).

Instead of coatings, designers have used other surface treatments to achieve surface finish that bone may grow into. Titanium has been shown to be successfully incorporated into bone and so instead of applying a coating, the implant can be blasted with special grit that roughens the surface to provide a porous surface that aids bony ingrowth.

It is essential that a good bearing surface is formed on the head of the hip stem so hard wearing materials are preferred that will produce minimal wear particles. This is significant area of research as the particles produced can cause aseptic loosening if they reach the interface between implant and bone. Titanium is not a good bearing material so cobalt-chromium and other alloys are often used with a modular design where the head fits onto a cylindrical taper at the top of the stem.

1.6. *Clinical results with cementless stems*

Clinically, cementless stems have been characterised by varying degrees of success; while some implants performed badly in clinical trials others have reported excellent results (Grubl *et al.,* 2003). Generally, comparative studies between cemented and cementless stems have shown that they have achieved similar success rates. One comparative bilateral study, where 70 patients were simultaneously given a cemented hip stem in one side and a cementless hip stem in the other side found that after an eight-year follow-up, 17% reported pain in the side that received an uncemented stems compared to 3% in the cemented side. There was no difference in the incidence of osteolysis (9%) for both cemented and cementless stems (Kim, 2002). Another study compared 36 patients who received a cemented total hip arthroplasty in one hip followed by a cementless total hip arthroplasty in the contra lateral hip. Clinical pain scores

between the cementless and cemented hips were very similar and patients either had no preference or preferred the cementless side (Hearn *et al.*, 1995).

1.7. *Failure of hip stems*

Modern THRs are characterised by relatively low failure rates: 90% survivorship at 10 years for cemented implants and 84% survivorship at 10 years for uncemented implants, for stems implanted from 1992 to 2003 (Swedish Orthopaedic Association, 2003). Even if characterised by a small percentage, failures affect a large number of patients due to the popularity and extended indications for surgery. The most common reasons for failure as recorded by the Swedish national hip register (2003) are outlined in Table 1-3 and discussed below.

Mode of failure (femoral)	**Total**	**Share**
Aseptic loosening	15,826	60.6%
Dislocation	2,789	10.7%
Deep Infection	2,171	8.3%
Fracture only	1,763	6.8%
2 stage procedure	1,074	4.1%
Miscellaneous	976	3.7%
Technical error	841	3.2%
Implant fracture	364	1.4%
Pain only	269	1.0%
(missing)	38	0.1%
Total	26,111	100%

Table 1-3 - Number of re-operations and modes of uncemented femoral component failure in Sweden from 1979 to 2003 (Swedish Orthopaedic Association, 2003)

Aseptic loosening is by far the most common cause of re-operation in cementless implants and it accounts for 60.6% of the total number of revisions. Aseptic loosening occurs when the stem loses fixation due to a breakdown of the implant-bone interface. This causes instability of the implant which, in turn compromises the function of the hip and causes pain. Poor surgical technique can lead to loosening, for example if the implant is not seated correctly in the

femoral cavity. In the long term, aseptic loosening can be caused by a lack of osseointegration (bone growing up to and into the implant) or by osteolysis (removal of bone). Osseointegration is important for cementless implants because bone ingrowth forms a micro-lock that supports and stabilises the implant (Berry *et al.,* 2003). For good osseointegration an implant is required to be very stable postoperatively (Doehring *et al.*, 1999; Buhler *et al.*, 1997a). If the geometry of the implant or its surface finish is inadequate to achieve postoperative stability then loosening will occur. The loads applied to the implant as a consequence of daily living and the resulting relative movement between the two bearing surfaces produce small wear particles (Kim and Kim, 1993; Goetz D.D *et al.,* 1994). Wear particles can penetrate the interfaces between the implant and the bone and cause osteolysis (Kim and Kim, 1993). Osteolysis is shown by a thin black line or dark shadow on X-rays. These particles have been found to be well within the bioactive range that can cause severe adverse reactions in the tissue (Ingham and Fisher, 2000). Osteolysis affects both cemented and cementless implants although cementless implants with coatings around the full circumference of the implant are less at risk. Researchers believe that as bone ingrowth occurs proximally it might provide a "seal" that blocks the particles reaching the bone/implant interface (Hirakawa *et al.,* 2004).

Although not as common as loosening, recurrent dislocation is a significant problem accounting for 10.7% of failures (Table 1-3). A single dislocation postoperatively is not a serious issue, however if the problem recurs then the implant may have to be revised. THR relies on tension in the muscles and ligaments around the joint pulling and locating the femoral head in the acetabulum. If these are left under tensioned then it is possible for the femoral head to dislocate causing severe discomfort. Other possible reasons for the dislocation can be a misaligned implant or bony projections that are common with arthritis. These projections and outgrowths cause impingement and can sometimes lever the femoral head out of its socket (Swedish Orthopaedic Association, 2003).

An infection deep within the hip joint or around the implants can lead to the need to remove the hip stem to treat the infection. This accounts for 8.3% of revisions in the Swedish Hip Register. This can be a particularly frustrating failure modality for both the patient and surgeon because the implant may be

successfully and securely fixed to the skeleton, however, it must be removed to access and eradicate the infection.

Implant fracture is now considered a rare occurrence and only accounts for 1.4% of failures recorded since 1979 in Sweden. Implant fractures are now more likely to be caused by manufacturing or materials defects undetected by factory quality control or by poor fixation to the skeleton (leading to high shear and bending forces) rather than flaws in the design of the implant.

1.8. *Conclusion*

The basic anatomy, function and structure of the healthy hip have been introduced alongside a brief outline of the main pathologies affecting this joint. A brief history of total hip replacement surgery has been presented to illustrate how small incremental improvements and the re-elaboration of old ideas have contributed to improve the success rates of the procedure. The main causes of failure for modern THRs have been described.

Chapter 2. Literature review - Current cementless hip stem testing and limitations

2.1. *Introduction*

Pre-clinical testing is an important stage in the development of joint replacements. Pre-clinical testing aims to reduce or, ideally, remove the risks associated with the introduction of a new implant. Under current regulations and directives, any system must be proved to be efficacious and safe prior to any implantation or small scale clinical trials (Prendergast and Maher, 2001). Many factors need to be considered when developing pre-clinical tests capable of discerning between good and bad stem designs. Among these it is important to recognise the main failure modalities for a determined class of implant, identify the mechanical reasons for failure and reproduce these in a suitable laboratory model. In the case of cementless implants, for instance, immediate postoperative hip stem stability is critical to the achievement of long lasting function and pain relief. Postoperative stem stability is dictated by the design features of the implant alongside factors beyond the control of the design engineer, such as the quality of the surgery and quality of the host tissue.

Given that aseptic loosening is one of the main causes of failure of stemmed components, it is surprising that to date no standardised test has been developed to distinguish between good and bad designs.

This chapter will review the current International and British Standards relating to implant performance. The range of mechanical pre-clinical tests for hip stem stability available from the literature will be examined and the limitations that still exist within the test protocols proposed will be critically evaluated.

The chapter concludes with a discussion highlighting improvements in the test methodologies that have the potential to add to the understanding of failure modalities and therefore could be included in a standardised method for the pre-clinical assessment of hip stem stability.

2.2. *Considerations of pre-clinical testing*

New designs of total hip replacement components are developed continually as researchers, surgeons and engineers try to improve the results of the procedure and reduce or eliminate failures. These changes can be based on sound logic and fundamental design principles but there is no way of determining whether they will survive in the long-term, let alone provide enhanced performance with respect to current products. Development and experimentation to improve and test new designs of implants are now strictly controlled by legislation and directives to prevent unsafe or inferior implants being implanted. In Europe this is controlled by the Medical Device Directive (1996). In the United States the Food and Drug Administration (FDA) regulates medical products through the Medical Devices Amendment (1976). Current acts ensure that devices are safe for implantation but do not always indicate if they are an improvement on existing implants (Prendergast and Maher, 2001). Before clinical trials can be started, legislation prescribes a set of protocols that require a certain amount of validation and experimental results to prove the safety of an implant. These experiments form a series of tests known as pre-clinical validation.

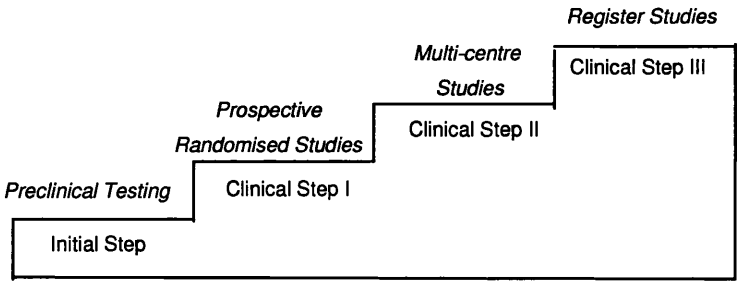

Figure 2-1 - A Diagram showing position of Pre-clinical testing in relation to clinical validation
(Malchau, 1995)

Pre-clinical tests represent only the initial step on the route to market for a medical device (Figure 2-1). If characterised by a successful outcome pre-clinical tests should be followed by prospective clinical trials and multicentre clinical studies prior to general release of a product on the market. In this methodology the pre-clinical tests should form a critical part of the development of a product and ought to provide three main functions:

1. ensuring the mechanical durability of a product,
2. highlighting the superiority of one design over another,
3. reducing the reliance on animal testing (Prendergast and Maher, 2001).

Pre–clinical tests can be classified into 3 groups: computational modelling, *in-vitro* laboratory testing and animal experimentation. Each of these can be used independently or in combination with others to facilitate the assessment of the implant in question. Computational modelling can be fast and inexpensive although the model is constrained by simplifications and limited by the understanding of the programmer. Laboratory tests can assess complex interfaces between implants and bone or substitute materials but can be time consuming. Finally animal tests are often expensive and sometimes controversial so researchers are keen to reduce reliance on the results by improving computational techniques and laboratory based work (Prendergast and Maher, 2001).

Prendergast and Maher suggest a protocol and methodology for developing pre-clinical tests (Figure 2-2). The methodology requires that the failure mode to be assessed is clearly understood so that quantities linked to this event can be measured. The environment and loading conditions need to be carefully established to model the hip environment, paying attention to all the factors that will affect the failure mechanism e.g. levels and patterns of load applied. Finally consideration is given to the necessary number of trials required to produce significant results and whether an accelerated test is possible.

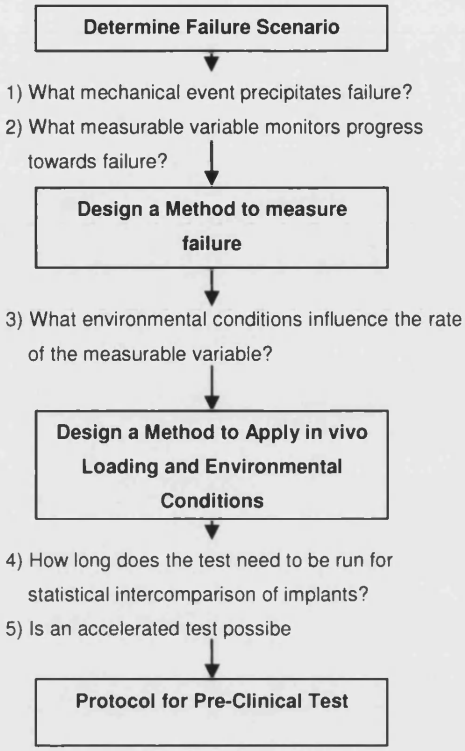

Figure 2-2 - Methodology for the development of a biomechanical pre-clinical test for an implant (Prendergast and Maher, 2001)

2.3. *Orthopaedic standards relating to hip stems*

The governing bodies responsible for formulating standards are the International Standards Organisation (ISO), the European Standards Body (CEN) and the British Standards (BS).

Standards in orthopaedics cover a wide range of areas from design to manufacture and surgery. The parties interested in the standards relating to THR include the patient, the surgeon, the theatre nurse, the purchaser, the manufacturer, the designer and possibly the lawyer (Paul, 1997). The standards affect so many people because of the broad range of areas covered including function, materials, shape, surface, sterility, packaging and labelling, with each of these having a varying effect on the parties concerned (Paul, 1997).

The standards most relevant to hip stems are mostly material related and described in the family of standards ISO 5832 but the main standard to be achieved by the designer is EN 12563 or BS EN12563:1999 detailing non-active surgical implants, in particular, joint replacement implants. As far as mechanical testing is concerned hip stems must conform to the following standards: -

- BS ISO 15032:2000 Prostheses – Structural testing of hip joints
- BS ISO 14242-1:2002 Implants for surgery — Wear of total hip-joint prostheses — Part 1: Loading and displacement parameters for wear-testing machines and corresponding environmental conditions for test
- BS ISO 7206-4:2002 Implants for surgery — Partial and total hip joint prostheses — Part 4: Determination of endurance properties of stemmed femoral components
- BS 7251-3:1997 ISO 7206-1:1995 Orthopaedic joint prostheses — Part 3: Specification for classification and designation of dimensions for hip joint prostheses
- BS 7251-4:1997 ISO 7206-2:1996 Orthopaedic joint prostheses — Part 4: specification for articulating surfaces made of metallic, ceramic and plastic materials of hip joint prostheses
- BS 7251-10:1992 ISO 7206-6:1992 Orthopaedic joint prostheses — Part 10: Method of determination of endurance properties of the head and neck region of stemmed femoral components of hip joint prostheses
- ISO 7206-4:1992 – Endurance testing of femoral components
- ISO 7206-6:1992 - Endurance properties of femoral components
- ISO 7206-9:1994 – Resistance to torque of modular heads of femoral components

These standards mainly concentrate on fatigue of the stem and wear of the articulating surfaces. The fatigue studies concentrate on the implant alone and not its interaction with the bone. ISO 7206 details test methods for fatigue testing of hip stems and specifies how to secure the implant and how to apply loading as shown in Figure 2-3. Since the introduction of this standard, hip stem fatigue has been almost totally eliminated as a mechanism of failure.

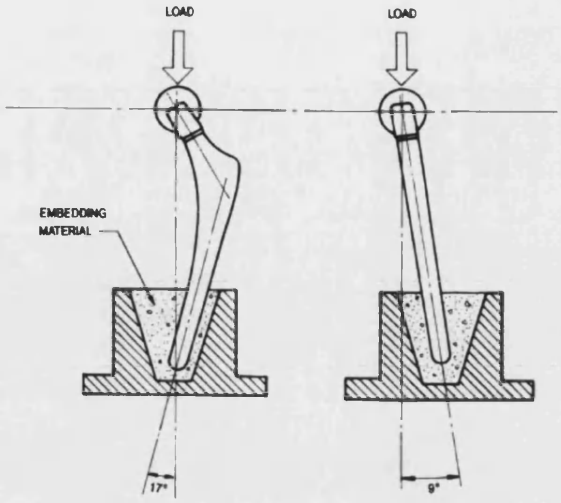

Figure 2-3 - Loading arrangement used (ISO 7206) to test fatigue properties of new implants

The standards relating to wear have been formulated from a large amount of research from hip simulators concerned with the articulating surfaces, friction of the joint, loading patterns and how best to measure wear (volumetric or gravimetric).

To date there are no standards with the aim of assessing the long term stability in terms of migration and micromotion of hip stems. There are many difficulties in establishing such a test due to the fact that movement at the stem bone interface is the result of the interaction between both materials, therefore a suitable bone mimic needs to be established. In addition to this, the amount of movement induced at the interfaces by the loading regime resulting from activities of daily living is a function of the geometry of the implant. For example, the torsional movement generated by out-of-plane forces arising from activities such as stair climbing will be greater in the case of stems characterised by wide medial-lateral dimension, as in this case the bone-stem interface is further away from the line of action of the force.

In addition to these simple geometric considerations it is important to recognise that, due to the changing demographics of the patients undergoing THR, new implants should be designed to cope with much more demanding environments. For example a middle aged man with an active lifestyle will have very different expectations from an implant than a patient who is aged 75 years or more with a

sedentary life style (Paul, 1997). This wide range of application causes much debate about the suitable values for applied loads and number of cycles.

These issues need careful consideration to develop a universally accepted benchmark test with the potential to become the basis for a standard concerned with bone implant motion. To work towards this benchmark test the previous micromotion research must be examined for the test methodologies, loading regimes and instrumentation techniques. The next section evaluates the contribution of various research groups involved with bone implant motion measurements and highlights potential areas of further study within the field.

2.4. *A summary of bone-implant motion studies*

Although there is no current standard concerning the stability of hip stems there have been many bone implant motion studies published over the last 40 years. These studies have been used to understand the mechanisms of aseptic loosening, prove new designs of hip stems and develop test protocols.

As mentioned in section 2.2 the regulatory route necessary for a stem to reach the clinical trial stage requires that it must be subject to rigorous pre-clinical validation before implantation in a patient. The aim of pre-clinical testing is to evaluate new implant designs and predict how well the implant is likely to perform *in vivo*. Thus screening out inferior implants and reducing the risk to the patient.

When designing a hip stem stability study a large number of factors need to be considered. These include the loading regimes to apply, whether to include muscle forces, the experiment configuration and the measurement apparatus. The ultimate goal is to design a realistic test that models the environment of the hip as physiologically as possible. However as there are no standard test protocols, various stability studies have been tried are described in the literature. These are characterised by diverse test environments and consequently the results are difficult to compare.

This section will provide a critical overview of some of the hip stem stability studies available in the literature. Common features of the different techniques

adopted will be highlighted with the main advantages and limitations of each methodology. Following this, the requirements and possible solutions to improve past methodologies will be discussed.

Bone implant motion studies are based on the premise that stable implants are more likely to achieve long term fixation and attain a successful clinical outcome. A clear link between osseointegration and long-term clinical success has been demonstrated (An *et al.,* 1998). For osseointegration to take place the stem must be stable postoperatively in order to allow bone growth onto and around the implant. Hip stem stability can be described by two different types of movement commonly called micromotion and migration (or subsidence). Micromotion defines the recoverable movement of an implant relative to the host bone under cyclic loading, a function of the elasticity of the bone-implant construct. Migration (or subsidence) defines the unrecoverable movement of an implant with respect to the surrounding bone; it reflects the micro-damage caused by the implant to the host tissue

In a canine study that assessed the level of motion between implant and bone, Pilliar reported that bone ingrowth can occur in the presence of some movement, albeit very small (up to 28 μm), while excess movement (150 μm or more) results in ingrowth of mature connective tissue (Pilliar *et al.*, 1986).

These small motion amplitudes are extremely difficult to measure accurately. In addition, the implant movement can occur in different directions: medial-lateral, inferior-superior and anterior-posterior translations and rotations about the axes. The small motions coupled with the complex bone-implant interface and six degrees of freedom mean that a sophisticated transducer is required to measure stability. Many different techniques and approaches are described in the literature to perform this measurement. A brief summary of some of these techniques highlighting the displacement they are capable measuring and how they have been developed is given below.

The first method of measuring implant bone motion was developed by Charnley in an attempt to eliminate any slip between implant and femur. While trying to assess the factors that led to early loosening of hip stems, Charnley devised a method of assessing the motion (or slip) between the implant and the host bone while load was applied. The femur was held in a vertical position while a

compressive load was applied to the head of the implant. The level of migration was assessed using a simple dial gauge accurate to 1/10,000th of an inch (Charnley and Kettlewell, 1965). This pioneering research highlighted the importance of bone implant motion; however the test only detected motion in one direction (axially along the femur) and relied on the researcher recording the deflection. Other researchers have also used dial gauges (Whiteside and Easley, 1989) however the technique becomes impractical when motions in more than two directions were required. Walker *et al.,* 1987, used a system of extensometers to offer a more complete picture of the motion. In Walker's experiment, the femur was also mounted in a vertical position in the sagittal plane while it was inclined by 12° in the coronal plane to simulate single leg stance. Vertical compressive loads were statically applied to the implant through pneumatic actuators up to a maximum of 1000N. The relative movement between the implant and the host cadaveric bone was recorded by a configuration of six extensometers that monitored the position of steel cubes attached to the implant. The cubes were rigidly secured to the stem via a push fitted rod that passed through an oversized hole drilled in the cortex of the femur. This system was capable of measuring translational motion in three orthogonal directions however rotation could only be measured in the superior-inferior and anterior-posterior axes. Walker demonstrated that well fitted cementless implants were only subject to micromotion amplitudes slightly larger than those of cemented implants (Walker *et al.,* 1987).

Schneider *et al.,* (1989) developed a new protocol for testing bone implant motion to overcome the shortcomings of previously adopted techniques such as the application of quasistatic loads, the restriction of only one stem and the use of a measurement system that failed to record the full extent of motion of the implant. In the study by Schneider, cadaveric femora were subjected to axial loads of up to 4 times bodyweight and torsional moments of 8Nm, the load was applied 2400 times at a frequency 0.5Hz. Motion of the implant relative to the bone was recorded by five transducers in conjunction with an x-y table to assess a combination of translations and rotations over the implant. The x-y table was used to transmit axial and torsional load, one transducer was dedicated to measuring transverse rotation and the remaining four transducers measuring motion at the bone implant interface at various levels. The results from this technique showed considerable differences between the motions of the five stems tested. This highlights that different geometry used in the design of the

implants will lead to altered behaviour in a femur. The instrumentation technique adopted was capable of recording the subsidence of the implant over the course of the test; however, the micromotion associated with each loading cycle was not recorded. The instrumentation was also capable of recording motion at various locations on the stems but could not measure the overall motion of the stem unless both the bone and implant are considered as rigid bodies.

Burke *et al.,* (1991) performed a cadaveric study to compare cemented to uncemented stems. The cadaveric femora were held in positions to represent single leg stance and stair climbing to replicate common loading regimes likely to be experienced at the hip. The study also acknowledged the likely effect of muscle loading on the hip stem and the experimental set-up included an abductor strap attached through a simulated pelvis. The knee joint was modelled as a pin jointed system to avoid non-anatomical bending forces acting on the test femora. The loads applied were kept low, 445N, to minimise risk of fracture in the cadavers and repeated three times with the displacement recorded both under load and after unloading to record permanent deformation. Motion of the implant relative to the bone was recorded by extensometers in three orthogonal directions. The experimental setup with extensometers is pictured in Figure 2-4. No 3D rotational data was recorded. The positioning of one sensor was 30mm distal to the collar as it was claimed that this is where the critical growth will occur hence the micromotion here was most important. By measuring both during loading and after unloading this study distinguishes between micromotion and migration however three cycles are insufficient to provide clinically relevant data.

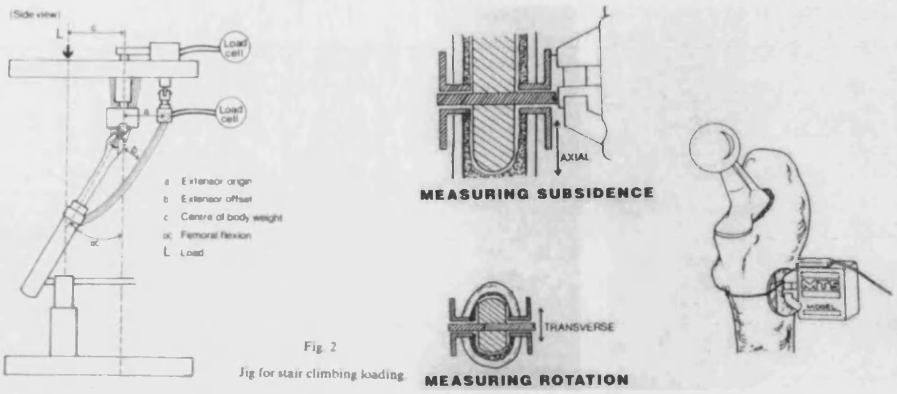

Figure 2-4 -Diagram showing measurement method used by Burke et al., 1991 (Burke et al., 1991)

Burke reported micromotions of up to 42µm in the cemented implants and 30µm in cementless implants for single leg stance. In stair climbing the performances reversed with 76µm in cemented implants compared to 280µm in the cementless. The results indicated that the cemented implants had a superior tolerance to stair climbing than cementless stems

The technique of using extensometers to record motions in three orthogonal planes was developed further by Callaghan *et al.,* 1992, who placed sensors at two locations to record the motion of the hip stem both proximally and distally. However, rotation of the implant was still not recorded and results were only recorded from the first loading cycle offering no data on the performance of the stem over time. The loads applied to the stem were also increased to 1500N in single leg stance to represent a more realistic experiment. The research suggested that the use of a curved stem in the anterior-posterior direction resulted in a lower micromotion than an equivalent straight stem. Callaghan also suggested that micromotion studies should be performed when femoral prostheses are being considered for use without cement.

McKellop *et al.,* 1991, took a new approach to the problem by attaching a rigid frame to the proximal femur which was instrumented with 3 strain gauge displacement transducers. The rigid frame was then brought into contact with the stem to monitor the relative motion between the two. The system was capable of measuring distal and medial displacement with anterior rotation with an accuracy of 2µm over a range of 3mm (McKellop *et al.,* 1991).

A more sophisticated method was developed later when Gilbert *et al.*, 1992, described a computer based method to calculate the position of a hip prosthesis relative to the femur. The technique was designed to measure the motion of the hip in six degrees of freedom and separate the results into migration and micromotion. The technique, shown in Figure 2-5, used the mechanics of rigid-body motion analysis and apparatus of seven linear displacement transducers to describe three-dimensional motion of the prosthesis during cyclic loading. Four transducers (LVDTs) measured the motion of a cube attached to the stem proximally and three transducers tracked the motion of a cube attached distally. Computer acquisition of the data and customised analysis software was used. The magnitude and direction of the motion of any point on the prostheses was calculated from the recorded motion of two points of interest on the device assuming that the stem behaved as a rigid body. The technique was tested on one cemented and one cementless hip stem implanted in cadaveric femora. Loads were applied sinusoidally between 40 and 200N at a frequency of 1Hz. Data was sampled from the LVDTs at 20Hz and the results were used to generate magnified animation models that could show the trends of motion experienced by the hip stems under loading. The authors claim a resolution of about 3-5 μm for each transducer. The largest limitation of this technique is that to compute the overall motion of the hip stem, both the bone and hip stem must be treated as rigid bodies. Considering the low level of force (200N) used in this study the assumption that both bone and implant behave as rigid bodies is acceptable however with larger, more physiological loads the assumption must be questioned.

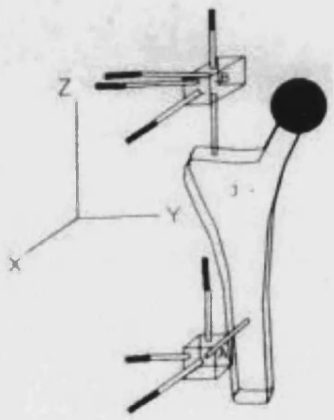

Figure 2-5 - Experimental setup of Gilbert's rig (Gilbert et al., 1992)

One year later, Berzins *et al.,* 1993, credited Gilbert for outlining an approach to developing a six degree of freedom transducer and produced the first system that could measure translational motion in orthogonal axes x, y and z and the rotations about these axes from a single point of attachment. Berzins combined the computer based technique with a measurement setup consisting of 6 transducers, previously used in spinal biomechanics by Panjabi *et al.,* 1976. The configuration of these transducers can be seen in Figure 2-6. The transducers monitor the position of three spheres rigidly attached to the lateral side of the hip stem via a frame. Using 6 transducers in a 3-2-1 configuration (3 superior-inferior, 2 medial-lateral and 1 anterior-posterior) allows six independent equations of motion to be generated and therefore motion in six degrees of freedom can be calculated.

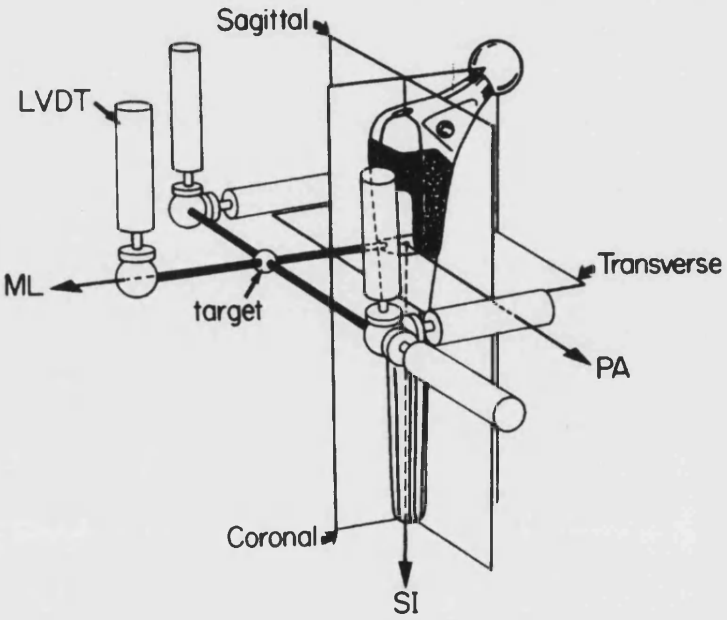

Figure 2-6 - Six degree of freedom measurement transducer (Berzins et al., 1993)

Berzins' experimental setup was used to investigate the initial relative bone-implant motion in a cadaveric study of two types of cementless femoral components, a straight stem and a curved stem. Torque of up to 32.9 Nm was applied at set angles to represent walking, stair climbing and rising from a chair. Stair climbing was shown to produce significantly more bone-implant motion than walking. The rotation of the implants was greater distally than proximally thus confirming that the rigid body assumptions that Gilbert used were not valid at higher loads. The conclusion was that the femoral component was

particularly sensitive to off-axis loads. As off-axis loads are normally induced by stair-climbing and rising from a chair, these activities should be avoided in the early postoperative period when a cementless, porous, coated stem has been used. The technique represented a significant step forward in the measurement of bone implant motion with full 3D motion recorded. Berzins acknowledges that the technique does not include a model of muscular forces and that the inclusion of muscle straps would affect the load on the femoral head.

A similar device to that developed by Berzins was used in a series of studies by the Bioengineering group in Trinity College, Dublin, Ireland. Maher *et al.*, 2001, measured the migration of hip stems with a target device consisting of six spheres mounted to the hip stem via two push fitted pins. The two pins prevented any rotation of the target device ensuring that the rotation measurements were reliable. The position of the six target spheres was continuously monitored by six LVDTs allowing computation of the motion of the hip stem relative to the outside of the femur in six degrees of freedom. The LVDTs were mounted on a composite femur by a ring clamp. Alignment of the target device and the LVDT bracket was achieved with a jig. Figure 2-7 shows the target device and LVDTs configuration used.

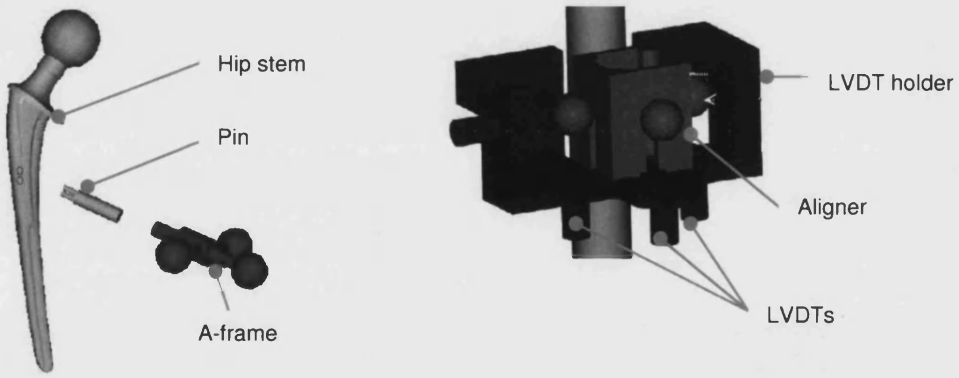

Figure 2-7 - Showing the measurement transducer and attachment to implant (Maher et al., 2001)

The transducer was mounted on the anterior side of the hip stem in a proximal location. No information was recorded at the distal tip. This rig was used to assess cemented and cementless stems showing the versatility of the method. The aim of Maher's work was the assessment of long-term fixation, so the cemented implants were loaded up to 1.8kN at 5Hz for 2 million cycles. The

results produced compared well to clinical trials showing high initial migration followed by a period of steady state subsidence, although the variability was high. It is important to note that the technique is for assessing cemented hip stems and measuring the long-term performance of the stem, hence 2 million cycles and only migration was recorded. Much shorter tests are relevant for cementless hip stems where immediate postoperative stability and micromotion are critical (Maher *et al.*, 2001).

The goal of these bone implant motion studies is to screen out bad hip stem designs. Maher and Prendergast used their motion transducer in another study with the aim of assessing the technique to see if the results produced could discriminate between two implants with known loosening characteristics (Maher and Prendergast, 2002). The two stems used were a Lubinus SPII prothesis and a Muller curved stem. These two stems were chosen as they are known to have different loosening rates *in vivo.* Both stems were implanted in composite femora and instrumented with the six DoF motion transducer. The specimens were subjected to compressive loads from 0.23 to 2.3kN at 5Hz for 2 million cycles. The results showed both hip stems migrating over time with the stem known for high loosening, the Muller curved stem (Krismer *et al.*, 1991), subsiding more than the Lubinus, known for low loosening (Malchau *et al.,* 1993). This agreed with the clinical loosening data, adding weight to a general view that this technique is capable of screening inferior stems.

Before an accepted benchmark test can be agreed, all the various factors that affect hip loading must be examined and assessed for their importance or significance. One of the main factors is the effect of muscle forces. Britton *et al.,* 2003, carried on the work of Maher and used the same six degree of freedom motion transducer to evaluate the effect of muscle forces. A method was used that could attach a strap to the femur to simulate the action of the abductors; the vastus lateralis and the tensor fasciae latae forces.

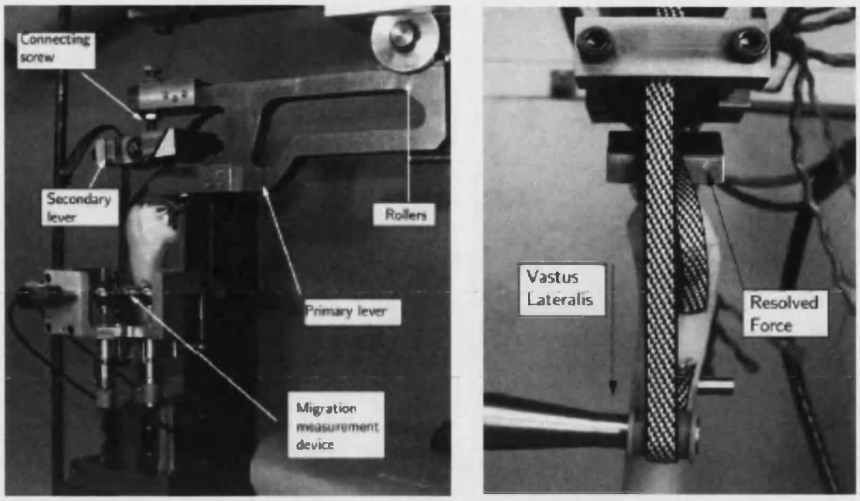

Figure 2-8 - Hip testing rig including muscle forces (Britton et al., 2003)

Britton's rig can be seen in Figure 2-8 which shows the loading rig and motion transducer. The loading rig includes a strap which acts to simulate the force of the abductor muscle Vastus Lateralis. The loading profile selected for these cemented stems was 1.5kN at a frequency of 5Hz for one million cycles, which was based on the work of Bergman et al., 2001. The results showed that applying muscle forces during the experiment produced less mean migration and a reduced experimental scatter leading to the conclusion that muscle forces should be included in any testing protocol to increase confidence in the obtained results (Britton *et al.*, 2003).

The Rizzoli research group in Bologna, Italy, have developed their own system for bone implant motion to investigate the effect of variation in surgical stem insertion and stem designs (Harman *et al.,* 1995). Eighteen composite femora were prepared by an experienced orthopaedic surgeon and three different stem designs were inserted with the aid of a mechanical system for repeatability. Stems investigated were; a hollowed Ti stem, a full Ti stem and a Cr-Co porous coated, collarless, anatomic uncemented hip stem. Positions of the stems in the femora were recorded by radiograph. The stems were statically loaded with a force of 1600N; the femur was mounted with 10° adduction. A single extensometer recorded axial micromotion. Although this measurement system is not as sophisticated as the ones used in earlier studies and the applied load was not cyclical, the study attained interesting findings. Stems characterised by shallow insertion (i.e. the stems sitting proud) displayed significantly larger micromotion than those which were inserted deeply. The use of a controlled

insertion technique was found to reduce the experimental scatter from 35% down to 20%.

Harman's method and femoral instrumentation were further developed by Baleani *et al.,* 2000, and used for testing three hybrid stem designs. This study used a set of eighteen composite femora with groups of six for each stem design. The three hybrid designs were an ANACAFIT cemented stem, ANACAFIT cementless stem and the CLU prototype (a partially cemented stem). After reaming and broaching of the composite femora, the cementless hip stems were inserted using a series of 100 compressive cycles at 1.7 kN. An initial study found that, after this preconditioning, no further axial subsidence could be detected by an extensometer when the compressive load was applied. The CLU stem was inserted into the composite femora and a cement gun was used to inject acrylic bone cement through specially designed holes. All three sets of stems were then subjected to a set of 1000 cycles with a sinusoidal torque applied up to 18.9Nm. This force was chosen to represent one month of stair climbing. The motion of the implants relative to the bone was recorded for the first 20 cycles and then for 1 entire cycle out of every 10 after that. This motion was recorded by an extensometer to measure subsidence and four LVDTs to record shear micromotion. The four LVDTs were strategically placed at the medial point on the femur neck resection plane, medial point 7mm above the tip of the stem, half way between the previous mentioned positions and the anterior point on the femur resection plane. A side study investigated the error caused by removal and reattachment of the LVDTs and extensometer and it was found that the accuracy was better than 5μm. The cementless stem was the least stable implant, while the hybrid stem had similar motion levels to the fully cemented stem.

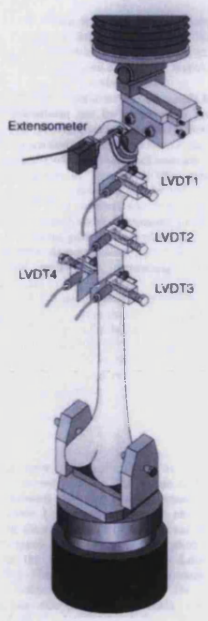

Figure 2-9 - Cristofolini's rig with extensometer and LVDTs (Cristofolini et al., 2003)

Further research by this group (Cristofolini *et al.*, 2003) was carried out using a very similar instrumentation configuration and setup to that of Baleani (Figure 2-9). An extensometer was again used to measure the subsidence along the axis of the femora and a set of LVDTs was used to record the shear (interface motion) between the bone and the implant. The aim of the study was to prove that the technique was sensitive to implant design and capable of discriminating between "good" and "bad" stems. The two stems used were the Lubinus SPII and the Muller curved, the same stems used by Maher and Prendergast in 2002 in a very similar study. In this investigation the number of loading cycles was increased from 1000 in Baleani's work to one million cycles of stair climbing with the femur subject to axial forces of 1683N and torques of 23.2Nm applied in the direction of intra rotation. The Muller curved stem was found to exhibit larger axial subsidence (172μm) than the Lubinus SPII (43μm). The protocol was designed with industrial pre-clinical validation in mind and the results confirm that the technique is capable of screening poor implants. However, no muscle loading was included.

A very different approach to measuring motion was developed by Buhler *et al.*, 1997a. After both numerical and experimental studies proved that neither the bone nor the implant could be realistically modelled as rigid bodies (Cheal *et al.*, 1992; Berzins *et al.*, 1993), Buhler developed a method of recording detailed

motion data at specific sites between the stem and bone. An optoelectronic sensor based on a silicon position-sensitive detector was used for this purpose. Three optoelectronic transducers were mounted on the anterior side of the stem at proximal, distal and middle locations along the length of the implant, as shown in Figure 2-10. The sensors were mounted onto the cadaveric femora, located onto the stem through oversized holes drilled in the femur and finally into machined hemispheres on the implant surface. This method allows direct measurement of the interface motion however the hemispheric depressions must be regularly checked and cleaned to ensure no tissue inhibits the location.

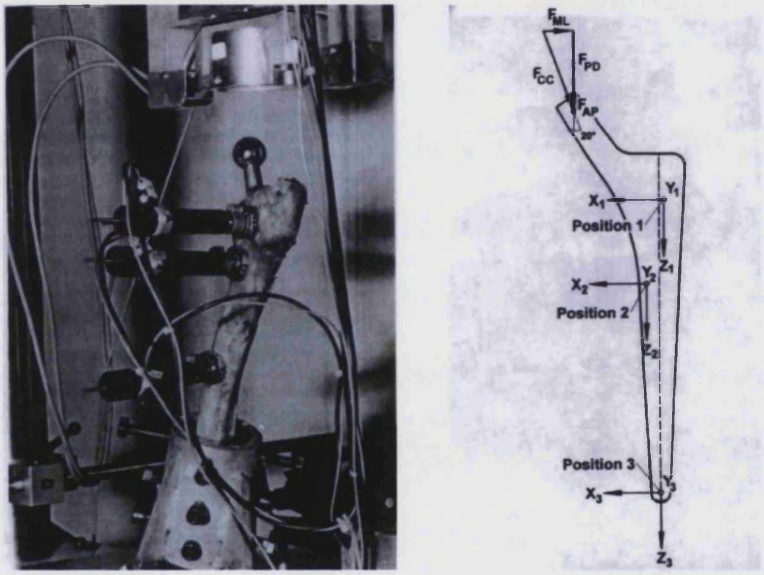

Figure 2-10 - Optoelectronic sensors mounted on a cadaveric femur and a diagram showing their attachment locations
(Buhler *et al.*, 1997b)

The accuracy of this technique was claimed to be 5µm over a range of 1.5mm and provides more localised information than previous studies by recording motion along the three orthogonal axes. The same year Buher *et al.*, 1997b, investigated the stability of the CLS stem (Spotorno) and the Cone prosthesis (Wagner) after implantation in seven paired cadaveric femora. The specimens were loaded with a force proportional to the donor's bodyweight in a series of increasing loads. On the final set of experiments the specimen was subjected to up to four times bodyweight axially at a frequency of 1Hz and 0.4 times bodyweight applied in the anterior posterior direction at a frequency of 0.5Hz. No abductor force was applied. The cone shaped stem concept demonstrated

less subsidence along the femur than the CLS stem with longitudinal ribs displayed less micromotion.

Speirs used the same setup in a cadaveric study with cemented stems and concluded that different patterns of motion could be due to surface finish and geometry (Speirs *et al.*, 2000).

Claes *et al.*, 2000, used the configuration of LVDTs shown in Figure 2-11 to analyse the stability of partially cemented stems in cadaveric models. The study was intended to prove the stability of a new hip stem in order to proceed with a clinical study. The loads applied were 1.6kN at 0.5Hz for three cycles with the motion data being analysed at the third peak. This reflected the original intention of the study: to assess initial stability rather than long-term stability. The six LVDTs used in this study allow one-dimensional measurements of displacement at several positions on the implant. The implications are that the translations measured are local and, due to possible flexing of the hip stem, cannot be used to extrapolate overall rotation or translation. Also, the set-up time will be considerable to ensure the sensors are correctly aligned.

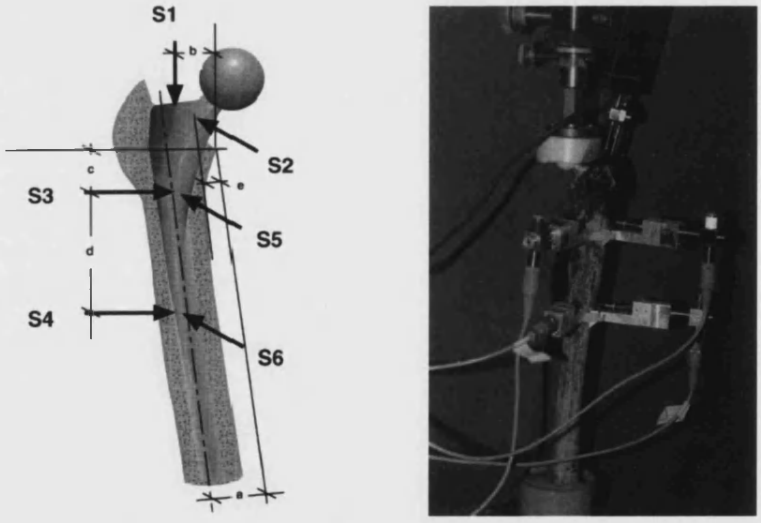

Figure 2-11 - Configuration of LVDTs used by Claes (Claes et al., 2000)

The study conducted by Claes is, nevertheless, very comprehensive and includes the effect of muscle forces (through an abductor strap). The implant is also assessed in different positions.

One of the most comprehensive methods of measuring bone implant motion was described by Doehring *et al.*, 1999, who used a technique similar to Berzins with a crucifix supporting three metal spheres that are tracked by six LVDTs at two locations, proximal and distal (Figure 2-12).

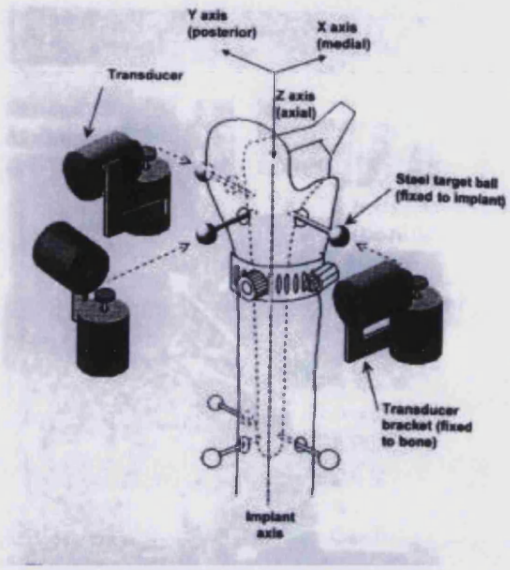

Figure 2-12 - Experimental setup of Doehring (Doehring et al., 1999)

The aim was to investigate the effect of modular neck length alterations on the initial stability of hip stems. Neck lengths are often increased to minimise the risk of dislocation of the hip stem from the acetabular component. A longer neck length though, increases the torque on the stem and might affect loosening. Doehring *et al.*, 1999 measured the stability of the stem by attaching a crucifix through the centre of the hip stem at proximal and distal locations (Figure 2-12). This configuration results in a rigid system for transferring the motion of the hip stem to the LVDTs, however, the complexity of the setup of the experiment is also increased. The LVDTs are attached to the cadaveric femur by a device similar to a jubilee clip; however the design of the frame holding the LVDTs is not clear. It is critically important that there is no relative motion between the LVDTs as this would affect data recorded during the test. The system developed was capable of recording translational and rotational motion of the hip stem relative to the host bone. Motion of the hip stem was categorised into recoverable (micromotion) and subsidence (migration). The study was

performed with a set of six cadaveric femora implanted with hip stems with varying modular components to increase the neck length by 12.5 mm and 25 mm. Loads were applied to the femora mounted at 34° flexion and 15° adduction to represent stair climbing based on research by Andriacchi *et al.,* 1980. Quasi-static loads were applied at 0.05Hz between 0 and 445N. The inclusion of muscle modelling cables increased the applied load to 3.5 to 4 times bodyweight on the head of the hip stem. The results showed that long modular neck lengths increased micromotion by 38% suggesting that their use should be avoided.

The use of two transducers (proximal and distal) has been adopted at the Centre for Orthopaedic Biomechanics (COB), University of Bath. The transducers used for this research are based on the design first introduced by Berzins *et al, 1993.* A picture of this set up can be seen in Figure 2-13. A detailed description of the experimental procedure adopted at the University of Bath will be presented later in this document. (Clements *et al.*, 2005).

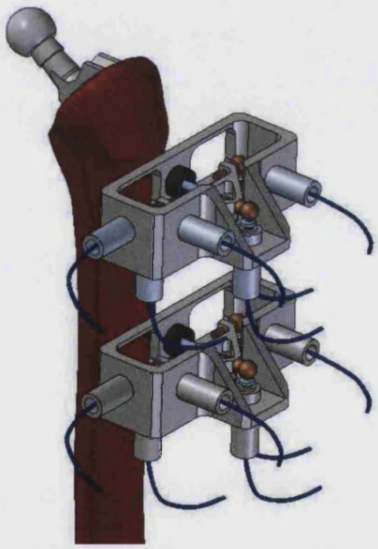

Figure 2-13 - Experiment setup used at the Centre for Orthopaedic Biomechanics (Clements et al., 2005)

Table 2-1 provides a summary of the main 3D bone implant motion detection techniques described above.

Another technique for measuring bone implant motion is Roentgen Stereophotogrammetry (RSA) which is capable of measuring hip stem migration

in vivo. This technique uses two x-ray images to show the position of markers on the bone and implant. The positions of the markers can traced over time to assess the motion between the hip stem and host bone and hence show the migration of the stem. Results have shown that high initial subsidence is linked with thigh pain and can predict the need for early revision of the stem (Karrholm *et al.*, 1994). It should be noted that the technique is the only current method of recording stability *in vivo* however the accuracy is of the order of 0.3mm and micromotion measurements are not possible.

All the tests presented so far have tried to replicate the environment of the hip to achieve a realistic model and produce meaningful and accurate results. However one characteristic of all these studies is that the femur is held statically, whilst the load is applied. *In vivo*, during the gait cycle the femur moves relative to the upper body so the forces on the head of the hip stem constantly change their line of action with respect to the long axis of the bone. This will change the loading pattern on the implant and potentially the pattern of relative motion between implant and bone, thus it is believed that a dynamic test of stability would best reflect the working environment of the implant.

Author and year	Specimen type and quantity	Stem Type	Specimen Position	Muscle Included	Type of test	Max Load	Variables measured	Transducer class	Transducer Configuration
Charnley and Kettlewell, 1965	Cadaveric x 8	Moore cemented Moore uncemented	0° Flexion 0° Adduction	No	Ramp	0.2 ton	Axial migration	Dial gauge	Sup-Inf
Walker *et al.*, 1987	Cadaveric x 25	Exact fit Type 1 Type 2	0° Flexion 12° Adduction	No	Ramp	1000N	Strain and Displacement	Extensometer	6 Independent
Schneider *et al.*, 1989	Cadaveric x 30	Straight Stem x 6 Muller 85 x 6 CLS x 6 PCA x 6 Zweymüller x 6	0° Flexion 7° Adduction	No	Cyclical	4 x BW	3D micromotion	Strain gauge based motion transducer	Independent
Burke *et al.*, 1991	Cadaveric x 7	Cementless x 7 then Cemented x7	SLS - 0° Flex 12° Add SC - 32° Flex 12° Add	Abductor	Ramp	445N	Axial and transverse micromotion	Extensometers	Independent
McKellop et al., 1991	Composite	3 Cemented Austin Moore uncemented	SLS - 0° Flex 12° Add	No	Cyclic	1000N	Axial and transverse micromotion	Strain gauge based motion transducer	Independent
Callaghan *et al.*, 1992	Cadaveric x 7 pairs	Harris Galante Curved (anatomic)	SLS SC	Abductor	Cyclical	1500N SLS 1200N SC	Axial micromotion	Extensometers	Proximal and Distal
Gilbert *et al.*, 1992	Cadaveric	Uncemented cemented	SLS	No	Cyclical	2kN	3D micromotion	LVDTs	2 Clusters
Berzins *et al.*, 1993	Cadaveric x 5 pairs	HG Multilock Curved (anatomic)	SLS 20° Flex 8° Add SC 34° Flex 8° Add	No	Ramp	19.9Nm 32.9Nm	3D micromotion	LVDTs	1 Cluster
Harman *et al.*, 1995	Composite x 6	Collarless anatomic uncemented	0° Flexion 10° Adduction	No	Ramp	1600N	Axial micromotion	Extensometer	Sup-Inf
Buhler *et al.*, 1997	Cadaveric x 7 pairs	CLS (Spotorno) Cone prothesis	0° Flexion 20° Adduction	No	Cyclical	4 x BW	Translational micromotion	Optoelectric sensors	3 Independent
Doehring *et al.*, 1999	Cadaveric x 6	HG Multilock	SC 34° Flex 15° Add	Abductor Adductor Extensor	Ramp	4 x BW	3D micromotion	LVDTs	2 Clusters
Baleani *et al.*, 2000	Composite x 18	CLU cemented CLU hybrid CLU cementless	SC	No	Cyclical	1.7 kN	Translational micromotion	LVDTs	4 Independent
Claes *et al.*, 2000	Cadaveric x 6 pairs	Option 3000	6° Flexion 8° Adduction	No	Cyclical	1600N	Translational micromotion	LVDTs	6 Independent
Speirs *et al.*, 2000	Cadaveric x 8 pairs	Prototype Charnley	0° Flexion 20° Adduction	No	Cyclical	4 x BW	Translational micromotion	Optoelectric sensors	3 Independent
Maher *et al.*, 2001	Composite x 5	Lubinus	0° Flexion 20° Adduction	No	Cyclical	1.8kN	3D micromotion	LVDTs	Cluster
Gortz *et al.*, 2002	Cadaveric x 7 pairs	Adaptiva Zweymüller	6° Flexion 8° Adduction	No	Ramp	2kN	Translational micromotion	LVDTs	Independent
Cristofolini *et al.*, 2003	Composite x 6	Lubinus Muller	SC	No	Cyclical	1.7 kN	Translational micromotion	LVDTs	4 Independent
Britton *et al.*, 2004	Composite x 6	Omnifit	9° Flexion 10° Adduction	Abductor	Cyclical	1.6kN	3D micromotion	LVDTs	Cluster
Clements *et al.*, 2005	Cadaveric x 5 pairs	Zweymüller	SLS 7° Flex 11° Add SC 32° Flex 11° Add	Abductor	Cyclical	1.2kN	3D micromotion	LVDTs	2 Clusters

Table 2-1 - Table summarising experimental setups of 3D Bone implant motion techniques in chronological order

2.5. *Dynamic hip stem testing*

Dynamic hip simulators are already used for predicting the wear characteristics of the artificial bearing surfaces of a THR. This is very different to assessing bone implant motion but the rationale underpinning both simulators the same: the achievement of a realistic, physiological, reproduction of the loads and kinematics of the hip joint. There has been a large amount of research into the loading and kinematics of wear simulators which could be transferred to hip stem stability studies. This section assesses the dynamic wear simulators available commercially and examines the current research aimed at developing a dynamic simulator for the purposes of hip stem stability evaluation.

Dynamic hip simulators have been developed over the past 20 years but their use has been almost exclusively for the assessment of wear debris generated by the articulating surfaces of hip replacements. This is based on the evidence that the debris causes osteolysis (Smith *et al.,* 1999), which is a contributing factor in late loosening. The basic concept of these simulators is to reproduce the locus of forces acting on a femoral head to simulate the effects of the gait cycle. The aim is to create comparable wear rates and patterns which total replacements are likely to show *in vivo.* From a theoretical point of view, loading and motion cycles of hip joints can only be closely reproduced by three rotational actuators and three force actuators (Viceconti *et al.*, 1996). However, in order to reduce the complexity of the equipment existing devices have been designed assuming that some of these degrees of freedom are negligible. An example of this is the commercially available Boston hip simulator (Figure 2-14). The Boston simulator comprises twelve stations for parallel testing; it provides rotation about three axes and loading profiles which replicate walking or stair climbing. Each specimen is immersed in a temperature-controlled test fluid containing bovine serum and saline. Each of the chambers is independent of all others so wear debris collected from each chamber can be independently analysed.

Figure 2-14 – Boston hip simulator for measuring wear of femoral head and acetabular cup (one side only)
(Design news, 2003)

Table 2-2 presents the loads and ranges of motion used in several commercially available wear simulators that may be relevant to the design of a hip stem stability simulator. Various ranges of motion are used to either investigate the effect of differing gait data or for alternative theories of "worst case" motion. A full analysis of these simulators and the force track path was performed by Calonius and Saikko, 2003, who were trying to identify a method for comparing results between simulators. Simulator studies are now controlled by ISO standard 14242-1 which states that the stem must rotate from 25° flexion to -18° extension in the sagittal plane; 7° Abduction to -4° adduction in the coronal plane and rotate from 2° internal rotation to -10° external rotation in the transverse plane.

Authors	Simulator	Motion Data			Peak Load (KN)	Pattern
		Sagittal	Coronal	Transverse		
(ISO Standards, 2002)	ISO 14242-1	25° to -18°	7° to -4°	2° to -10°	3	Double peak curve
(Saikko, 1996)	HUT - 3	23° to -23°	23 to -23	0	3.5	Square wave
(Dowson and Jobbins, 1988)	Leeds MkI	35° to -20°	7° to -7°	7° to -7°	2.6	
(Smith and Unsworth, 2001)	Durham MkII	30° to -15°	10° to -10°	5° to -5°	2.5	
(Barbour *et al.*, 1999)	Leeds Mk II	30° to -15°	10° to -10°	7° to -7°	3	Double peak
(Goldsmith and Dowson, 1999)	Pro Sim	25° to -23°	3° to -3°	0	2.87	Double peak

Table 2-2 - Table showing loads and angles used in wear studies

A survey of the literature has revealed that only one dynamic simulator has been used for the purposes of evaluating bone implant motion and was developed by Liu *et al.*, 2003. The design was based on the Durham hip joint simulator Mk III but was extended to contain the proximal section of a composite femur (Figure 2-15). The simulator synchronises the flexion extension movement of the femoral component with internal external rotation of the cup (pelvis) whilst dynamically loading the implant and composite femur. The flexion extension rotation was modelled as a sine wave, between 15° extension at toe off and 30° flexion at heel strike, this motion is characterised by a frequency of 1 Hz to represent walking pace. The internal and external rotation was similarly modelled with a sine wave between -5° and 5° in the transverse plane. Abduction and adduction were not included. The loads were applied to a peak of 2500N, which is about 3.5 times body weight, at an average 75Kg body mass, with a load profile taken from research by Crowninshield *et al.*, 1978. The aim of the simulator was to measure migration of a cemented hip stem and compare this to previous studies to assess the effect of the kinematics. The migration was measured using a similar device to Maher *et al.*, 2001, described earlier in this report. The results produce a complex migration pattern, which is claimed to be similar to that found in clinical data, no information was recorded with regards to micromotion.

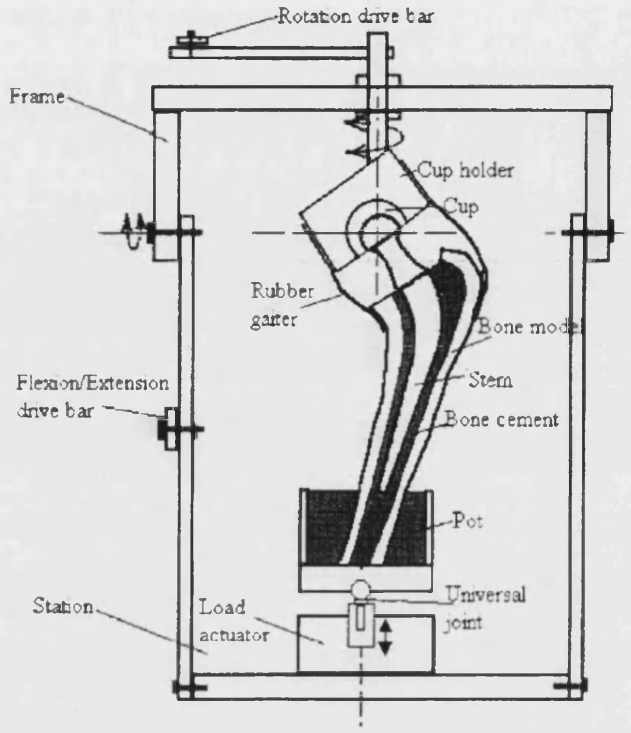

Figure 2-15 -Schematic drawing of Dynamic hip joint simulator
(Liu *et al.*, 2003)

2.6. *Discussion of current testing methods*

The medical device industry is heavily regulated. Each stemmed implant introduced into the market is required to exceed minimal levels of performance set out in National, European and International standards. It is the aim of the standards to ensure that implants are safe for implantation. Implant safety is assessed with a series of specific tests; however, additional tests are often performed by Orthopaedic companies. These, although relevant, might not be formalised in the standards or required by the regulators. Researchers agree that the longevity of cementless hip stems relies on immediate postoperative stability; currently there is no legislative requirement to assess stability of hip implants. A review of the literature revealed that the most popular technique of analysing bone implant motion involves the use of six LVDTs in the configuration first suggested by Berzins. Several research groups include muscles forces in their test setup to build a more accurate model of the hip. However, there are still limitations with the testing methods proposed in the literature. These will need to be fully researched and understood if this technique is to become a recognised standard test.

One of the largest challenges with a bone implant motion study is associated to the choice of the material used to represent the properties of bone. Cadaveric studies are widely used as, in this case the material properties are assumed to be very similar to those of living bone. However, the sources for cadaveric material are rare and require ethical approval and careful safety consideration, making handling and working with the material expensive and time consuming. This usually results in studies with small numbers of specimen samples. In addition, the quality of the bone can widely vary from cadaver to cadaver. This, coupled with small sample groups makes comparison between and within a group difficult and often undermines the power of the study. To avoid these problems, composite femora are often used as the next best alternative. These femoral models are made from a combination of epoxy glass resin and expanded foam to represent cortical and cancellous bone respectively. They are free from ethical consideration and can contribute to the limitation of the experimental scatter associated with cadaveric samples (Britton *et al.*, 2003). The overall properties of these bones, such as stiffness and elasticity, have been validated against those of cadavers (Cristofolini *et al.*, 1996) but their suitability for use in bone implant motion is yet to be established. Until a validation study can show that hip stems exhibit similar behaviour in composite femora and cadaveric femora this will remain a limitation of the technique.

With one exception, none of the bone implant motion studies include the effect of femoral kinematics on hip stem stability. All the tests, apart from the dynamic simulator described by Liu, hold the femora static in various positions, e.g. stair climbing or walking, whilst physiological loads are applied. The dynamic simulator by Liu was built to analyse cemented hip stems and measure the migration of the hip rather than its micromotion. None of the groups involved with stability of cementless implants have investigated the effect of dynamics on micromotion and migration in order to represent a more physiological model of human gait. With the inclusion of femoral kinematics, the direction of the loads on the femoral head will vary, this is likely to affect the relative movement between stem and femur. Increased amplitudes of relative motion could be generated as a consequence of the dynamic load applied. Should this be proved to be the case it would suggest that the current test setups are not adequate to assess stability of hip stems. Dynamic tests are inherently more complex than static ones, this affects the cost associated with such a test. The

question of how implant stability is affected by the dynamics of the joint needs to be answered prior to the development of a standard benchmark test of stability.

Pre-clinical tests attempt to model the loading conditions that cause the relative movement between stem and bone in order to gain an understanding of the *in vivo* behaviour of the stem. It is important that loads applied *in vitro* are as close to physiological patterns and magnitudes as possible. The hip is loaded in a very complex manner with 20 muscles spanning the joint (Pedersen *et al.*, 1997). These are activated at different times during the gait cycle to achieve motion (Heller *et al.*, 2001). However in many bone implant motion studies the muscles have been ignored; instead a resultant force is applied purely to the femoral head. This results in large bending moments being applied to the stem due to the offset of the stem and the lack of counteracting action of the ilio-tibial band. This arrangement has been used to assess critical failure loading but its suitability has been questioned (Heller *et al.*, 2005). Loading of the hip and the role played by different groups has been researched using Electromyography (EMG) in conjunction with numerical analysis. This type of research has shown that some muscles are more influential than others (Kassi *et al.*, 2005). The muscle group with the largest effect on the femoral head in normal walking is the abductor (Kassi *et al.*, 2005), this muscle group had been modelled by some investigators(Britton *et al.*, 2003; Burke *et al.*, 1991; Callaghan *et al.*, 1992; Clements *et al.*, 2005). In these studies a strap attached to the lateral side of the femur has been used in conjunction with a loading arm to effectively create a lever, thus applying the force to the femoral head in a direction and pattern similar to that experienced *in vivo*. Britton *et al.*, 2003, showed that the inclusion of this muscle group reduced experimental scatter. In a recent study (Kassi *et al.*, 2005), ropes with tensioners controlled by servo electric motors via pulleys have been used to represent the four main muscle groups acting on the hip, the abductors, tensor facia latae, vastus lateralis and vastus medialis (Figure 2-16).

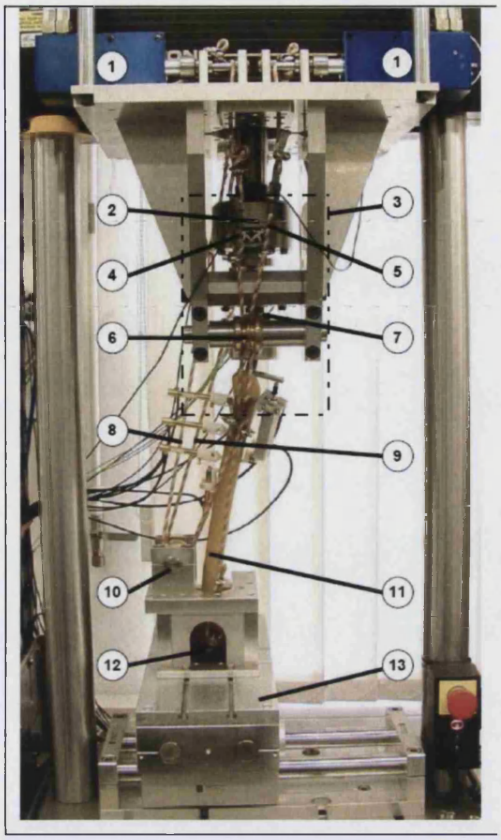

Numbers of note:-
1) Muscle Acuators
4) Loading rope – Tensor fascia latae
5) Loading rope – Abductors
6) Pulleys to adjust muscle action
8) Loading rope – Vastus Lateralis
7) 3D Load cell for hip contact force
9) Loading rope – Vastus medialis

Figure 2-16 - Experimental rig modelling four muscle groups (Kassi et al., 2005)

Most studies conclude that muscle loading has a significant effect on the stability of hip stems, therefore the main muscle groups acting on the hip should be included in a pre-clinical test (Britton *et al.*, 2003; Cristofolini *et al.*, 1995; Kassi *et al.*, 2005; Heller *et al.*, 2005). The inclusion of muscles does increase the complexity of the test and therefore cost but with good understanding of the loading, strategic muscles can be represented to achieve a reasonable physiological model.

2.7. *Conclusions of literature review*

Immediate postoperative stability has been established as a key factor in the longevity of cementless stems. Stability is a result of the geometry of the stem and the surgical technique. A review of the studies analysing bone implant motion has been presented. The use of six degrees of freedom motion transducers has been shown to give insights for a full understanding of implant stability *in vitro*. It has been shown that muscle forces should be included in the laboratory model to produce physiological conditions of the hip.

It is evident that there is limited knowledge of the contribution of femoral kinematics when combined with loading on hip stem stability. With one exception, bone implant motion studies are performed quasi-statically. Therefore the development of a simulator to apply the dynamic loads generated during the gait cycle to a stem/bone construct could add important knowledge for the development of a standard bench mark test for implant stability.

In addition, although the use of composite femora is wide spread, there is a need for a validation study to directly compare the stability of hip stems in a composite model to a freshly implanted hip stem in a cadaveric host. This research is vital to validate the femoral model that will be used to assess the inclusion of femoral kinematics in hip stem stability testing.

Chapter 3. Biomechanics of the Hip

3.1. *Introduction*

The goal of a pre-clinical test is to evaluate factors that contribute to the eventual failure of the system. In THR, several failure mechanisms and related tests have been identified and investigated in the previous chapters. The most common cause of failure of THR is aseptic loosening caused by instability of the hip stem. A series of tests known as bone implant motion tests are currently used to evaluate stability of hip stems, however, there is no current standard for this test. The tests aim to recreate the *in vivo* mechanical conditions of the hip however only one bone implant study has investigated the effect of the kinematics of the femur. The influence of femoral kinematics on hip stem stability is not fully understood and therefore needs to be investigated before a comprehensive standard can be specified. To investigate the effect of femoral kinematics on bone implant motion it is important to understand the mechanical environment of the hip including the forces and muscle actions during a gait cycle.

This chapter outlines the current knowledge of the mechanical environment of the hip including daily living cycles and hip loading during various activities. The research investigating femoral kinematics and muscle action during normal gait is presented to form the basis for the design of a dynamic hip joint simulator for evaluating bone implant motion.

3.2. *Gait cycle and daily living*

The primary goals of total hip replacement are pain relief and restoration of function of the joint. This means that a successful total hip replacement will ideally restore, to the maximum possible extent, 'normal' gait.

In order to develop a simulator to reproduce expected motion of the hip, it is important to understand the biomechanical function of the joint during the gait cycle alongside expected levels of motion during everyday living.

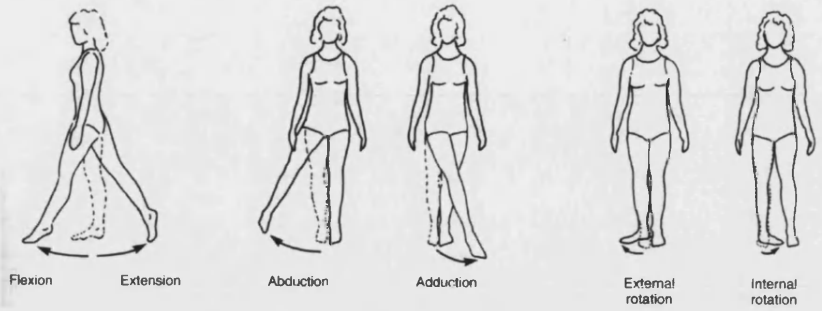

Figure 3-1 – Descriptors of hip motion (Nordin and Frankel, 1980)

In a normal healthy hip rotation occurs in all three planes: sagittal (flexion extension) coronal (abduction adduction) and transverse (internal external rotation) as shown in Figure 3-1. The total ranges of these rotations and their limitations over age (even without disease) are shown in Table 3-1. Diseases of the joint limit the range of motion. The purpose of a THR is to restore flexibility as closely as possible to the normal values shown in Table 3-1 in order to restore the normal function during gait.

Motion	**Direction**	**Age Group (yr)**		
		25-39	40-59	60-74
Sagittal	Flexion	122° ± 14°	120° ± 14°	118° ± 13°
	Extension	22° ± 8°	18° ± 7°	17° ± 8°
Coronal	Abduction	44° ± 11°	42° ± 11°	39° ± 12°
Transverse	External	33° ± 7°	31° ± 8°	30° ± 7°
	Internal	34° ± 8°	32° ± 8°	29° ± 9°

Table 3-1 – Range of normal hip motion (Roach and Miles, 1991)

Gait is defined as the *"pattern of locomotion"* the study of which has involved many research groups. The effect of different variables (including age, sex, height and skeletal deformities) on the patterns of movement in the lower limbs has been widely investigated.

Figure 3-2 shows images of the lower body through a full gait cycle combined with a schematic diagram showing the stages of the gait cycle. By convention, the description of the gait cycle begins at the heel strike with the following stages of stance, double stance and swing described as a percentage of the cycle up to the next heel strike. The main four phases of gait can be further

broken down into 8 stages (Perry, 1992) which are described later in this chapter together with the function of muscles at specific times during the cycle.

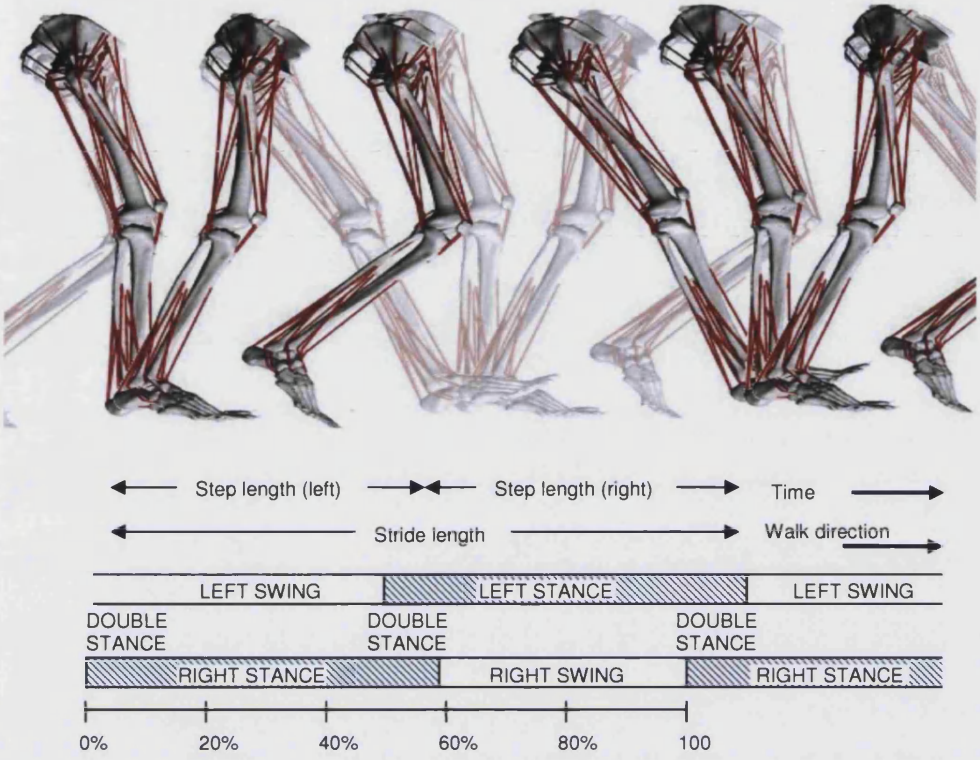

Figure 3-2 A schematic diagram illustrating typical gait pattern combined with images of the leg through the gait (left leg faded for clarity) (Heller et al., 2001)

To develop a physiological hip simulator including the femoral kinematics, it is critical to understand the levels of motion in all three planes of the hip joint so that suitable parameters can be included in the design specification. One of the first researchers to publish data about gait patterns in adult humans was Murray, 1967, who took measurements of the femur in the sagittal plane and showed that the femur was maximally flexed during the late swing phase of gait i.e. as the limb moved forward for heel strike, and maximal extension was reached at toe off. This information is useful for some boundary levels for modelling gait with simple sine waves but provides no data in the coronal and sagittal planes. More comprehensive studies have used electromagnetic goniometers to measure joint angles in all three planes during gait. The findings of Elftman (1966), Murray (1967), Johnston and Smidt (1969), Smidt and Heller *et al.*, (2001) have been summarised in Figure 3-3 to 3-5. This data will provide the basis for the specification of the gait cycle of the hip simulator. It is important to

notice that all these studies evaluated 'normal' gait with the exception of Heller who investigated postoperative gait after a THR.

In the sagittal plane there is general agreement on the angle of the femur over the course of a stride between the included studies (Figure 3-3). The maximum flexion occurs just prior to heel strike and the angle of flexion reported by these authors varies between 32° and 25° for normal gait but is reduced to 22° flexion for postoperative gait in the study of Heller *et al.* The other extreme of motion occurs at toe off, extension ranges from -9° to -12°; the postoperative gait is within this range at -10°. The set of data displayed in Figure 3-3 can be reasonably simplified to a sine wave, ranging from 32° flexion to -10° extension, to provide a basis for the hip simulator specification. This is shown as a red dashed line in Figure 3-3.

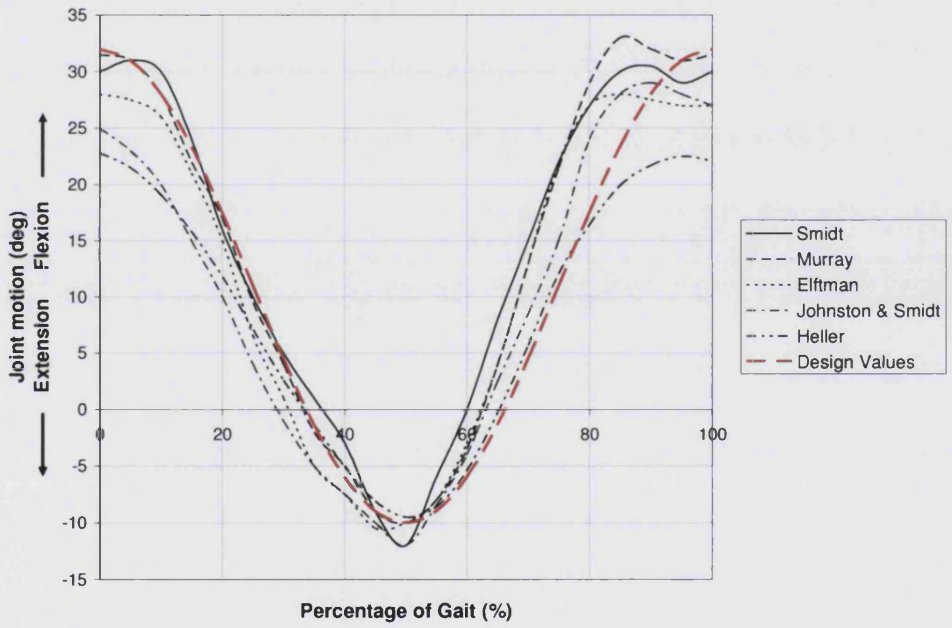

Figure 3-3 Hip range of motion in sagittal plane

Less information is available in the coronal plane (Figure 3-4), in addition this is characterised by less agreement between the different studies than in the sagittal plane. However, general patterns can be detected; during the stance or loading phase of gait (the first 60% of the cycle), The maximum adduction of the femur varies between -2° and -4° as the pelvis moves over it to achieve stability. During the swing phase the femur moves into abduction (between 6° and 8°) as the leg swings around the contralateral leg to begin the cycle again. In the postoperative data set the angle of adduction is reduced to -1° but the abduction

level is similar to normal at 6°. It was felt best to model the largest range of motion in the coronal plane as this would represent the most severe working conditions for the implant and therefore result in a 'worst case' scenario for the assessment of hip stem stability. Thus, the coronal range of motion was approximated to a sine wave ranging between -4° adduction and 8° abduction (red dashed line Figure 3-4).

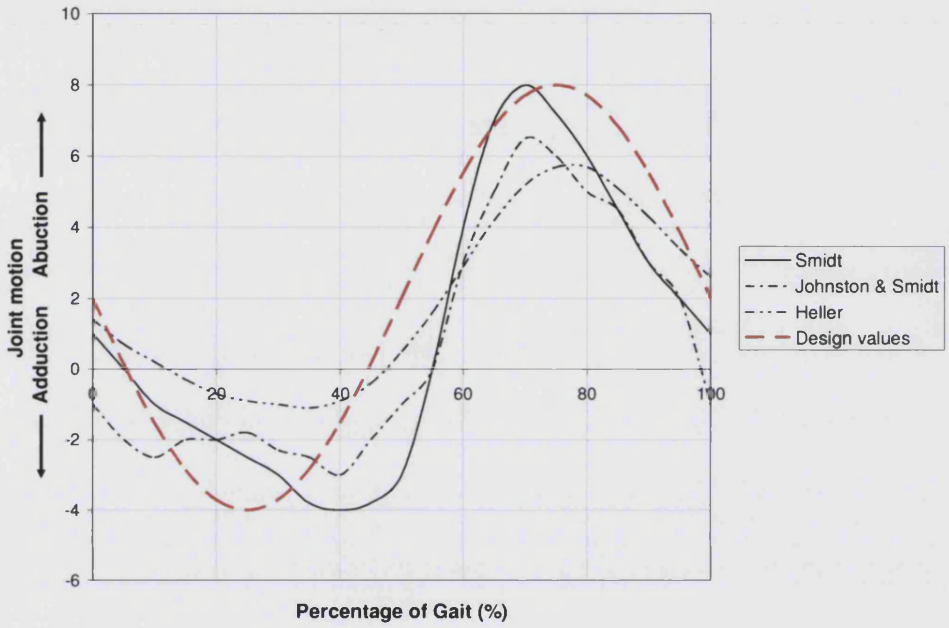

Figure 3-4 – Hip range of motion in coronal plane

In the transverse plane at heel strike the femur is characterised by internal rotation rising up to levels of 4° during mid stance. During the swing phase the femur is externally rotated up to levels of - 6° during the mid swing phase (Figure 3-5). A worst case approach was adopted similarly to that which ha been modelled for the coronal plane. This resulted in the transverse motion being modelled by a sine wave oscillating between 4° and -6° (red dashed line Figure 3-5).

It is important to notice that the sine wave that will represent the transverse plane movement of the femur in the simulator even though this deviates significantly from the pattern of gait obtained by Heller for postoperative gait.

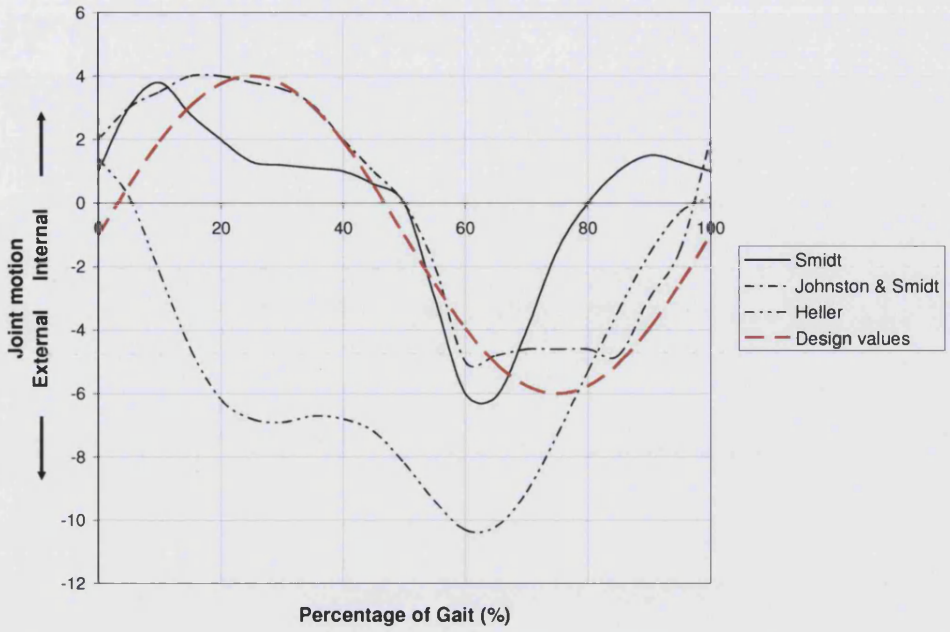

Figure 3-5 - Hip motion in the transverse plane

All the data shown in Figure 3-3 to Figure 3-5 are representative of a medium paced gait but it should be noted that speed is a large factor in gait patterns. At a normal walking pace of about 5/6 km/h the foot will spend around 60% of the total gait cycle in load bearing. As walking speed increases the time of load bearing decreases and more time is spent in the swing phase (Nordin and Frankel, 1980). Age also has an effect on gait patterns.

A second study by (Murray *et al.,* 1969), based on a group of 67 men between the ages of 20 and 87 demonstrated that older men had decreased hip flexion and hence, shorter strides with decreased flexion of the ankle.

In their study Heller *et al.,* (2001) used high-speed cameras to film patients to evaluate gait with several strategically placed markers. Image analysis software was then used to calculate the relative positions of the markers at any point in time thus inferring the position and speed of various body segments during gait. A summary of this information is presented in Figure 3-6 and Figure 3-7, which show the gait patterns seen from orthogonal views for walking and stair climbing. The coronal and transverse plane views show the abduction and adduction that occur during the gait.

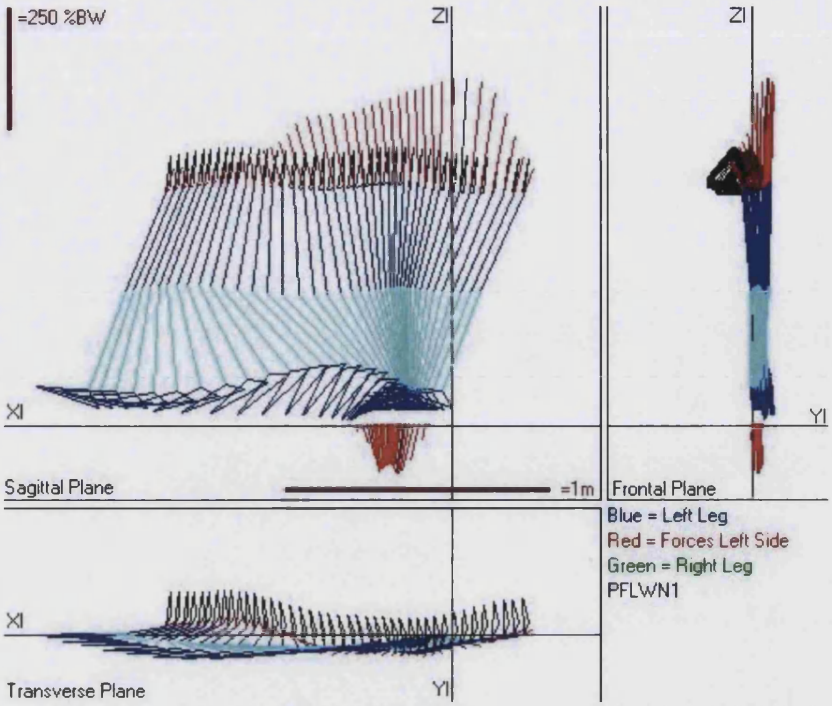

Figure 3-6 - Gait pattern during normal walking (Heller et al., 2001)

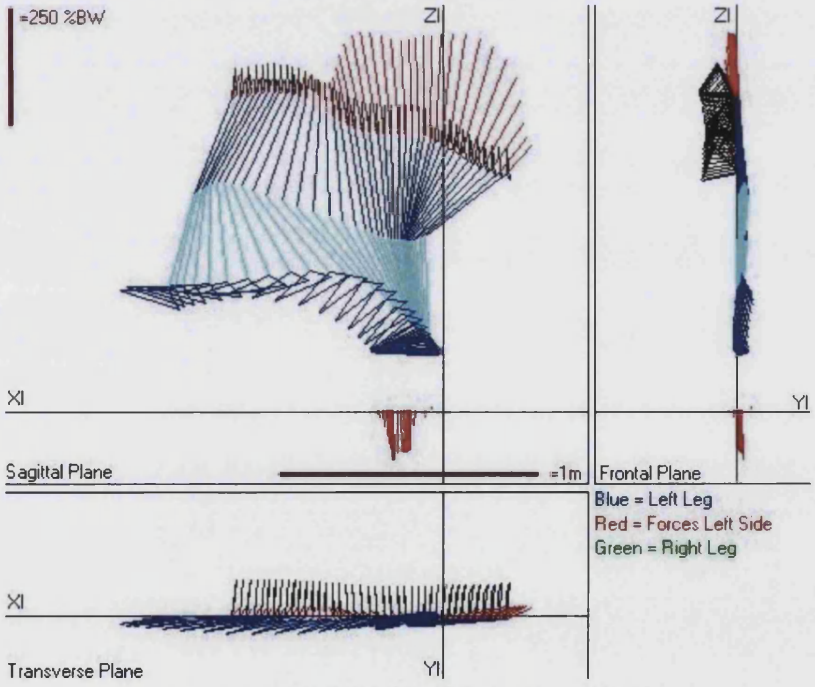

Figure 3-7-Gait pattern during stair climbing (Heller et al., 2001)

3.3. *Hip contact forces*

Musculo-skeletal loading plays an important role in the primary stability of joint replacements (Heller *et al.*, 2001). The forces loading the hip are a combination of ground reaction forces and the action of the muscles aiming to stabilise the joint while providing locomotion.

Many investigators have contributed to this field of research and the studies can be divided into two separate catagories, external measurement using force plates and internal *in vivo* measurements using instrumented hip stems. In the force plate method the body is treated as a series of rigid links each described by equilibrium equations for moments and forces. The ground reaction force can be measured experimentally and hence the reaction at each joint can be calculated through the gait cycle using equilibrium considerations. This approach was first adopted by Paul (1966) and resulted in the force on the hip being described by a double peak curve (Figure 3-8), also known as the Paul cycle.

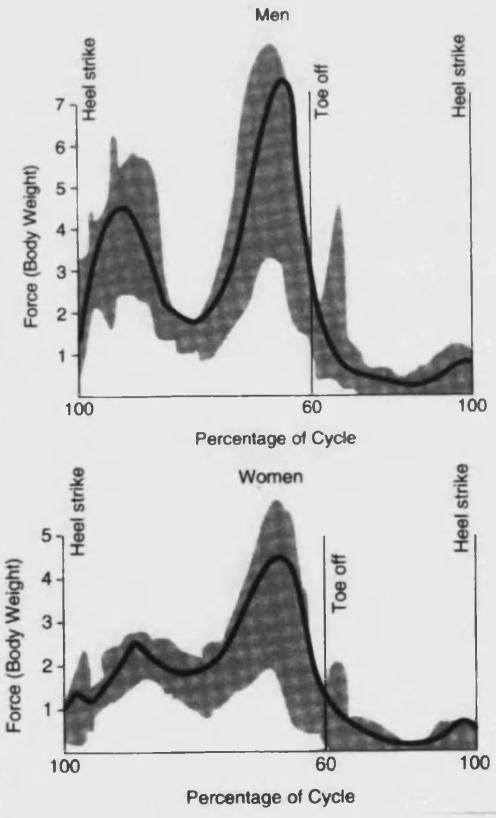

Figure 3-8 - Typical gait pattern showing double pattern in men and women (Paul, 1966)

Paul was able to correlate the peaks to specific muscle activity which was recorded electromyographically by electrodes attached to the skin. In men, two peak forces were produced during the stance phase when the abductors contracted to stabilise the pelvis. The first maximum (4 x bodyweight (BW)) occurred after heel strike and the second (7 x BW) just before toe off. In women, the pattern was similar but the second maximum was lower, only reaching (4 x BW). This could be explained by either a wider pelvis, a difference in neck to shaft angle of the femur or a different pattern of gait.

A number of studies similar to that of Paul have been summarised in Table 3-2. While there is general agreement on the overall shape of the curve there are some discrepancies on the relative magnitudes of the two peaks.

Author and Speed	Joint Contact Force	
	1st Max (xBW)	2nd Max (xBW)
(Paul, 1966)	4.9	7
(McLeish and Charnley , 1970)	2-3	
(Crowninshield *et al.*, 1978a)		
0.28 m/s Old Person	3.31 ± 1.18	n/a
0.83 m/s Old Person	3.81 ± 1.18	
1.39 m/s Old Person	4.42 ± 1.18	
0.28 m/s Young Person	3.44 ± 1.4	
0.83 m/s Young Person	4.29 ± 1.34	
1.39 m/s Young Person	5.85 ± 1.51	
(Crowninshield *et al.*, 1978b)		
0.94 m/s	3.6	1.9
3.83 m/s	5.62	2.92
(Rohrle *et al.*, 1984)		
0.69 m/s	2.6 ± 1.65	3.6 ± 1.65
1.25 m/s	4.4 ± 1.65	5.55 ± 1.65
1.75 m/s	6.20 ± 1.65	7.55 ± 1.65

Table 3-2- Data showing magnitudes of 1st and 2nd Peaks in gait cycle for force plate studies

Crowninshield *et al.* (1978b) clearly shows a higher first peak at heel strike whilst, Rohrle *et al.* (1984) shows higher forces at toe off. At low walking pace there is a general agreement between the authors with a force of about 2 -3.5 times body weight which correlates with the early study by Mcleish and Charnley, 1970. The maximum force is also shown to increase with the speed

of the patient (Crowninshield *et al.*, 1978a; Crowninshield *et al.*, 1978b; Rohrle *et al.*, 1984).

A method to assess joint forces *in vivo* was popularised by Bergman (1993) and has been further developed by a number of other researchers. This involves the use of instrumented implants to directly assess the load on the hip joint (Bergmann *et al.*, 2001; Kotzar *et al.*, 1991; English and Kilvington, 1979; Rydell, 1966). The most comprehensive of these studies is that of the group led by Bergman. Their findings have been widely published (Bergmann *et al.*, 2001; Heller *et al.*, 2001; Morlock *et al.*, 2001) and have been summarised in a CD-Rom (Hip 98). An instrumented femoral prosthesis with a telemetric data transmission system was implanted into four patients enabling measurement of *in vivo* hip contact forces. These data were combined with gait analysis data (Heller *et al.*, 2001), muscle activity data, monitoring of daily living activities (Morlock *et al.*, 2001) and CT scans to build the sophisticated musculo-skeletal model of the lower extremity shown in Figure 3-9. This model was used to calculate muscle and joint contact forces using an optimisation algorithm.

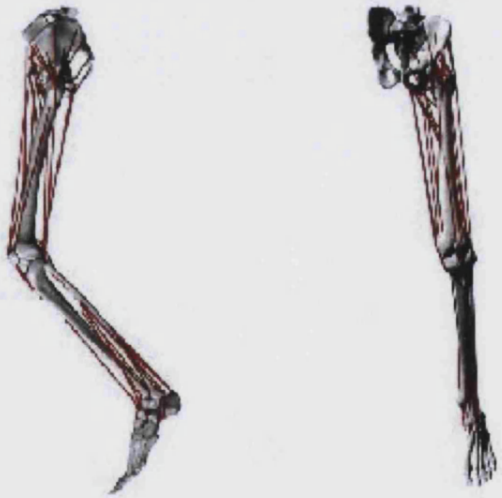

Figure 3-9 - Musculo-skeletal model of the lower extremity during walking (Bergmann et al., 2001)

Measurements were performed on patients during the most frequent activities of daily living including fast and slow walking, climbing and descending stairs. The results for normal walking showed a maximum hip force of about 2.6 times body weight but the second peak predicted from the force plate studies was not always present or was characterised by reduced magnitude (Figure 3-10). This

is not always in agreement with research using instrumented implants carried out by other groups, a summary of which is presented in Table 3-3. The reason that these force patterns differ from those measured by the force plate studies is probably due to the hip stem altering the force distribution and gait leading Bergmann to conclude that the second peak is not always present in a patient who has previously undergone a hip replacement.

This poses the question of whether a pre-clinical test should model the forces that an implant is likely to experience or the force experienced if 'normal' gait has been restored.

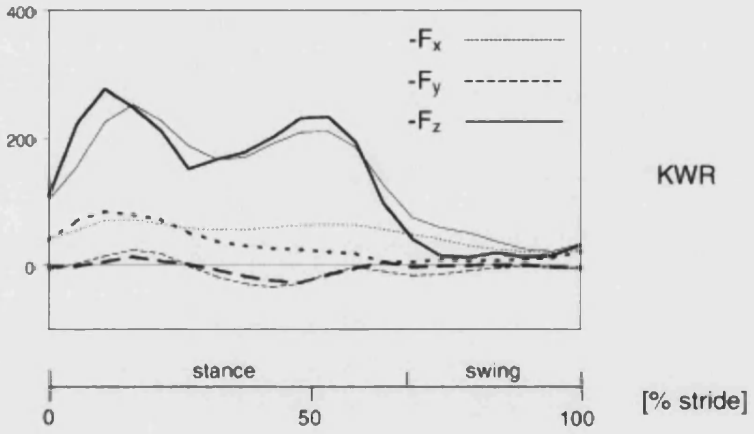

Figure 3-10 - Forces profile during a slow walking gait cycle (Bergmann et al., 2001)

Author	Joint Contact Force	
	1st Max (xBW)	2nd Max (xBW)
(Rydell, 1966)	1.8	3.3
(English and Kilvington, 1979)	2.7	
(Kotzar *et al.*, 1991)	2.7	3.6
(Bergmann *et al.*, 2001)	2.7	

Table 3-3 - Data showing magnitudes of 1st and 2nd Peaks in gait cycle measured by instrumented implants

3.4. *Muscles active in the gait cycle*

An understanding of the influence of muscles on the pattern of forces experienced on the hip is vital for the design of a pre-clinical tests of implant stability.

There are many muscles acting at the hip with varying roles and strengths. These can be grouped as; - hips flexors, extensors, abductors, adductors and rotators (Hay and Reid, 1988).

Hip flexion is primarily controlled by the *iliopsoas*, which originates from the lumbar vertebrae and upper iliac fossa and inserts at the lesser trochanter. This muscle has also been shown by electromyographical methods to be active at irregular intervals during erect standing (Hay and Reid, 1988). Hip extension is mainly controlled by the large quadrilateral shaped *gluteus maximus*. This powerful muscle is mainly active during running and stair climbing. The major hip abductors of the hip joint are the *gluteus medius* and *gluteus minimus.* These muscles do the majority of work during single leg stance effectively balancing the body weight. Hip adduction is controlled by the group of muscles including the *gracilis, pectineus, adductor magnus* and *adductor longus.* They are generally long and slender inserting into the medial posterior surface of the femur.

Muscle action during the gait cycle has been described in detail and separated into eight stages (Perry, 1992)

1. *Initial contact* – the gait cycle is defined as beginning at the initial contact of the heel with the ground (heel strike). The thigh is forward with the femur in hip flexion of about 30°. At the moment of contact the hip is in an unstable position

2. *Loading response* – the sagittal and coronal positions are maintained and hip extensor muscles restrain flexor momentum. The hamstrings and gluteus maximus are active. In the coronal plane rapid transfer of body weight onto the loading limb demands active stabilisation of the pelvis over the hip which is achieved through the abductor muscles.

3. *Mid stance* – the hip is progressively extended toward 0° flexion as the limb rotates and the pelvis moves directly over the femur. The abductor muscles have returned the pelvis to a neutral alignment in the coronal plane so the gluteal muscles relax and the tensor fascia lata takes over

4. *Terminal stance* – the body weight rolls over the fore foot rocker and puts the thigh into a trailing position. The anterior fascia lata responds to restrain the rate of extension and provides the partial abduction force for stabilisation. Here the body's centre of gravity is at its most lateral point and it begins to retreat toward the midline causing a passive abduction force

5. *Pre-Swing* – the ankle begins to advance to the tibia which starts to carry the thigh forward. The rectus femoris assists with hip flexion which begin to accelerate the femur into the swing phase

6. *Initial Swing* – as the limb unloads motion of the femur becomes rapid. Two muscles that display activity here are the gracilis and satorius providing adduction, internal rotation and flexion. The three dimensional path of the femur could represent the fine balance of these muscles.

7. *Mid Swing* – momentum continues the motion of the femur and the hip flexor muscles remain passive.

8. *Terminal Swing* – finally the motion of the femur is stopped by the hamstring muscles. The gluteus medius counteracts the earlier adducting muscles and leaves the femur optimally positioned for initial contact when the cycle begins all over again.

Figure 3-11 shows the levels of the individual muscle actions during one gait cycle:-

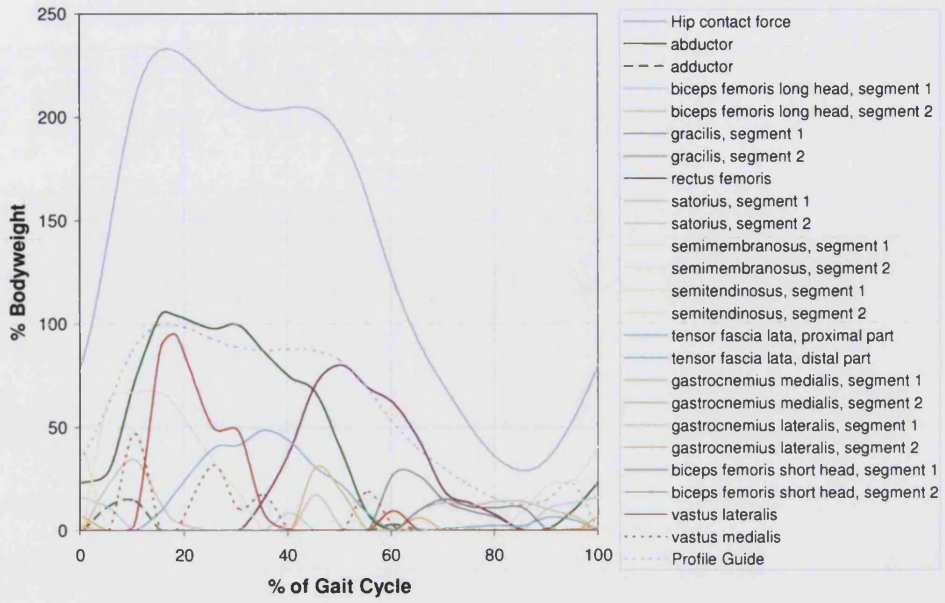

Figure 3-11- Levels of muscle activity during one gait cycle (Heller et al., 2001)

3.5. *Conclusion*

Information from this chapter will be extremely important for the development of a physiological hip simulator and the following observations will be used as criteria for making decisions about the inclusion of certain parameters.

The motion of the femur can be described in three distinct planes sagittal, coronal and transverse. The predominant motion during a normal gait is in the sagittal plane with levels of motion from 30° flexion to about 10° extension followed by motion in the coronal plane, varies from 8° abduction to 4° adduction. The lowest levels of motion are in the transverse plane, from 6° external to 4° internal rotation.

Loading of the hip is predominantly vertical and medium paced walking produces a femoral head contact force of approximately 2-3 times bodyweight. The shape of this force pattern can be described by a double peak curve and HIP 98 provides an excellent source of data to be used as a loading profile. Loads from anterior to posterior and medial to lateral are lower than those

experienced vertically, however their inclusion would provide a more realistic simulation of the functional loads of the hip.

Muscle loading of the hip has been shown to have an effect on hip stem testing however the inclusion of muscles can be complex. The muscle group with the highest level of loading has been shown to be that of the abductors. These should be included in the rig if possible.

Chapter 4. Aims and Objectives

Pre-clinical testing of hip stems is a critical area to ensure that implants are safe for use and to screen out inferior designs before implantation in a patient. Currently there is no standard protocol for the evaluation of bone implant motion and there is a need for further research in the area before a standard can be comprehensively specified.

The aim of this thesis is to investigate the influence of femoral kinematics on hip stem stability with a view to supplying important information to be incorporated in a standard protocol for the pre-clinical test of hip stem stability.

To achieve the stated aim there are a series of objectives that are necessary to validate test materials and instrumentation techniques in addition to the manufacture of test rigs. The key tasks will be described by the following chapters and are specified below.

Objectives

1. Validation of the use of Sawbones composite femora - Many research groups use composite femora, however their use for hip stem stability studies is yet to be validated. This validation will be performed by a comparative test with cadaveric material.
2. Comparison of long and short term stem stability - Clinical data suggests that the initial stability of cementless hip stems is vital for long-term survival. The bone-implant motion will be measured in long-term surviving implants and compared to freshly implanted femora in cadaveric materials.
3. Design and development of a dynamic hip joint simulator capable of replicating the kinematics and loading of the femoral head for the assessment of bone-implant motion.
4. Investigation of the inclusion of femoral kinematics in a bone-implant motion test and their effect on hip stem stability.

Chapter 5. Cadaveric Studies

5.1. *Introduction*

Immediate postoperative stability of cementless hip stems is one of the key factors for the long-term success of total hip replacement (Draughan and An, 2003). Good initial stability promotes early osseointegration between the implant and the host bone, leading to a better fixation over time. The ability to discriminate between stable and unstable stems in the laboratory constitutes a desirable tool for the orthopaedic industry, as it would allow the identification of unsuitable stem designs prior to clinical trials.

As already highlighted in Chapter 2, much of the research in this field has been performed using composite femora. The first step towards the development of a standard technique to assess implant stability requires the validation of the bone model adopted. This was carried out by comparing the stability of the same stem design, the Zweymüller type stem, in cadaveric and composite femora (objective 1). In addition, the clinical observation that, in cementless stems, initial stability is paramount for long term survival was tested by comparing migration and micromotion of freshly implanted and long living stems in cadaveric femora (objective 2).

This validation work is presented in the following pages as two individual case studies. Both cases were subject to the same experimental protocol, developed and validated at the Centre for Orthopaedic Biomechanics (Clements *et al.*, 2005) and described in the next few sections.

Stem stability was assessed in terms of micromotion and migration. Micromotion was defined as the recoverable movement of the implant relative to the bone under cyclic loading, a function of the elasticity of the bone-implant construct. Migration was defined as the non-recoverable movement of the implant with respect to the surrounding bone, and reflects the micro-damage caused by the implant to the material in its immediate surroundings. A graphical representation of these motions is shown in Figure 5-1.

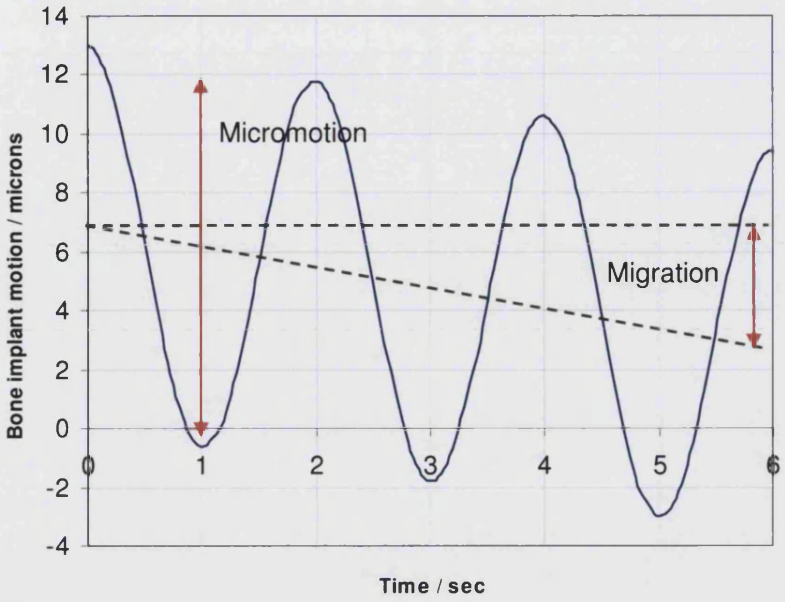

Figure 5-1 - Definition of micromotion and migration

5.2. *The Zweymüller Implant*

The Zweymüller hip stem is a cementless and collarless implant and is made from Titanium-aluminium-niobium alloy (Ti-6Al-7Nb). The design relies on a diaphyseal press fit for initial stability and has a grit-blasted surface with a 3-5μm micro-structure to achieve secondary fixation through bone on-growth. The geometry of the stem is a rectangular cross section to provide rotational stability with a double taper distally for axial location. Clinical results of the Zweymüller stem have shown excellent survivorship at 10 years (Pieringer *et al.*, 2003; Delaunay and Kapandji, 2001; Grubl *et al.*, 2002). Stems characterised by the same geometry are the marked by Zimmer (Alloclassic) and Plus Orthopaedics (SL-Plus).

5.3. *Micromotion transducers and coordinate system*

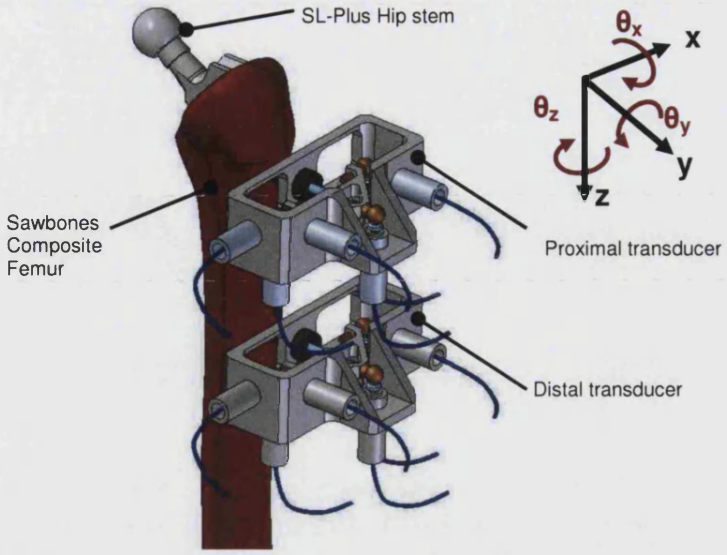

Figure 5-2 - CAD model of the two motion transducers

The displacement transducer is attached to the stem and cortical shell of the femora to measure the relative movements between the implant and cortical bone in six degrees of freedom (Figure 5-2).

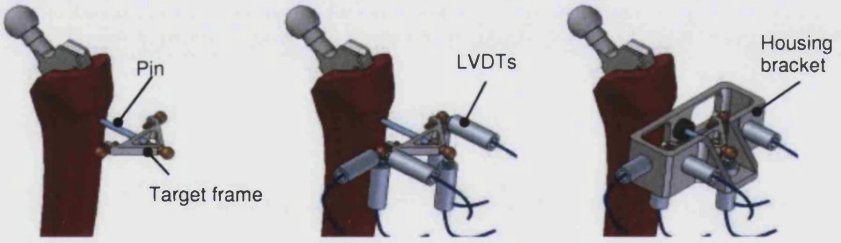

Figure 5-3 - Transducer components

Each transducer is composed of the following parts, Figure 5-3:

1. a pin push-fitted into a hole drilled into the lateral face of the implant and protruding out of the femur via an oversized hole,
2. a target frame, attached to the pin, holding three target spheres,
3. Six linear variable differential transformers, LVDTs, (Marposs, UK, AF050).
4. a housing bracket fixed rigidly to the femur to hold the LVDTs,

Two transducers, one mounted proximally and one mounted distally are used to give comprehensive information on the motion of the implant within the bone. The protocol used for calibration of each LVDT can be found in Appendix III

5.4. *Specimen preparation*

5.4.1. Introduction

The two case studies are based on three sets of specimens, two cadaveric and one composite. The two sets of cadaveric specimens each comprised of six paired femora harvested in Austria and brought to the UK for testing. Each pair consisted of one femur that had received a Zweymüller type stem while the patient was alive (long-term group) and the contra lateral femur that had been implanted with an SL Plus hip stem at post-mortem (freshly implanted group). The sizes of implants used in the freshly implanted group are shown in Table 5-1. Stem sizes were not available for the long living group. The exact age, sex and body mass index of the femoral donors were not known to ensure that the study was blinded. This study was part of a larger body of research on the specimens so the donor details were not available even after testing; the specimen identification numbers are also as labels.

Specimen ID	Stem size (Freshly Implanted group)
81	7
215	12
326	9
413	6
433	8
504	9

Table 5-1- Sizes of implants used in freshly implanted specimens

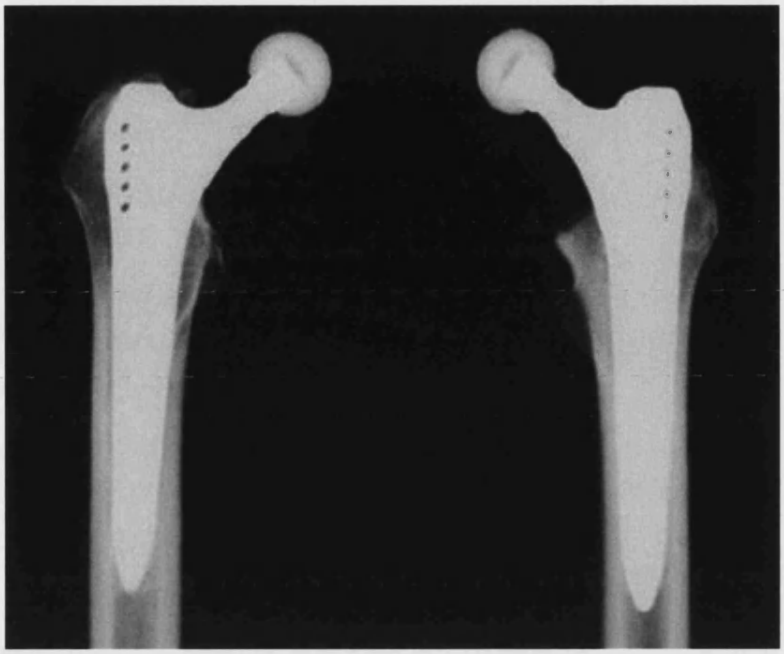

Long term implanted SL Plus Stem Freshly implanted SL Plus stem

Figure 5-4 - X-ray showing the stems implanted in the cadaveric hosts

Figure 5-4 shows X-rays taken of the pair of femora labelled "81" showing the right sided (from the patient's perspective) femur implanted with a long term hip stem and the left sided femur with a freshly implanted SL Plus stem. The stem sizes implanted were the largest that would fit and hence the x-ray shows the stem position very proud in the host bone. Implantation of all hip stems into the cadaveric material was performed by surgeons experienced with the "Zweymüller" hip stem or the very similar SL Plus hip stem.

The initial steps taken to prepare the specimens differ for the two materials used (composite and cadaveric) however the final step, concerning the attachment of the transducers and muscle cables, is identical for both materials. The steps of preparation are;-

1. Implantation of the hip stem
2. Drilling of holes in the stem to attach the motion transducers
3. Drilling of oversized holes in the femur through which the attachment for the transducers will pass
4. Attachment of the abductor strap
5. Mounting and set up of the motion transducers
6. Setting the femur in 'Woods metal' pots

5.4.2. Preparation of Cadaveric femora

The cadaveric femora used in this study arrived at the laboratory frozen in dry ice and were transferred to the freezer for storage. The hip stems were already implanted in the femora and skin and muscle had been removed, however there were still soft tissues attached to the cortical bone. The soft tissue, mainly muscle attachment sites, was removed with scalpels before the femora were returned to the freezer until required for testing. A typical femur before any preparation can be seen in Figure 5-5.

Figure 5-5 - Photograph showing cadaveric femur before preparation for testing

The femora required two holes drilled for the attachment of transducers, one at the proximal end of the hip stem and one distally, 44 mm and 118 mm respectively from the shoulder of the implant. Each hole would require drilling in two stages. The first stage consists of a 2 mm hole being drilled through the cortical bone and into the hip stem itself. This provides a location point for the pin supporting the target frame section of the transducer, see section 5.3. The second stage consists of drilling an 8mm hole coaxially aligned with the original hole but passing only through the cortical bone. This provides access for the pin through the cortical shell and eventually to allow attachment of the outer support bracket to the femur. To ensure that these holes were always in the exact location for each stem a jig was designed. On the freshly implanted stems (SL Plus) the rig was located onto a screw feature on the shoulder of the implant

(Figure 5-6). This is normally used for assistance in implantation. However, not all the hip stems were characterised by the same shoulder geometry as the design of the stems in the freshly implanted specimens had changed marginally from the long term stems implanted up to 20 years previously.

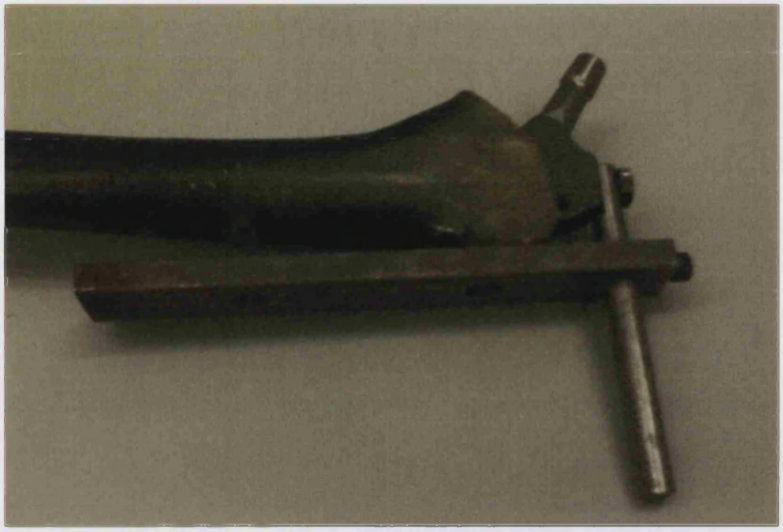

Figure 5-6 - Photograph of the drill jig used to prepare the proximal and distal holes

The screw feature was absent on some of the long term implanted stems so a new jig was developed. On this jig, the head of stem was used as the main location component and screws were used from either side to stop the femur rotating. A pilot hole was drilled near the tip of the stem to confirm alignment and then the same procedure was used to drill the holes. The femora were then returned to the freezer for storage until required for testing.

On the day that the femora were required for testing the specimens were removed from the freezer and allowed to defrost for 2 hours.

5.4.3. Preparation of Composite femora

The composite femora required less specialist handling than the cadaveric femora. However implantation of the SL Plus stem was required. Advice from Plus Orthopaedics suggested using the size seven SL Plus hip stems in the Sawbones femora and all the necessary surgical equipment was supplied. To assist with a reproducible fit a jig was used to make the neck cut. The jig consisted of a mould of the proximal femur with a slot to pass a saw blade through (Figure 5-7). The angle and position of the neck cut were set with advice from Plus Orthopaedics.

Figure 5-7 - Jig used to cut the neck of the Sawbones femora

To minimise the effect of the surgeon's influence on stability, the femora were all implanted with the SL Plus hip stem by an experienced orthopaedic surgeon. An example of an implanted femur can be seen in Figure 5-8. The position of the shoulder of this stem is very high with respect to the greater trochanter of the composite femur; this was intended to mimic the fit of the hip stems in the cadaveric specimens. The greater trochanter is also cut back to allow attachment of the muscle cables.

Figure 5-8 - Sawbones composite femora with SL Plus stem implanted

The SL Plus stems used in the Sawbones were similar in design to the stems freshly implanted in the cadaveric femora, except for the variation in size of implants used in the cadavers. The identical geometry of the stem ensured that the same drill jig could be used to drill the pin holding hole in the hip stem and the access hole in the shell (representing cortical bone) ensuring the location of the transducers would be identical both on either Sawbones or cadaveric models.

5.4.4. Instrumentation and attachment of muscle cable

To achieve a physiological loading profile, an abductor strap was included in the experimental setup. The abductor strap was modelled using a steel cable secured to the femur and extending upwards to a lever arm plate acting as a substitute pelvis. The geometry of the substitute pelvis developed a force of approximately 100% of bodyweight so the attachment of the muscle cable must be secure. Attaching the muscle cables to the femur was difficult with the SL Plus hip stems as the stem is designed to achieve a good lateral fill of the proximal femur. This high degree of fill leaves very little space on the lateral side of the femur so the muscle cables were attached just either side of the hip

stem posteriorly and anteriorly. The holes were drilled from these positions down to just below the proximal hole for the transducer. The path of the holes drilled is shown as a dotted red line in Figure 5-9. The cable selected was a 3 mm high tensile steel wire.

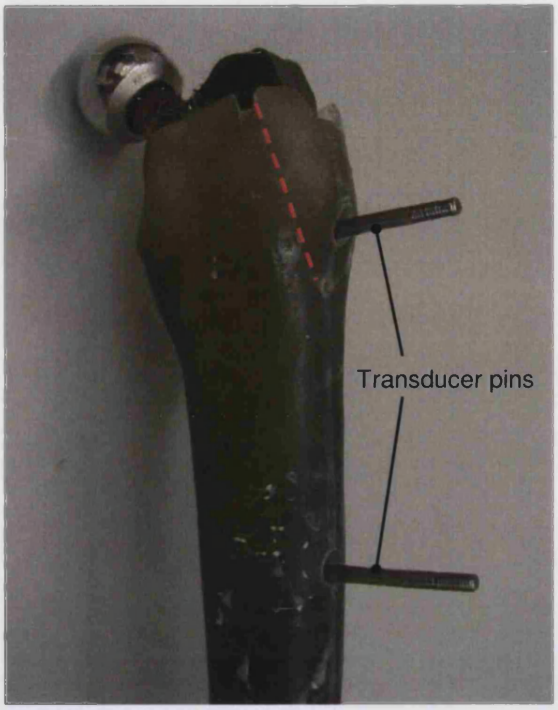

Figure 5-9 - Femur with transducer pins inserted into the proximal and distal holes

The next steps were all concerned with the attachment and alignment of the motion transducers. These start with the insertion of the transducer pins into the hole drilled in the hip stem. The pins were designed as a press fit and were additionally secured to the stem with super glue to prevent rotation. The transducer pins are shown in Figure 5-9.

The motion transducers were then assembled around the two pins. The LVDT frame was mounted over the pins and the target frame attached to the pin via two nuts. The LVDT frames were held in place by another jig designed to mount on the screw feature on the shoulder of the SL Plus implant. This jig held the transducers aligned exactly with the implant and to one another with the balls on the target frame positioned over the screw threads that would eventually hold the LVDTs. With the transducer held rigidly in the correct alignment, then bone cement was prepared and applied around the femur and motion transducers. Other studies have used a device similar to a jubilee clip (Burke *et al.*, 1991) to

support the transducers on the femur, however there is a concern that this may impede motion of the hip stem and affect the stability recorded. Bone cement is capable of moulding to the complex shape of the femur and holding the transducer rigidly to the host bone without affecting the stability of the stem. The jig used to align and hold the transducer while the bone cement was applied can be seen in use in Figure 5-10. Simplex (Stryker) bone cement was used on the Sawbones femora; however more success was achieved with Palacos bone cement (Biomet Merck) on the cadavers. The surface of each composite femur was roughened to improve the 'grip' of the bone cement. The transducer jig could not be attached to the long term cadaveric femora, however it was used to hold the transducers aligned to each other and the alignment with the implant was achieved with clamps.

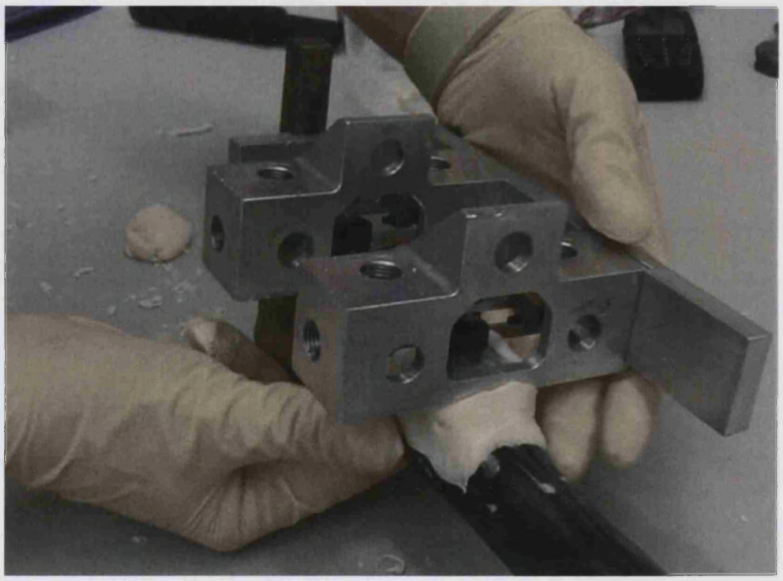

Figure 5-10 - Motion transducers held in the jig with bone cement being applied

The femoral condyles of the specimens were then potted in Woods metal (MCP 75) to hold the femur at the correct angle for the tests. Woods metal was used as it is a low melting point (75°C), lead-based alloy that could be melted and set to hold the specimens rigidly at any angle desired. On the Sawbones femora a hole in the base of the knee could be used to locate on a jig that would ensure a consistent set up angle.

The specimens were then clamped onto the materials testing machine and the muscle loading plate and the LVDTs screwed into the motion transducers. To minimise the risk of any of the transducers reaching the end of their 1mm stroke

the LVDTs were set to their mid position at the beginning of each test. This was determined by adjusting the mounts until the voltage output from the LVDTs was at its mean value.

5.5. *Loading configurations*

The specimens were loaded by an Instron servo-hydraulic materials testing machine (Model No 8511). The load was applied to the head of the implant through a pelvic substitute as shown in Figure 5-11. The pelvic substitute acted as a lever arm with load applied from the Instron at one end of the plate and the abductor strap modelled by a steel cable reacting the applied load at the other end. The geometry of the pelvis substitute and abductor strap induced a load on the femoral head of 2.7 times the force applied by the materials testing machine. The specimen set up on the load testing machine can be seen in Figure 5-12.

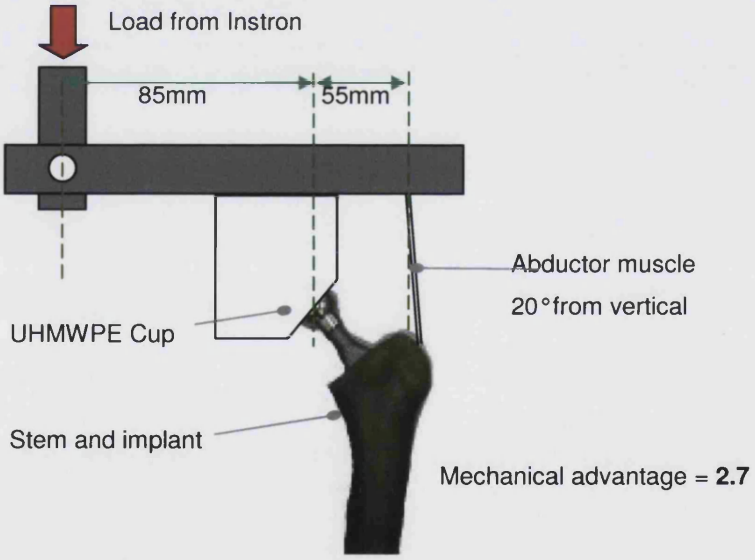

Figure 5-11 – The pelvic substitute and muscle setup for test specimens

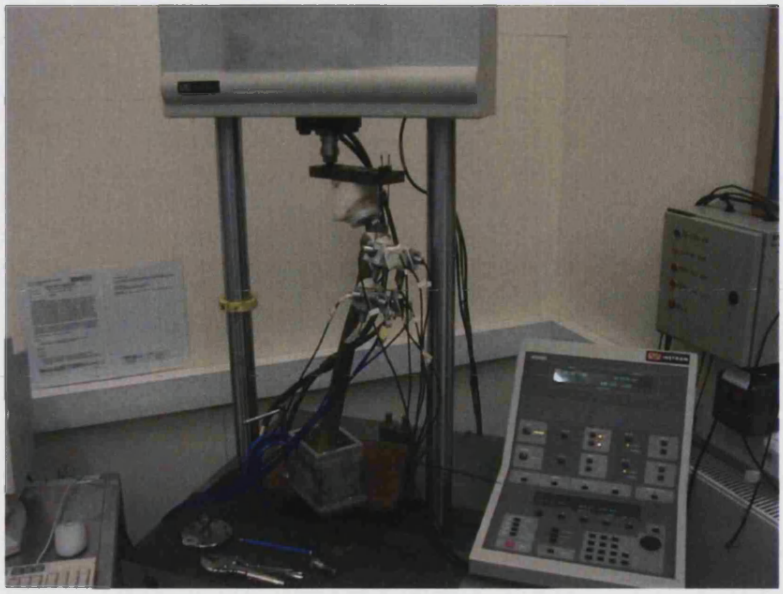

Figure 5-12 -Photograph of specimen and six degree of freedom motion transducers during a SLS experiment

Each femur was tested in two different loading configurations: single leg stance and stair climbing. To simulate single leg stance (SLS) the femur was positioned in 11° of adduction and 7° of flexion (Andriacchi *et al.*, 1980). During stair climbing (SC) the femur was positioned in 11° of adduction and 32° of flexion (Andriacchi *et al.*, 1980). The angle of the femur was changed by melting the woods metal in a water bath then resetting the femur to the desired angle and allowing the alloy to reset.

Preconditioning of the hip stems implanted in the three bone models was not used as the long-term implanted stems will have been loaded *in vivo* and any loads applied to the freshly implanted stems may compromise the comparison. Instead, both sets of specimens were initially loaded at low loads which were later increased as confidence increased that the specimens would not fracture.

The loads were applied from the actuator of the testing machine to the rig as compressive sinusoidal cycles. During single leg stance, each femur was subject to three sets of 200 load cycles oscillating from 0 to 540N, 0 to 810N and 0 to 1080N on the femoral head each separated by resting period of 30s. The load was applied at a frequency of 0.5 Hz to represent a slow walking pace. A graph of the loads applied from the materials testing machine and the load on the femoral head can be seen in Figure 5-13. The grey lines represent the

loads applied to the pelvic substitute from the Instron machine and the green lines represent loads on the femoral head.

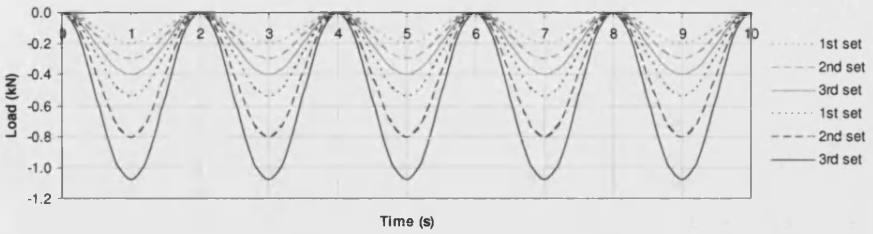

Figure 5-13 - Applied and femoral head loads during single leg stance loading

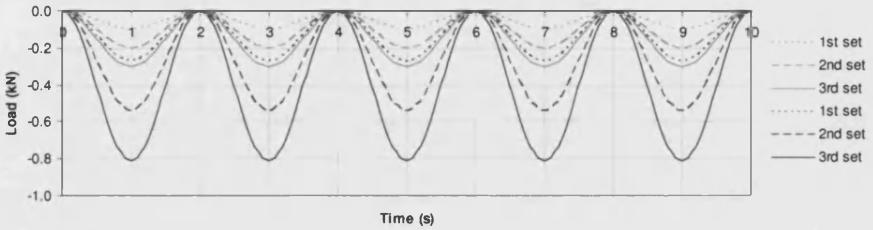

Figure 5-14 - Applied and femoral head loads during stair climbing

In stair climbing the compressive sinusoidal load cycles on the femoral head oscillated between 0 to 270N, 0 to 540N, and 0 to 810N. These loading patterns can be seen in Figure 5-14. In this case the lower loads were used due to the risk of fracturing the bone as a result of the larger torque on the bone caused by the angle of flexion.

5.6. *Data acquisition and processing*

The voltage output from the LVDTs was acquired at a frequency of 50 Hz and stored on a computer. The captured data was post-processed by a MATLAB routine and converted into translations and rotations of the stem with respect to the bone according to the local coordinate system defined in Figure 5-2. A Fast Fourier transform algorithm was used to evaluate the amplitude of micromotion. Migration was evaluated by a second order polynomial fit through the centre point of the oscillations as illustrated in Figure 5-15.

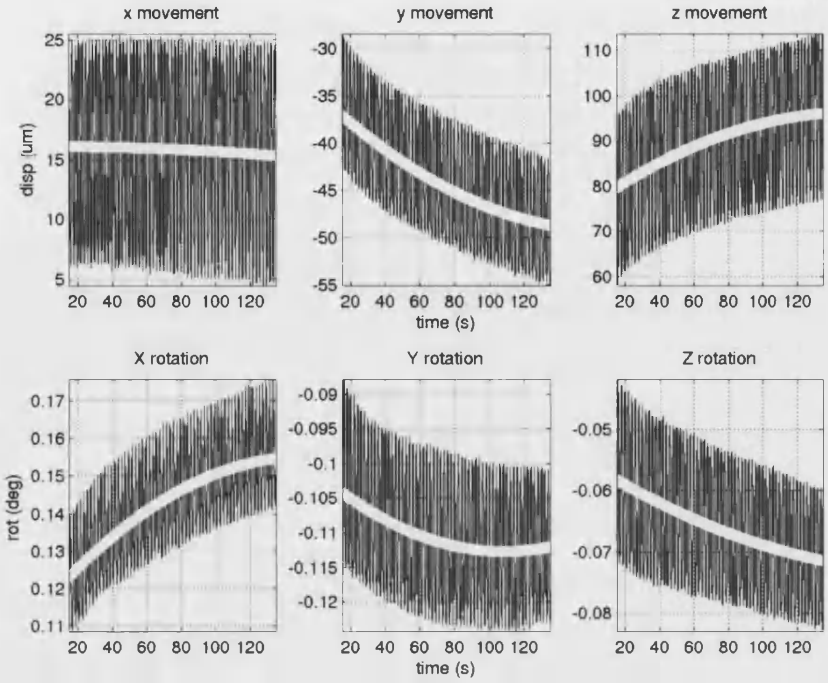

Figure 5-15 - Typical results obtained for migration (white line at the centre of the plot) and micromotion (amplitude of oscillations)

5.7. *Case Study 1: Validation of Sawbones composite femora (Objective 1)*

5.7.1. Introduction

Pre-clinical testing of total hip replacement stems employs cadaveric femora to evaluate the stability of new design concepts or modifications to the design of these stems (Baleani *et al.,* 2000; Gotze *et al.,* 2002; Buhler *et al.,* 1997a; Chareancholvanich *et al.,* 2002). In vitro cadaveric testing is the closest representation of the *in vivo* environment and bone properties that exist. However, bone quality and mechanical properties can vary widely in cadaveric specimens resulting in a large spread of experimental data. There are also problems associated with the availability, handling and preservation of cadaveric material. The combination of these factors result in expensive and time consuming tests and, frequently, only allows for a small number of femora to be used. The large experimental spread and small groups can make statistical comparison unreliable and can prevent the detection of small differences

between experimental groups. Due to these limitations research groups have tended to use composite femora as an alternative.

Pacific Research Laboratories Inc (Vashon, WA) has produced composite femora for biomechanical testing since 1991 and their products are known by the trade name Sawbones. The design of their 3rd generation femur models natural cortical bone uses a mixture of short e-glass fibres and epoxy resin which are pressure injected around a polyurethane foam core used to represent cancellous bone. The shaft area has an intermedullary canal. The gross mechanical properties of this type of femora have been found to be comparable to those of cadaveric femora (Heiner and Brown, 2001), however, post-operative stem stability is dictated by the type of material directly supporting the stem rather than the mechanical properties of the whole bone.

Sawbones are readily available and can produce more consistent results than cadaveric material, enabling the effect of small design changes to be highlighted. The use of composite femora as an alternative to cadaveric bone has become wide spread (Maher *et al.*, 2001; Liu *et al.*, 2003; Maher and Prendergast, 2002) although their use specifically for hip stem stability studies is yet to be validated.

Characterisation studies performed by Szivek *et al.,* (1993) showed that the polyurethane foam has similar stress strain curves to those obtained from human trabecular bone and a Young's Modulus between 62 and 104MPa which is well within the human range (Martens *et al.,* 1983). It is therefore reasonable to postulate that the performance of a hip stem in this foam would be similar to the in vivo situation; however this hypothesis requires validation.

The freshly implanted set of cadaveric femora obtained from Austria offered a chance to perform a validation of Sawbones. The stems had been implanted at post mortem so no bone remodelling could have occurred. The absence of osseointegration makes the specimens comparable with that of an immediate postoperative condition and could be compared with new data acquired from a set of composite bones implanted with an SL Plus stem.

This study aimed at establishing whether Sawbones composite femora are suitable for the assessment of migration and micromotion of a cementless hip stem.

5.7.2. Method

The composite specimens were 3rd generation Sawbones left sided femoral models (Pacific Research Laboratories, Sweden). The stems were implanted by an experienced orthopaedic surgeon using template guides. The stem selected according to the templates was a size 7. Both composite and cadaveric specimens were subjected to loading cycles as described in section 5.5. An example of a cadaveric specimen with instrumentation is shown in Figure 5-16.

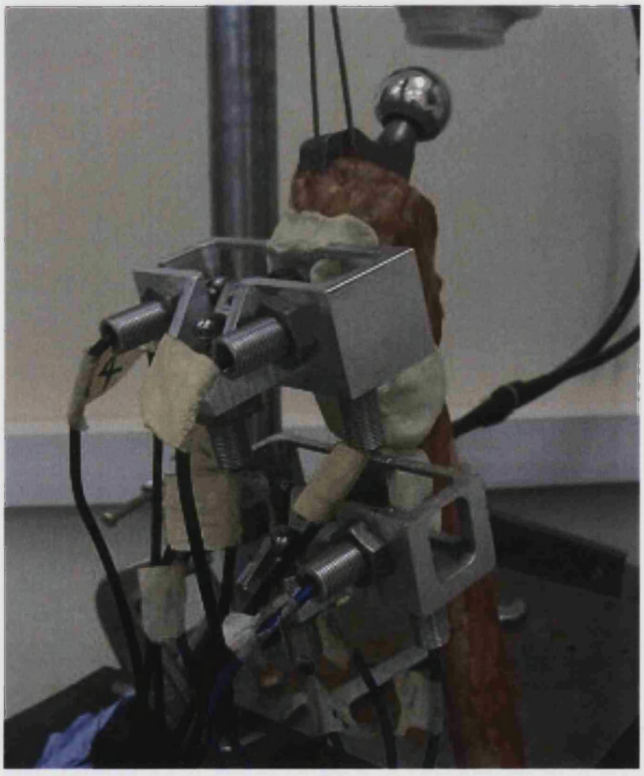

Figure 5-16 - Photograph of cadaveric specimen and six degree of freedom motion transducers

5.7.3. Results

Data from the final set of 200 cycles were used for statistical analysis as the largest forces induced the largest motions of the implant. The results are represented graphically in the form of box-plots, an example of which is shown in Figure 5-17, and numerically as medians (25th – 75th percentiles). Differences between the groups were evaluated with the Mann-Whitney U test, statistical significance was assumed for $p<0.05$.

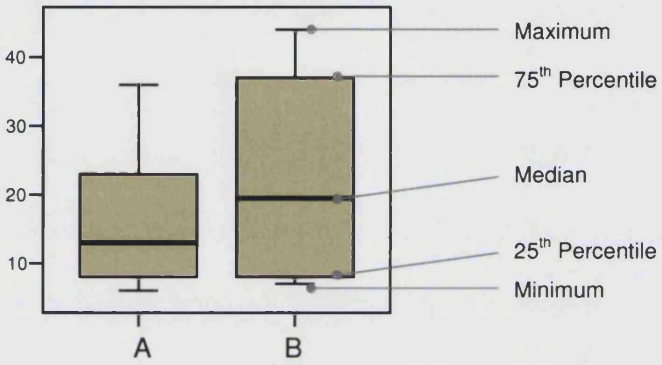

Figure 5-17 - Example of box plot and description of features

Figure 5-18 to Figure 5-19 show the principal directions for micromotion and migration during single leg stance (SLS) and Figure 5-20 and Figure 5-21 show the principal directions for micromotion and migration during stair climbing (SC). The graphs are displayed in sets of 4 to show the prevalent motion for translational and rotational micromotion (a and b) on the top row and translational and rotational migration on the bottom row (c and d).

Outliers in the data sets are defined are values between 1.5 times and 3 times the inter-quartile range outside the upper or lower edge of the box and are shown on the graphs with circles. Extreme values are defined as those more than 3 inter-quartile ranges from the upper or lower edge of the box and are shown on the graphs as stars.

Data from the second composite bone tested were removed from the analysis due to persistent outliers indicating a probable error in the experimental set up.

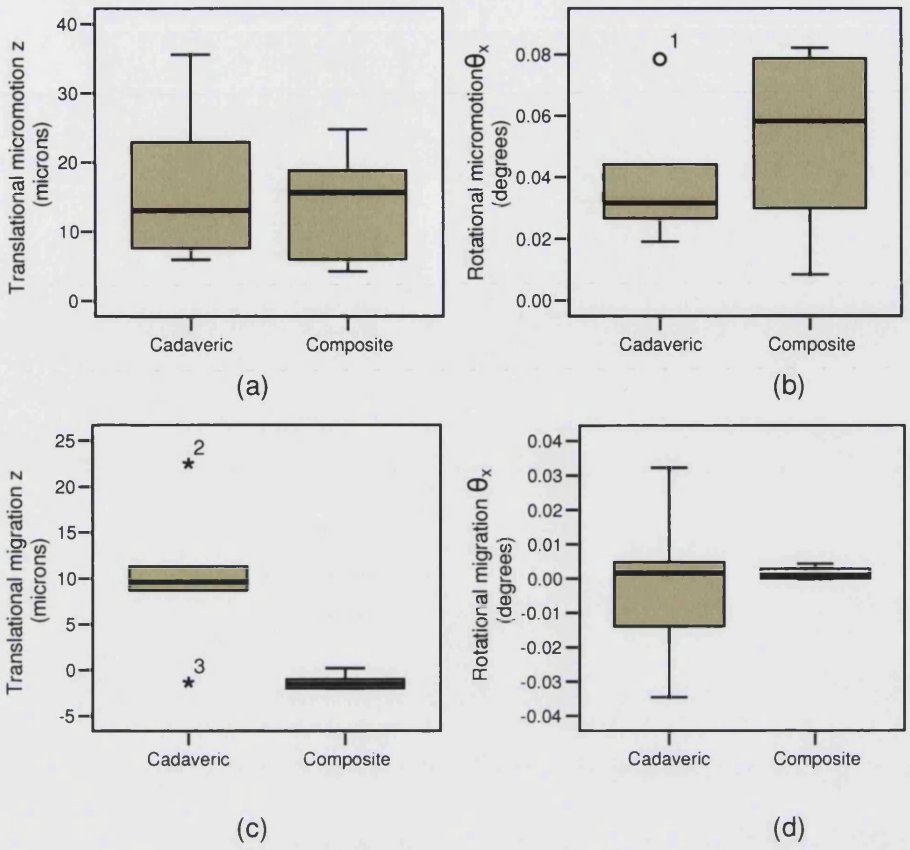

Figure 5-18 - Prevalent motion measured in the proximal transducer during SLS

In the SLS experiments the largest amplitudes of micromotion measured by the proximal transducer were oscillations parallel to the longitudinal axis of the femur (z in Figure 5-3). These amounted to 13 μm (8μm - 23μm) for the cadaveric bones and 16 μm (6μm - 19μm) for the composite Sawbones® models, see Figure 5-18a. The proximal rotations measured during SLS stance were also similar between the two materials, both producing small rotations of the same order of magnitude. The largest rotations measured proximally were about the x-axis (θx), these can be seen in Figure 5-18b, in the cadaveric bone they were 0.03° (0.03° – 0.04°) compared to 0.06° (0.03°-0.08°) in the composite bone models.

The non-recoverable motion, or migration, was low in the cadaveric femora but negligible in the composite femora. The largest proximal migration during SLS was in the same direction as the largest micromotion, along the axis of the femora (z) for translations and about the x-axis (θx) for rotations. Figure 5-18c shows the prevalent translational migrations recorded along the z-axis,

measuring 10μm (9μm – 11μm) in the cadaveric bone. The composite model produced lower levels of migration (-2μm (-2μm – 0μm)). These differences were statistically significant ($p<0.05$). In this case the use of the composite model in isolation would have lead to underestimating migration.

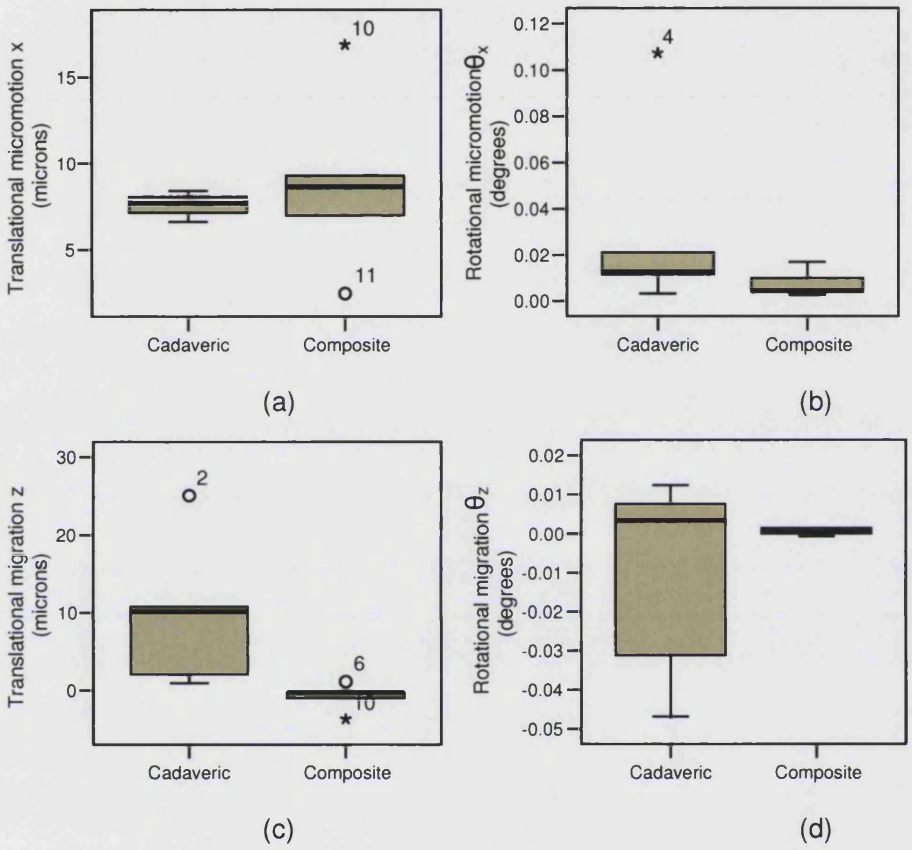

Figure 5-19 - Prevalent motion measured in the distal transducer during SLS

At the distal location the migration and micromotion results during SLS were all very low indicating excellent stability and fit in with the design philosophy of the implant. The graphs for the prevalent motion at the distal measuring location can be seen in Figure 5-19. The largest distal micromotion was a translation along the x axis and the two models compared favourably, cadaveric bone 7μm (7μm – 8μm) and 9μm (7μm – 9μm) in the composite bone model, Figure 5-19a. The levels of rotational micromotion were also similar between the models yet were so low that they could be considered negligible, Figure 5-19b. Figure 5-19c shows that the largest distal migration, in the cadaveric femora during SLS, was along the z axis 10μm (2μm – 11μm); however this predominant migration was not recorded in the same axis in the composite femora where this

motion was negligible, 0μm (0μm – 1μm). This difference was statistically significant ($p<0.05$).

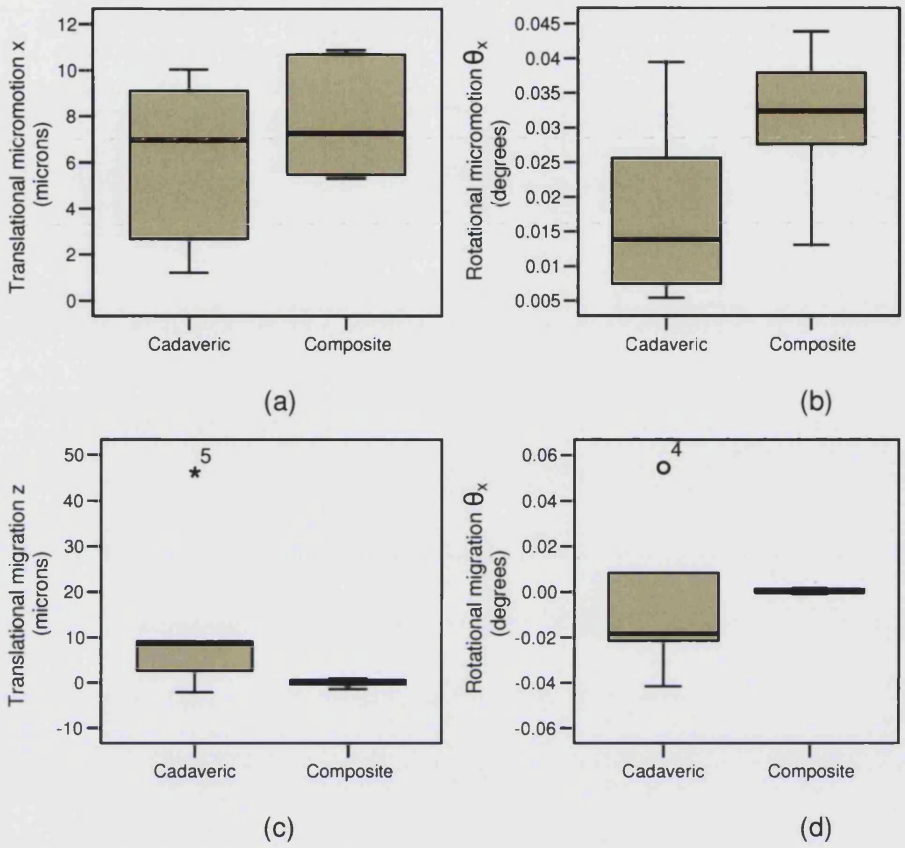

Figure 5-20 – Prevalent motion measured in the proximal transducer during SC

In the SC experiments translations and rotations about the x-axis (θx) became predominant (Figure 5-20). The prevalent linear micromotion movement consisted of oscillations parallel to the x-axis (Figure 5-20a) which were greatest in the proximal part of the implants inserted in the cadaveric femora, amounting to 7μm (3μm - 9μm). In the case of composite femora, oscillation amplitudes along the x-axis were very similar 8μm (5μm - 11μm). The rotational micromotion (Figure 5-20b) was highest about the x axis in the composite stems 0.03° (0.03° - 0.04°) and although in the cadaveric femora the rotations were lower 0.01° (0.01° - 0.03°) both models showing the same predominant motion. The migrations followed similar patterns to the SLS results with the cadaveric femora showing low but measurable levels of migration and the implants in the composite femora showing significantly different results ($p < 0.05$) with zero levels of non recoverable motion (Figure 5-20c). The proximal rotations recorded in the composite femora were significantly larger than those measured

distally (p=0.009) and larger than those measured proximally in cadaveric hosts but not significantly so.

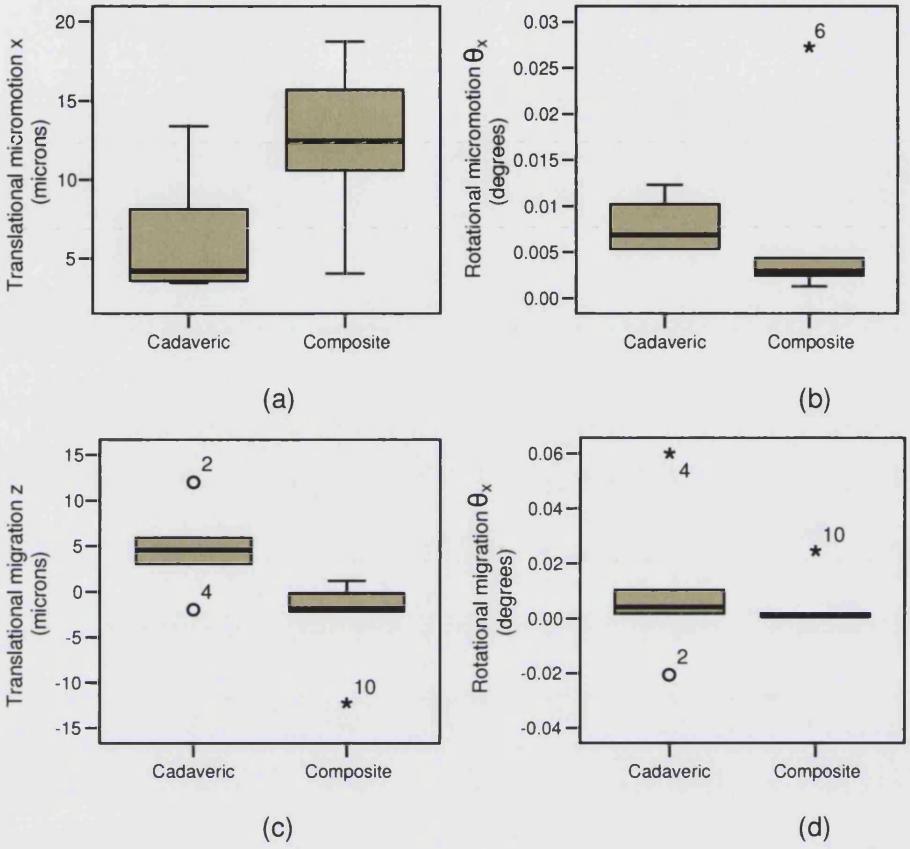

Figure 5-21– Prevalent motion measured in the distal transducer during SC

At the distal location the implants appeared very stable in both the cadaveric and the composite femora during stair climbing (Figure 5-21a-d). The prevalent micromotion of the hip stem (Figure 5-21a) was in the x axis amounting to 4μm (3μm – 11μm) in the cadaveric model and larger motions of 12μm (7μm -17μm) in the composite femora. The implant proved to be rotationally stable with the largest rotational micromotion recorded about the x axis (Figure 5-21b) with values of 0.01° (0.00° – 0.11°) and 0.00° (0.00° – 0.02°) in the cadaveric and composite models respectively. The migration results for prevalent translation and rotation presented in Figure 5-21c and d, followed the same trends as other results with low values recorded in the cadaveric model and negligible results recorded in the composite model.

5.7.4. Discussion

The need for a synthetic bone model for assessment of hip stems in pre-clinical tests as a standard bench test model is a desire commonly expressed in the field (Heiner and Brown, 2001; Prendergast and Maher, 2001). The results from this study show how the SL Plus stem respond to loading in single leg stance and stair climbing and provide data that directly compares *in vitro* cadaveric testing with the Sawbones composite bone substitute. When the two different materials investigated (cadaveric bone and composite bone model) are subjected to load, they respond with predominant motions in the same direction. In single leg stance the force applied was almost vertical relative to the implant and host bone and the micromotion was predominantly along the longitudinal axis of the femur. When the implant and bone were rotated to represent stair climbing the rotational motion about the x-axis became the principal motion, as the force applied is offset from the point of measurement creating a torque on the stem. The levels of micromotion, in both translation and rotation, were similar with comparable medians and there were no significant differences between the groups. Distally the micromotion results were very low which is in accordance with the design philosophy of good initial fixation by a press fit taper.

The similarity in behaviour between the two models was maintained when the migration or non-recoverable motion was assessed. The migration values in the cadaveric study were typically less than 20μm however this value was reduced to almost zero, i.e. no migration, when the stems were implanted in composite femora. This low motion could be due to the Sawbones internal foam having a higher elastic modulus/stiffness than the cadaveric bone or due to the internal shape of the composite femora. This is characterised by a narrow intra-medullary canal that could be offering some additional support to the stems that is not present in the cadaveric bones. It is also possible that the low motion is a combination both of higher stiffness and intra-medullary narrowing in the composite femora. Stems characterised by narrower distal tips may not make contact with the narrow medullary canal allowing the stem to migrate in this particular model. The low migration in composite femora was an important result as the use of composite femora could lead to a gross underestimation of a stems resistance to migration. The highest levels of migration were commonly found in the same direction as the largest micromotion.

One of the limitations of this study is the low number of specimens, which is ultimately responsible for the low power of the statistics used. This makes it difficult to draw strong conclusions about the femoral models.

Another difficulty is represented by the risk of femoral fracture during the experiments. One of the cadavers had already been fractured during implantation reducing the data set and further reduction could not be afforded. To minimise the risk of fracture during testing the forces applied to the femora were not full body weight but still comparable to those applied in another study (Britton *et al.,* 2004). The force applied at the hip during normal gait in the patient is proportional to their body weight; however for comparative reasons the force used in this study was kept constant between the specimens. An average hip contact force has been shown to be about 2.3 times body weight (Bergmann *et al.*, 2001; Paul, 1966). With an average weight of about 75Kg, the force resulting at the hip joint would be 1.7kN, which is greater than the forces used in this study. Levels of micromotion and migration were recorded at three loading levels for each regime. However the data from the test did not show clear enough trends to reliably scale the results for comparisons to other studies. Even if the data of load against level of motion had produced a linear trend over the range tested there was no further evidence to suggest that this would continue up to physiological loads in the same pattern. The data can be used to comparatively assess the suitability of using composite femora in preference to cadavers.

In general the SL Plus stem exhibited a stable behaviour, with most micromotion values in both cadaveric and composite femora under the 30μm threshold, a value suggested by Pilliar *et al.*, 1986, to be required for good bone in-growth. In particular, the rectangular cross section of this stem gives good rotational stability and distally the stem is very secure. The low rotational values and distal fixation fit well with the highly successful clinical performance of the implant type and would suggest that the composite model is suitable for assessing micromotion. However, this study can only report the suitability of the model for one stem. A further study of interest would be to use a hip stem considered inferior with known design flaws to see if the composite model provides a reliable test to detect and display design flaws. A similar study was used to show that good and bad stems could be differentiated by loading

protocols (Cristofolini *et al.*, 2003), however this has not been repeated for cementless implants in composite bones. A composite femur for validating hip stems is desirable for pre-clinical testing, although as the use of composite femora is increased it is important that hip stems are not optimised only to perform well in the composite femora to pass pre-clinical tests (Cristofolini *et al.*, 1996).

5.7.5. Conclusion

This study has demonstrated that Sawbones composite femora provide an effective model to establish micromotion with oscillation patterns and orders of magnitude similar to cadaveric bone. The micromotion levels recorded in this study are low but they could be attributed to the cautious loading regime adopted. It is important to note that this was a comparative study between the two femoral models and not a study aimed at comparing the SL-PLUS stem to other designs. Migration was not modelled as effectively as micromotion. Migration is much more dependent on the quality of fit and the internal geometry of the femur and therefore more caution should be placed on interpreting migration data from Sawbones models.

5.8. *Case study 2: Post-operative and long-term stability of the SL Plus hip stem (Objective 2)*

5.8.1. Introduction

The "Zweymüller" type stem has been implanted in over 350,000 patients since its introduction in 1979 and reports have shown 99% survivorship after 10 years (Delaunay *et al.*, 2001 and Grűbl, 2002). The long-term success of this implant, like any cementless hip prosthesis, is dependent upon achieving primary postoperative stability between the implant and the host bone to promote early osseointegration. The design of the stem is claimed to offer both primary and long-term stability. The rectangular cross section is intended to anchor the stem rotationally and the tapered geometry provides axial fixation.

The aim of this study is to compare the initial postoperative stability to the stability after several years implantation of Zweymüller type stems by evaluating micromotion and migration levels between the stem and the host bone.

5.8.2. Method

This case study used the six paired femora described in section 5.4 with long term "Zweymüller" hip stems in one femur and freshly implanted SL Plus stems in the contra-lateral side. One pair from the set had to be removed from the study as the transducers could not be fitted to the long-term femur and in the contra-lateral side a fracture was produced in the proximal region during the implantation of the SL Plus stem. Patient consent and ethical approval were obtained for the harvest of the femora and testing by the operating team.

The remaining femora with implanted stems (5 for each group) were then subjected to loading cycles described in section 5.5. The stability was assessed in terms of micromotion and migration which are defined in Figure 5-1.

5.8.3. Results

The same considerations outlined in section 5.7.3 apply to this set of results; differences between the groups are analysed using the Mann-Whitney U test assuming a value of $p<0.05$ for statistical significance. The boxplots of Figure 5-22 to Figure 5-25 show the principal directions for micromotion and migration during single leg stance (SLS) and stair climbing (SC).

Data from the last long-term stem tested were removed from the analysis as they constantly presented outliers. The larger motion of this implant may be eventually explained by the histology examination.

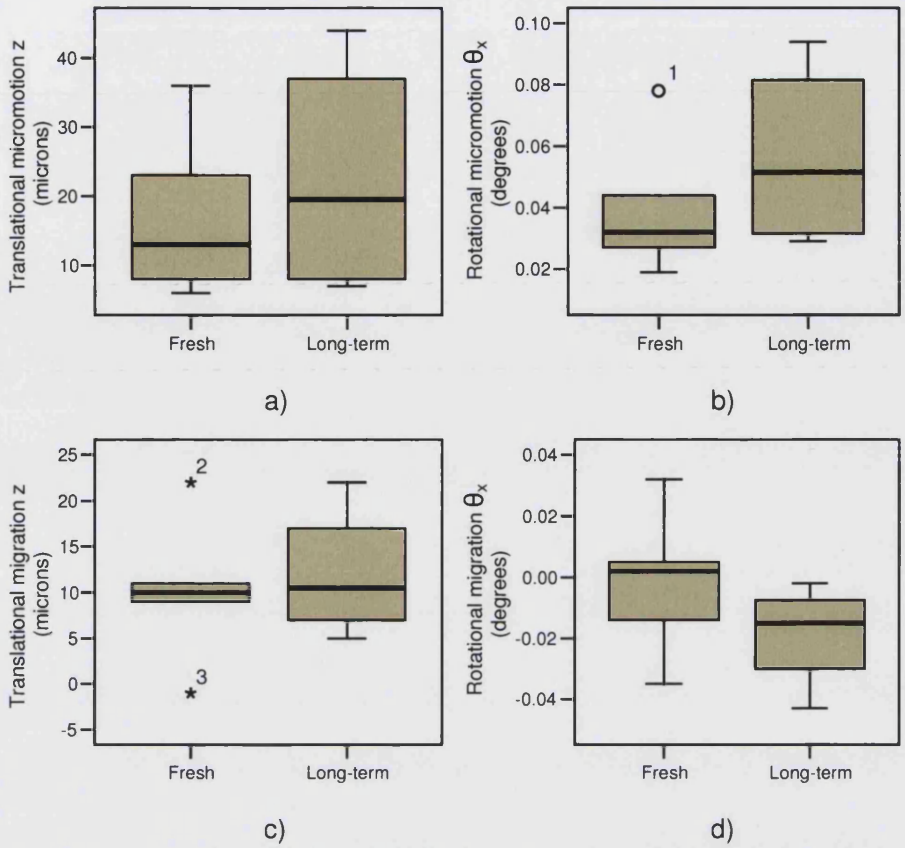

Figure 5-22 – Prevalent motions in the proximal transducer during SLS

The largest micromotion movements recorded during the SLS experiments consisted, for both sets of tests, i.e. freshly implanted and long term stems, in oscillations parallel to the longitudinal axis of the femur (z in Figure 5-2). These amounted to 13μm (7μm - 30μm) for the freshly implanted hip stems and 19μm (8μm - 40μm) in the case of long term surviving implants (Figure 5-22a). The prevalent rotation recorded in the proximal transducer was about the x axis (θ_x) with recorded motions of 0.03° (0.03° – 0.04°) in the freshly implanted stems and 0.05° (0.03° – 0.08°) in the long-term surviving implants (Figure 5-22b). The micromotion is marginally larger in the long-term femora than in the freshly implanted but comparable in terms in magnitude and range. These differences were not statistically significant.

The highest migrations recorded during SLS consisted of translations along the z-axis (as shown in Figure 5-22c) and rotations about the x axis (θ_x) (Figure 5-22d). The translational migration measured had identical medians of 10μm for both freshly implanted femora and long term surviving femora but the range of translational migration was higher in the case of the long-term implants. The

rotational migrations were comparable between the models with the freshly implanted femora producing values of 0.00° (-0.02° - 0.02°) and the long-term surviving femora -0.01° (-0.04° – 0.01°). There were no statistical differences between the two sets of data.

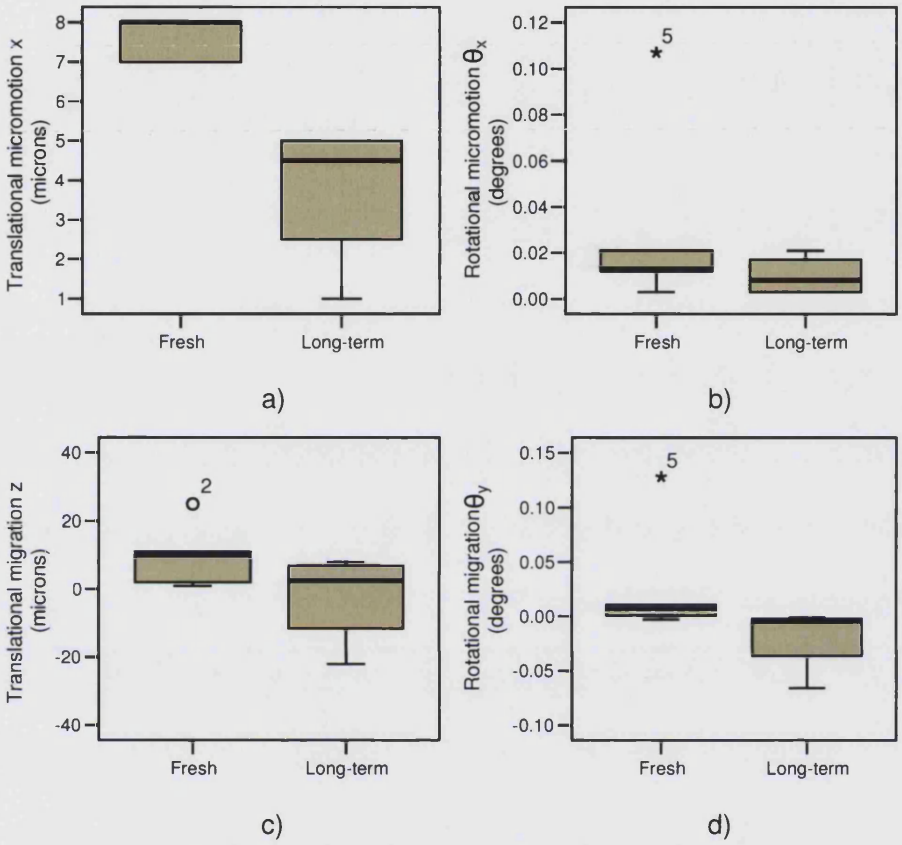

Figure 5-23 – Prevalent motion in the distal transducer during SLS

The levels of axial micromotion (i.e oscillations along the longitudinal axis of the femur) recorded by the distal transducer were significantly lower than those recorded proximally ($p < 0.001$). The prevalent translational micromotion was measured along the x-axis, and seen in Figure 5-23a, with the hip stem moving from anterior to posterior producing results of 8µm (7µm - 8µm) in the freshly implanted hip stems and 5µm (2µm - 5µm) in the long term surviving implants. The difference between these micromotion results was significant ($p < 0.05$) but this was the only direction in which a statistical difference was detected. The prevalent rotational micromotion recorded in the distal transducer was about the x axis and shown in Figure 5-23b. The recorded values were of the same order of magnitude for both hosts, 0.01° (0.01° – 0.06°) in the freshly implanted femora and 0.01° (0.00° – 0.02°) in the long-term surviving implants.

Figure 5-23c shows the highest migration results at the distal location which was measured by the transducer along the z axis. This produced some unexpected results: in the freshly implanted femora the median migration was 10μm (2μm – 18μm) however in the long-term surviving implants it was 3μm (-17μm - 8μm). The negative value for the 25th percentile in the long-term results indicates that some of the hip stems were migrating upwards against the direction of the loading during the tests, Figure 5-23c. This is could be experimental artefact introduced by the way which the load is applied to the head of the implant. If the implant rotates about a point between the head and the transducer then that may induce an upward motion at the transducer. The prevalent rotational migration in the distal transducer was about the y axis, as shown in Figure 5-23d.

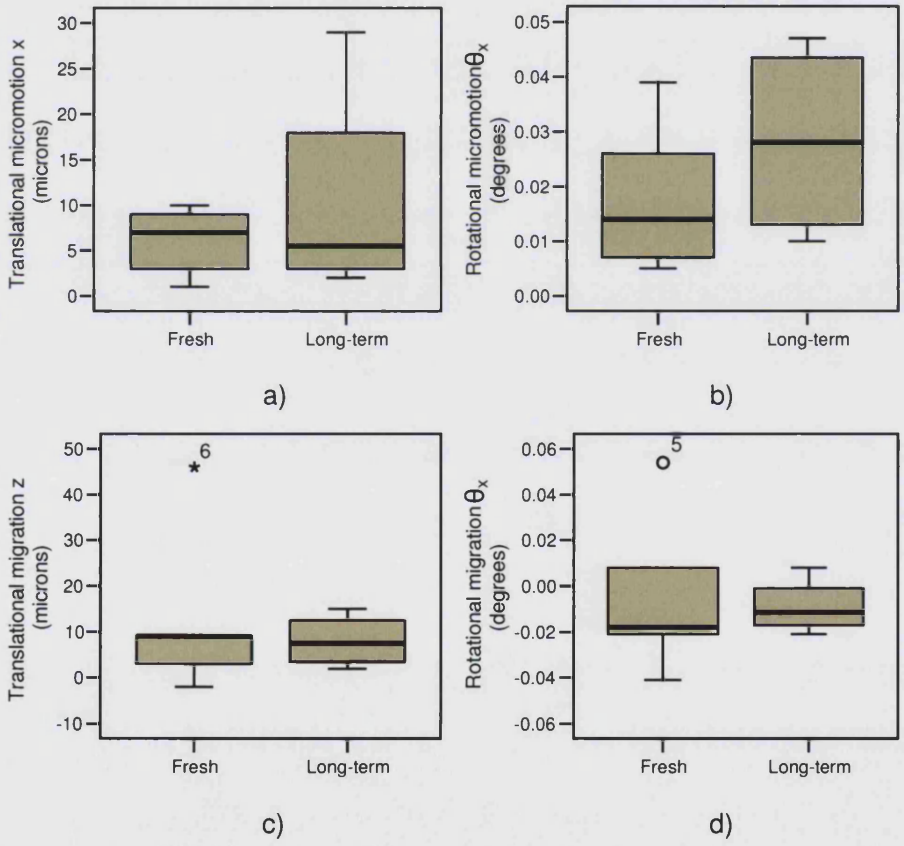

Figure 5-24 – Prevalent motion recorded at the proximal transducer during Stair climbing

During the stair climbing (SC) loading regime the prevalent translational micromotion was parallel to the x axis for both the cadaveric models, this can be seen in Figure 5-24a. The values for this translational micromotion were similar for both hosts producing 4μm (3μm -11μm) for the freshly implanted femora and

9μm (4μm -20μm) in the long term surviving implants. The prevalent rotational micromotion for both femoral models was about the x axis and is shown in Figure 5-24b. Comparable values were obtained for the two experimental groups; 0.02° (0.01° – 0.03°) for freshly implanted stems and 0.03°(0.01° - 0.04°) for the long living ones.

Like the migration results in the SLS regime the prevalent migration in the SC regime resulted in translations along the z axis and in rotations about the x-axis (Figure 5-24c and d).

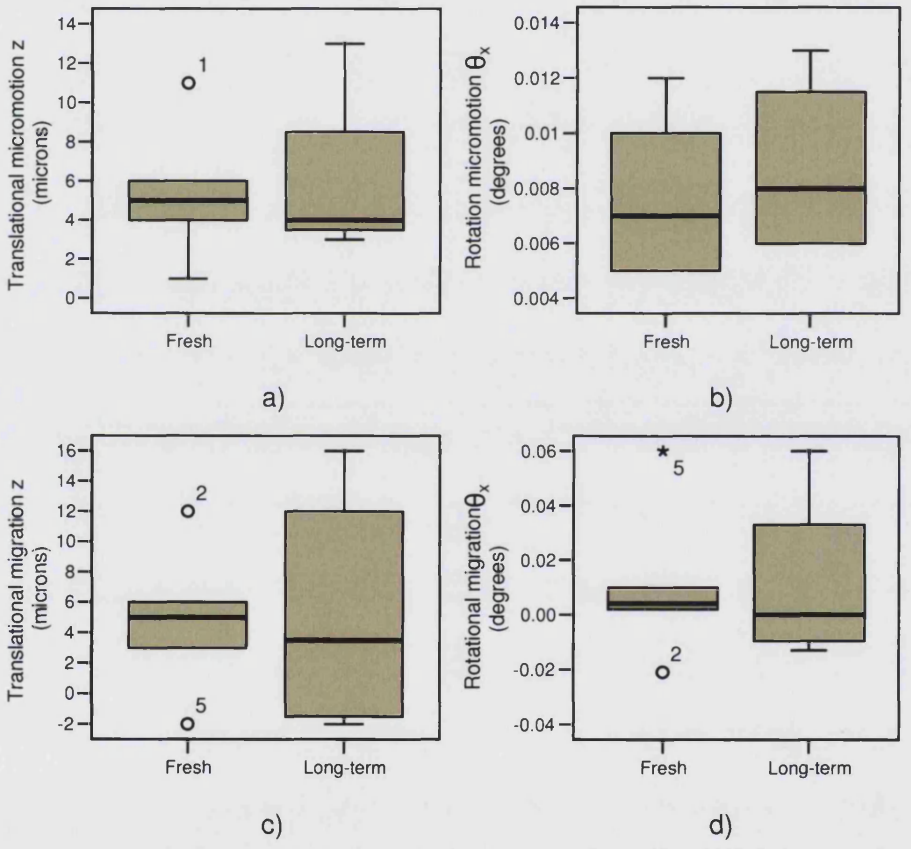

Figure 5-25 – Prevalent motion recorded at the distal transducer during stair climbing

At the distal location during SC the prevalent micromotion and migration were parallel to the z axis in translation and about the x axis in rotation in both cadaveric models (Figure 5-25 a – d). The prevalent translational micromotion results are shown in Figure 5-25a. Both groups were characterised by similar micromotion; 4μm (3μm - 11μm) in the freshly implanted and 9μm (4μm –

20μm) in the long-term surviving implants. The rotational micromotion was minimal with results only ranging from 0.00° to 0.01°.

The distal migration showed similar median values between the freshly implanted stems and the long-term ones however the long-term implants were characterised by larger ranges of motion between specimens in both translational and rotational migration.

In general there was no statistically significant difference between most of the values for translation motion recorded between the long-term and freshly implanted stems. The highest micromotion amplitudes were recorded in both groups proximally, independently of the loading configuration.

5.8.4. Discussion

The predominant motion of the hip stems examined in both loading regimes was generally aligned with the direction of the forces applied to the head of the implant. In SLS the predominant motion in both fresh and long-term implant stems was along the z axis, with the main rotation about the x axis. In SC the predominant motion was along the x axis with rotations about the x axis. The two groups (freshly implanted and the long-term implants) also showed similar levels of micromotion and migration in most of the directions analysed. With only 4 pairs for comparison (1 pair excluded for fracture and 1 pair for outlying results) strong conclusions about which group produced the higher motion is difficult.

Both models showed larger motion proximally rather than distally and the levels of motion recorded in this study are all well below the 30μm threshold generally recommended for good osseointegration. However, the levels of load used in this study were lower than the forces experienced *in vivo*. Femoral head load has been reported in studies at about 2.3 times body weight (Paul, 1966; Bergmann *et al.*, 2001). For an average bodyweight of 75kg, a 2.3 times increase would induce a femoral head force of 1.7kN which is above the forces used in this study. The levels of load in this study were conservative due to the risk of femoral fracture especially during the stair climbing regime where the angle of flexion induces large torque at the base of the femur. The results from

the tests performed at lower loads on the cadaveric bones do not provide enough data to extrapolate these results reliably to physiological load levels.

The results obtained in the case of cadaveric bone models show large variation between specimens. This could be due to a number of factors which are difficult to control during the test including variation of bone quality, surgical technique and differences in the geometry of the bones. The variability of the bone quality alongside with differences in the geometry of the femora is probably the highest factor of inter-specimen variation. This study was blinded so there is no data on the donors of the bones regarding their sex, age, weight and other factors that may affect bone quality which could offer extra information to explain some the variation.

Another source of possible variation in stability studies such as the one performed here is the quality of the surgery which relies on the experience of the operating surgeon. In this study the hip stems were implanted by surgeons very experienced with the SL Plus hip stems, hence the variation due to surgical technique should be minimal.

In Figure 5-23 the results showed that negative migration was recorded at the distal transducer during SLS. This is an unexpected result and there is no clear explanation for this pattern of motion. A possible explanation could be a movement of tissue underneath the distal tip of the implant preventing the tip returning to its initial position after a loading cycle. The upward motion recorded at the transducer could also be an effect of the rotation or large bending moments. Both the bone and stem have not been assumed to be rigid structures and therefore the exact centre of rotation cannot be derived. If this centre of rotation is between the head of the implant and the pin attachment point then rotation would actually lift the lateral side of the implant which would be recorded at the transducer. Other results for migration have shown small amounts of upward motion however the magnitudes were only 1 micron (lower than the accuracy of the transducer) therefore these values have not been taken into account.

Finally errors in the experimental setup contribute to the variation in the results. Jigs were use to minimise most of the setup issues such as the positions of the pin holes and alignment of the motion transducers and a program was

developed to set the LVDTs to their mid position minimising the risk of the sensors reaching the end of their travel. One area that could be improved is the set up of the muscle cable. If the cable is over tensioned then this will produce higher loads on the head of the hip stem and affect the levels of micromotion.

5.8.5. Conclusion

This study has demonstrated that a double-tapered rectangular stem is stable in both single leg Stance and stair climbing giving low micromotion values especially in rotation. The amplitudes of movement recorded in freshly implanted stems are comparable to those recorded in long living implants. Therefore it is concluded that this type of stem offers immediate postoperative stability and that this stability is maintained in the long-term. Clinical evidence suggests that initial stability is key to long-term success; the findings of this partially explain the reasons for the success of the implant geometry.

Chapter 6. Design of a Dynamic Hip Simulator(Objective 3)

6.1. *Introduction*

In the previous chapters the importance of hip stem stability has been highlighted. The survey of the literature identified that the current bone implant motion studies are performed with the femora held statically and hence the influence of femoral kinematics on implant stability is not fully understood. The aim of this study was to investigate the influence of femoral kinematics on hip stem stability. This will enable a comparison of the results of experiments with the femur held statically to the results when the femur is moved through a gait cycle to replicate normal walking. This has been achieved by developing a simulator to drive the femur through the various angles experienced during normal gait and simultaneously load the femur with physiological forces. Background information on the kinematics, contact forces and muscle loading experienced in the hip joint is presented in Chapter 3. This formed the basis for the design.

The simulator was designed to accommodate Sawbones composite femora, the use of which in bone implant motion studies has been validated in Chapter 5. Another important consideration for the design was availability of a multi-axis materials-testing machine. The capacity and suitability of its actuators are detailed.

This chapter includes an assessment of the kinematics and loading other dynamic simulators (used for wear tests) and defines the ideal simulator to comprehensively model a hip joint. The kinematics and loading directions required in the simulator are prioritised to aid the decision making of which should be included in the design. Concepts of the dynamic simulator are presented and evaluated to choose the most suitable design.

The development of the dynamic hip simulator was planned in three stages;

1. development of flexion-extension mechanism,
2. development of abduction-adduction mechanism,
3. inclusion of muscle loading.

Each phase was designed with consideration for the future stages and rigorously tested before proceeding to the next stage. This chapter describes the key design decisions that were made throughout the stages and presents the results of the ongoing testing. Finally the tests evaluating the performance of the simulator are analysed.

6.2. *Aims*

The aim of the simulator was to establish the effect of femoral kinematics on implant stability. This was to be achieved through the design of a rig capable of replicating human gait for use with a multi axis materials testing machine. This simulator should simulate normal human gait combined with synchronised physiological loading of the femoral head.

6.3. *Resources and materials*

6.3.1. Zwick multi axis load testing machine

The design for the simulator was based around the multi axis servo hydraulic materials testing machine (Zwick – HBT 25-200). This machine was the most suitable to provide the actuators for a hip simulator due to its versatility. The machine is comprised of two independent linear actuators placed horizontally and vertically and a torsional actuator rotating about the vertical axis. Basic details of these actuators are listed in Table 6-1

Actuator	Load cell	Stroke
Horizontal	5 kN	100mm
Vertical	25 kN	150mm
Torsional	200Nm	90°

Table 6-1- Multi axis actuator capacity

The multi axis machine is programmed through a PC based software suite supplied with the machine (Workshop Release 21), a Windows based system capable of generating synchronised control signals based on waves or

programmed profiles. The software is also capable of recording load and stroke data from each of the actuators.

6.3.2. Sawbones composite femora

A decision was made to base the design around the Sawbones composite femora shown in Figure 6-1. The use of composite femora in pre-clinical testing is widespread (Britton *et al.*, 2003; Clements *et al.*, 2004; Heiner and Brown, 2001) and in this study, they were selected for the reasons stated below:-

1. Composite femora provide a more consistent material for biomechanical testing than cadaveric specimens
2. Composite femora are widely available and provide a cheaper alternative to cadaveric materials,
3. Cadaveric materials require ethical approval and special handling requirements which can lengthen the time taken to perform experiments.
4. The availability of 3D CAD models for a composite femur which could be used in the design phase to make geometric decisions about the rig.
5. The use of Sawbones composite femora has been validated in Chapter 5 for the assessment of micromotion

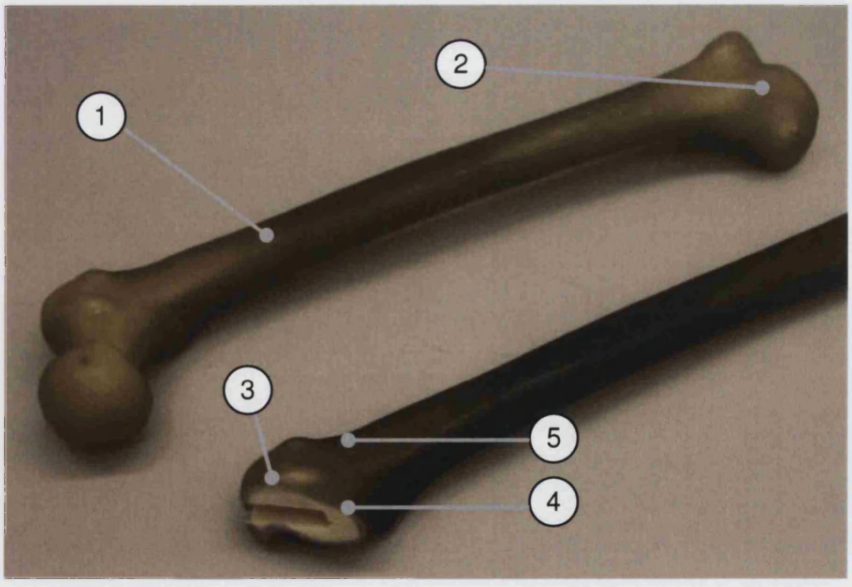

1) Sawbones composite femur
2) Condyles of the knee
3) Femur with neck resected
4) Expanded polyurethane modelling cancellous bone
5)Epoxy E-glass modelling cortical bone

Figure 6-1 – Sawbones® composite femora

6.3.3. Instrumentation

The stability of the hip stem in the dynamic study was to be assessed with the same six degree of freedom transducers as all the earlier studies (Chapter 4). A detailed description of the transducers can be found in section 5.3 and overall dimensions can be seen in Appendix II.

6.4. *Design considerations and prioritisation of parameters*

The hip joint is a complex system and to comprehensively model the system would require a larger number of actuators. Before the generation of conceptual designs the parameters for the simulation need to be considered and prioritised with reference to other hip joint simulators designed to date (Section 2.5). The majority of these are wear simulators which have different objectives to bone implant motion simulators. Because there is only one current dynamic bone implant motion simulator (Liu *et al.*, 2003) it is important to consider the parameters used in wear simulators. Despite the measured quantities in a wear simulator being different to those measured in a bone implant motion simulator the parameters of force and kinematics used to simulate the *in vivo* conditions are the same. A discussion of these simulators and a classification system is offered by Viceconti *et al.* (1996). The classification system describes the ability of a simulator to reproduce motion and loading forces using a coded bracket as follows.

(degrees of freedom (motion); configuration / degrees of loading; configuration).

e.g. (2; x-z / 1; z)

The first half of the bracket refers to the motion modelled in the simulator and their configuration. The second half of the bracket refers to the loads applied in the simulator and directions in which they are applied. The example given (2; x-z / 1; z) would produce motion in the x and z axis whilst loading in the z axis. If a load is applied in two orthogonal directions but the loads are not independent then the hyphen is removed i.e a load applied that acts y and x axis would be written 2: yz. Viceconti's study offers a suggestion that two sets of three actuators are ideally required to comprehensively model a hip joint. One set of three would be used to produce motion in sagittal, coronal and transverse

planes. The second set of three would be used to provide orthogonal loading conditions at the hip in x, y and z. Following the notation above the ideal simulator would be classified as (3; x-y-z/3; x-y-z).

The ideal simulator requires six actuators but only three were available (two linear and one rotational) for this study; consequently, a choice had to be made about which features of motion and loading would be used in the simulator. The three motions and loads were ranked in order of importance for inclusion in the simulator. Assuming that the largest motion would have the greatest potential influence on hip stem stability the motions were ranked from highest to lowest according to data compiled in section 3.2.

1. Flexion Extension – (32° to -10°)
2. Abduction Adduction – (8° to -6°)
3. Internal External rotation – (4° to -5°)

The importance of the loads applied from the three orthogonal directions were also ranked in importance according to magnitudes of bodyweight component during normal walking (Bergmann *et al.*, 2001).

1. Superior to Inferior - (2.3 x BW)
2. Lateral to medial – (approximately 0.5 x BW)
3. Anterior to posterior – (approximately 0.3 x BW)

Due to the potential complexity of the simulators design and the need to understand each component a decision was made to include the various features incrementally throughout the development.

6.5. *Concepts and selection of chosen design*

Concepts were originally developed and categorised into two main areas

Concepts A) a static design with loads applied through forces resolved to include femoral kinematics

Concept B) a series of rotation frames to physically rotate the femur whilst loads were applied

These two concepts are described in the following sections and evaluated for how realistically these could be implemented and their potential capability to simulate the *in vivo* hip conditions.

6.5.1. Concept A - Static femur with 3D loading to represent gait

One option was hold the femur in a fixed position and apply known 3D hip contact forces and gait data to produce theoretical hip loading curves in orthogonal directions x, y and z through a gait cycle (Figure 6-2). This data would then be used in a configuration of three loading actuators to independently load the head of the hip stem in the composite femur. The fixed femur idea was considered but rejected because of the lack of a third linear actuator and the reliance on modelling assumptions possibly leading to large errors.

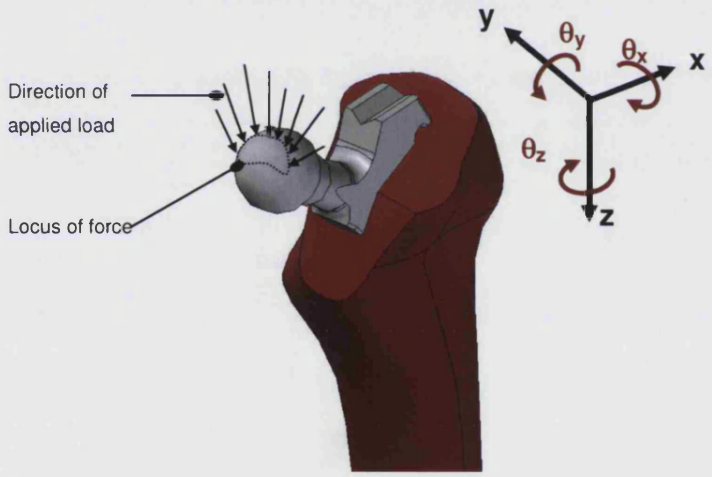

Figure 6-2 – Concept A showing loading of a static femur with theoretical dynamic loading

6.5.2. Concept B - Rotating frames synchronised with vertical loading

The basis of this design is a primary mechanical frame used to hold the femur and allow it to rotate in flexion extension (Figure 6-3). An additional femoral bracket can be added to increase the number of motions included. The feasibility of this concept depends on the methods used for actuation of the frames. Ideally, stepper motors would be used on the axis of each frame to

move the two frames independently to model a gait cycle. However, the load testing machine has only one torsional actuator and it is not conveniently located to provide flexion extension or abduction adduction. The use of stepper motors would also require additional control systems and resources beyond the budget of the project.

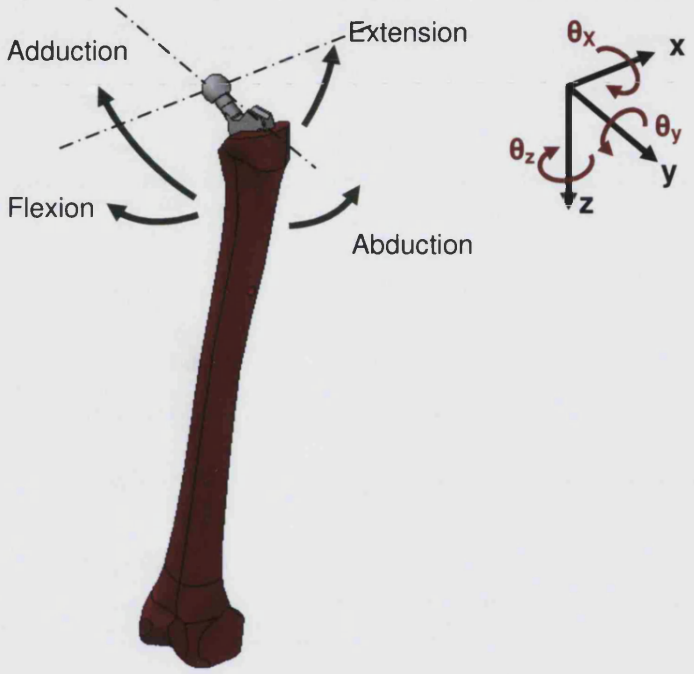

Figure 6-3 - Concept B showing the desired motion of the femur in a mechanical frame

With the current configuration of the actuators on the Zwick machine, the vertical actuator is best suited to providing the hip contact force and the horizontal actuator can be used with a linkage mechanism to drive the primary rotating frame. A cam and follower mechanism was suggested to control the motion of the femur in the coronal plane providing the abduction adduction movement of the hip. A selection of cam plates could be used to simulate a variety of gait patterns (slow/fast walking, stair climbing or rising from a chair). Using cam plates to control rotations would reduce the flexibility of the simulator for varying the levels of rotation but could provide an inexpensive solution.

The rotating mechanical frames concept was taken forward as the basis for the design and was implemented in three design stages.

The first phase was to include the largest motion, flexion extension (rotation in the sagittal plane), with loading applied from a vertical direction (superior to inferior). This would be achieved through the development of a rig capable of supporting a full composite femur and rotating through a mechanism powered by the horizontal actuator on the Zwick machine. The vertical actuator would provide the loading on the femoral head. Using Viceconti's classification this would be described as (1; x / 1; z).

The second phase of the design would include the rotation of the femur in the coronal plane (abduction adduction) with the development of a cam and follower mechanism and addition of a secondary rotating mechanism inside the primary frame (2; x-y / 1; z).

The final phase of the design would assess the feasibility of adding an abductor muscle to replicate loading in the lateral to medial direction. The final result would be a simulator with two degrees of freedom for the motion and loading from two directions. This could be represented using Viceconti's classification as (2; y-x / 2; zy) which would make this dynamic simulator the most comprehensive bone implant motion simulator available. When compared to wear hip simulators this classification would give this dynamic simulator a high degree of motion and loading simulation. Viceconti's classification of a number of wear simulators is presented in Table 6-2.

Simulator	Classification
Stanmore MK2	{3; x-y-z / 1; z}
Munchen	{3; x-y-z / 1; z}
WALKER	{1; y / 1; yz}
MMED	{2; x-y / 1; z}
LEEDS	{3; x-y-z / 3; x-y-z)

Table 6-2 - Viceconti's classification of a number of wear simulators
(Viceconti *et al.*, 1996)

6.6. *1st Stage – Design of the primary rotating frame for flexion extension*

6.6.1. Aim of 1st stage simulator

To produce a simulator capable of replicating femoral motion between 32° flexion and 10° extension in synchronisation with a vertical loading force comparable to *in vivo* data. The design of the simulator should make allowance for future developments (the next two stages) whilst providing a robust frame with high stiffness.

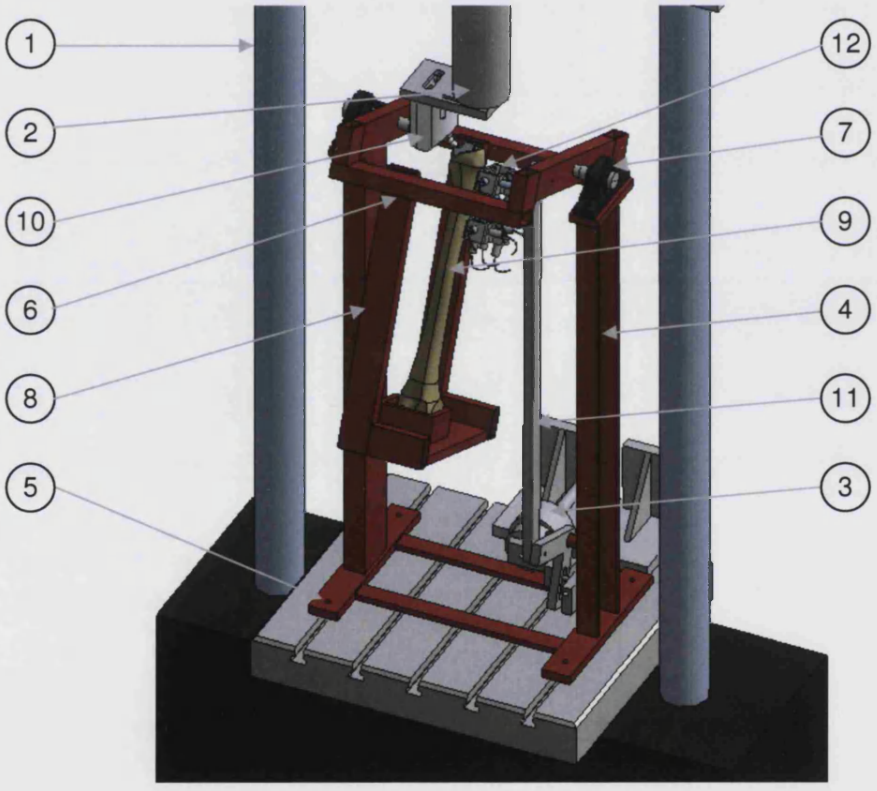

1) Zwick Load testing machine frame
2) Vertical Actuator
3) Horizontal Actuator
4) Rig uprights
5) T-slots
6) Primary frame
7) Bearings
8) Femoral bracket
9) Femur
10) Acetabulum
11) Flexion/Extension mechanism
12) Transducer

Figure 6-4 -Concept of 1st stage rig showing main features of the design

6.6.2. Design of the primary frame and supporting brackets

The design comprises two large uprights pictured in Figure 6-4 constructed from 75 x 35 mm of U section steel. These uprights and all structural components of the rig were designed with a large safety factor to provide high stiffness so that deformation of the frame would be negligible. The base plates of these uprights were braced together for stiffness and were secured to the base of the Zwick mutli-axis machine via large T-slots. Bearings were mounted at the top of the uprights to support the primary frame. The primary frame, connected to the uprights via 25 mm axles, was made from rectangular (50 x 25 x 3 mm) tubular steel forming a square. At this stage the primary frame supported a bracket that secured the base of the femur. This securing point was adjustable so that the head of the hip stem in the femur could be aligned with the axis of the primary frame. Loading to the hip stem head was applied through an acetabular cup mounted in a polythene holder and attached through a loading plate on the vertical actuator. The primary frame was driven by a strut connected to the horizontal actuator via an L-shaped pivot converting the motion from horizontal to vertical. The geometry was modelled on a spreadsheet so that the primary frame could be driven from 32° flexion to -10° extension by the 100mm actuator stroke.

6.6.3. Initial testing

Once the manufacture of the 1st stage simulator was complete, a testing phase was undertaken to evaluate the performance and suggest improvements that would be needed to start the next phase of the design. The simulator was cycled to replicate femoral rotation in the sagittal plane from 32° flexion to -10° extension at 0.5 Hz (to represent a slow walk) with a loading cycle on the vertical axis from 0 to -600N run at 1Hz synchronised with the flexion extension movement in order to achieve a loading peak at the heel strike and toe off positions, see Figure 6-5. Both inputs were modelled as sine waves for simplicity at this early development stage and sent to the actuators by the cycle generator in the program. The input to the horizontal actuator was set by adjusting the rig to the maximum flexion and extension and reading the positions

of the actuator, these values could then be used in the cycle generator to drive the frame.

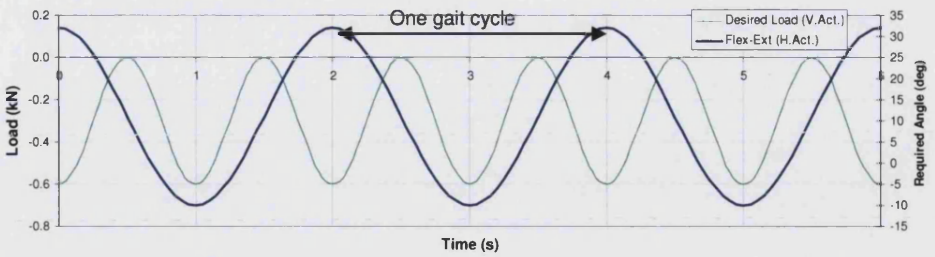

Figure 6-5 - Simulator inputs for vertical and horizontal actuators

The performance of the rig is shown in Figure 6-6 and Figure 6-7. This data shows the load and stroke of each actuator over the first six seconds of testing.

The graphs can be used as a method of evaluating the performance of the simulator to check that the desired levels of motion and loading are achieved with correct synchronisation and minimal vibration. The horizontal actuator data (Figure 6-6) shows that although the stroke is smooth and achieves the correct levels of flexion extension, the load is affected by a large degree of noise, visible as small high frequency oscillations in the system. The vertical actuator (Figure 6-7) shows that the load cycle is achieving the desired levels; however the there was also a high frequency vibration that was unsatisfactory.

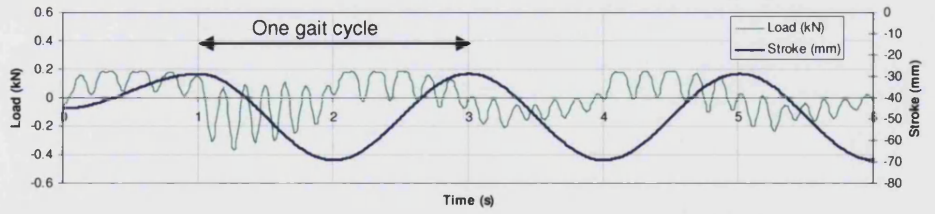

Figure 6-6 - Horizontal actuator load and stroke data (1st stage)

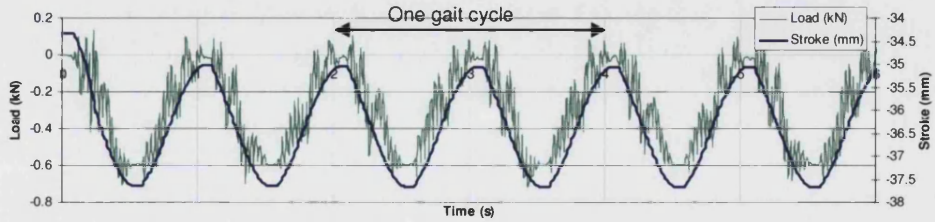

Figure 6-7 - Vertical actuator load and stroke data (1st stage) before autogain

An investigation into the cause of the vibration revealed that both actuators were running with unsuitable gains set in the control system. The auto gain function on the simulator control was used and visibly improved the systems performance. At this stage the simulator was deemed to be working satisfactorily and the next phase was initiated.

6.7. *2nd Stage – Introduction of abduction and adduction to the gait cycle*

6.7.1. Aim

The aim of this phase was to introduce the motion in the coronal plane with an abduction adduction cycle through the inclusion of a cam and follower mechanism.

The mechanism was placed in the space left in the phase one design under the primary frame. The design of this mechanism was divided into three parts.

- adding bearings on the primary frame to allow motion of the femoral support in the coronal plane,
- the design of a cam to replicate knee motion and
- a follower mechanism to the cam plate.

6.7.2. Design

The femoral bracket was disconnected from the primary frame and reattached using the same type of bearings as those supporting the primary frame. Care was taken with the alignment between two frames to ensure that the axis of motion would be orthogonal with the primary axis and projected through the centre of the acetabular loading cup.

Once the femoral bracket was set up and aligned, the femur held in the assembly was free to pivot about the femoral head of the hip stem in the sagittal and coronal plane. The rig now had the desired number of degrees of freedom

but it required a constraint to produce the desired gait pattern. A cam and follower concept was developed to control the motion which was based on the gait research presented in section 3.2. The gait data obtained from the literature describes the motion of the femur utilising the angles through which it passes during a complete gait cycle in the sagittal and coronal plane. Trigonometry was used in a spreadsheet to project these angles onto an imaginary plane in the rig where a cam would be located, Figure 6-8. The result produced an irregular shape that would involve high local acceleration and undesirable load spikes if it was to be developed into a cam. The gait was therefore simplified by the adoption of an elliptical cam shape in order to achieve smooth movement. The ellipse was generated with two sine wave functions that control the shape in sagittal and coronal planes. The simplified gait pattern was also projected onto the imaginary plane and adjusted until a good approximation was achieved. The final result is shown in Figure 6-8. The projections were used to build a model of the cam in Solid Edge (a CAD package), this process is illustrated in Figure 6-9. From this model it was clear that the follower would have to extend a large distance to follow the curve to the maximum flexion position, which introduced bending forces and the risk of dislocation from the groove. By inclining the cam plate, the maximum extension could be minimised. A simple recalculation of the cam plate geometry led to the plate pictured in Figure 6-9. The cam surface was manufactured as a deep groove on the surface of an aluminium plate, which was mounted on the two main uprights supporting the rotating frames.

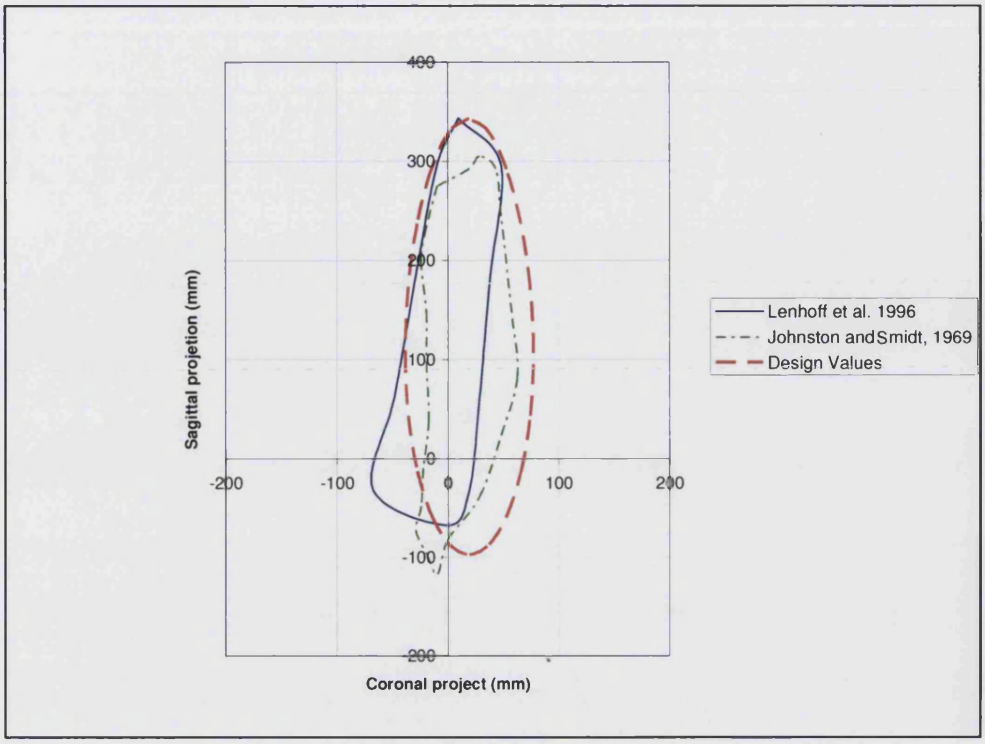

Figure 6-8 – Graph of the cam shape comparing design choices with known gait data

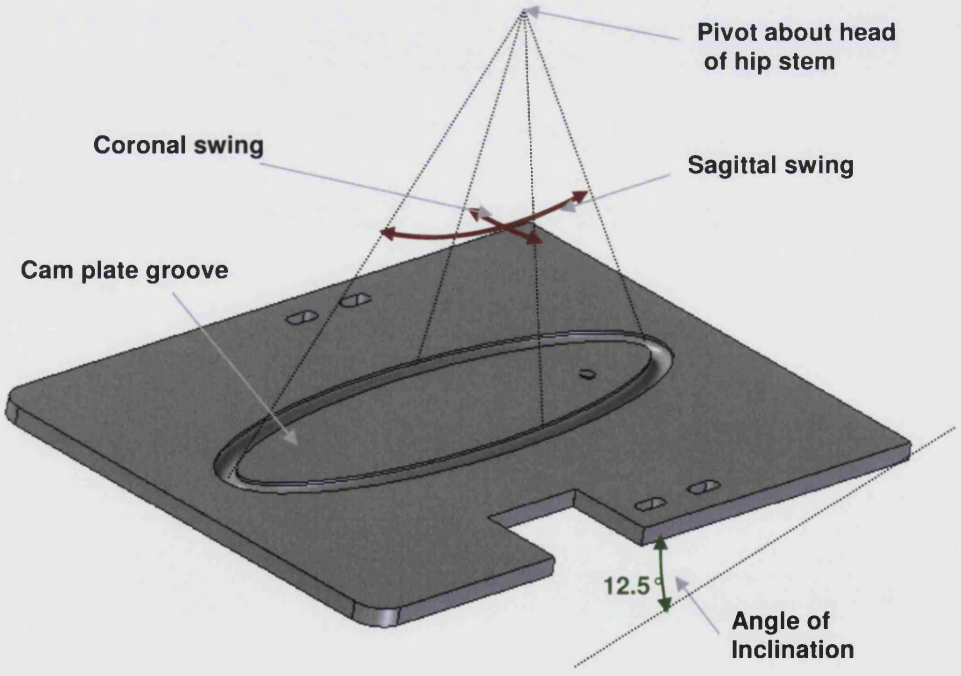

Figure 6-9 - Model of the cam plate to constrain the rotating frames

The follower of the cam plate consisted of a nylon sphere (to ensure low friction with aluminium) supported on a steel rod that was allowed to slide against a

spring applying pressure on the follower in order to keep the ball in the groove. Careful consideration was given to the geometry of the follower to ensure minimal chance of dislocation whilst providing a system capable of withstanding the forces generated and allowing the angular range of motion required.

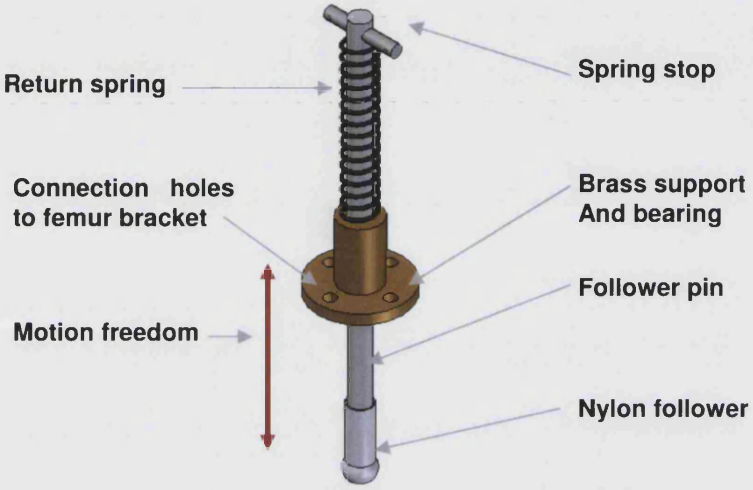

Figure 6-10 - Model of the cam follower mechanism

The cam was supported by two L shaped brackets located on the existing uprights and the follower mechanism was mounted on the base of the femoral bracket, the follower pin passed through a hole in the base of the frame to provide access to the cam plate. The original mechanism from stage 1 was used to provide flexion extension with the cam governing the motion in the coronal plane. A full CAD model of the rig can be seen in Figure 6-11.

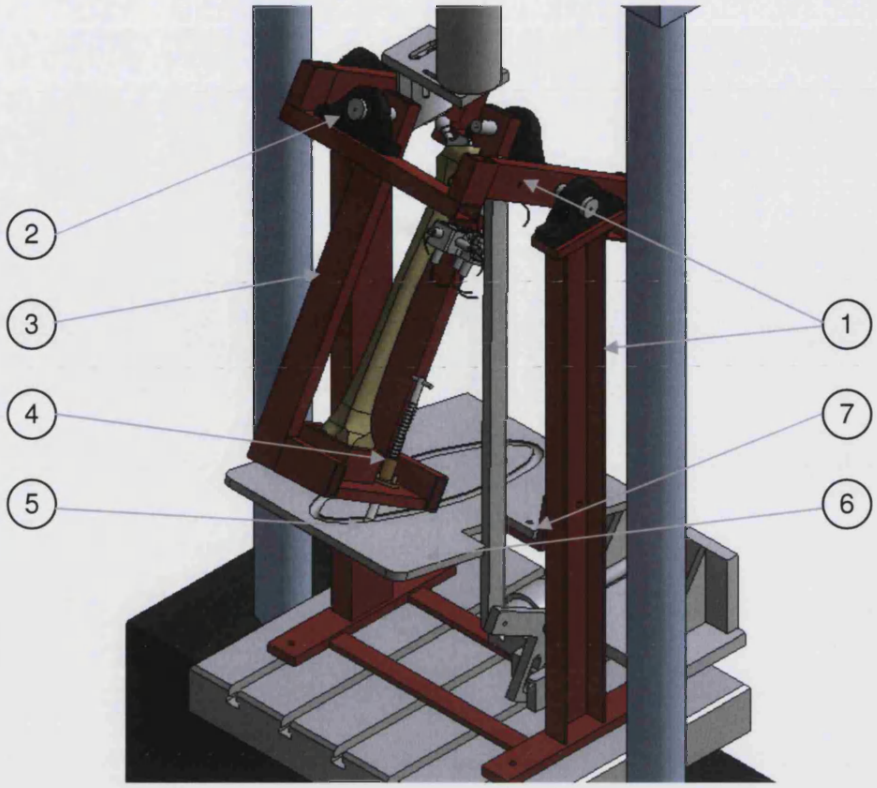

1) Original uprights and primary frame from 1st stage design
2) Femoral bracket bearings
3) Femoral bracket
4) Cam follower
5) Follower head locating in groove
6) Cam plate generating effective knee motion
7) Cam plate supports

Figure 6-11 - CAD model of the 2nd stage of the simulator

6.7.3. Initial testing

To assess the introduction of the cam and follower mechanism the rig was initially cycled using manual controls to check that the mechanism would produce the desired motion of the femur without problems. Once the femur had successfully moved round a complete gait cycle then the computer software could be used to control the actuators. The actuators were programmed to drive the primary frame in the sagittal plane to each end of the cam plate. While the primary frame repeated this motion the cam would cause the follower to move the femoral bracket in the coronal plane and generate motion from -4° and 8° to produce a simplified gait pattern. Figure 6-12 shows the desired gait pattern in both sagittal and coronal planes. Due to the complexity of the rig, the frequency

of the gait cycle was slowed to 0.3Hz. The loading cycle was in turn slowed to 0.6Hz to maintain the double peak curve.

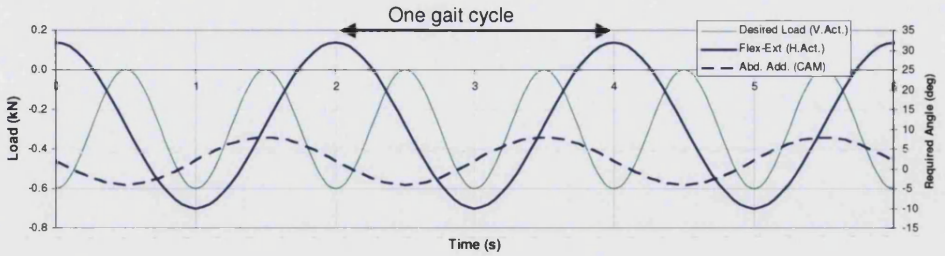

Figure 6-12 - Desired motion and loading in 2nd stage hip simulator

Initial tests showed that the femoral bracket did not make the transition from one side of the cam to the other at the heel strike and toe off positions in a satisfactory manner. The intention was that the momentum of the femoral bracket would carry the cam follower to the opposite side of the cam. However, it was found that the controller of the horizontal actuator driving the flexion extension movement had to be set very carefully. If the actuator started to pull the frame back too soon it would impact on the inside of the cam (Figure 6-13a) producing a large vibration in the machine and often resulting in an actuator overload, stopping the machine. If the actuator started to drive the frame too late then the follower would start to ride up the outside of the groove back towards the apex of the cam (Figure 6-13c). When the actuator started to draw back the follower would again strike the apex either inducing large vibration or stopping the machine through over load. If the control levels of the actuator were set up exactly, then the change of direction of the actuator would occur just after the apex (Figure 6-13b) and the simulator would complete one cycle. However, the rig was sensitive to small disturbances and it was found that the follower would not make the transition sufficiently reliably for the required test program.

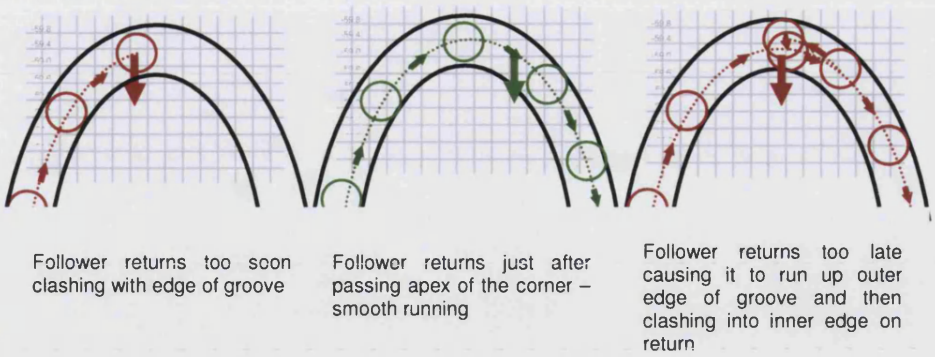

Figure 6-13 - Diagram demonstrating the critical levels of control for the follower in the groove

An external force was required to ensure that the follower made the transition to the opposite side of the cam and enable the simulator to run smoothly. This meant that two additional forces had to act on the femoral bracket. At the toe off end the follower had to be pulled onto the abduction side of the gait. At the heel strike end the follower had to be pulled onto the adduction side of gait. A solution was found using springs attached to the femoral bracket. One spring was attached to the front of the frame whilst a second was attached to the back. Both were secured on the cam plate close to each upright. At heel strike, the first spring is pulled taut whilst the second is slack, pulling the frame one way. At toe off the second spring is pulled taut whilst the first is slack pulling the frame the other way. The concept was shown to work with steel cable and springs but the slack cables often interfered with the follower. An alternative material was found with natural rubber tube as shown in Figure 6-14. The band identified (1) is attached to the front of the femoral bracket and to the adduction side of the cam. The band identified (2) is attched to the rear of the femoral bracket and the abduction side of the cam. The rubber tubes provided a better length differential between slack and taut and worked almost silently. The bands were mounted on small turntables that ensured the forces applied to the bands were always linear minimising stress on the bands and adding to the differential between slack and taut that enabled the concept to work. The concept was refined by adjusting the length of the rubber to ensure that there was just enough force to pull the femoral bracket over to the opposite side of the cam while creating minimal impact on the cam surface.

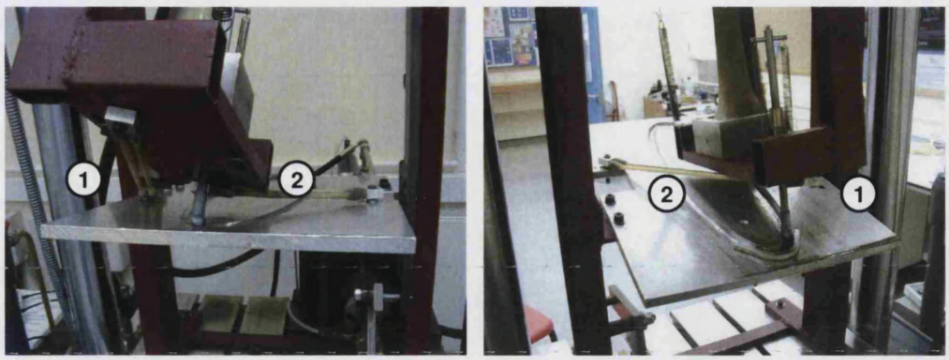

View from the front showing transition from abduction to adduction at heel strike

View from the back showing transition from adduction to abduction at toe off

Figure 6-14 - Photographs showing band transition concept

With the rig making full cycles between the abduction and adduction sides of the cam plate, attention turned to reducing some of the vibration that was evident both visually and in the data downloaded from the horizontal actuator (Figure 6-15). At this stage the vertical actuator was not used. Initially the source of the vibration on the horizontal actuator was thought to be associated to the levels set for the actuator change of direction; however the vibration did not reduce after trialling a range of different values. After further investigation and understanding of the load testing machine it appeared that adjusting the control system levels could provide an answer. The actuators are controlled with a PID (Proportional Integral Differential) system with the option of adjusting the gain for each of the components: proportional, integral, and differential. The largest effect on the vibration was produced by the proportional component, however the actuator became unstable at times. The best result was seen when the actuator was set up with the auto gain function in software package 'Workshop release 21'. The auto gain function was used, moving the actuator between levels approaching each end of the elliptical cam. These levels were set conservatively as the actuator tended to overshoot during this setup phase and cause damage to the rig. Once the gains had been set automatically, the rig was cycled again and the results can be seen in Figure 6-16. The vibration is not totally absent but significantly reduced and the motion was smoother. The overall shape of the load on the horizontal actuators is governed by the resistance of the elastic bands, oscillating the load between 0.5kN and -0.4kN.

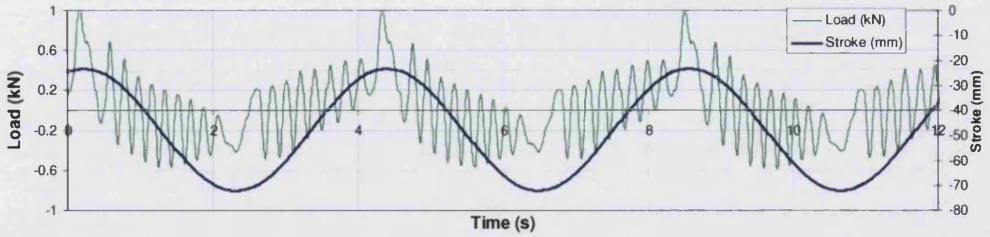

Figure 6-15 – Horizontal actuator results with double band working, prior to auto gain

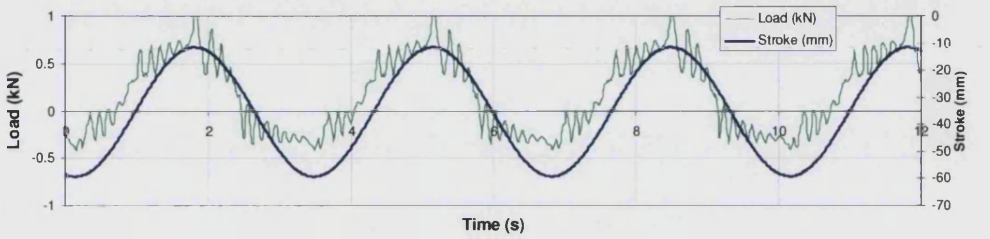

Figure 6-16 – Horizontal actuator results after gain set up

Once the horizontal actuator was operating acceptably the vertical actuator was reintroduced. During the first cycles of the simulator it became apparent that even though the loads applied were relatively low the vertical actuator has to move a large distance to apply the load. This is due to the bending of the composite femur under loading at high levels of flexion where the loads on the femur are more in the anterior-posterior direction. To solve this problem a clamp was introduced to support the femur proximally thereby reducing stroke required by the loading actuator would need to move. The position of this clamp was important as the more proximal the clamp then the shorter the effective length of the femur thus offering the best possible chance that the head of the hip stem remains aligned with the axis of motion. However, any clamp must not interfere with the stability of the hip stem. Polgar *et al.*, 2003 suggested that in order to clamp a femur without affecting the proximal strains the clamp must be positioned at a distance of at least one diaphysis below the distal tip of the stem. In Sawbones composite femora the diaphysis measures 35mm and the tip of the SL PLUS stem reaches approximately 180 mm along the length of the femur measured from the femoral head. Therefore, the highest possible position of the clamp is at least 215 mm below the head of the stem. At this point the shape of the shaft of the Sawbones femur makes it awkward to hold so a cast was taken and a split clamp was made that could be compressed around the shaft by anterior and posterior screws. The clamp located against a lateral plate that ensured the position of the femur in the coronal plane. The overall assembly is

shown in Figure 6-17 and was attached to the femoral bracket via four screws.

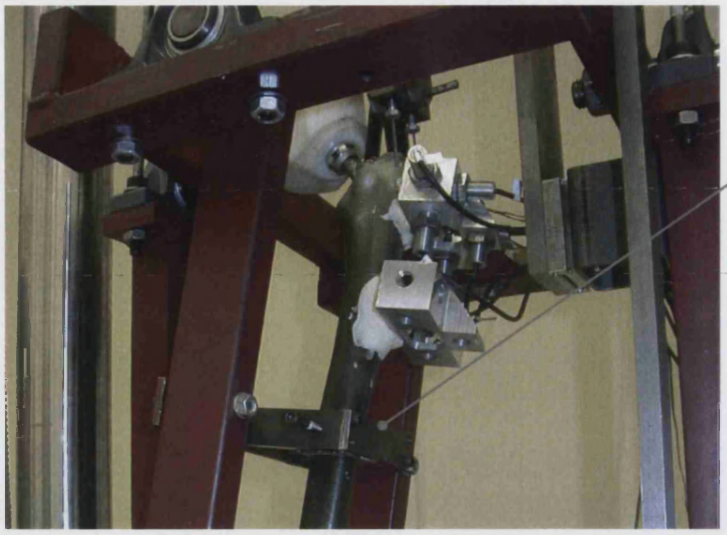

Figure 6-17 - The femoral clamp used to minimise any deflection of the composite femur during loading

The addition of the femoral clamp reduced the deflection of the composite femur during loading and lowered the levels of displacement recorded from the vertical actuator. This improved the ability to accurately control the load applied on the femoral head and allowed more complex load patterns to be included.

Previously as a first approximation in the development of the simulator, the loading pattern on the femoral head had been represented by a sine wave at twice the frequency of the gait. The Zwick testing machine is capable of running user defined loading profiles so it was possible to implement a more physiological loading regime. Section 3.3 presents data from Hip 98 which provided data on *in vivo* hip contact forces. This data was used by the profile generator program in the Zwick loading machine software. The Zwick load testing machine required that the same control methods must be used for both actuators. To achieve this, a spreadsheet was written to produce control data for both actuators instead of the normal sine wave cycle generator. The spreadsheet used 'average' data compiled from patients presented in HIP 98 (Bergmann *et al.*, 2001) to produce a double peak wave normalised (from 0 to 1) for the vertical load and a synchronised sine wave that would drive the horizontal actuator between the two transition points on the cam.

The profiles were programmed into the software used to control the Zwick machine, the hip contact force being used to control the vertical actuator and the sine wave used to control the horizontal actuator. The two profiles were cycled on the simulator and the resulting load and stroke data were downloaded from the machine. Initially, when the data from the actuators was compared with the demand profiles there was a small time lag between the profiles. Small offsets and scaling coefficients were applied to the input profiles and the simulator was run through iterative steps until the data downloaded from the actuators matched the initial demand. The synchronised data downloaded from the actuators is shown in Figure 6-18.

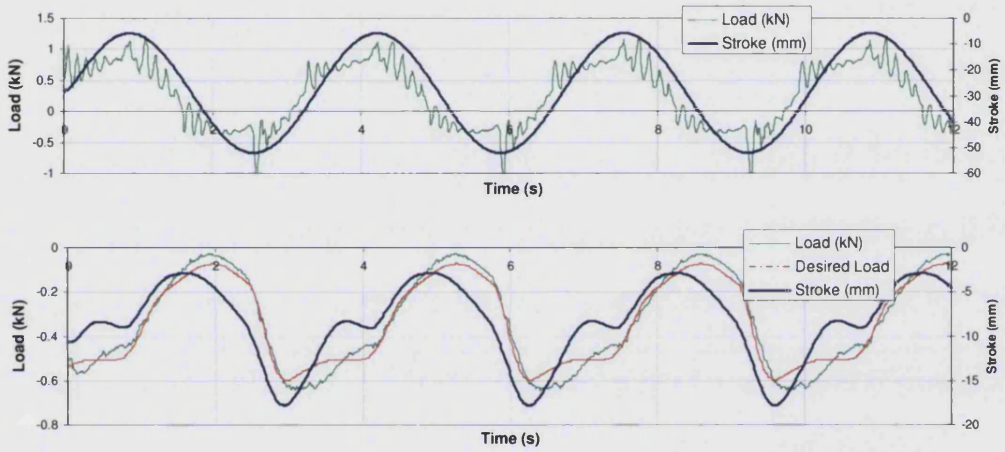

Figure 6-18 – Profiled loading regime is use, horizontal actuator (top) Vertical actuator (bottom)

The results in Figure 6-18 show the horizontal actuator in the top graph performing with low vibration and achieving the transition from abduction to adduction. The performance of the vertical actuator is shown in the lower graph where the demand load is shown in a red line which can be compared to the actual load downloaded for the actuator. A comparison between the demand and actual load shows several key similarities,

1) a similar magnitude of peak load is achieved,
2) the peak load is applied at the desired time and
3) the swing phase of the gait cycle is synchronised with the femur on the abduction side of the cam.

The only difference between the demand and actual load is around the plateau after the main peak in the demand where the actual load reduces. In early trials there was vibration between the main peak and the plateau but this was reduced by automated adjustment of the gains. The gains of the PID controller were adjusted manually as the auto gain could only optimise the controller to produce a simple sine wave.

The status of the simulator at this stage was a fully synchronised rig producing flexion extension and abduction adduction of the femur with a loading cycle reproducing a pattern similar to those measured in postoperative gait. The simulator at this stage equalled the degrees of freedom modelled by the Liu simulator (2003). The major difference is that the coronal rotation of the femur is replicated rather than transverse rotation. The simulator in this state would be capable of assessing the effect of femoral kinematics on hip stem stability. However it was decided to include muscle load on the simulator in order to make the results more comparable with the static studies already presented in section 2.4 (Clements *et al.*, 2005; Britton *et al.*, 2003; Claes *et al.*, 2000).

6.8. *3rd Stage – Including an abductor muscle in the simulator*

6.8.1. Aim

The aim of the 3rd stage simulator was to include a muscle loading system that would replicate the action of the abductor muscles. This muscle group was highlighted as the most influential muscle groups on femoral head loading in section 6.4. The system was designed to apply a force to the femur at specific times and magnitudes in order to model the action of the abductor muscles as they act *in vivo*.

6.8.2. Design

The normal setup of a muscle loading system for a hip stem stability test can be seen in section 5.5. In the static studies muscle loading alters the direction of the load applied to the femoral head and applies a mechanical advantage that

increases the magnitude of the applied force. Including a system to replicate muscle forces in a dynamic simulator introduces a problem with the line of action of the abductor muscles as this changes throughout the gait cycle while the femur rotates in both the sagittal and coronal planes.

The design parameters for the inclusion of the action of the abductor muscles were based on the same data as the femoral head contact force pattern used in the previous section: HIP 98 (Bergmann *et al.*, 2001). The desired timing and magnitude of the muscle loading is presented in Figure 6-19.

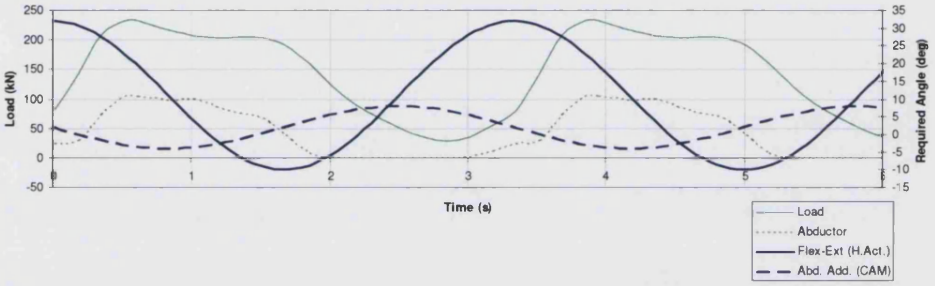

Figure 6-19 - Desired motion and load for the 3rd stage rig including the force pattern for the abductor muscle

The first iteration of the design concentrated on mounting the plate connecting the vertical actuator to the acetabular cup (Figure 6-20). The plate used to transfer load to the femoral head was replaced with a similar plate (3) to that used during the static studies to act a as 'pelvic substitute', (see page 77). This was intended to maintain the geometry adopted during the static studies to make the results from the dynamic simulator comparable to the static ones. A second plate (the offset plate 1) was directly connected to the vertical actuator and a pillar was use to apply the actuator load to the pelvic substitute. The muscle strap (6) was attached to the femur in the same way as in the static studies and joined to the mounting plate via a rocker (5) that allowed it to move with the flexion extension cycle of the femur. The initial setup is pictured in Figure 6-20.

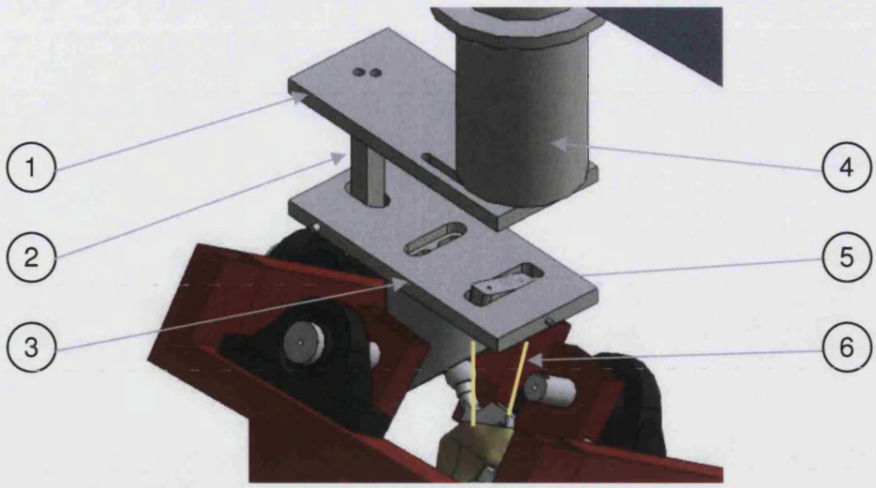

1) Offset plate
2) Vertical pillar
3) Pelvic subsitute
4) Vertical actuator
5) Muscle rocker plate
6) Muscle wires *(highlighted in yellow)*

Figure 6-20 - Initial attempt at including muscle loading system in the dynamic rig

This system was tested in the simulator but failed in two key areas. The main problems were caused by off-axis loads generated on the vertical actuator and by dislocation of the follower in the cam groove. The off-axis load on the vertical actuator was caused by the direct connection of the offset plate which induced instability in the actuator. This instability produced unpredictable motion and caused large vibration which was reflected in the downloaded data. The extent of this vibration could not be reduced with gain setup. The dislocation of the cam was caused by the force of the muscle trying to rotate the femur towards the abduction side of the cam and lifting the follower out of its shallow groove. Neither of these problems could be solved with minor adjustments and resulted in significant changes having to be made to the simulator.

To counteract the off-axis load on the vertical actuator the direct connection between the rig and the vertical actuator had to be removed. The load would have to be applied through a ball-on-plate set up that would not constrain the rig horizontally. This would achieve the desired compressive load without transferring any off axis loads onto the vertical actuator. The muscle loading system was changed to a bracket attached to the main uprights via a linear slide. This system operated satisfactorily and can be seen in Figure 6-21.

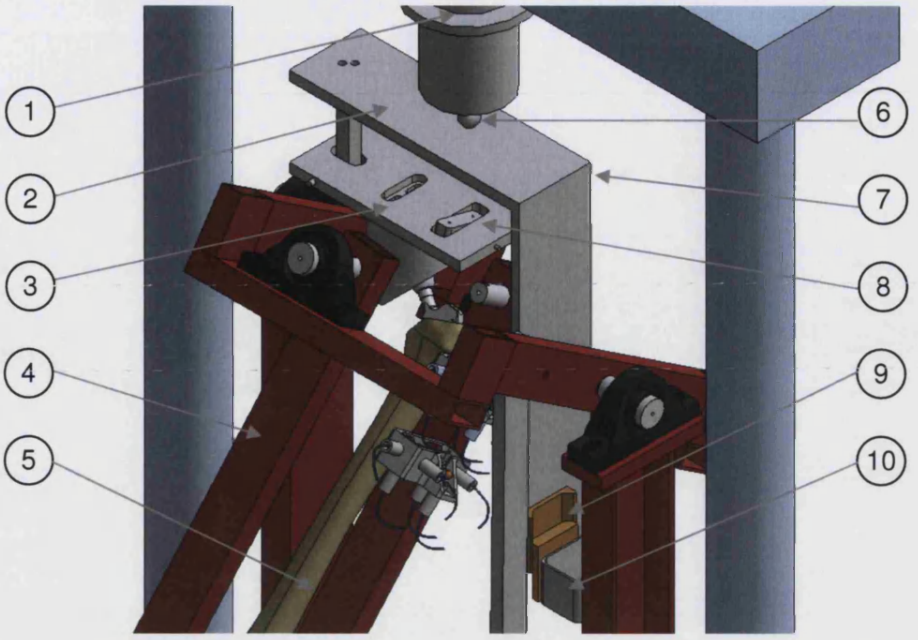

1) Vertical Actuator
2) Muscle system support bracket
3) Pelvic substitute
4) Femoral bracket
5) Composite femur
6) ball on plate loading
7) Welded joint
8) Muscle rocker plate
9) Linear slide
10) Slide mount

Figure 6-21 - 3rd stage design of simulator

The dislocation of the cam follower was a harder problem to solve. This resulted in a large design change to the main cam plate in order to secure the follower more satisfactorily and avoid dislocations. The new design had to be capable of reacting the force generated by the abductor muscle so that the femur could still follow round the cam generating the desired motion.

Initial ideas to solve this problem included building up the groove wall or using a mushroom shaped follower that could be restrained in the groove. Attempts to implement these ideas failed to stop the dislocation and a re-design of the cam system was initiated. The new concept adopted a cylindrical roller on a rigid follower that would be guided along the side of the cam. The follower would require contact with the full perimeter of the elliptical cam therefore an additional support to hold the cam was provided from below. Alignment became an important part of the setup. The edges of the new cam were all rounded to prevent wear on the follower and material on the outer parts of the cam was removed to prevent the transition points at heel strike and toe off from being over constrained. The new plate was machined on a multi axis milling machine from the design shown in Figure 6-22.

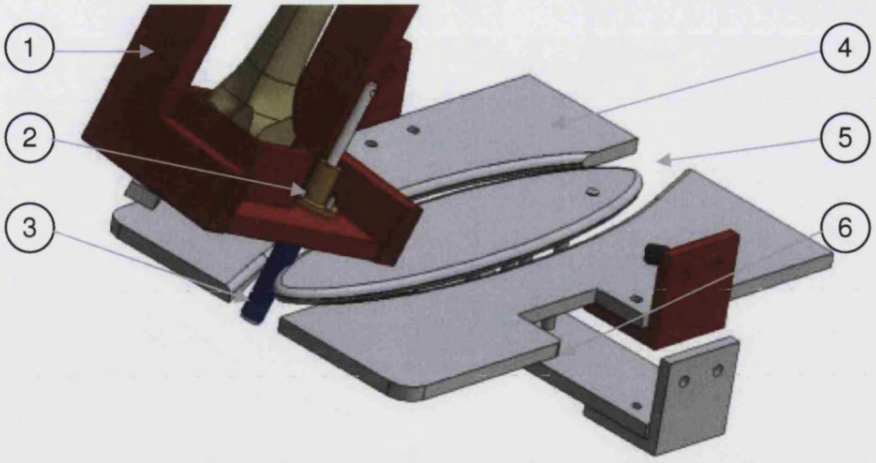

1) Femoral bracket
2) Rigid follower
3) Roller follower
4) New cam plate
5) Material removed to reduce constraints
6) Support bracket for central section

Figure 6-22 - Redesigned cam plate with follower and support bracket

6.8.3. Initial testing

The testing began by checking the performance of the new cam. Initially a sine wave was used to drive the horizontal actuator between the two transition points on the cam at the heel strike and toe off positions. Small adjustments were made with the position of the cam plates until the transitions were reliable. The vertical actuator was then tested separately with the muscle loading system. Loads were applied up to 1kN by the vertical actuator to ensure that the abductor cable and assembly did not fail. Once both systems had been checked, the simulator was tested with both actuators running simultaneously. The inputs to the actuators were the same as those used initially in the 3rd stage and are presented in Figure 6-19.

The load and stroke data downloaded from both actuators are shown in Figure 6-23. The horizontal actuator successfully guided the cam follower around the cam and the transitions at the toe off and heel strike positions were achieved with minimal vibration. The motion on the vertical actuator was not consistent with the force applied and the whole machine experienced a high frequency vibration at some stages of gait. Figure 6-23 shows this vibration in the load cycle of the vertical actuator at about 1.8, 4.6, 8.2 and 9.8 seconds. These times coincide with the swing phase of the gait as the femur is guided towards the abduction side of the cam.

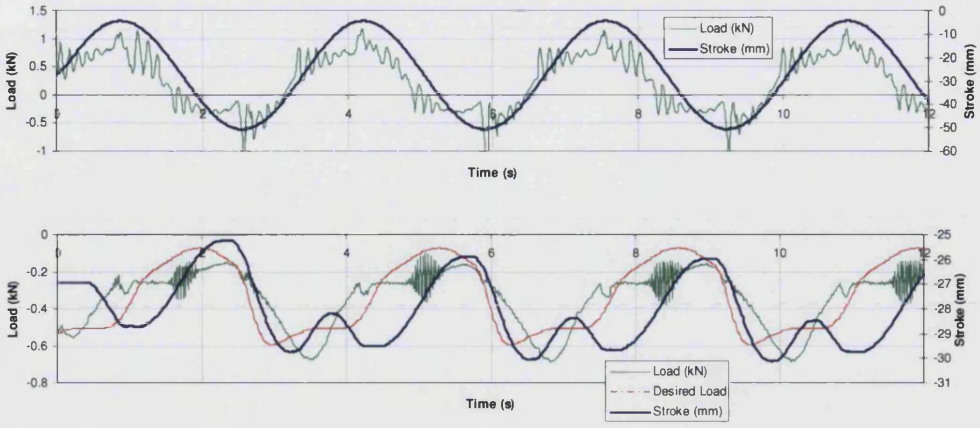

Figure 6-23 - First results from the 3rd stage simulator (Horizontal actuator top – vertical actuator bottom)

Previous problems with vibration had been solved with manual adjustment of the PID controller but a similar approach was not successful. Technical advice from the manufacturers of the materials testing machine (Zwick) suggested the use of a Butterworth filter in the control system for the actuators. The suggestion was made as the inclusion of a steel cable, modelling the abductor muscle, had added another degree of compliance to the system and so a 2nd order control system was required. The Butterworth filter removed high frequency feedback from the actuators. The simulator was tested again using the same actuator inputs and a Butterworth filter removing any control signals over 10 Hz. Figure 6-24 shows the load and stroke data downloaded from the actuators. The high frequency vibration visible in Figure 6-23 on the vertical actuator was reduced to minimal levels and the simulator ran smoothly with the femoral bracket making satisfactory transitions across each side of the cam.

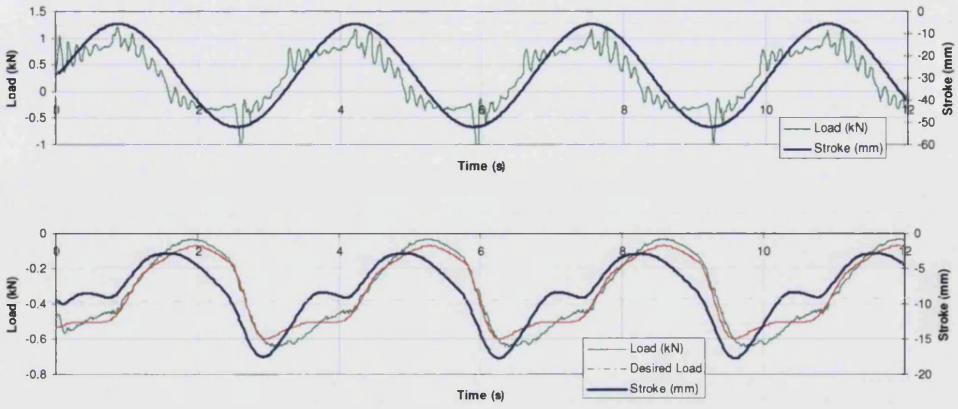

Figure 6-24 - 3rd stage simulator running including the Butterworth filter, horizontal (top) and vertical actuator (bottom)

The simulator at this stage was operating reliably and satisfactorily thus the design phase was complete. However before using the simulator to assess the original research objective, it was fully evaluated and tested to ensure that this prototype design was robust enough to provide reliable data.

6.9. *Evaluation*

In section 6.4 the ideal simulator was considered and the parameters required to create a physiological model of the hip were ranked in accordance to their importance. During the development phase mechanical features were incrementally included through three stages until the simulator performed reliably and achieved a reasonable representation of the physiological loads and motions during the gait cycle. The 2nd stage of the simulator, where motion was modelled in two planes was comparable with the Liu simulator (Liu *et al.*, 2003). The further development aimed at including muscle forces resulted in the hip stem in the simulator experiencing a more physiological loading pattern. It was then important to assess each of the loads and motions to check that there was no negative interaction between the features and that the prototype was robust enough to reliably allow the application of the number of loading cycles required for each micromotion test. The motion, load and endurance are assessed in this section by comparison with values described in Chapter 3.

6.9.1. Motion

The desired motion of the simulator was developed from data available from the literature on gait studies. These offered comprehensive data on the exact motion of the femur during the gait cycle. To model any of these studies exactly was deemed too complex a task so an elliptical motion was adopted. The demand cycles were modelled by two sine waves to represent the motion in the sagittal and coronal planes. The design values thus obtained are shown as a reasonable approximation in Figure 6-25 as red lines (demand). The sagittal demand motion ranged from 32° flexion to 7° extension and the coronal motion ranged from 8° abduction to 4° adduction. The blue lines in Figure 6-25 display the actual angles achieved by the femur as it passed around the cam. Comparisons between the demand and actual position of the femur indicate that the cam achieved the desired timing for the femur position and ranges of motion of the gait cycle with good accuracy. This combined with the design changes applied to the follower, ensured that the motion generated by the simulator was smooth and characterised by low friction.

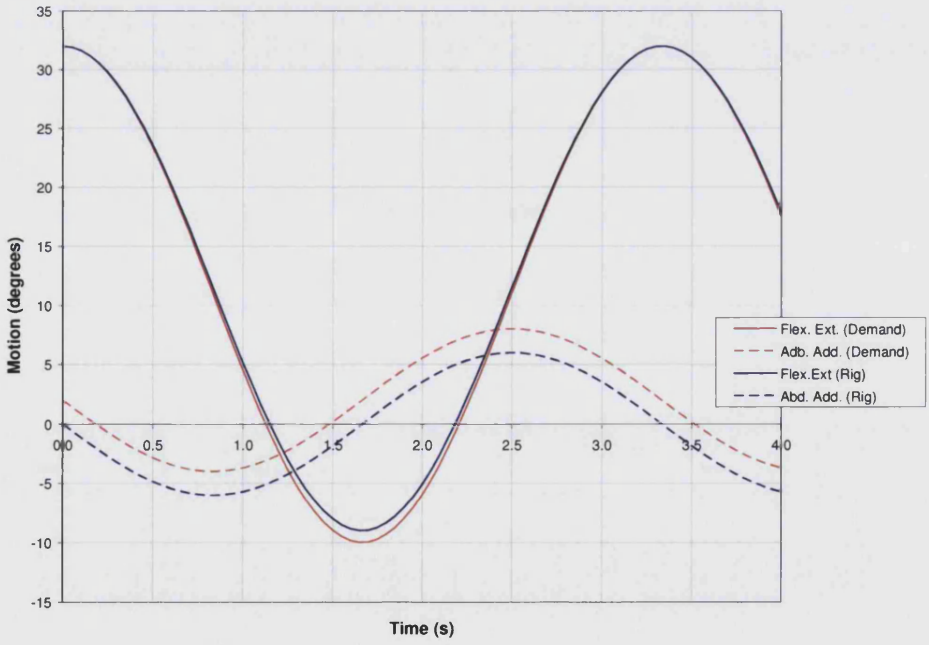

Figure 6-25 - Motion of the simulator with the demand positions compared to actual motion of the femur

The discrepancy between the demand and actual position of the femur was caused by small adjustments to the alignment of the cam plate. These

adjustments were necessary to ensure that the follower made the transitions across to each side of the cam. Ideally the two curves for the demand and actual position of the femur would match exactly. This could be achieved by repositioning the cam plate laterally but as the simulator performance was good in other areas, the small differences were accepted.

6.9.2. Applied load

The loading cycles on the simulator were based on *in vivo* values obtained by Bergmann *et al.*, 2001 and sourced from the data available in Hip 98. Figure 6-27 compares the demand loads that the simulator was designed to achieve (red) and the actual loads (green) measured in the simulator. At this stage the femoral head load was calculated from the applied load multiplied by the mechanical advantage of the muscle system. The muscle forces were measured directly by strain gauges attached to the muscle cables (Figure 6-26). Design notes and calibration of the gauges can be found in Appendix III.

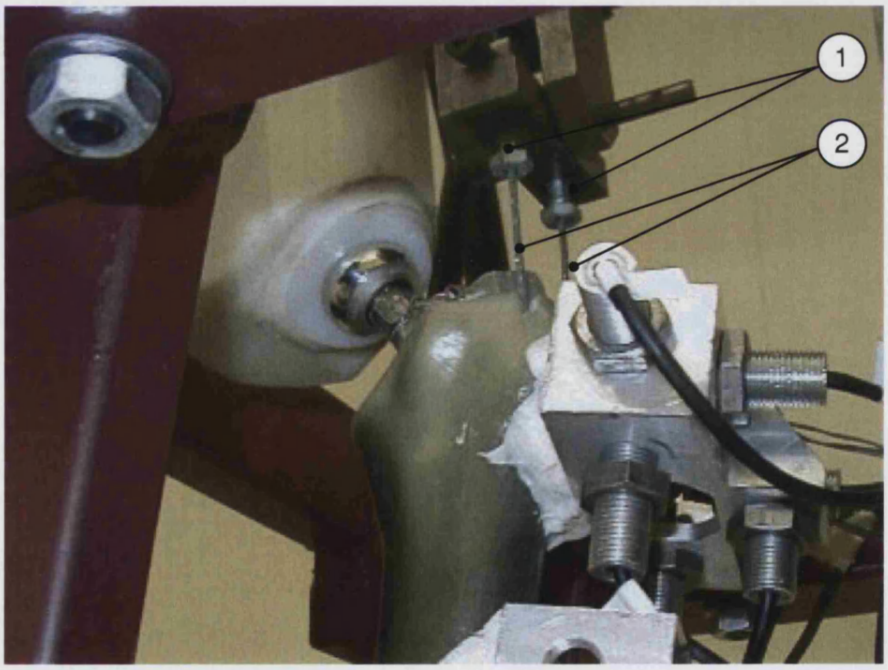

1) Tension adjusting screws
2) Muscle Cable

Figure 6-26 - Photograph of the muscle cables

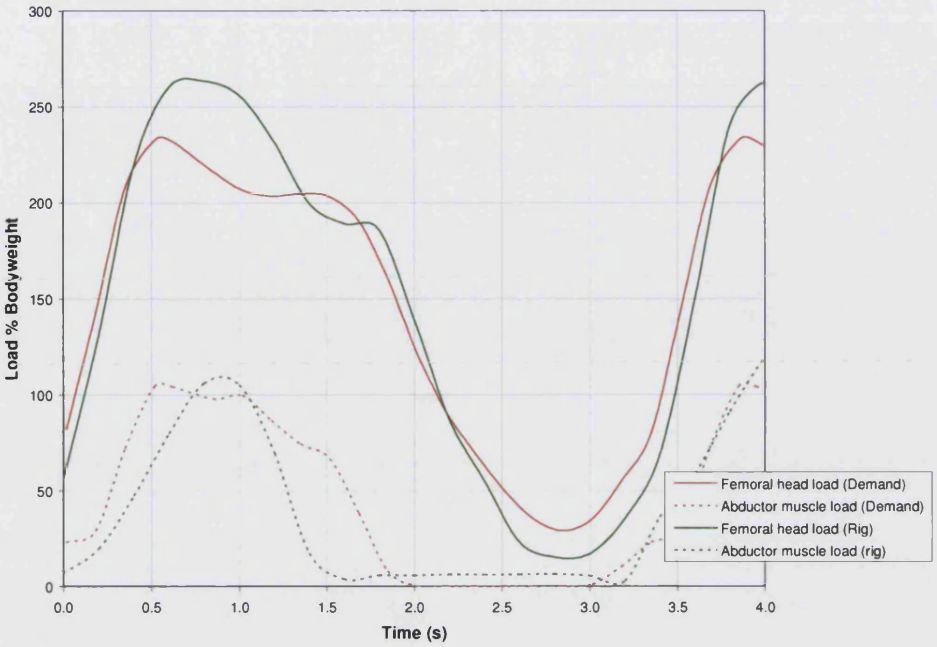

Figure 6-27 – Femoral head and muscle loads in the simulator compared to in vivo data

The loads shown in Figure 6-27 are presented as a percentage of bodyweight in order to facilitate comparison with the Hip 98 data. The demand and actual load compare favourably for both the muscle and the femoral head loads (Figure 6-27). The estimated femoral head load was higher than the demand, this assumed to be due to the overshoot of the vertical actuator due to the high gains used. This head load could be reduced in the experiment phase by setting the demand slightly lower. The peak load of the muscle force was applied at a very similar time to the peak force of the abductor muscle recorded *in vivo* during the gait cycle. This occurred because the muscle system acted as a lever system synchronising the femoral head and muscle loads. One initial concern about the muscle loading system was the change in length of the muscle cable as the femur moved from abduction to adduction. This rotation will increase the distance between the greater trochanter and the substitute pelvis, effectively stretching the cable and applying tension. This action actually seems to have assisted the operation of the muscle system as the vertical actuator travels a shorter distance to tension the muscle and apply the femoral head load.

In general the loading of the simulator during the dynamic gait cycle was satisfactory as the loads were appropriately synchronised with the phases of gait and the correct magnitudes were achieved. In this state the simulator is the

only current simulator available to include femoral kinematics with a muscle loading system. This simulator should provide comparable data to assess the results produced when the simulator is dynamically cycled to the results produced when the femur is held static. Thus the simulator is capable of exploring the research objective 4 (Chapter 4).

6.9.3. Endurance testing

The final part of the assessment was to ensure that the simulator would be robust enough to run a full loading cycle of 200 repetitions without any adjustment or failure of any components. The endurance test involved running the simulator through 1000 cycles, i.e. five times longer than any of the experimental tests. The test was intended to predict possible failure mechanisms and highlight signs that could be used as an indicator of impending failure. A longer endurance test was considered but, as the simulator was still at a prototype stage and the risk of component failure leading to the possibility of a large machine failure was considered unacceptable, the test was kept reasonably short. Any technical problems with the simulator could be fixed between experimental batches of 200 cycles. The endurance test was performed over 1000 cycles which were carefully monitored for any irregularities which could be indicators of problems.

The endurance test identified some areas where small features of the design were unreliable but in general these were fixed with simple changes. The simulator is capable of running far longer than the individual series of 200 cycles, however, any failure could be a serious event with the potential of damaging the equipment. This could result in time delays and expensive repairs and therefore it was decided that the simulator should be monitored throughout all testing. A small amount of maintenance work that will keep the machine functioning in good order is suggested in Table 6-3. This maintenance can be performed between each set of 200 cycles and after femur changeovers.

The simulator completed the 1000 cycles without any breakdown but there were signs on the machine that would have led to possible failures had the test continued. These observations and failures are noted in Table 6-3.

Observation	Cycle	Probable Failure	Action	Recommendation
Degradation of rubber tubing when rubbing on sharp surface	550	Rubber tubing failure – disabling the transition from one side of the cam to the other	Surfaces near tubing filed smooth	Tubes should be inspected after each batch of 200 cycles
Loosening of screws on femur clamp	770	Femur loosening leading to poor results	Thread lock used on all screws	Tightening of screws in the mechanism at each femora change (6 sets of 200 cycles)
Squeaking of roller	820	High friction leading to early wear on the roller	Roller lubricated	Apply lubrication to roller after each set of 200 cycles
Muscle cable lengthening	900	Vertical actuator gradually moving further to apply load – generating possible clash with primary frame	Muscle cable changed for stiffer variety and clamping mechanism altered	Monitor carefully during test but the small redesign should have removed this failure

Table 6-3 - Observations from endurance test

6.10. *Conclusions*

The final design of the 3rd stage simulator is capable of producing a normal gait whilst synchronised physiological loads are applied through a pelvic substitute; these include the force generated from the action of the abductor muscles. The main parameters of performance for the simulator are listed below:-

Motion

- In the saggittal plane the simulator replicates femoral motion from 32° flexion to -8° extension
- In the coronal plane the simulator replicates femoral motion from 6° adduction to 6° abduction

Loading

- Femoral head loads achieved are 260% of load applied to the rig and physiologically profiled which is an excellent replication of *in vivo* hip loading.

- Abductor muscle forces achieved are very close those experienced *in vivo* and synchronised to act at physiological times

Endurance

- The simulator is capable of running up to 1000 cycles
- Regular checks are advised between each set of 200 cycles

Test specimens

- The simulator is designed for use with Sawbones composite femora implanted with SL Plus hip stems
- The use of which has been validated in Chapter 5

The simulator could be represented using Viceconti's classification as (2; yx / 2; zy). This classification means that this simulator is the only bone implant motion simulator to include the effect of femoral kinematics in the coronal plane and the effect of abductor muscle loading during gait.

The simulator is capable of loading test specimens both statically or dynamically. Therefore, the simulator characterised by these loading and motion parameters, allows the investigation of the influence of femoral kinematics on hip stem stability (Objective 4).

Chapter 7. Dynamic Testing (Objective 4)

7.1. *Introduction*

Pre-clinical testing of cementless hip stems is an essential stage in their development. During these tests it is important that all factors that could affect the longevity of a hip replacement are considered and modelled. The immediate postoperative stability of cementless hip stems is critical to is the long-term survival and the testing methods have concentrated on loading levels, measurement techniques and selections of muscles to be included in the models but only one other study has investigated the effect of kinematics on hip stem stability (Liu *et al.,* 2003). Consequently, most of the data available from the literature results from experiments where the femur is held statically in either single leg stance (SLS) or stair-climbing (SC) (Callaghan *et al.*, 1992; Clements *et al.*, 2005; Berzins *et al.*, 1993; Britton *et al.*, 2003).

The aim of this study was to assess the effects of the kinematics of the femur on the bone implant motion in a composite femur. The assessment was performed using the simulator developed in Chapter 6 (and shown in Figure 7-1) mounted on the Zwick multi-axis materials-testing machine. The simulator replicates the movements of the femur in the coronal and sagittal plane, these are synchronised to replicate a standard gait loading cycle which is applied with the use of an abductor muscle strap.

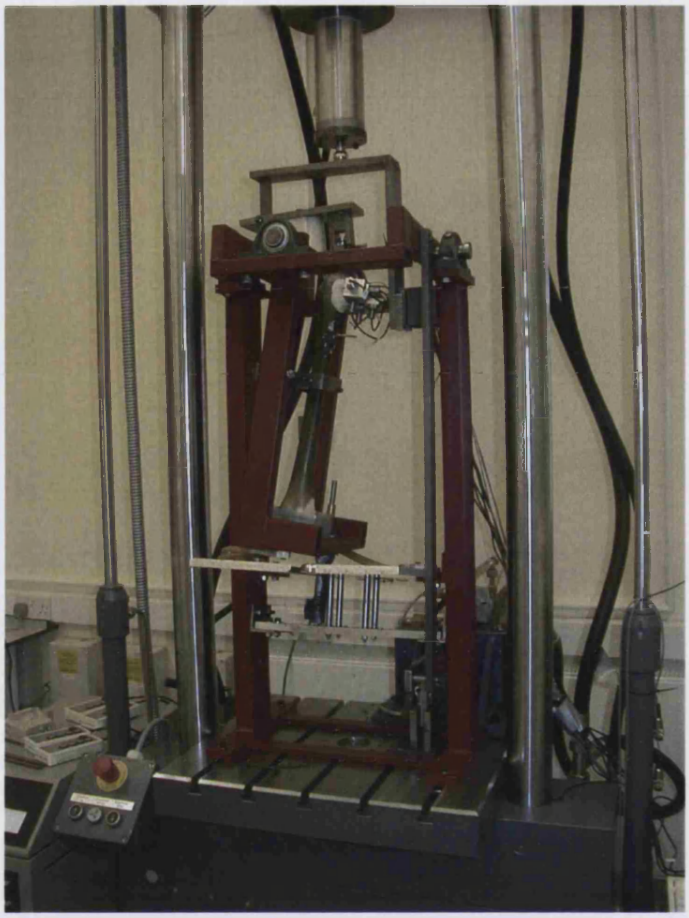

Figure 7-1 - Photograph of the experimental rig

During this testing most of the load was applied to the femur at varying angles. To ensure that potential differences between the results are not purely due to application of the load at different angles, part of this study consisted of the assessment of stability at different "static" positions around the gait cycle. Therefore a set of static studies was performed at strategic phases in the gait cycle for comparison to the dynamic data.

7.2. *Test specimens – Sawbones composite femora*

Six size 7 SL Plus stems (PLUS Orthopaedics AG, CH) were implanted into Sawbones® composite femora (Pacific Research Laboratories Inc (Vashon, WA). An abductor strap was attached to the greater trochanter and motion transducers were mounted on the lateral side of the femur as described in section 5.4. The specimens were mounted to the femoral bracket at the knee joint fitting into an aluminium pot. Woods metal was then melted and poured

around the knee section to ensure that the specimen was securely fixed. The specimen was then ready to be mounted on the simulator.

7.3. *Preparation of the simulator for dynamic and static testing*

The specimen, as prepared in the previous section, was mounted onto the dynamic simulator described in Chapter 6. The specimen was attached to the femoral bracket via two bolts through the woods metal pot. At this point care was taken to align the head of the hip stem exactly with the two orthogonal axes of the primary frame and femoral bracket. Alignment of the head with the bearings of the primary frame was achieved by careful positioning of the base and alignment of the head with the femoral bracket was achieved through adjustment of the mid femoral clamp.

The steel cables modelling the abductor muscle were then passed through the tensioning bolts, clamped by grub screws and tightened until the cables were of approximately equal tension. Tensioning of the steel wires was performed with the femur in a vertical position on the adduction side of the cam. This was the optimum position to tension the cables as it represents the phase of gait where the maximum tension would be reached during the simulators gait cycle therefore offering the best chance to control the motion of the muscle loading plate. Earlier in the development of the simulator, transducers with strain gauges were used to set the tension. However, since a minor redesign of the abductor strap mount, bringing the pivot point of the abductor strap in line with the femoral head, the transducers were removed due to space constraints.

The simulator was then manually moved through a full cycle of the cam to the toe off position of gait at the back of the cam and then up the abduction side to the heel strike position at the front of the cam and back to the upright position. This ensured that: -

- the motion transducers did not impinge the muscle loading bracket
- the transition from adduction to abduction at toe off was smooth
- the transition from abduction to adduction at heel strike was smooth
- the head of the hip stem maintained alignment with the axes of the primary and femoral bracket
- there were no unexpected events or motions that may indicate a problem

The femur was repositioned for better alignment or the tension of the muscle cables was adjusted until the operation was satisfactory. Setting the tension of the muscle was critical, too high a level of tension and the femoral bracket would not move across at the heel strike transition zone, too low a level of tension and the toe off transition was too harsh causing large vibration through the femur. The strain gauged muscle cables would have been advantageous for setting the cable tension. However, it was assumed that as long as the femur completed cycles of the cam with minimal vibration the tension in the cables would be governed by the load applied from the vertical actuator.

Once satisfactory manual running had been achieved, the stroke of the horizontal actuator was recorded at the positions of the toe off and heel strike transition. These two actuator positions were entered into a spreadsheet used to create a sine wave profile for the load testing machine software. The values were labelled as Level A for toe off and Level B for heel strike. The sine wave created in the spreadsheet was imported into the 'Profile' software of the Toolkit suite and the simulator was cycled with just the horizontal profile to ensure that it had been programmed correctly. The vertical profile was also programmed from the same spreadsheet with the original data from Bergman and Hip 98(Bergmann *et al.*, 2001). The spreadsheet was used to normalise the Bergman loading profile from 0 to 1 and the load testing machine software was later used to scale this profile to the desired magnitude of force. A function was also used to offset the profile forwards or backwards in time to ensure synchronisation with the profile used on the horizontal actuator. The two profiles (loading on the vertical actuator; motion on the horizontal actuator) were then cycled together and final adjustments of the rig were made to maintain smooth running.

Once the simulator was running reliably the femur was moved around the cam to the single leg stance position defined in Figure 7-2 and the vertical load was applied at 600N through 200 cycles to allow the hip stem in the femur to bed in thus removing the high initial migration often seen during stability tests. The same 'run in' cycle was used in the cadaveric studies seen in sections 5.8 and 5.7 but at lower loads of 200N, and 300N (Gheduzzi *et al.*, 2003; Clements *et al.*, 2003).

7.4. *Loading Configurations and dynamic motions*

7.4.1. Introduction

The aim of this study was to assess the effect of including femoral kinematics on hip stem stability. Six composite femoral implanted with an SL-Plus hip stem were tested with various static and dynamic loading regimes on the dynamic hip simulator described in Chapter 6. The simulator developed for this purpose has been designed to replicate a slow walk which in Chapter 5 has been represented by the loading regime single leg stance (SLS). SLS is characterised by the femur being held statically in 11° adduction and 7 ° flexion. It is important to note that static results were obtained from a rig fitted on a different materials testing machine and differences between the rigs and loading machines may affect the results, consequently the static trials were repeated on the dynamic simulator. A simple comparison between a dynamic gait (including the motion of the femur in the sagittal and coronal plane) against a static regime modelling SLS was considered. However the peak load (which has been shown to induce peak motion) during a dynamic loading cycle is not applied with the femur at the same angle as in the static single leg stance study. Any difference in the results could be attributed to the angle of the femur rather than to the dynamic motion. Therefore it was decided that static studies should be performed at strategic positions around the gait cycle applying an identical loading regime to the dynamic motion. Analysis of the results would then highlight which static regime provided the best model for a slow walk.

7.4.2. Static loading configurations

The positions for static trials were set along the adduction side of the gait. During abduction the femur is swinging back to the heel strike position and is mainly unloaded therefore loading trials were inappropriate.

Heel Strike (HS)	Initial Stance (IS)	Single Leg Stance (SLS)	Toe Off (TO)
			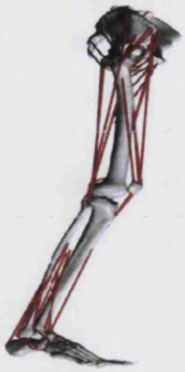
0% Gait	18% Gait	30% Gait	50% Gait
32° Flexion	20° Flexion	7° Flexion	7° Extension
3° Abduction	6° Abduction	6° Abduction	0° Abduction
Machine load - 600N	Machine load - 600N	Machine load - 600N	Machine load - 600N

Figure 7-2 - Definition of angles tested statically

The first loading of the hip joint occurs just after heel strike (HS) so this was chosen as the first static trial with the femur set at 32° flexion, -3° abduction. Three more static trials were set at even spacing until the toe off position (TO). At initial stance (IS) 20° flexion, 6° adduction; single leg stance (SLS) 7° flexion 6° adduction and at the toe off position (TO) 7° extension, 0° abduction, a summary of these is illustrated in Figure 7-2. Due to the design of the gait cycle cam it was not possible to test the femur at the same angle utilised in the static tests described in section 5.5.

7.4.3. Dynamic motion

During the dynamic trial (DYN) the femur was subject to complete cycles around the elliptical cam from 32° flexion to 8° extension and from 6° abduction to 6° adduction. An additional dynamic cycle (*Dynamic One Side* or DOS) was also used where the femur was cycled purely on the adduction side of the cam to rule out any errors being recorded by the LVDTs as a result of any vibration during the transition of the cam follower at the heel strike and toe off positions. During DOS the femur moved from 32° flexion to 5° extension and from 0°

abduction to 6° adduction. The DOS does not extend as far as the DYN cycle as the cam follower had to be stopped short of the transition point on the cam. The angle of the femur for both dynamic studies is shown in Figure 7-3, the load is shown in grey to for clarity.

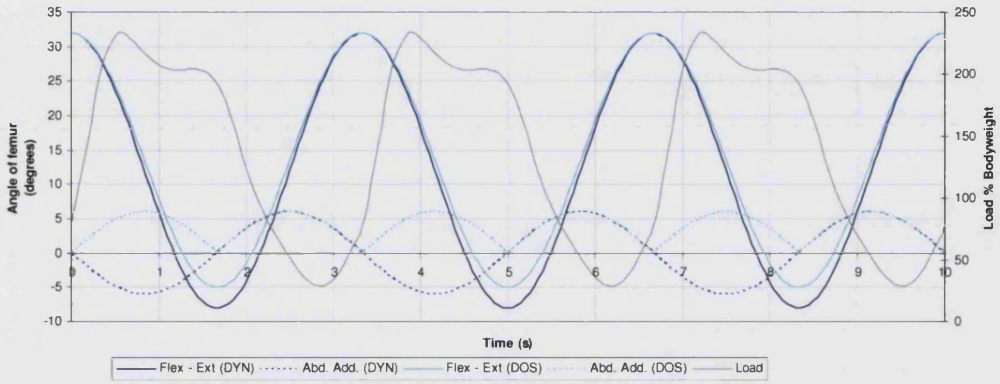

Figure 7-3 - Angle of the femur through the two dynamic cycles DYN and DOS

7.4.4. Loading patterns

During all six loading regimes (HS, IS, SLS, TO, DYN, and DOS) the muscle loading system was applied with a physiological loading profile peaking at 0.6kN from the vertical actuator. The applied load was then magnified by the muscle loading systems (theoretically by 2.7 times) producing a peak force of 1.6KN on the head of the stem.

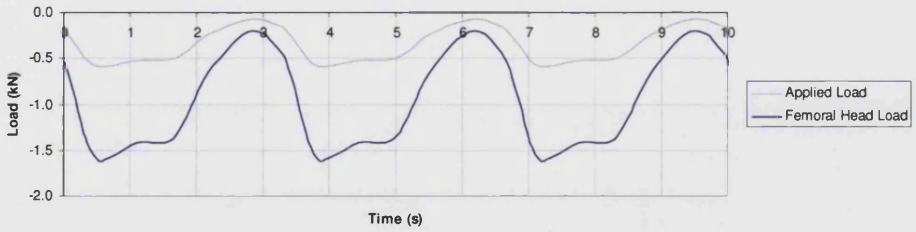

Figure 7-4 - Loading pattern used for static and dynamic cycles

The shape and loading levels of both the applied load and femoral head load can be seen in Figure 7-4. Each test consisted of 200 loading cycles applied at a frequency of 0.3 Hz. The number of cycles and speed would ideally match the cadaveric studies (0.5 Hz) but during the development a frequency of 0.3 Hz

was considered to be the maximum speed at which the simulator performed with greatest reliability.

7.4.5. Testing protocol and sequence of specimen testing

One of the concerns raised during this dynamic vs. static study was the possibility that the order in which loading regimes were applied to each femur would affect the stability of the hip stem in the later tests. For example if a HS cycle always followed by a SLS regime then it could be argued that there was some effect due to the test sequence. To eliminate this problem, the loading regimes were applied to each of the six specimens in a different order each time. The pattern of regimes used tried to ensure that the initial test performed on each femur was a different regime. The final order of loading regimes chosen ensured the results of a regime were not affected by its position in the order of testing; the sequence of testing adopted during the experimental phase is listed in Table 7-1.

Femur	**Order of loading regime**					
	1st	2nd	3rd	4th	5th	6th
1	SLS	HS	TO	IS	DYN	DOS
2	DOS	DYN	IS	TO	HS	SLS
3	TO	IS	DYN	DOS	SLS	HS
4	HS	SLS	DOS	DYN	IS	TO
5	DYN	DOS	SLS	HS	TO	IS
6	IS	TO	HS	SLS	DOS	DYN

Table 7-1- Order of loading regimes for the 6 femora

7.5. *Micromotion transducers and data acquisition*

The movement of the implant with respect to the surrounding bone was monitored by the same transducers as described in section 5.3. Plates were mounted around the transducers to protect the leads of the LVDTs from potential damage.

The method of data acquisition from the transducer was identical to the system used in the cadaveric studies and described in section 5.6.

7.6. *Calculations of nominal load applied to the head of the implant when femoral kinematics are included*

The six degree of freedom motion transducer is capable of detecting the translations and rotations of the stem with respect to the bone in a coordinate system defined about the femur. Understanding of these results is enhanced by modelling the forces applied to the hip stem so that the recorded motions can be compared with the forces applied. The forces applied to the hip stem are known in a machine coordinate system, which has to be translated onto the femur coordinate system for the various loading regimes, including those whilst the femur is in motion. To aid the analysis of micromotion and migration, a mathematic model describing the loading of the femoral head was developed using matrices to perform a coordinate transform translating the machine loads in orthogonal directions onto the same coordinate system as the motion transducers.

Definitions of the machine and hip stem coordinate systems and notation used in this model can be seen in Figure 7-5.

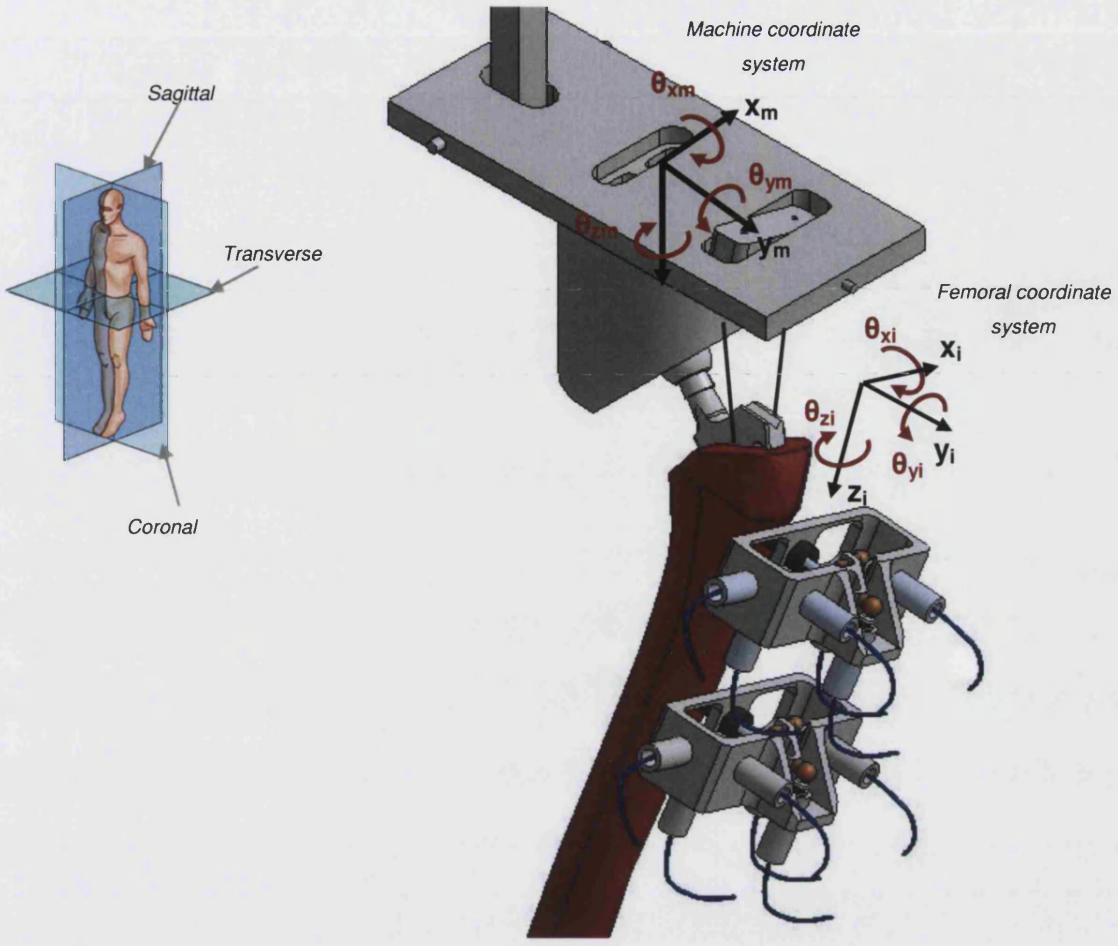

Angular relationship of machine coordinate system and femoral coordinate system

Θ = rotation in sagittal plane

α = rotation in coronal plane

Φ = rotation in transverse plane

Figure 7-5 - Definition of Coordinate systems and relationship; machine and implant

During the loading regimes the hip stems are re-positioned in the sagittal and coronal axes and during implantation the hip stem rotated in the transverse plane. The model incorporated each of these rotations by a 3 x 3 matrix shown in Equation 7-2

Rotation in sagittal plane

$$A = \begin{bmatrix} \cos(\theta) & 0 & \sin(\theta) \\ 0 & 1 & 0 \\ -\sin(\theta) & 0 & \cos(\theta) \end{bmatrix}$$

Rotation in coronal pane

$$B = \begin{bmatrix} 1 & 0 & 0 \\ 0 & \cos(\alpha) & \sin(\alpha) \\ 0 & -\sin(\alpha) & \cos(\alpha) \end{bmatrix}$$

Rotation in transverse plane

$$C = \begin{bmatrix} \cos(\phi) & \sin(\phi) & 0 \\ -\sin(\phi) & \cos(\phi) & 0 \\ 0 & 0 & 1 \end{bmatrix}$$

Equation 7-1 - 3 x 3 matrices defining rotations about sagittal, coronal and transverse planes

The loads from the machine were calculated by a model of the muscle loading system that used the loading profile to calculate the forces applied from the machine, x_m, y_m and z_m. Equation 7-2 was then used to define the relationship between the two coordinate systems, and the matrices were multiplied out for use in the the loading spreadsheet. The spreadsheet allowed the positions of the femur in the individual loading regimes (e.g. HS, SLS, DYN) to be entered so the graphs showing the loading on the implant in the orthogonal directions x, y and z could be calculated (femoral coordinate system). For the two dynamic trials the positions of the femur during the gait cycle were entered as an array so that the change in position through time was included.

$$\begin{bmatrix} x_m \\ y_m \\ z_m \end{bmatrix} = ABC \begin{bmatrix} x_i \\ y_i \\ z_i \end{bmatrix}$$

$$\begin{bmatrix} x_m \\ y_m \\ z_m \end{bmatrix} =$$

$$\begin{bmatrix} \cos(\phi)\cos(\theta) & -\cos(\phi)\sin(\theta)\sin(\alpha)+\sin(\phi)\sin(\alpha) & \cos(\phi)\sin(\theta)\cos(\alpha)+\sin(\phi)\sin(\alpha) \\ -\sin(\phi)\cos(\theta) & \sin(\phi)\sin(\theta)\sin(\alpha)+\cos(\phi)\cos(\alpha) & -\sin(\phi)\sin(\theta)\cos(\alpha)+\cos(\phi)\sin(\alpha) \\ -\sin(\theta) & -\cos(\theta)\sin(\alpha) & \cos(\theta)\cos(\alpha) \end{bmatrix} \begin{bmatrix} x_i \\ y_i \\ z_i \end{bmatrix}$$

Equation 7-2- Rotation matrix used to calculate theoretical femoral head forces

The results of this study are used for comparison with the prevalent micromotions and migrations discussed later in this section but two graphs are shown in Figure 7-6 to highlight some of the expected differences between SLS and the dynamic test DYN. The theoretical forces expected during the other loading regimes are shown in Appendix VI.

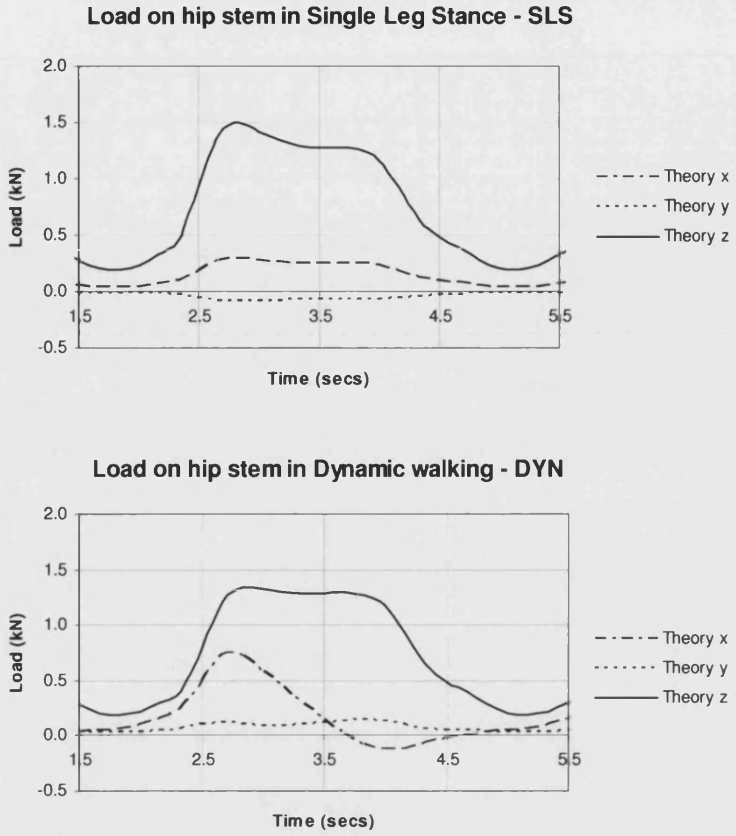

Figure 7-6- Theoretical forces applied in the implant coordinate system

The curves representing the calculated component of the applied load along the coordinate system (x, y, z) for the SLS and DYN experiments show interesting features suggesting that the dynamic motion experiments of the femur may affect the stability of the hip stem. In the z axis (defined along the length of the femur) the same basic shape of force is expected between the two loading regimes although for the dynamic regime (DYN) there may be a flattening of the peak shown in Figure 7-6 at about 2.7s or 25% gait. This flattening occurs as the femur is rotated in flexion and the force is applied in the x direction (from anterior to posterior). The peak force in the z direction is reduced which may lead to reduced micromotion values along the axis of the femur. In the dynamic regime the femur rotates from flexion to extension so the force in the x direction is applied from anterior to posterior and then later in the gait cycle from posterior to anterior. This could lead to higher micromotion levels than the peak force may indicate. The smallest force is predicted in the y direction (from medial to lateral) and the theory suggests that the forces, and hence the motion, between these regimes will not be changed significantly.

However the forces may not directly predict levels of motion as, due to the shape of the hip stem, the stiffness in each orthogonal direction will not be equal. To predict exact levels of motion a full FE analysis would be required.

7.7. *Micromotion and migration results of static vs. dynamic testing*

Differences between the six loading regimes were analysed with the Kruskal-Wallis test for more than two independent groups. Statistical significance was assumed for $p<0.05$. Results are expressed as median (25^{th} quartile – 75^{th} quartile) and shown graphically as stem and leaf plots.

Figure 7-7 to Figure 7-9 show the prevalent micromotions and migration between the loading regimes recorded at the proximal transducer. In this section, only the largest motions in any one direction are reported. A full set of results can be found in Appendix VII

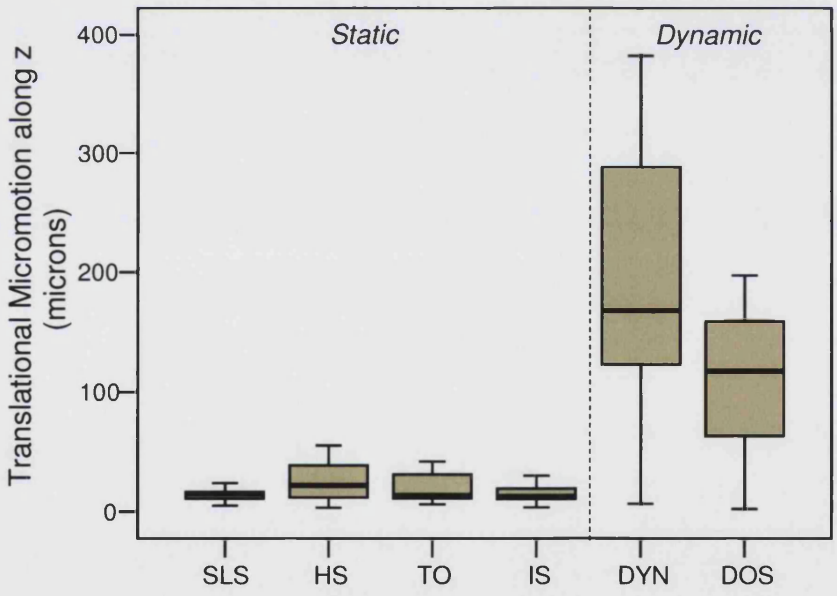

Figure 7-7 - Prevalent translational micromotion during the static and dynamic testing

Motions reported in this section are all in the implant coordinate system as defined in Figure 7-5. In the proximal transducer the largest translational motion was recorded in the dynamic test along the axis of the femur (along the z axis) which is consistent with the direction of the applied load. Figure 7-7 shows

clearly that the dynamic test designed to reflect a slow walk (DYN) produced much larger motions 170μm (110μm – 290μm) than the static regime often used to model walking (SLS) 15μm (11μm -17μm). The difference between the dynamic cycle representing a slow walk (DYN) and the static SLS regime results were statistically significant. The largest results measured along the z axis during the static study were recorded during the HS regime 22μm (11μm - 39μm); however these results were still significantly different even from the lowest measured dynamic results, DOS 118 μm (63μm - 159μm).

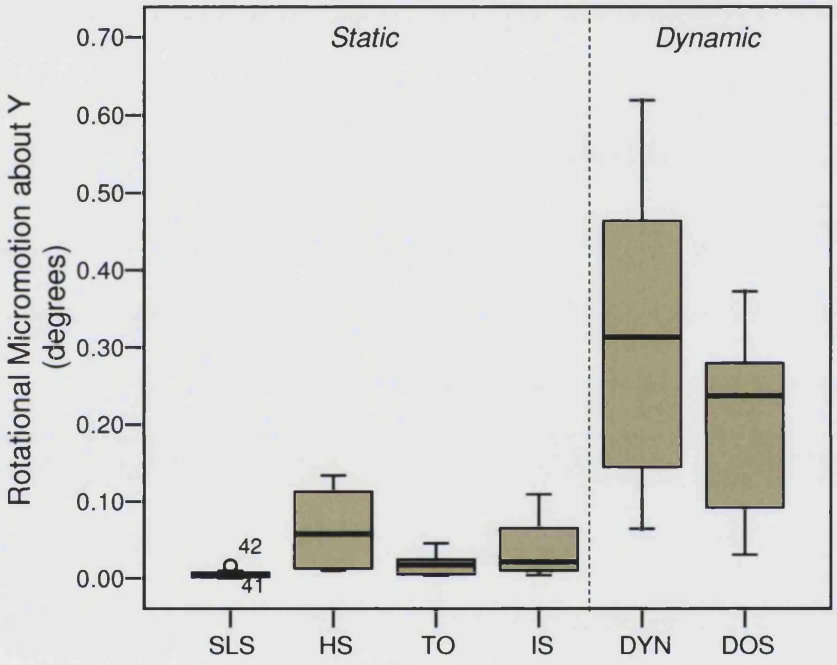

Figure 7-8 - Prevalent rotational micromotion during static and dynamic testing

The rotational micromotion results showed prevalent motions recorded about the y axis (θy) and are shown in Figure 7-8. Both dynamic studies DYN 0.31° (0.14°-0.46°) and DOS 0.24° (0.09°-0.28°) recorded significantly larger rotational micromotion than all of the static studies, the highest of which was HS with levels of 0.06° (0.01°-0.11°). It is interesting that the prevalent rotational micromotion was about the y axis in the dynamic studies whereas in the cadaveric static studies the prevalent rotational motion was about the x axis. This could be due to the action of the muscle cable as the femur moves through the maximum adduction. The lowest rotation was measured during the SLS regime 0.01° (0.00°-0.01°).

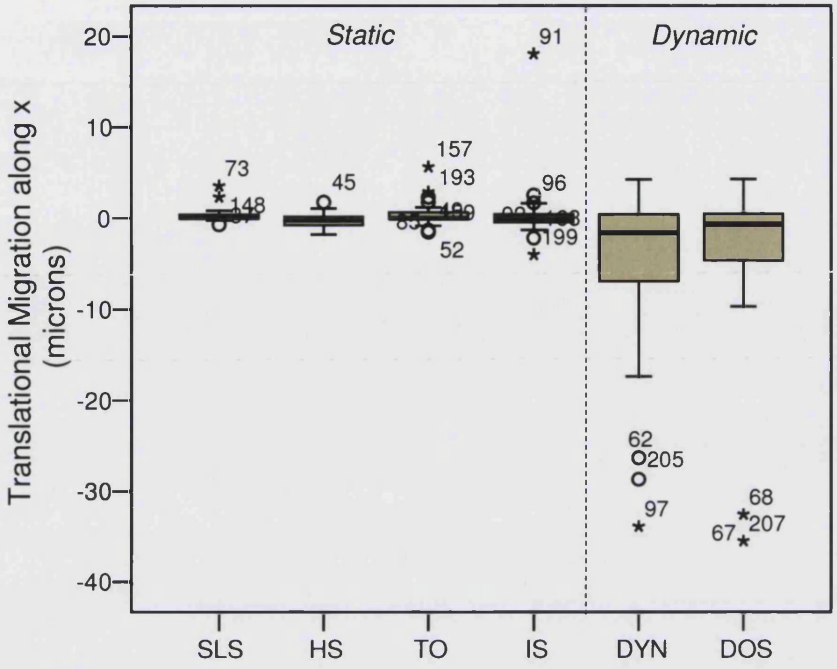

Figure 7-9 - Prevalent migration at the proximal transducer

The largest migration recorded in the proximal transducer in the dynamic loading regimes (DYN and DOS) was along the x axis. Figure 7-9 presents the migration results and shows that the static studies induced negligible migration, the largest in HS 0μm (-1μm - 0μm), and only small values of migration in the dynamic test DYN -1μm (-8μm - 0μm). Although most of the values are small the results are characterised by several outliers. This level of inconsistency in the results possibly indicates that migration is not a continuous motion. The cadaveric studies previously presented (section 5.7) show that Sawbones models often lead to an underestimation when assessing migration, so care must be used when trying to interpret these results. The results for migration along z and y and the rotations about all three axes show similar patterns of negligible migration, and in the majority of cases the dynamic results produced significantly higher levels of migration than the static ones (Figure 7-10). Although only the prevalent micromotion and migration at the proximal location are presented in Figure 7-7 to Figure 7-9 the statistical analysis reported that proximal micromotion and most migration results were significantly different when comparing static regimes to dynamic regimes. Figure 7-10 presents the relationships between each regime using a tick to indicate a statistically different relationship ($p < 0.05$).

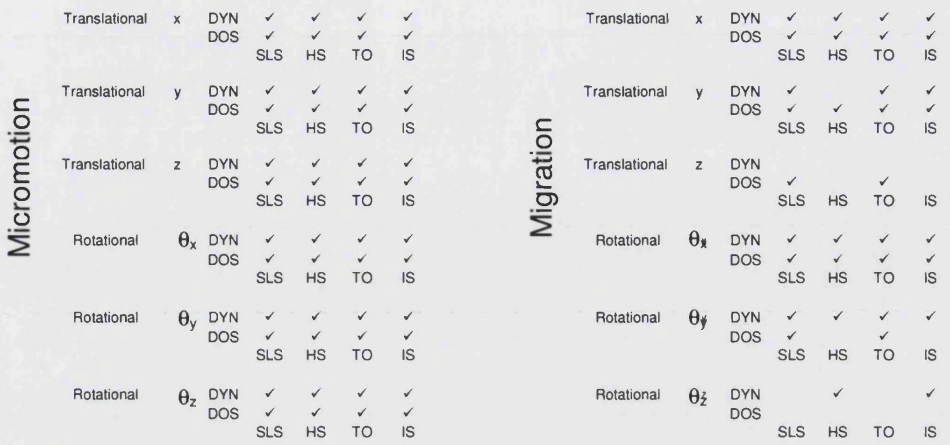

Figure 7-10 - Statistical differences between dynamic and static loading at the proximal location (tick indicates statistically different relationship)

At the distal location the prevalent translational micromotion was along the z axis, the same direction as the prevalent micromotion in the proximal transducer, and is shown in Figure 7-11.

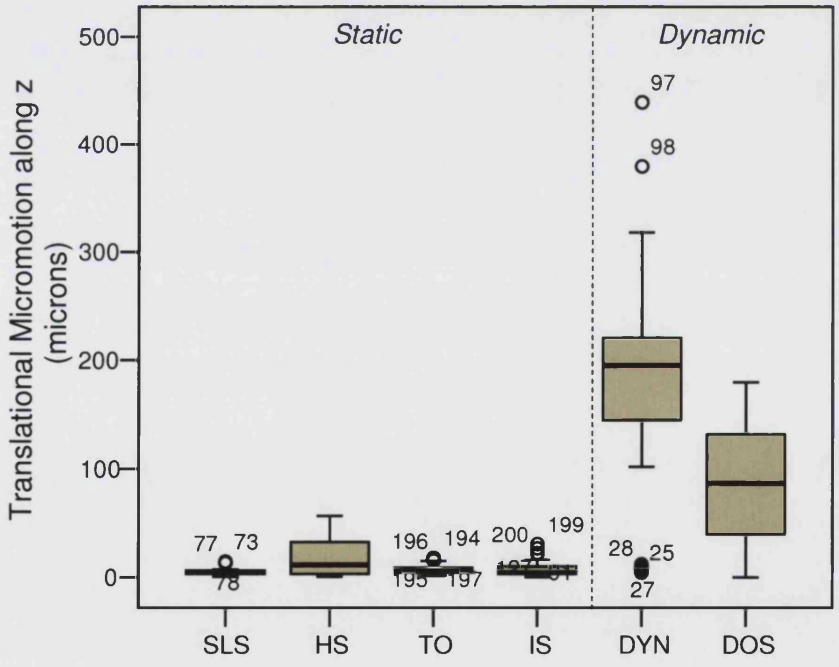

Figure 7-11 - Prevalent translational micromotion recorded at the distal transducer

The highest translational micromotion along the z axis measured by the distal transducer was recorded during the dynamic test DYN 195µm (144µm -223µm).

This motion is significantly higher ($p < 0.05$) than all the results of the static tests, the highest of which was again during HS 12µm (3µm – 33µm). The rest of the static tests produced very low levels of micromotion that could be considered negligible, e.g. zero or below the resolution level of the transducers. Like the proximal results the translational micromotion along z during the DYN regime was higher than when the simulator was cycled on just one side of the track in DOS 90µm (27µm – 132µm)

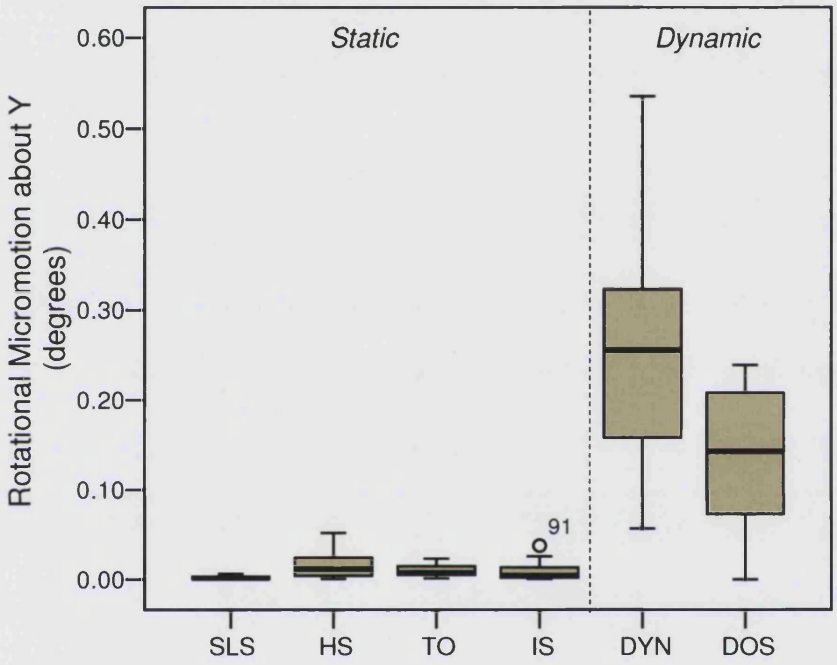

Figure 7-12 - Prevalent motion rotational micromotion recorded at the distal transducer

The prevalent rotational micromotion recorded in the distal transducer was about the Y axis as it was in the proximal transducer with the highest motion during DYN 0.25° (0.15°- 0.33°) with similar but lower values in DOS 0.14° (0.07°-0.21°). The micromotion levels obtained from both dynamic regimes were significantly larger than all the static regimes, again with HS 0.01° (0.00°-0.02°) producing the highest levels of the static regimes. This pattern of motion was reflected in the prevalent distal migration shown in Figure 7-13: the dynamic test consistently produced significantly higher motions than the static tests. A summary of the results obtained by the distal transducer is presented in Figure 7-14, a tick in this figure indicates that the difference between the two testing configurations was statistically significant (Krustal-Wallis, $p<0.05$). A

comprehensive set of graphs to describe all the micromotions and migration during the various regimes can be found in Appendix VII.

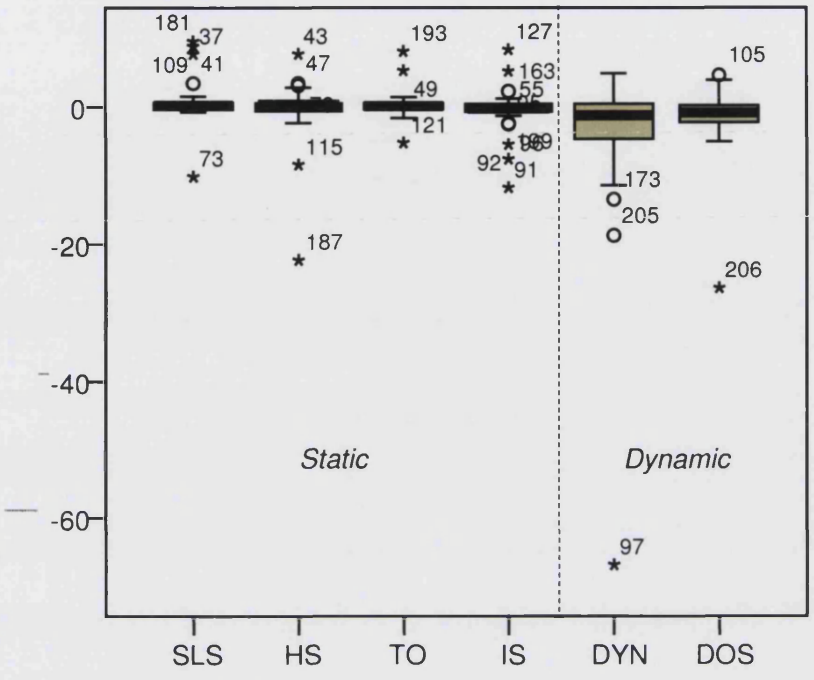

Figure 7-13 - Prevalent migration recorded distally

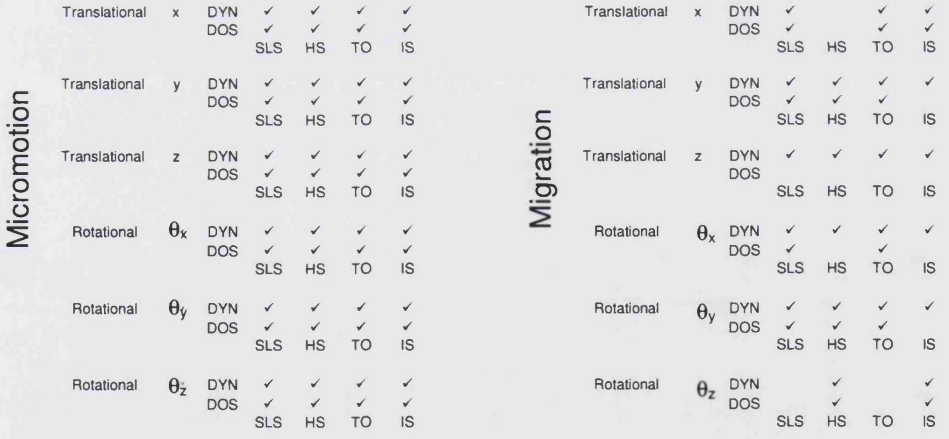

Figure 7-14 - Statistical differences between dynamic and static loading at the distal transducer

7.8. *Investigation of high motion during dynamic regimes*

The results presented thus far show that the dynamic trials produced far higher levels of micromotion and migration than the static ones. The differences between static and dynamic tests were significant both in terms of migration and in terms of micromotion. The calculated loading (section 7.6) suggested that patterns of motion may change but did not predict any difference between the levels of micromotion and migration so this needs to be investigated further. The initial thought was that the levels were higher due to transition of the femoral bracket from abduction to adduction and vice versa. Vibrations experienced at these transitions maybe affecting the LVDTs and therefore recorded by the motion transducers. This was proved not to be the case when the motion data produced by the MATLAB programs was analysed to show the motion during the gait. A graph showing a sample of the motion of the implant from the MATLAB results over one loading cycle is presented in Figure 7-15. This has been compared to the predicted theoretical force experienced by the stem along the coordinate axes (x, y and z). If the high motions recorded were due to vibration at the transition points then these would appear as a higher frequency disturbance superimposed on the motion of the stem. However the motion captured at 50Hz shows no sign of vibration or spikes indicating that the high motion is probably due to a cause other than the vibration of the transitions.

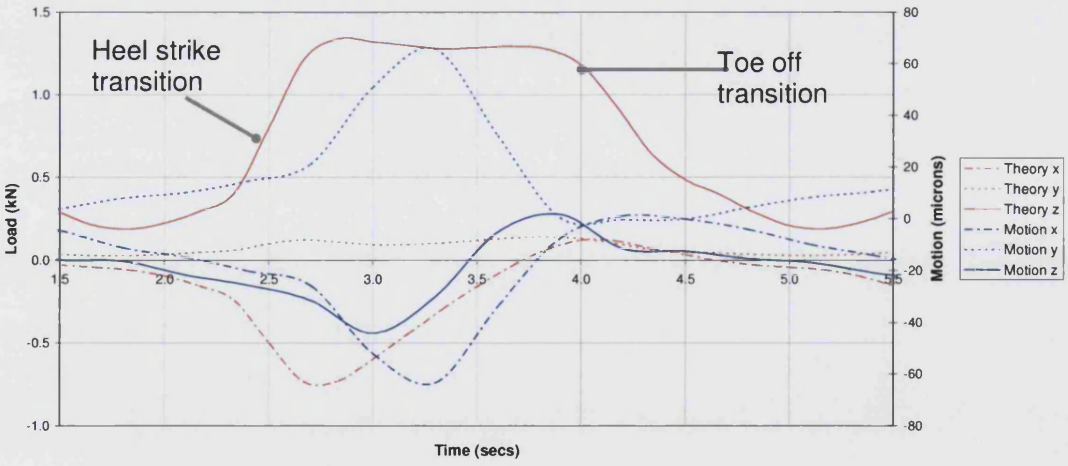

Figure 7-15 - Motion of the implant (right axis) during a dynamic cycle compared to the theoretical load (left axis) on the implant

Since vibration was not the cause of the higher recorded load it was important to check that the applied loads were not higher during the dynamic studies. The plots of the applied loads during the 6 loading regimes applied to this bone are shown in Figure 7-16

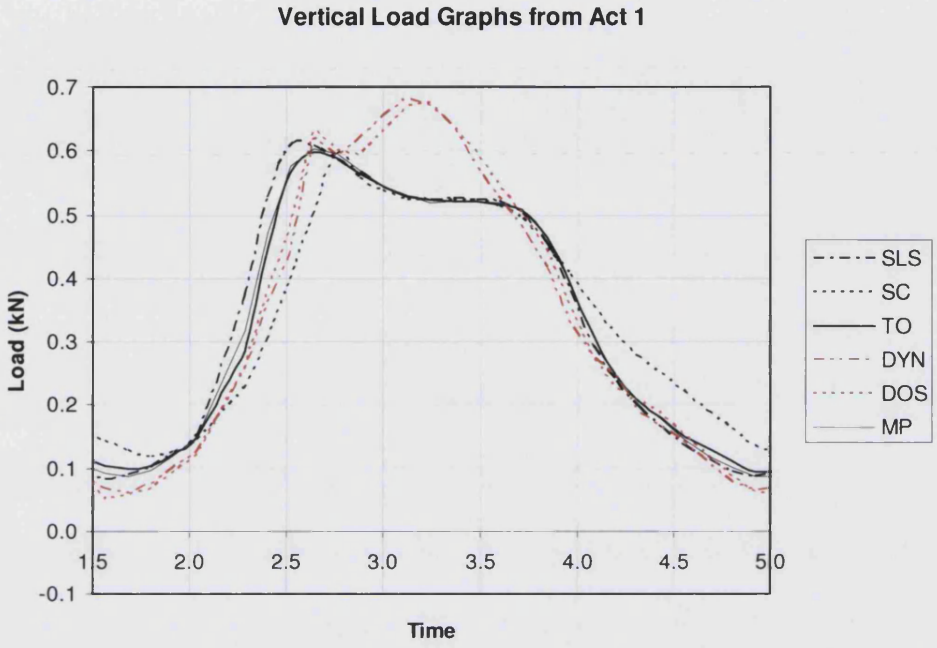

Figure 7-16 - Loads downloaded from the vertical actuator for femur 5

Results from the two dynamic regimes are shown in red for clarity. The two dynamic (DYN and DOS) trials display slightly differing shapes to the static trials, which are very consistent, and it is clear that the levels of force applied are not significantly higher than the static trials and therefore, not the cause of the higher micromotion. Having discounted vibration and the vertical actuator then the next possible source of force generation is the muscle loading system.

One explanation for the higher motion levels may be the constraint of the head of the hip stem in the acetabular cup whilst the femur moved round its cycle, producing unwanted forces on the head. To evaluate this problem the simulator was cycled through its dynamic cycle with no load applied from the vertical actuator and the muscle cables left connected as normal. The resulting motion of the hip stem is presented in Figure 7-17. The motions recorded were minimal but some motion was induced in the hip stem which when evaluated by the MATLAB routine was found to be about 4 μm, 5 μm and 7 μm along the axes x, y and z respectively Figure 7-17.

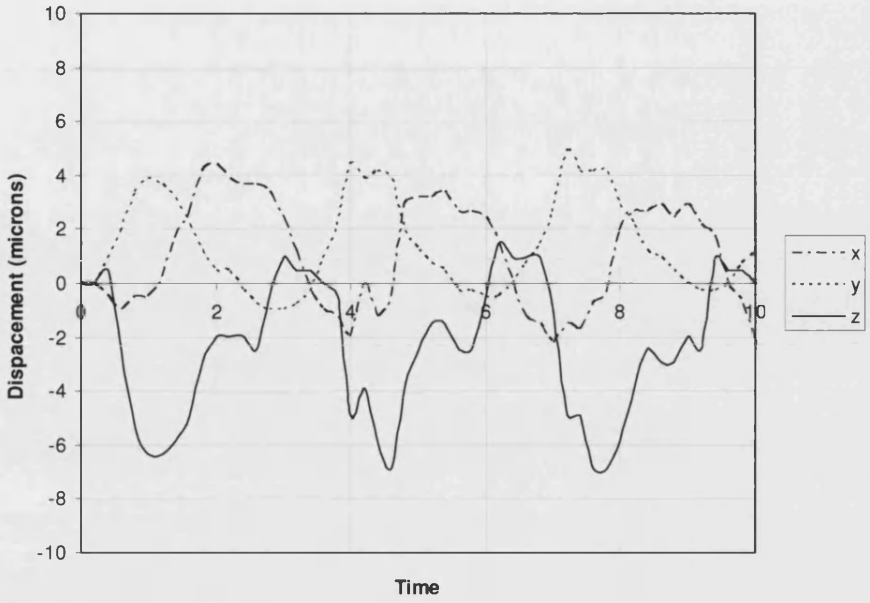

Figure 7-17 - Results from the No- load dynamic cycles

The magnitude of displacement recorded in the transducers without any vertical loading shows that the high micromotion recorded during the dynamic testing regimes are not solely due to the inclusion of the muscle loading system. However, there are patterns evident over time suggesting that the muscle loading system is inducing displacement of the hip stem due to an over constrained system. When the vertical load is applied this could increase the action of the abductor muscles and could be responsible for the high levels of micromotion recorded during the dynamic regimes. The theory that the system is over constrained would suggest that when the load is applied the head of the femur is being driven off the axes around which the simulator rotates (i.e., the 2 axes defined by the 2 pairs of bearings which allow motion in the sagittal and coronal planes) and therefore is subject to high loads. There is currently no data to prove this theory but when the head of the hip stem was observed during a full loading and gait cycle there was some visual evidence of the head moving off the desired axis of rotation. One way to analyse the forces directly applied on the head of the hip stem would be to use strain gauges on the neck of a hip stem that would be subjected to the loading regime and gait cycles in the simulator.

The dynamic test with the femur only moving on one side of the rig, the DOS regime, always produced lower median levels of micromotion than when the

femur was moved around the whole gait cycle in DYN. The difference between the results was not statistically significant but the pattern was repeated in all femora tested. The simplest explanation for this would be that during the regime when the femur is cycled purely on the adduction side of the cam the femoral head experiences a lower load. One reason for the reduced force differential could be the fact that simulator was run through a slightly lower flexion extension cycle to ensure that the femoral bracket would not make the transition to the other side of the cam. Another possible explanation for the lower results during the single sided dynamic cycle is that during the swing phase of the gait on the full cycle DYN, the muscle cables were at their lowest tension and therefore not exerting any force on the femoral head. In the DOS loading regime whilst the femur cycles back up the adduction side of the cam, the force on the head may be sustained by the increased tension in the muscle cables therefore reducing the overall change of force on the head of the hip stem. Strain gauging the neck of a hip stem may provide information on whether this is the case.

The cadaveric studies performed to validate the use of sawbones as an appropriate bone model suggest that the migration results often produce lower levels than those seen in cadaveric bone. This would suggest that caution should be given to the migration results recorded during the dynamic studies because they are obtained from Sawbones femora. The very low results produced in static regimes in this study show good agreement with the composite validation results obtained on the material testing machine used in section 5.7. The dynamic loading regimes also produced low levels of migration but these were still significantly different from the static studies in most of the directions measured (Figure 7-10 and Figure 7-14).

At this point the migration results should be considered in the context of the micromotion results. The micromotion results are considerably larger than the static ones so it could be expected that the migration would also be increased. The effect of higher forces (eg. > 1.5 kN) on micromotion and migration is not currently understood and needs to be investigated before it is possible to draw conclusions whether the higher levels of motion are due to dynamic regimes.

In summary, when the simulator is cycled dynamically the micromotion and migration levels recorded are significantly higher than those recorded statically.

However, the reason for these higher levels of motion it is not clear. The higher levels of motion were not predicted by the initial calculation relating to the load experienced by the implant therefore is it is not possible to attribute the higher magnitudes of motion directly to an increase in applied load resulting from the dynamic test regime. It is possible that the higher magnitudes of motion are due to internal forces in the muscle loading system producing undesired extra force on the head of the implant. Further investigations to explain these results are required to:

1. Investigate the response of the SL Plus hip stem to ever increasing load levels,
2. Assess the forces on the head of the implant during a dynamic cycle by strain gauging the neck of the hip stem

7.8.1. The effect of increasing load levels on the SL-Plus hip stem

The effect of increasing the load magnitude applied to the head of the SL Plus in a Sawbones femur needs to be understood before conclusions about how the dynamics of the simulator affect the patterns or levels of bone-implant motion. To justify the time and expense of strain gauging a hip stem a pilot study was performed to investigate how the micromotion and migration levels were affected by increasing the load on the hip stem.

A composite femur with an SL Plus hip stem was prepared and set up as described in section 5.4. The prepared femur was then mounted on the Instron materials testing machine (model 8511). Loading cycles were applied to the femur through a substitute pelvis in the SLS configuration used in the cadaveric and composite studies reported in section 5.5 were used but this time increasing load levels were applied. These consisted of repeated sets of 200 cycles applied to the head of the implant. In this set of experiments the load applied to the substitute pelvis varied between 100N and 1200N at intervals of 100N. The substitute pelvis rig produced a force magnification of 2.7, the resultant applied loads for each set of 200 cycles are summarised in Table 7-2. Repositioning the femur between loading cycles was not possible due the sensitivity of the setup procedure.

Set	Instron load (kN)	Femoral head load (kN)
1	0.1	0.27
2	0.2	0.54
3	0.3	0.81
4	0.4	1.08
5	0.5	1.35
6	0.6	1.62
7	0.7	1.89
8	0.8	2.16
9	0.9	2.43
10	1.0	2.7
11	1.1	2.97
12	1.2	3.24

Table 7-2- Loads applied to the substitute pelvis and resultant femoral head load due to 2.7 mechanical advantage

The data acquired from the motion transducers was processed using the same MATLAB programs as described in section 5.6.

The results were plotted for micromotion and migration (translational and rotational) against load for the proximal and distal transducer. Similar patterns were observed in all the graphs, which can be found in Appendix VIII, and the translational micromotion and migration in proximal transducer are shown in Figure 7-18 and Figure 7-19 to demonstrate the main points.

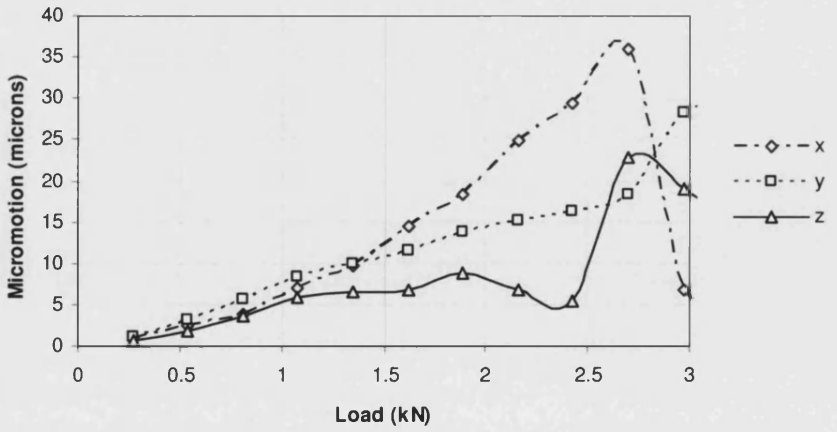

Figure 7-18 - Proximal micromotion against femoral head load

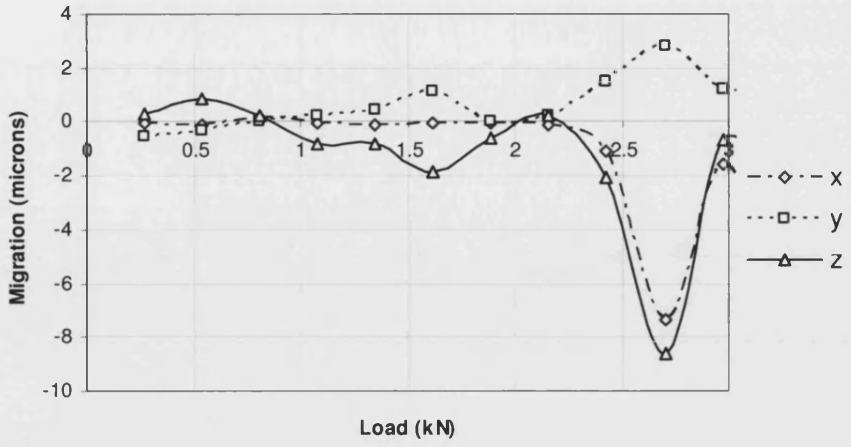

Figure 7-19 - Proximal migration against femoral head load

The results for proximal micromotion against femoral head load displayed in Figure 7-18 show that the levels of micromotion are approximately linear up to a femoral head load of 2kN in all three directions recorded. The largest motion is recorded along the x axis, however in the previous tests performed on composite femora (section 5.7) the predominant motion has been along the z axis. This anomaly could be a result of a poor fitting stem in the anterior posterior direction. The motion recorded below 0.5 kN head load is within the accuracy of the motion transducer (3μm) therefore caution must be used with this data point. Above 2 kN the level the micromotion in the z direction reduced with increased load. This mode change is also visible in the migration data where migrations are negligible up to 2kN load; above this level migration data becomes larger but erratic (Figure 7-19). It is possible that at this level of loading (2kN) there is a material failure occurred in the foam representing the cancellous bone in the model therefore changing the mode of motion.

The migration results in the x, y and z axes are all below 2μm up to 2kN. (Figure 7-19). Migration values recorded above 2 KN vary with no relationship to the applied load. The data for this femur suggest that a material failure has occurred at about 2.0 KN which has affected the later results.

The maximum level of motion occurred when the hip stem was loaded at 2.5kN producing a micromotion of 35μm along the x axis. Considering the levels of micromotion reported in the composite validation study (section 5.7.3) and the applied load in this experiment, 35μm is lower than expected. If the study were

repeated then higher levels maybe expected due to the statistic spread of results. Whether the levels recorded dynamically (> 400μm) would be reached is unclear.

Even with a 3kN load the levels of motion achieved in the dynamic study (> 400μm) were not observed. This study was only performed on one femur with an implanted SL Plus stem so no firm conclusions are possible, however, it does demonstrate that with greater load, higher levels of micromotion can be expected. This raises the question of what force is required to induce the level of motion recorded during the dynamic loading regimes and underlines the need for measuring the forces applied to the head of the hip stem during the various loading regimes.

The study indicates that, in this particular experiment, up to a certain load level (approximately 2kN) the results display a linear trend. However, this result is based on a sample size of one and therefore more experiments are required to characterise the hip stems response to increasing loading levels.

7.8.2. Assessing the force on the femoral head during dynamic loading regimes

The results from the dynamic loading regimes produced much larger micromotions than expected. A calculation of the femoral head loading (section 7.6) predicted that there would be changes to the pattern of the motion but did not predict the large micromotions measured. The reason for the high forces is thought to be caused by small errors in the set up of the simulator and the femoral head being driven off its axis of rotation. To confirm this an implant was fitted with strain gauges to record the femoral neck strains and tested in the dynamic simulator to report the forces experienced during dynamic and static cycles.

A system of strain gauges was configured to measure the strain on the neck of the hip stem in 3 orthogonal directions. The gauges were attached to the neck of the implant and measured the axial force with an 8 gauge bridge and the vertical and horizontal forces each with a 4 gauge bridge as shown in Figure 7-20. This configuration was chosen to minimise cross talk between the

channels. The two four gauge bridges were used to record the strain due to bending of the neck by evaluating each bridge as two pairs. The difference between the voltages developed in one pair of gauges was used to calculate the difference in strain while the other pair was used as a dummy gauge to remove the strain due to the axial compression. The axial strain was recorded by the 8 gauge bridge. Four gauges were used to record the axial strain and two pairs of dummy gauges were used to remove the effective strain from the bending in the orthogonal directions.

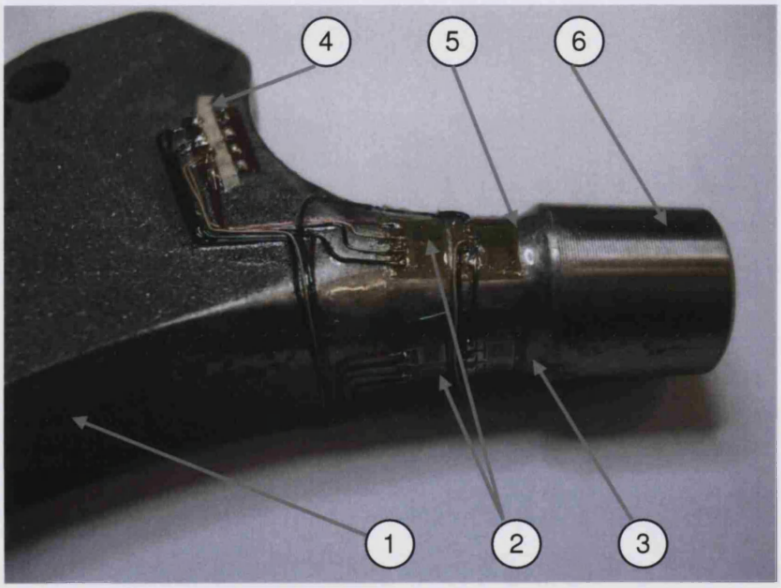

1) The SL Plus implant
2) An 8 gauge bridge forming a ring round the neck (4 pairs) – Axial load
3) A 4 gauge bridge (2 pairs) opposite pair on unseen side – Vertical load
4) Connections for wires
5) A 4 gauge bridge (2 pairs) opposite pair on unseen side – Horizontal load
6) A tapered section of the implant where the head locates

Figure 7-20 - Strain gauge configuration used on the SL Plus implant

Each set of gauges was calibrated by mounting the instrumented implant in a position where the strain gauges should only record in the direction of the applied load. Load was applied by an Instron load testing machine (Model No. 8511). Details of the calibration can be found in Appendix III.

Once the calibration was complete the instrumented stem was implanted into a Sawbones femur which was then prepared following the protocol as described in section 5.4. In this study, one of the data acquisition computers was required to

capture data from the strain gauges. The other data acquisition computer was used for the proximal transducer, as proximal results had recorded the higher levels of motion in previous studies. The instrumented stem and femur was then mounted onto the simulator and setup as described in section 7.3. The simulator was cycled through the same loading regimes as used in the dynamic study with the same range of motion and level of vertical load. The specimens were tested in the order DOS, SLS, HS, TO, IS and finally DYN. Data from the strain gauges was acquired using an HPVEE program adapted from that used in section 5.6 (Appendix X).

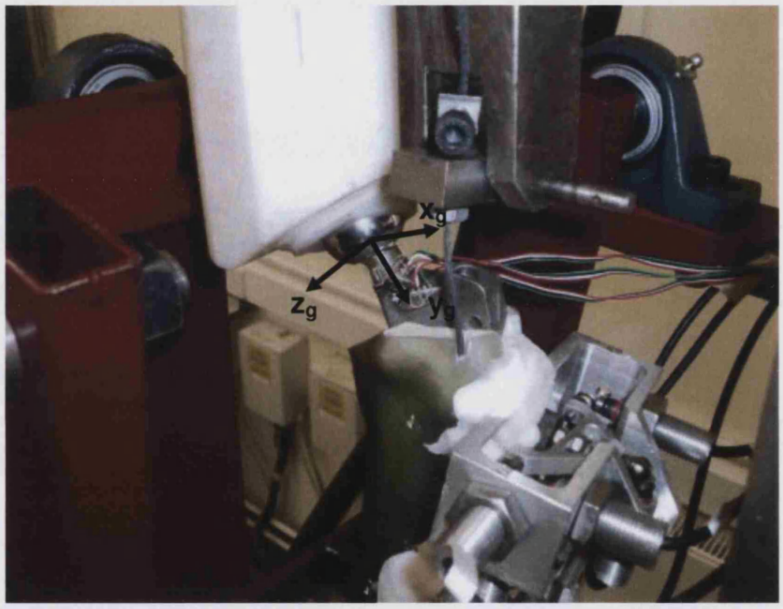

Figure 7-21 – SL Plus hip stem implanted in a femur and mounted in the dynamic simulator; showing coordinate system of the strain gauges

Figure 7-21 shows the coordinate system of the strain gauge bridges. To relate the strain gauge coordinate system to the implant motion coordinate system a rotation matrix was used, see Equation 7-3. This allowed the motion results from the transducers to be directly compared in the same axes with the forces on the hip stem.

$$\begin{bmatrix} x_i \\ y_i \\ z_i \end{bmatrix} = \begin{bmatrix} 1 & 0 & 0 \\ 0 & \cos(\alpha) & \sin(\alpha) \\ 0 & -\sin(\alpha) & \cos(\alpha) \end{bmatrix} \begin{bmatrix} x_g \\ y_g \\ z_g \end{bmatrix}$$

α = 40° to represent the angle between the neck of the implant and the coordinate system of the motion transducers

Equation 7-3 – Coordinate rotation from gauge to implant coordinate systems

With the results presented in the same coordinate system as used for the motion transducer the micromotion recorded in the experiments can be compared with the forces experienced by the head of the implant. Figure 7-22 shows the femoral head load experienced along the z axis and the resulting micromotion along the same axis during single leg stance (SLS). The force exerted by the vertical actuator and expected values calculated in Section 7.6 are also shown.

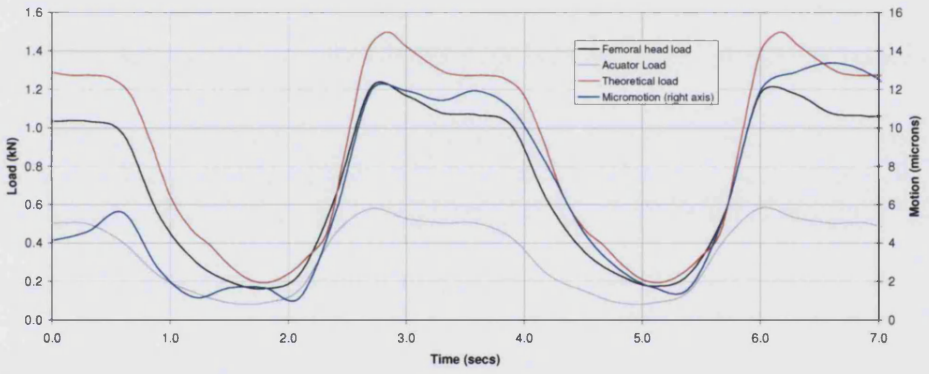

Figure 7-22 - Micromotion and femoral head load along the z axis during Single leg stance (SLS)

Results for this experiment are presented from data recorded along the z axis. This was the principal loading axis and also the axis in which the prevalent motion was recorded. The theoretical loading of the hip stem predicted that the maximum load on the hip stem during SLS would be 1.5kN. The largest force recorded along the z axis by the strain gauges was 1.2kN which showed reasonable agreement with the calculated loading as the principal force. Throughout the loading cycle the force recorded on the femoral neck during SLS was approximately 80% of the level predicted by the theory. This difference is probably due to some elasticity in the system resulting in imperfect transmission of force from the vertical actuator to the head of hip stem. The theory modelled the system as perfectly rigid while in the loading system, elasticity will be

introduced by deflection of the femur and stretching of the muscle cables. This deflection of the femur and other mechanical losses will account for the lower levels of load recorded. The vertical actuator force shows that the control system achieved the profile programmed in the actuator inputs and the level of loading required.

The micromotion of the hip stem is plotted from data recorded by the 6 DOF transducer and processed by the MATLAB routine is also plotted in Figure 7-22 (blue line). The amplitude of the micromotion recorded was 14µm along the z axis. The shape of the hip stem motion line closely follows that of the force applied displaying the initial peak followed by a fall and brief plateau then reducing back to repeat the pattern again. Similar patterns of micromotion and femoral head loading were observed in the x and y axes. The resultant motion and loading can be seen in Appendix IX.

The results from the instrumented hip shows that in the static loading regime (SLS) the simulator was working as desired and that the hip stems motion is a direct response to the direction of force applied with similar patterns of motion to the load applied.

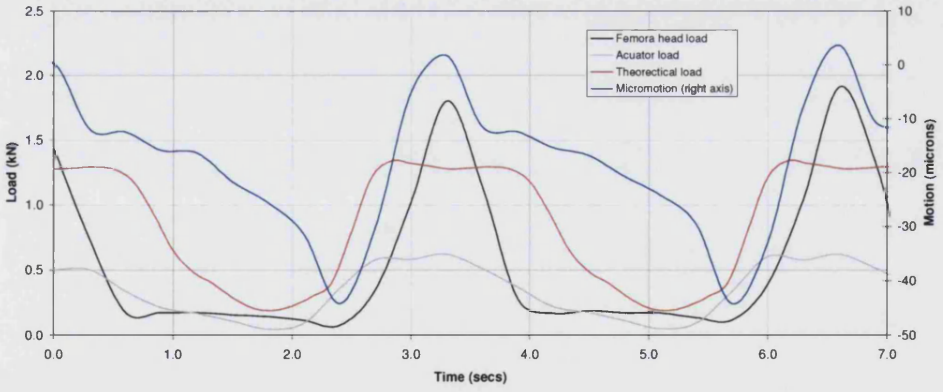

Figure 7-23 - Micromotion and femoral head load along the z axis Dynamic running (DYN)

Figure 7-23 shows the femoral head load experienced along the z axis during the full dynamic motion cycle (DYN). The theoretical loading, actuator load and hip stem motion are also shown. In this loading regime the force experienced at the femoral head does not follow the predicted theoretical loading. The shape of the force experienced on the femoral head shows a sharp peak rather than the plateau predicted in the theory. The level of force on the femoral head (max

1.8kN) is also much higher than that predicted by the theory (1.4kN). The data from the vertical actuator was analysed to see if it produced any clues to explain this discrepancy of loading shapes. The shape of the load recorded from the vertical actuator is distorted slightly from the input load however the desired input force of 0.6kN is achieved. When the applied force and the femoral head force are compared, the shapes of the graphs differ with the femoral head force showing a much sharper peak. This discrepancy between the shape of applied load and femoral head load shows that the femoral head load is not a direct response from the applied load and therefore a separate factor is affecting the femoral head force. When the levels of the force are compared, the 0.6kN applied to the substitute pelvis is increased to 1.8kN which is just greater than the 2.7 mechanical advantage that the system is designed to achieve. This is a positive result to validate the simulator however does not explain the high levels of motion.

The micromotion recorded by the motion transducer produced amplitude of 46μm and can be seen in Figure 7-23 as the blue line. The micromotion and femoral head force show very good agreement rising sharply to a narrow peak and then reducing at a similar rate. The motion pattern initially reduces in synchronisation with the force but then slows once the forces flatten at approximately zero until the start of the next cycle. This slower recovery could be explained by the natural stress relaxation rate of the internal foam inside the Sawbones. When the simulator was run in the dynamic cycle on one side similar patterns were seen and are shown in Appendix IX.

The aim of the instrumented hip was to try and explain why the dynamic loading regimes (DYN and DOS) produced higher levels of micromotion than the static regimes (SLS, HS, TO and IS). The strain gauges and motion transducers describe the loading and motion of the hip in detail for each loading regime. A graphical representation of this is presented in Appendix VII. Table 7-3 shows the resultant peak forces recorded on the femoral head, in the vertical actuator and the levels of micromotion calculated from the MATLAB routines for all the loading regimes tested with the instrumented hip stem.

Loading regime	Femoral head load (kN)	Actuator load (kN)	Theoretical load (kN)	Micromotion (microns)
SLS	1.15	0.6	1.53	14
HS	0.86	0.6	1.53	56
TO	1.1	0.6	1.53	20
IS	1.0	0.6	1.53	23
DYN	1.95	0.6	1.53	100
DOS	1.53	0.6	1.53	130

Table 7-3 –Maximum resultant loads and micromotion measured in loading regimes

In this study all the vertical actuator loads recorded were consistent for each loading regime (this was also the case in the full dynamic study shown in Figure 7-16) so it is clear that the vertical actuator is responding as expected and this is not the reason for the larger forces. The results in the DYN line of Table 7-3 show that this was the highest force on the femoral head and produced the second largest micromotion. The dynamic trials DOS and DYN again produced much larger levels of micromotion but not as high as some of the values reported in the original study. However, it was during these tests that the highest femoral head forces were experienced. This confirms the hypothesis that these larger micromotions are due to increased femoral head loading during the dynamic cycles.

The micromotions and loads in the static study are reasonably consistent with levels of about 20 μm and a 1.1kN force applied with the exception of the results from the heel strike regime (HS). It was during this regime (HS) that the highest levels of micromotion were recorded in the static regimes of the original study but the instrumented hip shows the forces here were lower than the other static regimes. The lower forces could be due the angle of the flexion of the femur allowing a greater deflection of the femur. The higher motion could be due to different material stiffness around the hip stem or because the hip stem is preconditioned only in SLS and hence when the HS cycles are run some "bedding in" could be occurring.

In conclusion it appears that the muscle loading system is creating some large internal forces during the dynamic loading regimes that were not observed or measured by the evaluation at the end of the design phase. These probably account for the larger micromotion recorded. The shape of the force profile

recorded on the hip is not currently explained and requires further investigation. In the static studies the strain gauges on the hip stem have shown that the muscle loading system was working well in producing the desired force profiles and that the motion of the hip stem also follows this profile. However, it is likely that the forces experienced on the head of the implant were only about 80% of those calculated.

7.9. *Discussion*

The results presented earlier in this chapter suggest that dynamic testing produced far higher levels of micromotion than static tests. The reason for the larger motion was thought to be either the inclusion of femoral kinematics on the gait cycle or the fact that the simulator was producing undesired levels of loading on the hip stem due to the errors in the systems. The increased load applied was proven not to be associated with the control of the vertical actuator after analysis of the load and stroke data recorded during the tests. The cause of the higher loads applied was therefore attributed to the substitute pelvis and muscle system. Two investigations were undertaken to investigate this possibility: by assessing of the effect of higher loading on the hip stem followed by strain gauging the hip stem to record the femoral head force.

The effect of increasing loads on the femoral head indicated that higher loads could be responsible for the higher levels of motion recorded. It should be noted that the conclusion from this study was based on a single specimen and thus gave only an indication of the cause of high motion. However there was a clear trend between the loads applied and hip stem micromotion.

The investigation of the load on the femoral head during gait using strain gauging of the implant allowed a more in-depth analysis of the simulator. The results of the investigation showed that levels of force on the head of the hip stem were much larger than those measured during the static studies. However, the exact cause of the higher loading was unknown and graphs were plotted of the force over the gait cycle were plotted to show where the peak force was applied. The shape of the magnitude and patterns of loading in the x, y and z directions were plotted and compared to *in vivo* data produced by Bergman *et al.*, (2001). Figure 7-24 shows the forces on the head of the hip

stem in orthogonal directions x, y and z in the simulator during a full gait cycle (DYN) and in the human body.

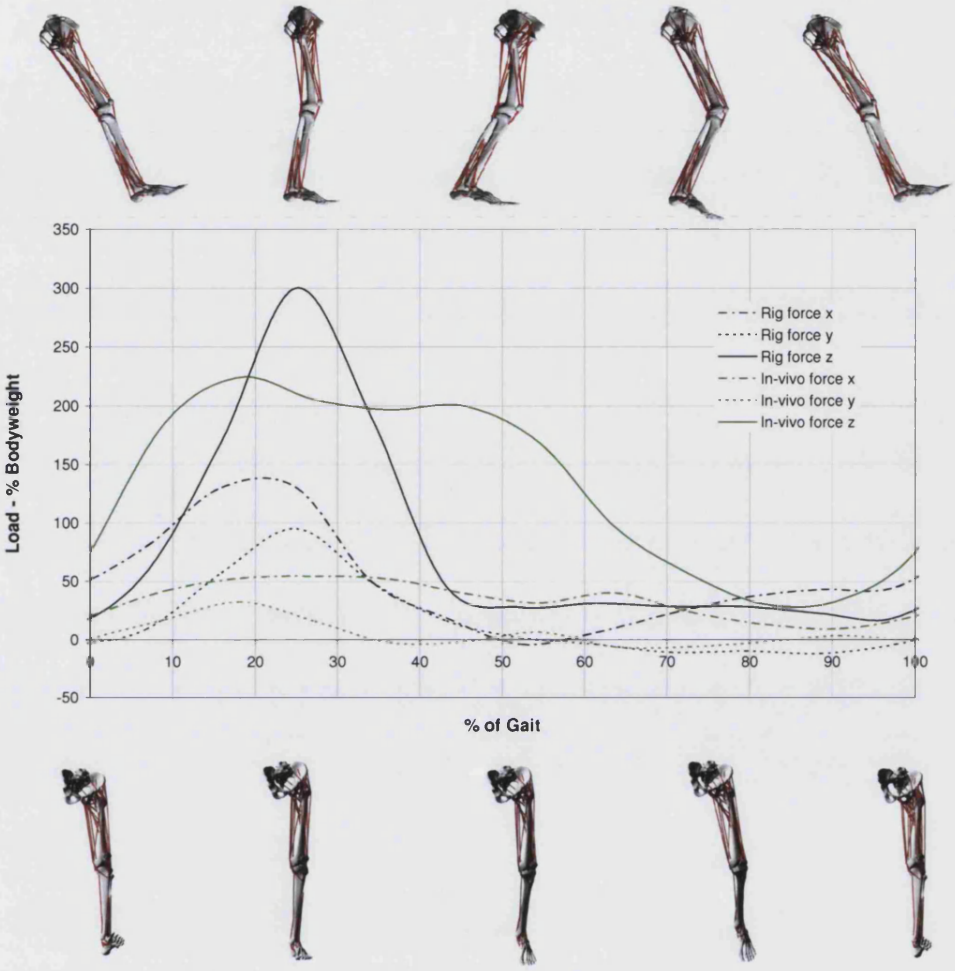

Figure 7-24 - Femoral head force in the dynamic simulator through out the gait cycle compared to in vivo data

The data is shown as percentage bodyweight to directly compare the levels of loading. The higher level of loading can clearly be seen in the simulator as the forces in the all axes (x, y and z) peaks at higher levels than their equivalent levels in the *in vivo* data. In this example the simulator produces 2.6, 2.9 and 1.3 times higher loading in the x, y, and z axes respectively, than the data measured *in vivo*. This shows that the earlier assumption made during the evaluation phase (section 6.9), that the muscle loading system was producing 2.7 times the force applied from the vertical actuator onto the femoral head, does not apply during dynamic loading. This implies that the muscle strap is not behaving according to the assumptions made in calculating the hip stem load.

The shape of the curves acquired from the instrumented hip stem suggests a reason why the muscle loading system is failing. The shape of the curves on the instrumented hip is very different from the profiles programmed into the vertical actuator, see Figure 7-24. The peak force occurs at the maximum level of adduction and the gradient either side of this peak is even. The maximum peak load should occur closer to the heel strike position as shown in the in vivo data but appears linked to the level of adduction.

One possible explanation for this shift of the peak force is that the muscle cable is tensioned as the femur passes to the adduction side of the cam and then the shape of the cam applies increasing tension in the muscle cable until the maximum adduction is reached (at 25% gait) when the femur moves back toward a neutral level of adduction unloading the muscle cable. The extra tension is acting on the muscle loading system and producing high loads on the head of the hip stem. This effect is increased with the application of load from the vertical actuator as shown in Figure 7-25.

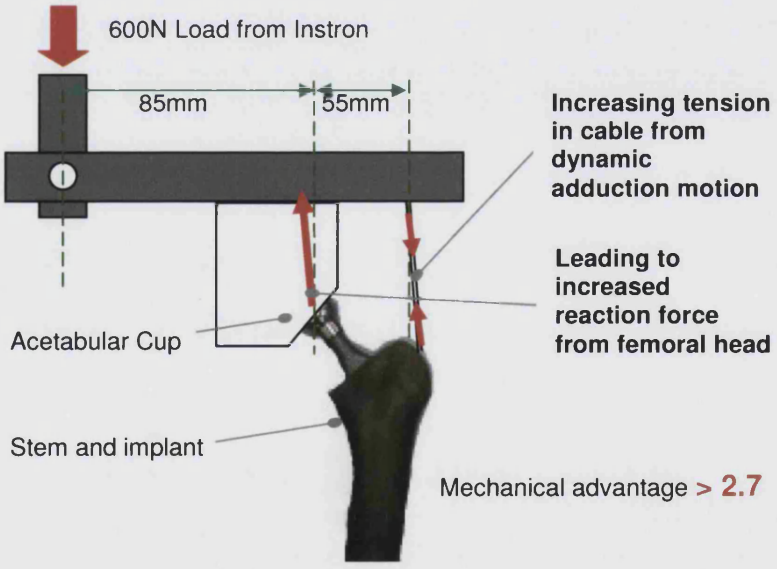

Figure 7-25 - Diagram of increased muscle cable loading

Initially it was thought that the muscle cable applying the force would be in more tension on the adduction side of the cam thereby loading the femoral head. However, it appears that the initial set up of this muscle could be the reason why it is not producing consistent results. When first introduced the muscle strap was setup with two strain gauges to record the tension in the cable however

when the muscle loading system was redesigned to bring its pivot in line with the femoral head there was no longer any room for the strain gauges so they were omitted. It was also felt that the muscle cable would only act in reaction to the force applied from the vertical actuator so the level of tension would be a direct result of the force applied. This is clearly not the case in the dynamic loading regimes as the muscle length is changing and therefore tension in the cable varies. This increase in tension, combined with the substitute pelvis increasing the force by a magnification of 2.7, could explain why the femoral head force recorded was 1.8kN when the theory predicted only 1.4kN. If the muscle tension could be setup correctly and consistently when the femur is mounted on the femoral bracket, then it may be possible to cycle the simulator with the muscle loading. However for a consistent setup the strain gauges will have to be reintroduced requiring a redesign of the muscle loading system.

Even with a better muscle cable setup the femoral head load may still be dominated by the effect of the muscle so three ways are suggested below to remove the effect of the changing muscle tension.

- The first way would be to cycle the simulator without any abduction adduction motion. Then the muscle length would not change and the muscle loading system should perform as it does in the static loading regimes. This could be achieved without too much redesign to the simulator. The cam plate would be removed and the femoral bracket fixed to the primary frame as was the case in the first stage of the simulator but with muscle loading.

- The second way to cycle the simulator without the errors caused by the changing length of the muscle would be to cycle the simulator as described at the end of the 2nd stage of the design, without the muscle loading system but including both motions of flexion extension and adduction abduction.

- Finally an additional actuator could be used to control the muscle tension governed by a profile measured *in vivo*. Suitable data for this is presented in section 3.3 by Bergman *et al.* Adding a further actuator to control muscle tension was considered in the initial concept however it

was considered that this would require a large design change which was not possible within the time scales of the project.

The inclusion of muscles in a hip stem stability test has been highlighted as important by several studies (Britton *et al.*, 2003; Kassi *et al.*, 2005). Therefore, the more desirable method to continue this research would be to eliminate the abduction adduction motion from the simulator. This would allow the simulator to model kinematics in the sagittal plane. This method would still be capable of achieving the research objective proving an understanding of what effect femoral kinematics have on hip stem stability and should prove less prone to setup errors than the more "physiologically" correct simulator used in this study.

One possible reason for the higher motion discussed earlier was the problem that the vertical loading was displacing the head of the hip stem away from the axes of rotation dictated by the primary and seconds swings thereby causing unwanted loads on the hip stem due to an over-constrained system. It is not clear from the strain gauge results on the neck of the hip stem whether this is occurring. The force profiles displayed in Figure 7-24 show that the dominant loading is caused by the tension in the muscle cable. A solution to this problem might be to redesign the simulator using an actuator to apply the load from under the knee. The problem stems from the application of load to the hip stems head which requires the acetabular cup to move downwards. However as soon as the cup moves it cannot be exactly in line with the axes of the primary and femoral bracket. If the acetabular cup were fixed in position then the load would have to be applied from under the femur at the knee position. The actuator would then move with the femur on the double mechanical frames, this is how the only dynamic simulator operates described in the literature (Liu *et al.*, 2003). This concept also has some problems of its own when considering the capacity of the actuator required and its power supply. A actuator capable of supplying 2-3 KN will add a significant inertia to the rotating frame and require careful design to fit into the space constraints. The hydraulic fluid supply and control wires may also impede the action of the simulator. Therefore the use of an actuator under the knee will require a major redesign to the rig and may not be necessary if the muscle loading issues can be rectified.

7.10. *Conclusions*

This study set out to achieve the research objective 4: the investigation of the inclusion of femoral kinematics in a bone-implant motion test and their effect on hip stem stability. This investigation employed the simulator designed in Chapter 6. This dynamic simulator was capable of replicating motion of the femur in the sagittal and coronal plane whilst applying physiological loads to the head of the hip including the action of the abductor muscles. This is only the second dynamic simulator to be reported for measuring hip stem stability and the only simulator to include motion of the femur in the coronal plane and loading of the femoral head via the action of the abductor muscles.

The initial results suggested that the inclusion of the kinematics of the femora in a bone implant micromotion study had a significant effect on the levels of micromotion. However, further investigation demonstrated that this was a result of excessive force developed by the abductor muscle during dynamic motion. The simulator in its current state is too sensitive to setup errors to assess the effect of the kinematics on hip stem stability however suggestions have been made as to how future work can overcome this with minor changes to the experimental rig. The most feasible of these suggestions would be to eliminate the abduction adduction motion from the rig and to make a preliminary assessment of how the flexion extension affects stability. If these results demonstrate an effect on hip stem stability then the simulator can be developed with more actuators to assess more degrees of freedom of the femur and alternative loading pattern e.g. dynamic stair climbing and rising from a chair.

The static results obtained as part of the study show that the loading regime modelling the heel strike of the gait pattern yielded the largest micromotion results and proved a worst case scenario for hip stem loading.

Although this study did not lead to a definitive conclusion about the effect of femoral kinematics on hip stem stability it has progressed the knowledge in this area and identified further work that will enable a clear conclusion.

Chapter 8. Final Conclusions

Total hip replacement surgery (THR) has become a very successful procedure through the introduction of many innovations (Chapter 1). This success has widened the potential age group suited to THR, including younger and more active patients and as a result the need for long term surviving hip replacement has increased. The Swedish hip register reports that the largest cause of revision operations is aseptic loosening of the hip replacement components is associated with osteolysis and the destruction of the implant bone interfaces. Long-term survival of cementless hip stems is characterised by postoperative initial stability which is crucial to allow osseointegration of the stem in the host bone. Many research groups have investigated hip stem stability and suggested new concepts of fixation and also methods to quantify the stability of hip stems (Section 2.4). Critical analysis of this research revealed the importance of pre-clinical testing and limitations with current hip stem stability studies. In particular a review of literature highlighted the need to understand how femoral kinematics during gait may affect the results of a hip stem stability study and the need for a validation of Sawbones composite femora with respect to bone implant motion.

Four objectives for this thesis were defined (Chapter 4) and are summarised as:

- to validate the use of composite femora for use in hip stem stability testing (Case study 1 - 5.7)
- to investigate the premise that good initial stability is vital for the long term survival of a hip stem (Case study 2 - 5.8)
- to design a test rig that will cycle a femur in the sagittal and coronal plane defining a gait cycle and replicating *in vivo* loading of the head of the hip stem including the action of muscle forces (Chapter 6)
- to investigate the effect of femoral kinematics during gait on hip stem stability (Chapter 7)

The first objective (Section 5.7) was to validate the use of composite femora for use with hip stem stability testing. This was achieved through comparative testing of Zweymüller type hip stems implanted in both composite and cadaveric femoral specimens. Typically cadaveric specimens have been used to assess new design of hip stems as they represent the closest environment to that which

a stem would experience *in vivo*. However, the limited availability of cadaveric material, the special handling requirements and large spread of experimental data make their use for the detection of design improvements difficult. Many research groups use Sawbones composite materials as an alternative to cadaveric specimens. Studies have validated the gross mechanical properties of Sawbones composite femora before the implantation of a hip stem; however their properties for hip stem stability tests require validation. Testing of cementless hip stems for initial postoperative stability involves testing before osseointegration would have occurred. Six SL-Plus stems were implanted into cadaveric femora and Sawbones femora. The test femora were instrumented with a six degree of freedom motion transducers to assess micromotion and migration. The specimens were set-up in single stance and stair climbing configurations to represent early postoperative gait, then subjected to loads representing those experienced *in vivo* through the use of a substitute pelvis with cables to simulate the action of the abductor muscles.

The results showed that both models (cadaveric and composite) produced similar levels of micromotion between the stem and host bone. However, the migration levels recorded in the composite femora were almost negligible compared to those recorded in the cadaveric specimens. The validation concluded that composite femora are suitable *in vitro* models for evaluating micromotion. However the migration values obtained with composite femora often lead to an underestimation of the cadaveric model values and therefore caution should be used when interpreting these results. This achieved objective 1 whereby it is valid to use composite femora in hip stem stability studies for the assessment of micromotion.

The second objective (Section 5.8) was to investigate the premise that good initial stability is vital for the long term survival of a hip stem. Initial stability is often quantified in a pre-clinical test to predict whether a stem is likely to survive in the long-term. Case study one (section 5.7) showed that Sawbones are a suitable model for the assessment of micromotion. Therefore the confirmation of the relationship between initial and long term stability in the same group of specimens and hip stems would provide further validation of the importance of initial stability on long term outcomes. Case study 2 compared two groups of cadaveric specimens, one group comprised of long term surviving implants and one with freshly implanted stems. The long term group were from donors that

had been implanted with Zweymüller hip stems a number of years ago. The second group were implanted with SL Plus stems (characterised by identical geometry to the Zweymüller stem) freshly implanted in the contra lateral cadaveric femur. The specimens were subjected to indentical loading regimes to those in case study one. The results showed similar levels of micromotion and migration (in translation and rotation) at both the proximal and distal locations. This study confirmed that initial and long term stability are linked and that this stem design demonstrated good stability both in translation and rotation that promotes good initial fixation which is continued in the long term.

A study of literature concerning hip stem stability tests highlighted that currently there is no accepted benchmark test for hip stem stability. Current tests are performed with a variety of femoral positions, loading regimes and motion transducers. The survey of the literature also showed that all but one study (the Liu simulator for cemented implants) were conducted with the femur static during the application of loading to the femoral head. This simplification of the loading environment means that the effect of femoral kinematics on hip stem stability is currently not understood. The inclusion of femoral kinematics will change the locus of the force on the femoral head and hence will be likely to alter the patterns and possibly the magnitude of forces experienced by the femoral head. Before a standard benchmark test can be established the question of the effect of femoral kinematics on hip stem stability must be resolved. The investigation into the effect of femoral kinematics on hip stem stability considered the literature on the gait cycle focusing on the range of motion in the sagittal, coronal and transverse planes; the magnitude and pattern of femoral head loading and the action of the associated muscle groups (Chapter 3).

A dynamic hip simulator was designed using the gait research data from Chapter 3 to assess the effect of femoral kinematics on hip stem stability (Objective 3 - Chapter 6). The dynamic simulator was developed through three stages to replicate *in vivo* conditions of femoral head loading and kinematics with evaluation performed at the end of each stage. The first stage simulated the sagittal motion of the femur whilst a simplified sinusoidal loading motion was applied to the head of the implant. The second stage progressed the concept of the first stage simulator by adding the motion of the femur in the coronal plane whilst a double peak loading cycle was applied to the head of the simulator.

Finally in the third stage a steel cable was added to the model to represent the abductor muscle, which was modelled in the most recent static hip stem stability studies (Britton *et al.*, 2003; Kassi *et al.*, 2005; Clements *et al.*, 2005).

The resulting dynamic simulator is the only current hip stem stability simulator to include the effect of femoral kinematics in the coronal plane and the effect of abductor muscle loading during gait. The simulator is also capable of loading hip stems statically in various levels of abduction-adduction and flexion-extension. Alternatively the simulator could be cycled, simultaneously modelling flexion-extension and abduction-adduction during a gait cycle whilst applying physiological levels of load to the head of a hip stem, including the influence of the abductor muscle group. A validation study showed that the simulator achieved the target specification for load levels and kinematics. The ability to load the femur statically or dynamically, achieving objective 3, facilitated the investigation of femoral kinematics on hip stem stability and the commencement of objective 4.

The effect of femoral kinematics on hip stem stability (Objective 4 - Chapter 7) was analysed utilising the dynamic hip simulator. The results obtained showed that the inclusion of femoral kinematics in combination with physiological loading had a significant effect on hip stem stability, producing large levels of motion at both the proximal and distal transducer. Calculations of the expected load in a dynamic cycle suggested that the patterns of loads were likely to change, producing differing levels of motion in the three orthogonal planes to those observed during static loading. However, large changes to magnitudes of micromotion were not expected. The data recorded from the actuators and motion transducers was analysed to assess the likely cause of the significantly higher micromotions experienced during dynamic testing. The data recorded in the vertical actuator showed that similar forces were exerted during both static and dynamic testing. The micromotions calculated from the transducers highlighted no unexpected peaks or vibration of the femur during the gait cycle that may have resulted in the higher values. With no explanation of the higher loading it was assumed that internal forces in the muscle loading system must be the cause and two short studies were performed to investigate this possibility.

The first study investigated the effect of increasing the load towards physiological levels on micromotion. The study showed that up to certain levels of load, the micromotion of the femur was approximately linear showing that increased levels of loading would result in larger micromotion. However the study did not record micromotions as high as those recorded during dynamic testing regimes. The results also showed that extrapolation of the data to predict motion at high load was unrealistic beyond 2kN. This was attributed to the properties of the Sawbones femora.

The second study assessed the force on the head of the stem using strain gauges on the neck of the implant. The hip stem with strain gauges attached was mounted in the simulator and subjected to each of the six testing regimes (4 static and 2 dynamic). Analysis of the data recorded from the strain gauges showed that the head of the hip stem was experiencing significantly larger forces during the dynamic cycles, peaking at the point of maximum adduction as the abductor strap was tensioned to its maximum level. The abductor strap system was sensitive to set up errors, producing problems with its action during the dynamic regime. Initially this cable was instrumented with strain gauges to ensure that the desired levels of loading were achieved and to assist with the correct setup of the abductor strap. However, once the concept was proven the instrumentation was removed due to space constraints and the limited channels for data capture. It was concluded that the abductor strap was developing too much tension, consequently producing higher than expected forces on the head of the hip stem and increasing the micromotions significantly. This increase in head force must be resolved before the true effect of femoral kinematics on hip stem stability can be quantified using this simulator.

The rig developed has made a significant step towards the identifying the effect of femoral kinematics on hip stem stability. In turn this development will provide answers to the question of whether kinematics are a necessary inclusion in a pre-clinical evaluation of cementless hip stems. The problems encountered could be overcome with the use of additional actuators or the simplification of the motions included. However, this was not possible within this study. With further research to solve the problems identified, the dynamic hip simulator shows promise for use in developing a standard pre-clinical test for assessing the stability of cementless hip stems.

In summary:

- The use of composite femora for use in hip stem stability testing has been validated against cadaveric bone demonstrating good correlation in terms of micromotion but limitations in terms of migration
- The premise that good initial stability is a reliable indication of the long term survival of a hip stem has been supported by comparisons of stability levels of freshly implanted vs. long term surviving implants in cadaveric bone. However, further work such as histology results are required before further conclusions can be made.
- The design of a test rig that will apply a loading cycle to a femur in the sagittal and coronal plane defining a gait cycle and replicating *in vivo* loading of the head of the hip stem including the action of muscle forces has been achieved
- The investigation of the effect of femoral kinematics during gait on hip stem stability and micromotion has indicated that higher levels of micromotion occur, but further development of this rig is required before definitive conclusions can be reached.

Chapter 9. Further work

Further evaluation of the influence of load level on micromotion to explore whether tests conducted at conservative loads to avoid fracturing test femora would be a useful area for further study. A large sample size is necessary to assess the pattern of stability compared to applied load. If a linear and consistent pattern could be shown, then this would promote confidence in using a lower load to reduce the risk of fracture. This would give guidance on how results from lower load level studies may be extrapolated. Initial results suggested that levels of micromotion in Sawbones are proportional to the applied load up to a certain level but further studies are necessary to establish this level. The work could be extended to include cadaveric bone models. Further work relating to the long term cadaveric will be a study of the histology of the cadaveric femora. These results may be able to explain some of the stability patterns recorded and relate these to types of tissue growth whether this is fibrous tissue or newly formed bone. This work is due to be carried out in Austria from where the cadaveric material was obtained.

In the dynamic study performed using the simulator, there is a need to reinstall the strain gauges used to monitor the tension of the muscle cables to assist the set up of the simulator. If improving the muscle cable set-up does not reduce the femoral head load there is a need to eliminate the changing muscle length of the abductor strap. Three alternative ways of cycling the dynamic simulator are suggested in Chapter 7 to remove the effect of the changing muscle tension.

- The first would be to cycle the simulator without any abduction adduction motion. The cam governing abduction and adduction would be removed from the simulator. With no rotation of the femur in the coronal plane the tension in the muscle strap would be governed by the load applied to the pelvic substitute and would achieve the desired levels of tension. However this would simplify the kinematics of the femur and the effect of coronal motion on hip stem stability could not be studied.

- The simulator could also be cycled with the system as described at the end of the 2nd stage of the design, i.e. without the muscle loading system

but including both motions of flexion extension and adduction abduction. This would enable the effect of sagittal and coronal femoral motion to be study in relation to hip stem stability. However, without the muscle strap, the simplification of the loads applied will change the magnitude and direction of the load of the head of the hip stem.

- Finally an additional actuator could be used to control the muscle tension governed by a profile calculated to represent *in vivo* levels. This method would enable the simulator to maintain kinematics in the sagittal and coronal plane and the application of load including a muscle strap. The rig modifications to incorporate an additional actuator would be significant and introduces the risk of alternative sources of error.

Suggestions are made in the discussion that the best way forward is to test the effect of the kinematics of the femur on hip stem stability without the abduction-adduction motion. With small changes to the rig, the effect of the flexion extension on the patterns and levels of micromotion can be assessed. If these results show significant change to the levels or patterns of micromotion then the other motions of the femur should be included. During investigations into the cause of higher micromotion (section 7.8.2) a hip stem was instrumented to assess the force experienced on the head of the hip stem whilst cycling in the simulator. This tool proved powerful for determining the levels and direction of applied loading on the head of the hip stem and should therefore be used in further developments of the simulator to ensure that these loads are in compliance with the desired loads. More in-depth studies will require larger changes to the rig and the introduction of more actuators. With the introduction of more actuators a feasibility study is suggested to establish if it possible to supply loading to the hip stem from an actuator mounted under the knee of the femur. This should prevent some of the off-axis forces that are expected to be seen after the muscle loading issues are resolved.

References

1. An,Y.H., Friedman,R.J., Jiang,M., LaBreck,J.C., Draughn,R.A., Butehorn,H.F., III, and Bauer,T.W. (1998) Bone ingrowth to implant surfaces in an inflammatory arthritis model. *J.Orthop.Res.* **16,** 576-584.

2. Andriacchi,T.P., Andersson,G.B., Fermier,R.W., Stern,D., and Galante,J.O. (1980) A study of lower-limb mechanics during stair-climbing. *J.Bone Joint Surg.Am.* **62,** 749-757.

3. Baleani,M., Cristofolini,L., and Toni,A. (2000) Initial stability of a new hybrid fixation hip stem: experimental measurement of implant-bone micromotion under torsional load in comparison with cemented and cementless stems. *J.Biomed.Mater.Res.* **50,** 605-615.

4. Barbour,P.S., Stone,M.H., and Fisher,J. (1999) A hip joint simulator study using simplified loading and motion cycles generating physiological wear paths and rates. *Proc.Inst.Mech.Eng [H.]* **213,** 455-467.

5. Bauer,T.W., Taylor,S.K., Jiang,M., and Medendorp,S.V. (1994) An indirect comparison of third body wear in retrived hydroxyapatite-coated, porous, and cemented femoral components. *Clin.Orthop.* **298,** 11.

6. BBC (2003a) 'Home in a day' hip replacements. *http://news.bbc.co.uk/1/hi/health/3153262.stm.*

7. BBC (2003b) 'Smart hip could treat itself'. *http://news.bbc.co.uk/1/hi/health/3153262.stm.*

8. Bergmann,G., Deuretzbacher,G., Heller,M., Graichen,F., Rohlmann,A., Strauss,J., and Duda,G.N. (2001) Hip contact forces and gait patterns from routine activities. *J.Biomech.* **34,** 859-871.

9. Berry,D.J., Morrey,B.F., and Cabanela,M.E. (2003) Uncemented Femoral Components. In *Joint Replacement Arthoplasty* (Edited by Lewallen,D.G.) Pp. 637-656. Churchill Livingstone, Minnesota.

10. Berzins,A., Sumner,D.R., Andriacchi,T.P., and Galante,J.O. (1993) Stem curvature and load angle influence the initial relative bone-implant motion of cementless femoral stems. *J.Orthop.Res.* **11,** 758-769.

11. Britton,J.R., Lyons,C.G., and Prendergast,P.J. (2004) Measurement of the Relative Motion Between an Implant and Bone under Cyclic Loading. *Strain* **40,** 193-202.

12. Britton,J.R., Walsh,L.A., and Prendergast,P.J. (2003) Mechanical simulation of muscle loading on the proximal femur: analysis of cemented femoral component migration with and without muscle loading. *Clin.Biomech.(Bristol., Avon.)* **18,** 637-646.

13. Buhler,D.W., Berlemann,U., Lippuner,K., Jaeger,P., and Nolte,L.P. (1997a) Three-dimensional primary stability of cementless femoral stems. *Clin.Biomech.(Bristol., Avon.)* **12,** 75-86.

14. Buhler,D.W., Oxland,T.R., and Nolte,L.P. (1997b) Design and evaluation of a device for measuring three-dimensional micromotions of press-fit femoral stem prostheses. *Med.Eng Phys.* **19,** 187-199.

15. Burke,D.W., O'Connor,D.O., Zalenski,E.B., Jasty,M., and Harris,W.H. (1991) Micromotion of cemented and uncemented femoral components. *J.Bone Joint Surg.Br.* **73,** 33-37.

16. Callaghan,J.J., Fulghum,C.S., Glisson,R.R., and Stranne,S.K. (1992) The effect of femoral stem geometry on interface motion in uncemented porous-coated total hip prostheses. Comparison of straight-stem and curved-stem designs. *J.Bone Joint Surg.Am.* **74,** 839-848.

17. Calonius,O. and Saikko,V. (2003) Force track analysis of contemporary hip simulators. *J.Biomech.* **36,** 1719-1726.

18. Centre for the History Science (2003) Total Hip Replacement. *http://www.chstm.man.ac.uk/images/hip-prothesis-2.jpg.*

19. Chareancholvanich,K., Bourgeault,C.A., Schmidt,A.H., Gustilo,R.B., and Lew,W.D. (2002) In vitro stability of cemented and cementless femoral stems with compaction. *Clin.Orthop.* 290-302.

20. Charnley ,J. and Kettlewell ,J. (1965) The Elimination of Slip etween Prothesis and Femur. *J.Bone Joint Surg.Br.* **47,** 56-60.

21. Cheal,E.J., Spector,M., and Hayes,W.C. (1992) Role of loads and prosthesis material properties on the mechanics of the proximal femur after total hip arthroplasty. *J.Orthop.Res.* **10,** 405-422.

22. Claes,L., Fiedler,S., Ohnmacht,M., and Duda,G.N. (2000) Initial stability of fully and partially cemented femoral stems. *Clin.Biomech.(Bristol., Avon.)* **15,** 750-755.

23. Clements,J.P., Gheduzzi,S., Webb,J.C.J., Schmotzer,H., Learmonth,I.D., and Miles,A.W. (2003) Measurement of the micromotion and migration of an un-cemented stem in an in-vitro test. IASTED Biomech.

24. Clements,J.P., Gheduzzi,S., Webb,J.C.J., Schmotzer,H., Learmonth,I.D., and Miles,A.W. (2004) An in-vitro comparison between the initial stability of a cementless stem in composite and cadaveric models. British Orthopaedic Research Society.

25. Clements,J.P., Gheduzzi,S., Zweymuller,K., Lintner,F., Schmotzer,H., Learmonth,I.D., and Miles,A.W. (2005) An in-vitro cadaveric biomechanical evaluation of the SL-Plus hip stem – comparison of long and short term stability. 51st Meeting of the Orthopaedic Research Society.

26. Cofield,R.H. (1984) Total shoulder arthroplasty with the Neer prosthesis. *J.Bone Joint Surg.Am.* **66,** 899-906.

27. Cristofolini,L., Teutonico,A.S., Monti,L., Cappello,A., and Toni,A. (2003) Comparative in vitro study on the long term performance of cemented hip stems: validation of a protocol to discriminate between "good" and "bad" designs. *J.Biomech.* **36,** 1603-1615.

28. Cristofolini,L., Viceconti,M., Cappello,A., and Toni,A. (1996) Mechanical validation of whole bone composite femur models. *J.Biomech.* **29,** 525-535.

29. Cristofolini,L., Viceconti,M., Toni,A., and Giunti,A. (1995) Influence of thigh muscles on the axial strains in a proximal femur during early stance in gait. *J.Biomech.* **28,** 617-624.

30. Crowninshield,R.D., Brand,R.A., and Johnston,R.C. (1978a) The effects of walking velocity and age on hip kinematics and kinetics. *Clin.Orthop.Relat Res.* 140-144.

31. Crowninshield,R.D., Johnston,R.C., Andrews,J.G., and Brand,R.A. (1978b) A biomechanical investigation of the human hip. *J.Biomech.* **11,** 75-85.

32. Delaunay,C. and Kapandji,A.I. (2001) Survival analysis of cementless grit-blasted titanium total hip arthroplasties. *J.Bone Joint Surg.Br.* **83,** 408-413.

33. Design news (2003) Boston Hip Simulator. *http://www.manufacturing.net/dn/index.asp?layout=article&articleid=CA151483.*

34. Doehring,T.C., Rubash,H.E., and Dore,D.E. (1999) Micromotion measurements with hip center and modular neck length alterations. *Clin.Orthop.Relat Res.* 230-239.

35. Dowson,D. and Jobbins,B. (1988) Design and development of a versatile hip joint simulator and a preliminary assessment of wear and creep in Charnley total replacement hip joints. *Eng Med.* **17,** 111-117.

36. Draughan,R.A. and An,Y.H. (2003) Mechanical Testing of the Bone and Bone-Implant Interface. *CRC Press LLC.*

37. Elftman,H. (1966) Biomechanics of muscle with particular application to studies of gait. *J.Bone Joint Surg.Am.* **48,** 363-377.

38. Engh,C.A., Hooten,J.P., Jr., Zettl-Schaffer,K.F., Ghaffarpour,M., McGovern,T.F., Macalino,G.E., and Zicat,B.A. (1994) Porous-coated total hip replacement. *Clin.Orthop.Relat Res.* 89-96.

39. English,T.A. and Kilvington,M. (1979) In vivo records of hip loads using a femoral implant with telemetric output (a preliminary report). *J.Biomed.Eng* **1,** 111-115.

40. Gheduzzi,S., Clements,J.P., Latimer,P., Schmotzer,H., Learmonth,I.D., and Miles,A.W. (2003) Post-operative stability of cementless hip stems: an in-vitro study under physiological loading conditions. 6th Congress of

the European Federation of National Associations of Orthopaedics and Traumatology.

41. Gilbert,J.L., Bloomfeld,R.S., Lautenschlager,E.P., and Wixson,R.L. (1992) A computer-based biomechanical analysis of the three-dimensional motion of cementless hip prostheses. *J.Biomech.* **25,** 329-340.

42. Goetz D.D, Smith E.J., and Harris,W.H. (1994) The prevalence of femoral osteolysis associated with components inserted with or without cement in total hip replacements. *J.Bone Joint Surg.Am.* **76,** 1121.

43. Goldsmith,A.A. and Dowson,D. (1999) A multi-station hip joint simulator study of the performance of 22 mm diameter zirconia-ultra-high molecular weight polyethylene total replacement hip joints. *Proc.Inst.Mech.Eng [H.]* **213,** 77-90.

44. Gotze,C., Steens,W., Vieth,V., Poremba,C., Claes,L., and Steinbeck,J. (2002) Primary stability in cementless femoral stems: custom-made versus conventional femoral prosthesis. *Clin.Biomech.(Bristol., Avon.)* **17,** 267-273.

45. Government Statistical Service (2003) Main Operations on NHS.

46. Greenwald,A.S. and Haynes,D.W. (1972) Weight-bearing areas in the human hip joint. *J.Bone Joint Surg.Br.* **54,** 157-163.

47. Grigoris,P., Roberts,P., Panousis,K., and Bosch,H. (2005) The evolution of hip resurfacing arthroplasty. *Orthop.Clin.North Am.* **36,** 125-34, vii.

48. Grubl,A., Chiari,C., Gruber,M., Kaider,A., and Gottsauner-Wolf,F. (2002) Cementless total hip arthroplasty with a tapered, rectangular titanium stem and a threaded cup: a minimum ten-year follow-up. *J.Bone Joint Surg.Am.* **84-A,** 425-431.

49. Grubl,A., Csepan,R., Delaunay,C., Gordes,W., Kaider,A., Parzer,R., Zenz,P., and Gottsauner-Wolf,F. (2003) Six to ten year results of use of the alloclassic hip prosthesis--a multicentre survival analysis. *Z.Orthop.Ihre Grenzgeb.* **141,** 303-308.

50. Gruen,T.A., McNeice,G.M., and Amstutz,H.C. (1979) "Modes of failure" of cemented stem-type femoral components: a radiographic analysis of loosening. *Clin.Orthop.Relat Res.* 17-27.

51. Gunston,F.H. (1971) Polycentric knee arthroplasty. Prosthetic simulation of normal knee movement. *J.Bone Joint Surg.Br.* **53,** 272-277.

52. Hanssen,A.D. (2003) Anatomy and Surgical Approaches. In *Joint Replacement Arthroplasty* Pp. 566-593. Churchhill-Livingstone, Philadelphia.

53. Harman,M.K., Toni,A., Cristofolini,L., and Viceconti,M. (1995) Initial stability of uncemented hip stems: an in-vitro protocol to measure torsional interface motion. *Med.Eng Phys.* **17,** 163-171.

54. Hay,J.G. and Reid,J.G. (1988) *Anatomy, mechanics, and human motion.* Englewood Cliffs, NJ: Prentice-Hall.

55. Hearn,S.L., Bicalho,P.S., Eng,K., Booth,R.E., Jr., Hozack,W.J., and Rothman,R.H. (1995) Comparison of cemented and cementless total hip arthroplasty in patients with bilateral hip arthroplasties. *J.Arthroplasty* **10,** 603-608.

56. Heiner,A.D. and Brown,T.D. (2001) Structural properties of a new design of composite replicate femurs and tibias. *J.Biomech.* **34,** 773-781.

57. Heller,M.O., Bergmann,G., Deuretzbacher,G., Durselen,L., Pohl,M., Claes,L., Haas,N.P., and Duda,G.N. (2001) Musculo-skeletal loading conditions at the hip during walking and stair climbing. *J.Biomech.* **34,** 883-893.

58. Heller,M.O., Bergmann,G., Kassi,J.P., Claes,L., Haas,N.P., and Duda,G.N. (2005) Determination of muscle loading at the hip joint for use in pre-clinical testing. *J.Biomech.* **38,** 1155-1163.

59. Hirakawa,K., Jacobs,J.J., Urban,R., and Saito,T. (2004) Mechanisms of failure of total hip replacements: lessons learned from retrieval studies. *Clin.Orthop.Relat Res.* 10-17.

60. Ingham,E. and Fisher,J. (2000) Biological reactions to wear debris in total joint replacement. *Proc.Inst.Mech.Eng [H.]* **214,** 21-37.

61. ISO Standards (2002) Implants for Surgery - Wear of total hip-joint prostheses ISO 14242-1. *ISO Standards.*

62. Johnston,R.C. and Smidt,G.L. (1969) Measurement of hip-joint motion during walking. Evaluation of an electrogoniometric method. *J.Bone Joint Surg.Am.* **51,** 1082-1094.

63. Judet J, Judet R, LaGrange J, and Duncover J (1954) Resection Reconstruction of the Hip. In *Arthoplasty with Acrylic Prothesis* E & S Livingstone, Edinburgh.

64. Kang,J.D., McKernan,D.J., Kruger,M., Mutschler,T., Thompson,W.H., and Rubash,H.E. (1991) Ingrowth and formation of bone in defects in an uncemented fiber-metal total hip-replacement model in dogs. *J.Bone Joint Surg.Am.* **73,** 93-105.

65. Karrholm,J., Borssen,B., Lowenhielm,G., and Snorrason,F. (1994) Does early micromotion of femoral stem prostheses matter? 4-7-year stereoradiographic follow-up of 84 cemented prostheses. *J.Bone Joint Surg.Br.* **76,** 912-917.

66. Kassi,J.P., Heller,M.O., Stoeckle,U., Perka,C., and Duda,G.N. (2005) Stair climbing is more critical than walking in pre-clinical assessment of primary stability in cementless THA in vitro. *J.Biomech.* **38,** 1143-1154.

67. Kempson,G.E., Spivey,C.J., Swanson,S.A., and Freeman,M.A. (1971) Patterns of cartilage stiffness on normal and degenerate human femoral heads. *J.Biomech.* **4,** 597-609.

68. Kim,Y.H. (2002) Bilateral cemented and cementless total hip arthroplasty. *J.Arthroplasty* **17,** 434-440.

69. Kim,Y.H. and Kim,V.E.M. (1993) Early migration of uncemented porous-coated anatomic total hip replacement: results at six years in a consecutive series. *J.Bone Joint Surg.Br.* **75,** 6.

70. Kotzar,G.M., Davy,D.T., Goldberg,V.M., Heiple,K.G., Berilla,J., Heiple,K.G., Jr., Brown,R.H., and Burstein,A.H. (1991) Telemeterized in vivo hip joint force data: a report on two patients after total hip surgery. *J.Orthop.Res.* **9,** 621-633.

71. Krismer,M., Klar,M., Klestil,T., and Frischhut,B. (1991) Aseptic loosening of straight- and curved-stem Muller femoral prostheses. *Arch.Orthop.Trauma Surg.* **110,** 190-194.

72. Liu,C., Green,S.M., Watkins,N.D., Gregg,P.J., and McCaskie,A.W. (2003) A preliminary hip joint simulator study of the migration of a cemented femoral stem. *Proc.Inst.Mech.Eng [H.]* **217,** 127-135.

73. Maher,S.A. and Prendergast,P.J. (2002) Discriminating the loosening behaviour of cemented hip prostheses using measurements of migration and inducible displacement. *J.Biomech.* **35,** 257-265.

74. Maher,S.A., Prendergast,P.J., and Lyons,C.G. (2001) Measurement of the migration of a cemented hip prosthesis in an in vitro test. *Clin.Biomech.(Bristol., Avon.)* **16,** 307-314.

75. Malchau,H. (1995) On the importance of stepwise introduction of new hip implant technology - assessment of total hip replacement using clinical evaluation, radiosterometry, digitised radiography and a national registry. Ph.D Goteborg University.

76. Malchau,H., Herberts,P., and Ahnfelt,L. (1993) Prognosis of total hip replacement in Sweden. Follow-up of 92,675 operations performed 1978-1990. *Acta Orthop.Scand.* **64,** 497-506.

77. Mandell,J.A., Carter,D.R., Goodman,S.B., Schurman,D.J., and Beaupre,G.S. (2004) A conical-collared intramedullary stem can improve stress transfer and limit micromotion. *Clin.Biomech.(Bristol., Avon.)* **19,** 695-703.

78. Martens,M., Van Audekercke,R., Delport,P., De Meester,P., and Mulier,J.C. (1983) The mechanical characteristics of cancellous bone at the upper femoral region. *J.Biomech.* **16,** 971-983.

79. McKellop,H., Ebramzadeh,E., Niederer,P.G., and Sarmiento,A. (1991) Comparison of the stability of press-fit hip prothesis femoral stems using a synthetic model femur. *J.Orthop.Res.* **9,** 297-305.

80. McLeish,R.D. and Charnley ,J. (1970) Abduction forces in the one-legged stance. *J.Biomech.* **3,** 191-209.

81. McMinn,D., Treacy,R., Lin,K., and Pynsent,P. (1996) Metal on metal surface replacement of the hip. Experience of the McMinn prothesis. *Clin.Orthop.Relat Res.* S89-S98.

82. Morlock,M., Schneider,E., Bluhm,A., Vollmer,M., Bergmann,G., Muller,V., and Honl,M. (2001) Duration and frequency of every day activities in total hip patients. *J.Biomech.* **34,** 873-881.

83. Murray,M.P. (1967) Gait as a total pattern of movement. *Am.J.Phys.Med.* **46,** 290-333.

84. Murray,M.P., Kory,R.C., and Clarkson,B.H. (1969) Walking patterns in healthy old men. *J.Gerontol.* **24,** 169-178.

85. Netter,F.H. (1997) *Atlas of Human Anatomy.* Rittenhouse Book Distributors Inc.

86. Nordin,M. and Frankel,V.H. (1980) Biomechanics of the Hip. In *Basic Biomechanics of the Musculoskeletal System* (Edited by Nordin M and Frankel V.H.) Lippincott Williams & Williams, Baltimore.

87. Oh,I. and Harris,W.H. (1982) A cement fixation system for total hip arthroplasty. *Clin.Orthop.Relat Res.* 221-229.

88. Panjabi,M.M., Brand,R.A., Jr., and White,A.A., III (1976) Mechanical properties of the human thoracic spine as shown by three-dimensional load-displacement curves. *J.Bone Joint Surg.Am.* **58,** 642-652.

89. Paul,J.P. (1966) Forces transmitted by joints in the human body. *Proc.Inst.Mech.Eng [H.]* **181.**

90. Paul,J.P. (1997) Development of standards for orthopaedic implants. *Proc.Inst.Mech.Eng [H.]* **211,** 119-126.

91. Pedersen,D.R., Brand,R.A., and Davy,D.T. (1997) Pelvic muscle and acetabular contact forces during gait. *J.Biomech.* **30,** 959-965.

92. Perry,J. (1992) Hip. In *Gait Analysis and Pathological Function* (Edited by Perry,J.) Pp. 111-129. Delmar Learning, NJ.

93. Pieringer,H., Auersperg,V., Griessler,W., and Bohler,N. (2003) Long-term results with the cementless Alloclassic brand hip arthroplasty system. *J.Arthroplasty* **18,** 321-328.

94. Pilliar,R.M., Lee,J.M., and Maniatopoulos,C. (1986) Observations on the effect of movement on bone ingrowth into porous-surfaced implants. *Clin.Orthop.Relat Res.* 108-113.

95. Polgar,K., Gill,H.S., Viceconti,M., Murray,D.W., and O'Connor,J.J. (2003) Strain distribution within the human femur due to physiological and simplified loading: finite element analysis using the muscle standardized femur model. *Proc.Inst.Mech.Eng [H.]* **217,** 173-189.

96. Prendergast,P.J. and Maher,S.A. (2001) Issues in pre-clinical testing of implants. *Journal of Materials Processing Technology* **118,** 337-342.

97. Roach,K.E. and Miles,T.P. (1991) Normal hip and knee active range of motion: the realtionship to age. *Phys.Ther.* **71,** 656.

98. Rohrle,H., Scholten,R., Sigolotto,C., Sollbach,W., and Kellner,H. (1984) Joint forces in the human pelvis-leg skeleton during walking. *J.Biomech.* **17,** 409-424.

99. Rothman Insitute (2005) Hip Arthroplasty. *http://www.rothmaninstitute.com/.*

100. Rydell,N.W. (1966) Forces acting on the femoral head-prosthesis. A study on strain gauge supplied prostheses in living persons. *Acta Orthop.Scand.* **37,** Suppl-132.

101. Saikko,V.O. (1996) A three-axis hip joint simulator for wear and friction studies on total hip prostheses. *Proc.Inst.Mech.Eng [H.]* **210,** 175-185.

102. Schneider,E., Kinast,C., Eulenberger,J., Wyder,D., Eskilsson,G., and Perren,S.M. (1989) A comparative study of the initial stability of cementless hip prostheses. *Clin.Orthop.* 200-209.

103. Seer's Training website (2005) Planes of the Body. *http://training.seer.cancer.gov/.*

104. Smidt,G.L. (1971) Hip motion and related factors in walking. *Phys.Ther.* **51,** 9-22.

105. Smith,S.L., Burgess,I.C., and Unsworth,A. (1999) Evaluation of a hip joint simulator. *Proc.Inst.Mech.Eng [H.]* **213,** 469-473.

106. Smith,S.L. and Unsworth,A. (2001) A five-station hip joint simulator. *Proc.Inst.Mech.Eng [H.]* **215,** 61-64.

107. Smith-Petersen (1939) Arthroplasty of the hip. A new method. *J.Bone Joint Surg.Am.* **37A,** 269.

108. Soballe,K., Toksvig-Larsen,S., and Gelineck,J. (1993) Migration of hydroxyapatite coated femoral prothesis: a roentegen stereophotogrametric study. *J.Bone Joint Surg.Br.* **75,** 681.

109. Speirs,A.D., Slomczykowski,M.A., Orr,T.E., Siebenrock,K., and Nolte,L.P. (2000) Three-dimensional measurement of cemented femoral stem stability: an in vitro cadaver study. *Clin.Biomech.(Bristol., Avon.)* **15,** 248-255.

110. Swedish Orthopaedic Association (2003) Swedish National Hip Register. *http://www.jru.orthop.gu.se/archive/AnnualReport-2003-eng.pdf.*

111. Szivek,J.A., Thomas,M., and Benjamin,J.B. (1993) Characterization of a synthetic foam as a model for human cancellous bone. *J.Appl.Biomater.* **4,** 269-272.

112. Utah Hip and Knee Centre (2005) History of Total Joint Replacement. *http://www.utahhipandknee.com/.*

113. Viceconti,M., Cavallotti,G., Andrisano,A.O., and Toni,A. (1996) Discussion on the design of a hip joint simulator. *Med.Eng Phys.* **18,** 234-240.

114. Walker,P.S., Schneeweis,D., Murphy,S., and Nelson,P. (1987) Strains and micromotions of press-fit femoral stem prostheses. *J.Biomech.* **20,** 693-702.

115. Whiteside,L.A. and Easley,J.C. (1989) The effect ofcollar and distal stem fixation on micromotion of the femoral stem in uncemented total hip arthroplasty. *Clin.Orthop.* **239,** 145-152.

116. Wood,J.B., Klassen,R.A., and Peterson,H.A. (1995) Osteochondritis dissecans of the femoral head in children and adolescents: a report of 17 cases. *J.Pediatr.Orthop.* **15,** 313-316.

Appendix I

Publications

Conferences Papers

"Post-operative stability of cementless hip stems: an in-vitro study under physiological conditions"
Gheduzzi S, **Clements J P**, Latimer P, Schmotzer H, Learmonth ID and Miles AW
Presented at 6th Congress of EFORT, Helsinki, June 2003

"Measurement of the micromotion and migration of an uncemented stem in an in-vitro test"
Clements J P, Gheduzzi S, Heal J, Learmonth ID and Miles AW
Proc. IASTED International Conference BioMECH 2003, Rhodes, June-July 2003, pp18-21 ISBN – 0-88986-359-8

"Design and Development of a Hemi Pelvis Loading Rig for Evaluating Biodegradable Fixation Techniques"
Clements J P, Moriarty N, Chesser T, Cunningham J
Presented at Institute of Physics and Engineering in Medicine (IPEM), Bath, UK, September 2003

"An in-vitro comparison between the initial stability of a cementless stem in composite and cadaveric models"
Clements J P, Gheduzzi S, Webb, JCJ, Schmotzer H, Learmonth ID and Miles AW
Presented at British Orthopaedic Research Society Meeting, Bristol, March 2004

"Post-Operative stability of the SL-Plus stem: an in vitro comparison between cadaveric and composite models"
Gheduzzi S, **Clements J P**, Webb JCJ, Zweymüller K, Lintner F, Schmotzer H, Learmonth ID and Miles AW
Presented at European Hip Society, Innsbruck, June 2004

"An In Vitro Cadaveric Biomechanical Evaluation of Cementless Hip Stem Comparison of Long and Short Term Stability"
Clements J P; Gheduzzi, S; Zweymüller, K; Lintner F; Schmotzer, H; Learmonth, I D; Miles A W

Presented at Orthopaedic Research Society (ORS), Washington, USA, 20-23rd February 2005

"In-Vitro Post-Operative Stem Stability using Composite and Cadaveric Models"
Gheduzzi S, **Clements J P**, Webb J C J, Schmotzer H, Learmonth I D, Miles A W
Presented at Orthopaedic Research Society (ORS), Washington, USA, 20-23rd February 2005

"Development of a Dynamic Hip Joint Simulator"
Clements J P
IMechE Showcase Lecture, University of Bath, 10th March 2005

IASTED International Conference BioMECH 2003

MEASUREMENT OF THE MICROMOTION AND MIGRATION OF AN UN-CEMENTED STEM IN AN IN-VITRO TEST

J.P Clements, S. Gheduzzi †, J. Heal †, I.D. Learmonth † and A.W. Miles
Centre for Orthopaedic Biomechanics, Department of Mechanical Engineering, University of Bath, UK
† Department of Orthopaedic Surgery, University of Bristol, UK

Abstract

Objective. This study investigates the postoperative stability of the cement-less IPS hip stem (De Puy) by means of measuring the relative motion of the implant with the host bone.
Background. Primary stability of a cement-less hip stem is considered as one of the key factors for promoting good oesteoingeration helping to achieve long-term clinical success. The motion of the implant relative to the bone is catagorised into two modes, micromotion and migration.
Method. Six IPS hip stems were implanted into six composite femora. A six degrees of freedom displacement transducer was attached to the implant and composite femur to record the motion under two loading regimes, single leg stance and stair climbing.
Results. The motions measured were very small in all three orthogonal directions. The displacement transducer did not record any significant migration as motions detected were within the error range.
Conclusion. The IPS hip stem is extremely stable and shows that the design philosophy of this stem is effective producing excellent postoperative stability.

Key Words

Orthopaedics, Hips and femurs, Total hip replacement, postoperative stability, micromotion.

1. Introduction

The initial stability of cement-less hip stems is one of the key factors for the long-term clinical success of total hip arthroplasty [1]. Good initial stability promotes osteointegration between the implant and the host bone, leading to a better fixation over time. Its has been noted (Pillar *et al* [2]) that if the relative movement between the implant and the host bone is less than 28µm then bone ingrowth can occur. However, the same researchers also noted that if the relative motion exceeds 150µm then formation of connective tissues is favoured.

The need for immediate postoperative stability and the estimated one million hip operations per year worldwide [3] has led to vast numbers of new implant designs based on different fixation philosophies. Many of these new implants are not rigorously tested in the laboratory prior to implantation and find widespread use with little knowledge of their immediate postoperative stability. To address this issue, several researchers have been involved in developing test methodologies suitable for a *priori* discriminating implants that, due to their geometry, will be inherently stable. The aim of this study was to evaluate the initial stability of the IPS hip stem (DePuy) using six degrees of freedom displacement transducer, similar to that developed by Berzins *et al* [4]. The stability of the stem was assessed in terms of micromotion and migration; Micromotion was defined as the recoverable movement of the implant relative to the host bone under cyclic loading, a function of the elasticity of the bone-implant construct. Migration was defined as the unrecoverable movement of the implant with respect to the surrounding bone, and reflects the micro-damage caused by the implant to the host tissue.

2. Method

Six IPS size 4, left sided stems, with 12mm offset head components, were implanted by an experienced orthopaedic surgeon into six Sawbones® third generation composite femora. The Sawbones femora were used to represent the gross mechanical properties of cancellous and cortical bone without the large natural variation seen with the cadaveric studies. The repeatability of the neck cut angle on the femur was ensured with a moulded rig to guide the saw blade along the same path each time.

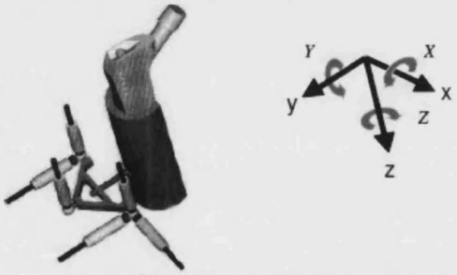

Figure 1 - *Schematic arrangement of the measuring transducer and co-ordinate system*

The displacement transducer was attached to the IPS stem and Sawbones® femur to measure the relative movements between the implant and host bone in six degrees of freedom.
The transducer was composed of the following parts:
(i) a pin push fitted into a hole drilled into the lateral face of the implant and protruding out of the Sawbones® femur via an oversized hole,
(ii) a target frame, attached to the pin, holding three target spheres,
(iii) a housing bracket fixed rigidly to the femur to hold the LVDT's in the configuration shown in figure 1,
(iv) six linear variable differential transformers, LVDT's, (Marposs, UK, AF050).

The push fitted pin was positioned on the lateral side of the stem, 35mm below the shoulder of the implant.

Each femur was tested in two different loading configurations: single leg stance and stair climbing. Single leg stance was modelled with the femur in 11^0 of adduction and 7^0 of flexion [5]. The load cycle consisted of a compressive haversine-loading curve oscillated between 60N and 600N. Stair Climbing was modelled with the femur in 11^0 of adduction and 32^0 of flexion [5], in this case the compressive haversine loading curve oscillated between 40N and 400N.

The loading was applied to the head of the implant at a frequency of 0.5 Hz for a duration of 200 cycles per test. Each test was repeated 6 times of each femur with a 30 second relaxation phase between tests. A custom data capture algorithm was programmed to acquire at a frequency of 50 Hz the voltage outputs from the LVDT's and from the materials testing machine.

Prior to testing, each femur with implant was run through a preconditioning sequence of 200 cycles of compressive cycles following a haversine waveform with the load oscillating between 60N and 600N at 0.5Hz.

The captured data was post-processed by a MATLAB routine in order to convert the voltages into translations, rotations and applied load. A Fast Fourier transform algorithm was used to evaluate the amplitude with a second order polynomial fit through the center point of the oscillations as illustrated in Figure 2.

3. Results

A typical output from the MATLAB routine is shown in Figure 2. The first row of graphs shows the translations of the stem, the second row shows the rotations with respect to the local coordinate system defined for the femur.

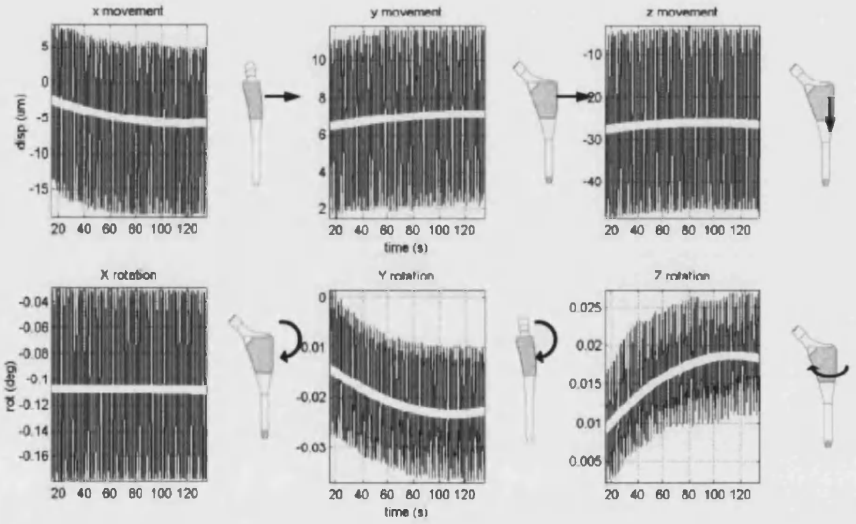

Figure 2 - *A typical set of results from a Stair Climbing test showing the micromotion and migration of the implants in orthogonal directions*

The flatness of the curves fitted to the graphs in Figure 2 demonstrates the very low migration measured in this test. The largest migration recorded was 2.5µm in the x direction during single leg stance. All other migrations (translations and rotations) recorded were so small that they were considered negligible with respect to the capability of the measuring transducer and setup.

The average translations of micromotion for femur 2 are shown in Figure 3 and the average rotations (micromotion) for the same femur are shown in Figure 4. A summary of all results for all femora is presented in Figure 5. In general the rotations measured were very small, the most significant being that about the X-axis with a magnitude of 0.05^0 (SD 0.02^0) and 0.04 (SD 0.016^0) for single leg stance and stair climbing respectively. This rotation is a consequence of the load being applied through the femoral head resulting in an off-axis force exerted to the stem. The largest micromotion amplitudes were recorded in the z direction for both loading regimes with an average of 8µm (SD 6µm) during single leg stance and 7µm (SD 6µm) during stair climbing.

The amplitude of micromotion along the x and y directions were smaller, with magnitudes of 6µm (SD 3µm) and 2µm (SD 1µm) respectively for single leg stance and 5µm (SD 3µm) and 2µm(SD 1µm) for stair climbing.

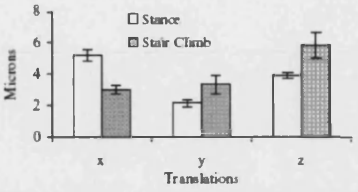

Figure 3 - *Translation in x, y and z for the IPS hip stem implanted in femur 2*

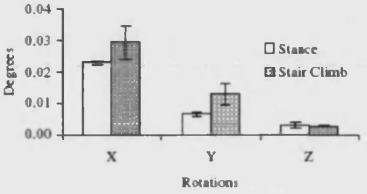

Figure 4 - *Rotations in X, Y and Z for the IPS hip stem implanted in femur 2*

	Micro-motion						*Migration*					
	Translation (µm)			*Rotation (deg)*			*Translation (µm)*			*Rotation (deg)*		
	x	*y*	*z*	*X*	*Y*	*Z*	*x*	*y*	*z*	*X*	*Y*	*Z*
Single Leg Stance												
Ave. Femur 1	4.7	3.6	7.5	0.059	0.006	0.011	-2.5	1.3	0.2	-0.002	-0.001	0.005
Ave. Femur 2	5.2	2.2	3.9	0.023	0.007	0.003	-1.3	1.4	-0.6	0.000	-0.001	0.004
Ave. Femur 3	8.7	2.1	15.3	0.069	0.015	0.014	-1.1	0.8	-1.6	-0.005	-0.002	0.004
Ave. Femur 4	6.2	1.4	3.4	0.065	0.013	0.008	-0.2	0.7	-0.1	-0.005	-0.001	0.005
Ave. Femur 5	1.0	1.6	1.5	0.031	0.005	0.008	-1.7	1.6	-1.5	0.001	-0.003	0.004
Ave. Femur 8	7.8	2.0	13.4	0.063	0.014	0.014	-1.6	0.6	-0.2	-0.003	-0.001	0.005
Overall Ave.	*5.6*	*2.2*	*7.5*	*0.052*	*0.010*	*0.010*	*-1.4*	*1.1*	*-0.6*	*-0.002*	*-0.002*	*0.004*
Stan Dev	*2.7*	*0.8*	*5.7*	*0.020*	*0.005*	*0.004*	*0.8*	*0.4*	*0.8*	*0.003*	*0.001*	*0.001*
Stair Climbing												
Ave. Femur 1	1.8	2.7	2.5	0.042	0.005	0.008	0.3	0.2	-0.2	-0.002	0.000	-0.001
Ave. Femur 2	3.0	3.4	5.9	0.029	0.013	0.003	-0.1	0.1	-0.2	-0.001	0.000	-0.001
Ave. Femur 3	8.8	2.3	13.8	0.063	0.021	0.012	0.3	0.2	-0.4	-0.002	-0.001	-0.001
Ave. Femur 4	4.3	0.7	2.0	0.052	0.014	0.007	0.0	-0.1	0.1	-0.002	0.000	-0.001
Ave. Femur 5	1.5	1.2	1.9	0.025	0.007	0.005	0.2	0.3	0.0	-0.001	0.000	0.000
Ave. Femur 8	8.8	2.5	13.3	0.059	0.019	0.009	0.2	-0.1	-0.3	-0.002	-0.001	-0.001
Overall Average	*4.7*	*2.1*	*6.6*	*0.045*	*0.013*	*0.007*	*0.2*	*0.1*	*-0.2*	*-0.002*	*0.000*	*-0.001*
Stan Dev	*3.3*	*1.0*	*5.6*	*0.016*	*0.006*	*0.003*	*0.2*	*0.1*	*0.2*	*0.001*	*0.000*	*0.001*

Figure 5 – *Table showing summary of all results for the six hip stems and femurs tested*

4. Conclusion

The average magnitude of micromotion recorded during this set of experiments were all well within the 28μm limit below which Pilliar *et al* [2] suggested for good oesteoingration. The values for migration recorded from this experimental set-up were extremely small, within the error of the testing apparatus. This has led to the conclusion that this implant is extremely stable and shows that the design philosophy adopted for this stem is effective in producing excellent postoperative stability. Additional development of the test rig to further increase the capability of resolving very small movements is not deemed to be beneficial as its current state it is adequate to assess implants movements well below the critical level 28μm [2].

5. Acknowledgements

DePuy International (Leeds) for supplying hip stems

Lab manager - Richard Weston, Centre for Orthopaedic Biomechanics, Department of Mechanical Engineering, University of Bath

References

[1] Y.H. An, R.A Draughan, eds. Mechanical Testing of the Bone and Bone-Implant Interface. *CRC Press LLC*

[2] R.M. Pillar, J.M. Lee, C Maniatopoulos, Observations on the effect of movement on bone ingrowth into porous-surfaced implants. *Clin. Orthop.*, 208: 108-113, 1986.

[3] D.W. Murray, A.J. Carr, C.J. Bulstrode, Which primary total hip replacement. *J Bone Joint Surg B* 1995; 77:520-7.

[4] A Berzins, D.R. Sumner, T.P Andriacchi, J.O Galante, Stem curvature and load angle influence the initial relative bone implant motion of cement less femoral stems. *J Orthop Res* 1991; 9:297-305.

[5] T.P Andriacchi, G.B.J Andersson, R.W Fermier, D Stern, J.O Galante, A study of lower-limb mechanics during stair climbing *J Bone J Surg* 1980; 62-A:749-757

IPEM September 2003

Design and Development of a Hemi Pelvis Loading Rig for Evaluating Biodegradable Fixation Techniques

J. Clements[1], N. Moriarty[1], T. Chesser[2], J. Cunningham[1],
[1]Centre for Orthopaedic Biomechanics, University of Bath, UK
[2]Frenchay Hospital, Bristol, UK

Background and purpose Pelvic ring injuries caused by trauma often require plate or screw fixation across the pubis symphysis (PS) to stabilise and reduce the fracture whilst healing occurs. New biodegradable materials have been produced to stabilise the fracture during the reparative stages then degrade into harmless substances naturally excreted by the body leaving the surgeon with no secondary surgery to remove the implant. These new materials need to be assessed for their mechanical fixation immediately postoperatively and as the implant degrades in the body environment over time. A test procedure is therefore required to discriminate which new techniques and materials will provide good pelvic stability. The aim of this study was to design and develop a method of simulating the degradation process and suitably loading a partially constrained hemi pelvis model to assess the new implants stability by measuring its motion with a six degree of freedom motion transducer.

Design The design of the rig was based around the Sawbones composite pelvis and was designed as a hemi pelvis model as composite models were only available for the left side. The hemi pelvis model was based on a full pelvis model by Simonian [1] where the pelvis is loaded through the L5 vertebra against two hip stems allowed to slide laterally and rotate about the inferior/superior axis. The new rig can be seen in Figure 1 where the individual features are shown. The hemi pelvis is supported on one side by a hip stem using the same constraints as Simonian[1]. The implant is attached across the PS joint with one side attached to the hemi pelvis and the other held rigid with respect to the loading machine. The pelvis is loaded on the L5 vertebra via a rod end allowing free rotation about all three axes.
The motion of the pelvis is recorded on a movement transducer based on research by Berzins et al [2] but developed to measure the larger motions of the pelvis. The displacement transducers are linear potentiometers arranged in a configuration that will record motions of three target spheres connected to the pelvis via a rigid pin attached locally at the PS joint.

Method In order to assess the performance of biodegradable implants it would be necessary to subject a number of samples to artificial degradation and periodically test their mechanical properties. This would provide information about how the implants properties change over time. Based on American and International standards [3] [4] a test method has been developed whereby the implants are placed in a buffered saline solution at physiological temperature. The implants are then periodically removed and tested to establish the effects of degradation on material and mechanical properties.

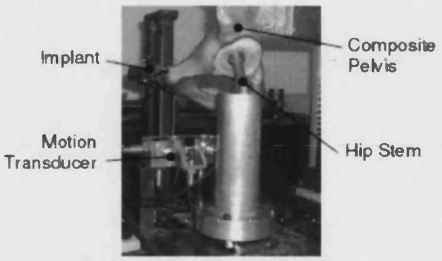

Figure 1 - The hemi pelvis rig setup

The load cycle applied through the L5 vertebra consists of a compressive haversine-loading curve oscillated between 60N and 600N at 0.5Hz to represent a slow paced walk. The captured data is post-processed by a MATLAB routine in order to convert the voltages into translations, rotations and applied load. A Fast Fourier transform algorithm is then used to evaluate the amplitude with a second order polynomial fitted through the centre point of the oscillations.
These results show the motions in six degrees of freedom, therefore giving a complete picture of how the pelvis and the implant are responding due to the loads applied.

Conclusions This rig and testing method have the capability to assess many techniques of fixation at the pubis symphysis. The results show how the implant maintains the stability of the pelvic ring and can be used to compare differing implants or analyse the performance of one implant at several stages throughout the degradation process. This hemi pelvis-testing rig therefore allows good analysis of pubis symphysis implants without the complications, time and expense of a cadaveric study.

References

[1] Simonian, Routt, Harrington, Tencer, Box plate fixation of the Symphysis Pubis *J. of Orthopaedic Trauma* Vol.8:476-482:1994
[2] Berzins A, Summer D, Andriacchi T, Galante J, Stem Curvature and load angle influence the initial relative bone implant motion of cement less femoral stems. *J Orthop Res* 1991; 9:297-305.
[3] ASTM, Standard test method for in vitro degradation testing of poly (L-lactic acid) resin and fabricated form surgical implants, *Annual Book of ASTM Standards*, Volume 13, F1635-95; 2001
[4] International Standard, Implants for surgery – Copolymers and Blends based on polylactide, In vitro degradation testing *ISO* 15814:1999

BORS 2004

A IN-VITRO COMPARISON BETWEEN THE INITIAL STABILITY OF A CEMENTLESS STEM IN COMPOSITE AND CADAVERIC MODELS

+Clements, J P; *Gheduzzi, S; *Webb, J C J; **Schmotzer, H; *Learmonth, I D; Miles, A W
Centre for Orthopaedic Biomechanics, University of Bath, UK

Introduction

Immediate postoperative stability of cementless hip stems is one of the key factors for the long-term success of total hip replacement. The ability to discriminate between stable and unstable stems in the laboratory constitutes a desirable tool for the industry, as it would allow the identification of unsuitable stem designs prior to clinical trials. The use of composite femora for stability investigations is wide spread [1,2] even though their use in this application is yet to be validated. This study is aimed at establishing whether Sawbones composite femora are suitable for the assessment of migration and micromotion of a cementless hip stem. The stability of two SL Plus stems (Precision Implants, CH) implanted into Sawbone was compared to that of two SL Plus stems implanted into cadaveric femora. Ethical approval was obtained for the harvest and use of cadaveric material.

Method

Stability was assessed in terms of micromotion and migration. Micromotion was defined as the recoverable movement of the implant relative to the bone under cyclic loading. Migration was defined as the non-recoverable movement of the implant with respect to the surrounding bone. Movement of the implant with respect to the surrounding bone was monitored at two locations on the lateral side of the stem by means of two custom made transducers based on the concept described by Berzins et al [3]. Each femur was tested in two different sinusoidal loading configurations: single leg stance (SLS-11^0 of adduction and 7^0 of flexion) [4] loaded up to 400N and stair climbing (SC-11^0 of adduction and 32^0 of flexion) loaded up to 300N. The effect of the abductor muscles was included in the model [5]. Each test consisted of 200 loading cycles applied at 50 Hz. The captured data was post-processed by a MATLAB routine and converted into translations and rotations of the stem with respect to the bone.

Results

The proximal part of the implant was subject to the highest amplitudes of micromotion in both loading configurations independent of the host. During SLS the largest micromotion was measured in the direction of the axis of the femur, this amplitude was in the order of 20 µm for the stems implanted in sawbones and varied between 13 and 39 µm for the stems implanted in cadaveric femora. The migration of the implants was minimal both in SLS and SC for both hosts with values measured in the sawbones model nearly on order of magnitude smaller than the cadaveric. In the case of SLS the prevalent movement consisted of a translation along the axis of the bone, while during SC the rotations became prevalent.

Discussion

This study has demonstrated that Sawbones provide an effective model to establish micromotion with oscillation patterns and orders of magnitude similar to cadaveric bone. However the migration is much more dependent on the quality of fit and the internal geometry of the femur and therefore more caution should be placed on interpreting migration data from Sawbones models.

References

1. Maher et al, 2001 Clin.Biomechanics; 12; 4 p307
2. Liu et al, 2003 Proc.Inst.Mech.Eng [H]; 217; 2 p127
3. Berzins et al, 1991 J.Orthop.Res; 11;5 p758
4. Andriacchi et al, 1980 JBJS; 62;5 p749
5. Tanner et al, 1988 J.Biomed.Eng; 10;3 p289

Affiliated Institutions for co-authors

Centre for Orthopaedic Biomechanics, University of Bath, UK *Department of Orthopaedic Surgery, University of Bristol, UK **Precision Implants AG, CH

ORS 2005

AN *IN VITRO* CADAVERIC BIOMECHANICAL EVALUATION OF A CEMENTLESS HIP STEM COMPARISON OF LONG AND SHORT TERM STABILITY

+*Clements, J P; ** Gheduzzi, S; ***Zweymuller, K; ****Lintner F., *****Schmotzer, H; **Learmonth, I D; *Miles, A W
+*Centre for Orthopaedic Biomechanics, University of Bath, UK
enpjpc@bath.ac.uk

INTRODUCTION:

The "Zweymuller" stem has been implanted in over 350,000 patients since its introduction in 1979 and reports have shown 99% survivorship after 10 years (Delaunay et al, 2001 and Grübl, 2002). The long-term success of cementless hip prosthesis is dependent upon achieving primary postoperative stability between the implant and the host bone to promote early osteointegration. The design of the stem is claimed to offer both primary and long-term stability with the rectangular form intended to anchor the stem rotationally and the tapered geometry for axial fixation. However, no current study has assessed the long-term fixation of this design philosophy. The aim of this study is to compare the initial postoperative stability to the stability after several years implantation by evaluating micromotion and migration levels between the stem and the host bone. Patient consent and ethical approval were obtained for the harvest of femora and cadaveric testing.

METHOD:

The study used five paired femora with a long term surviving "Zweymuller" stem implanted one side. The contralateral femur was freshly implanted with the latest version "Zweymüller" stem (SL-Plus, Plus Endoprothetik AG, CH), sized according to templates by an experienced orthopaedic surgeon. All femora with implanted stems were subjected to loading cycles and the stability was assessed in terms of micromotion and migration. Micromotion was defined as the recoverable movement of the implant relative to the bone under cyclic loading, a function of the elasticity of the bone-implant construct. Migration was defined as the non-recoverable movement of the implant with respect to the surrounding bone, and reflects the micro-damage caused by the implant to the material in its immediate surroundings.

Figure 1: The SL Plus stem with transducers and co-ordinate system.

The movement of the implant with respect to the surrounding bone was monitored at two different locations on the lateral side of the stem by means of two custom made transducers (Figure 1) based on the concept described by Berzins *et al.* (1991). Each femur was preconditioned at low load and then subjected to two different loading configurations representative of Single Leg Stance (SLS) and Stair Climbing (SC) (Andriacchi et al, 1980). These are summarised in Table 1. The effect of the abductor muscles was included in the model (Tanner et al., 1988)

Loading regime	Flexion	Adduction	Load (N)
Single Leg Stance (SLS)	7°	11°	1,080
Stair Climbing (SC)	32°	11°	800

Table 1: summary of the loading regimes applied to each femur.

Each test consisted of 200 loading cycles applied at a frequency of 0.5 Hz. The voltage output from the LVDTs was acquired at a frequency of 50 Hz and stored on a personal computer. The captured data was post-processed by a MATLAB routine and converted into translations and rotations of the stem with respect to the bone according to the local coordinate system defined in Figure 1. A Fast Fourier transform algorithm was used to evaluate the amplitude of micromotion. Migration was evaluated by a second order polynomial fit through the center point of the oscillations. Differences between the long term surviving stems and freshly implanted stems were analysed with the Mann-Whitney U test for independent groups. Statistical significance was assumed for $p<0.05$. Results are expressed as median (25^{th} quartile – 75^{th} quartile).

RESULTS:

Figure 2: Amplitudes of the prevalent micromotion oscillations recorded by the proximal transducers in the case of SLS (left) and SC (right).

Figure 3: Prevalent migration recorded by the proximal transducer in the case of SLS (left) and SC (right).

The largest micromotion movements recorded during the SLS experiments consisted, for both hosts, in oscillations parallel to the longitudinal axis of the femur (z in Figure 1). These amounted to 19µm (8µm - 40µm) in the case of long term surviving implants and 13µm (7µm - 30µm) for the freshly implanted ones. These differences were not statistically significant (Figure 2). In SC rotations about the x-axis became the prevalent. The data compared similarly with values of 0.027°(0.01° - 0.04°) for long-term and 0.014° (0.01° – 0.03°) for freshly implanted stems, respectively (Figure 2). The highest micromotion amplitudes were recorded in both groups proximally independently of the loading configuration. The highest migrations were recorded in SLS along the z-axis. These were similar between the two groups with values of 10µm (6µm -19µm) for long-term living stems and 9µm (4µm – 17µm) for the freshly implanted ones (Figure 3). In SC the largest rotational migration levels recorded were about the Z-axis with levels of -0.017°(-0.02° - 0.00°) long-term and -0.005° (-0.05° – 0.01°) freshly implanted (Figure 3). In general there was no significant difference between the values for translation motion recorded between the long-term and freshly implanted stems.

CONCLUSION:

This study has demonstrated that a double-tapered rectangular stem is stable in both SLS and SC giving low micromotion values especially in rotation. This is applicable both in the case of the freshly implanted stems and the long term surviving stems. The type of stem thus offers immediate postoperative stability and this stability is continued in the long-term. Clinical evidence suggests that initial stability is key to long-term success and the findings of the study show evidence of supporting this.

REFERENCES:

Delaunay et al, J Bone Joint Surg [Br] 2001; Grübl, J Bone Joint Surg, [A] 2002; Berzins et al, J Ortho Res 1991; Tanner et al., J Biomed Eng, 1988; Andriacchi et al, J Bone Joint Surg, 1980.

AFFILIATED INSTITUTIONS FOR CO-AUTHORS:

** Department of Orthopaedic Surgery, University of Bristol, UK
*** Orthop. Krankenhaus Gersthof, Vienna, A
**** Otto Wagner Spital, Vienna, A
***** PI Precision Implants AG, CH

Appendix II

Simulator Pictures

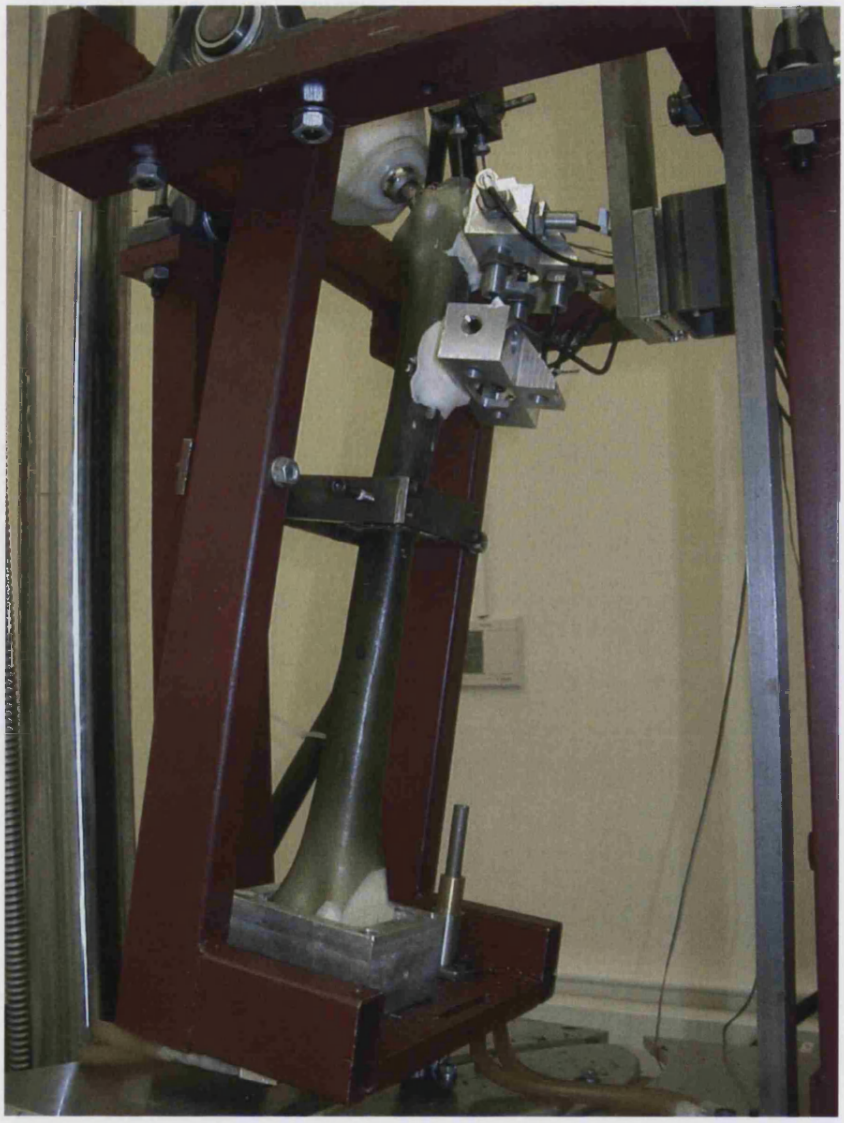

A view showing the femur clamped in the dynamic hip simulator

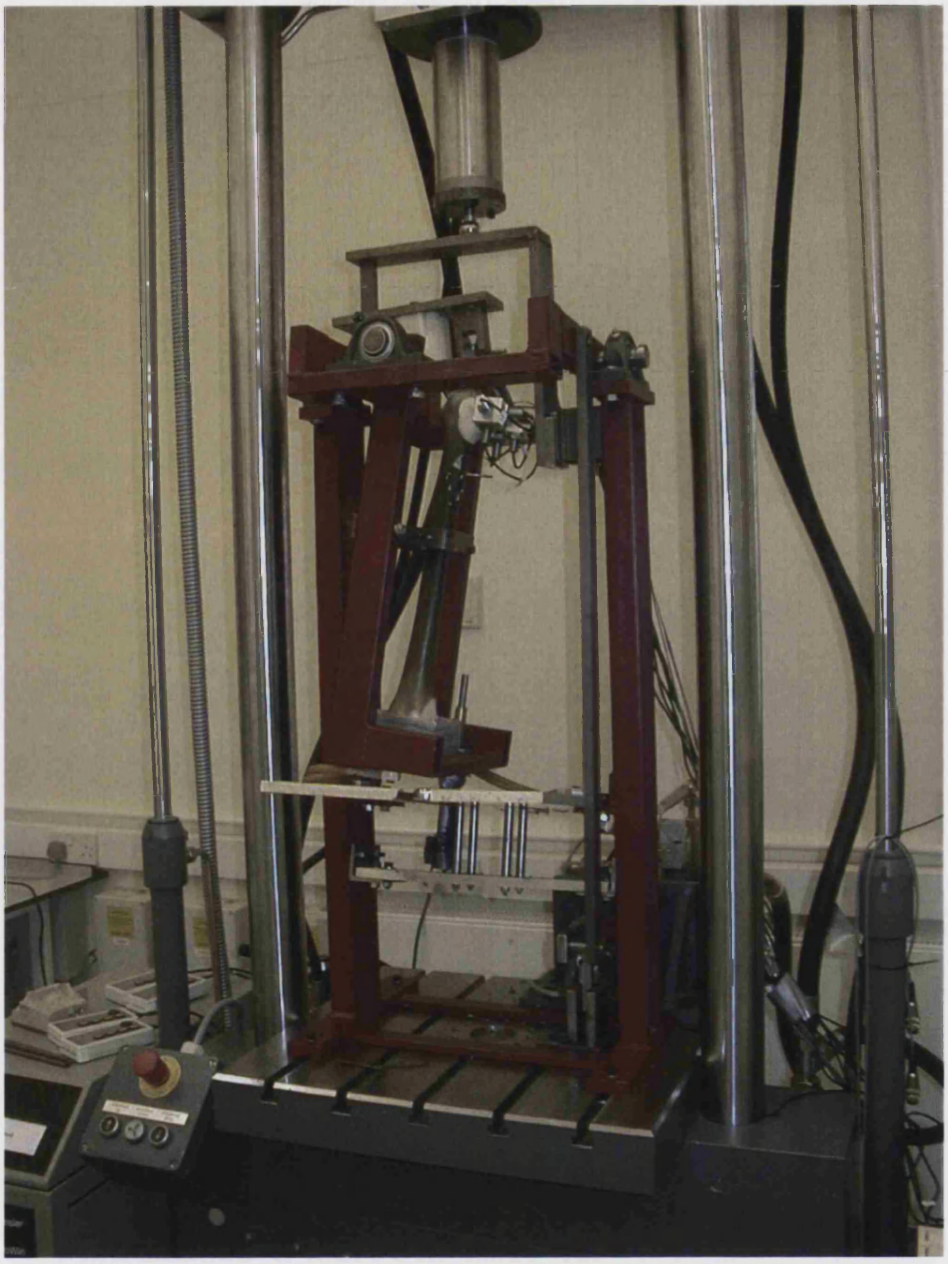

The dynamic simulator mounted on the Zwick multi axis materials testing machine

Appendix III

Equipment Calibrations

LVDT Calibration for micromotion studies

Calibration procedure as set by Hodey, 2001

1. Find the point at which micrometer just touches LVDT
2. Set zero using adjustment on cards to 0.75mm beyond this point
3. Move micrometer to a position -0.5mm relative to zero (set step 2) and adjust gain to an output voltage -5V
4. Move micrometer to a position +0.5mm relative to zero and check output (+5V) and adjust fain if necessary
5. Repeat steps 2 through 4 until reasonable results achieved (± 2μm)
6. Apply inputs to LVDT from -0.75mm to 0.5mm relative to zero in intervals of 0.25mm and record voltage intervals

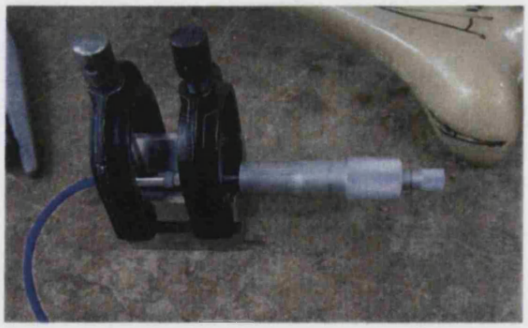

Calibration of Dog bone transducers used to record tension in muscle cables

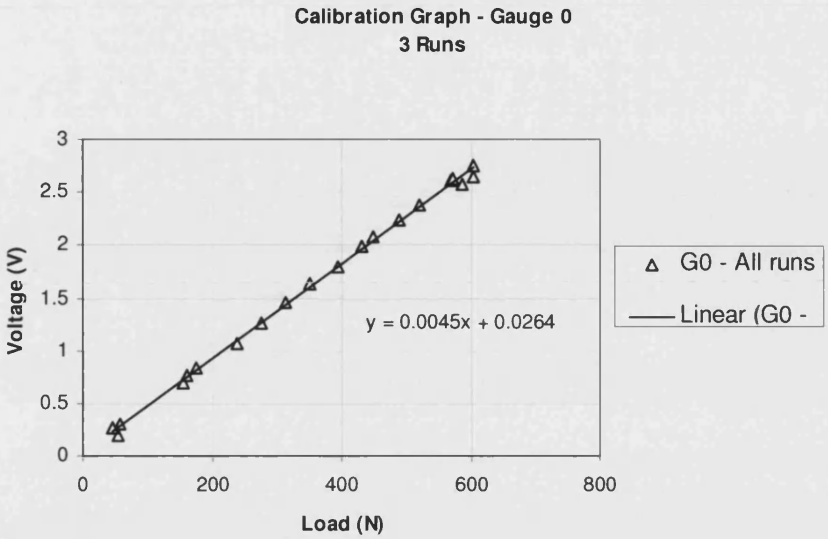

Gain = 222.2
Load = 222 x voltage

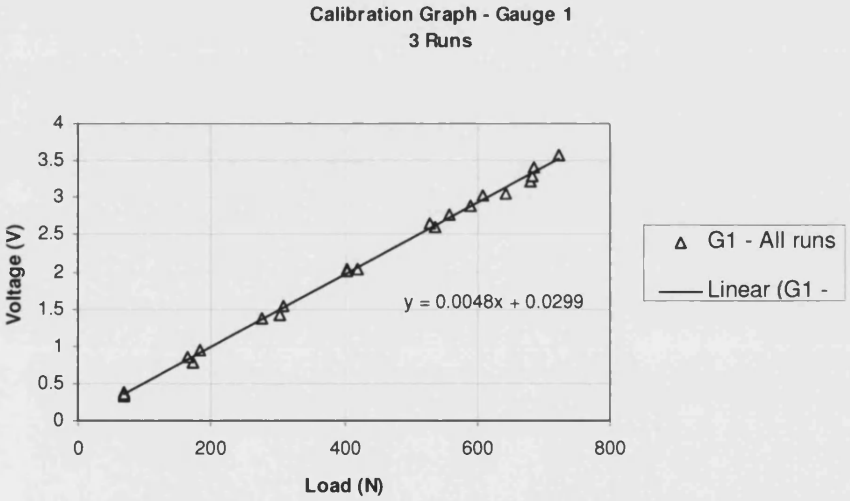

Gain = 208
Load = 208 x voltage

Calibration 3D Force Study

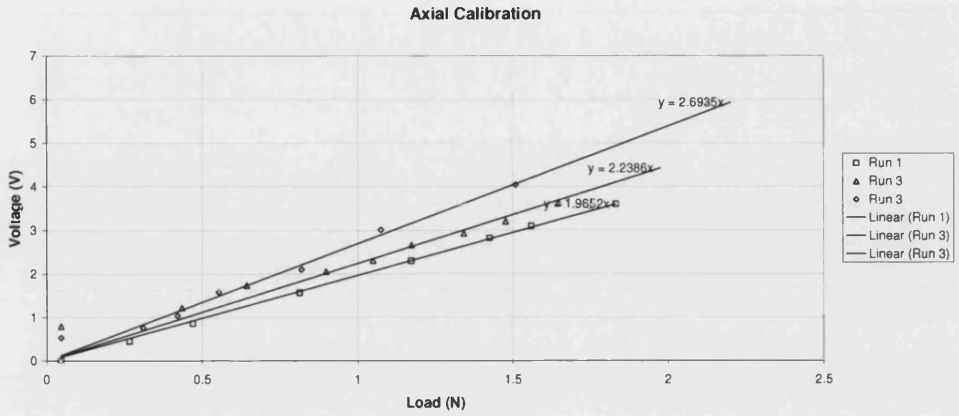

$Gain_{(axial)}$ = 0.435
Axial Load (kN) = 0.435 x voltage (V)

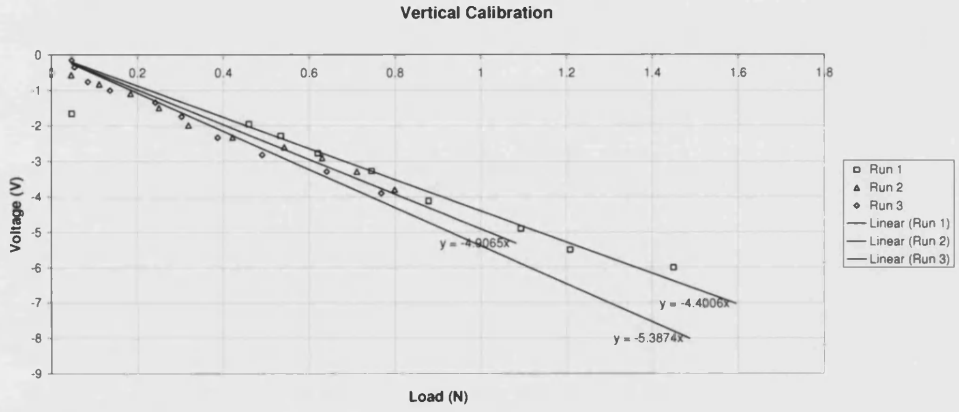

$Gain_{(Vert)}$ = -0.204
Vertical Load (kN) = -0.204 x voltage (V)

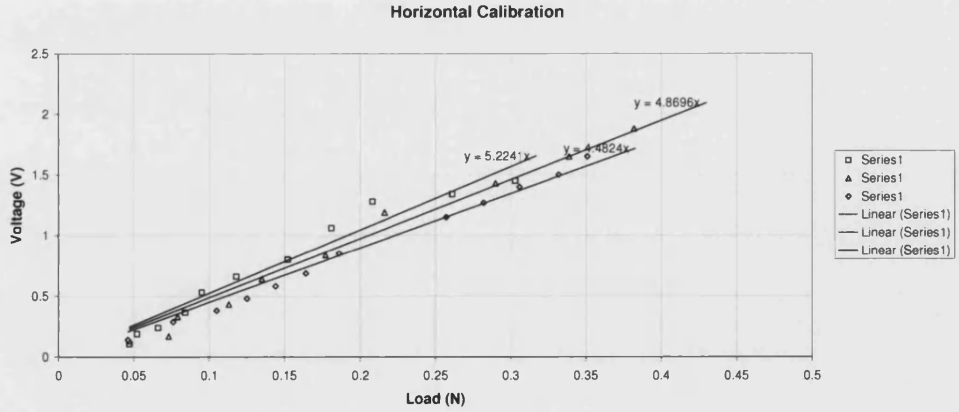

$Gain_{(Horiz)}$ = 0.205
Vertical Load (kN) = 0.205 x voltage (V)

Appendix IV

ux=micromotion along x
uy= micromotion along y
uz= micromotion along z
uxx= micromotion about x
uyy= micromotion about y
uzz= micromotion about z

mx=migration along x
my= migration along y
mz= migration along z
mxx= migration about x
myy= migration about y
mzz= migration about z

Results Fresh v Long-term

SLS Proximal

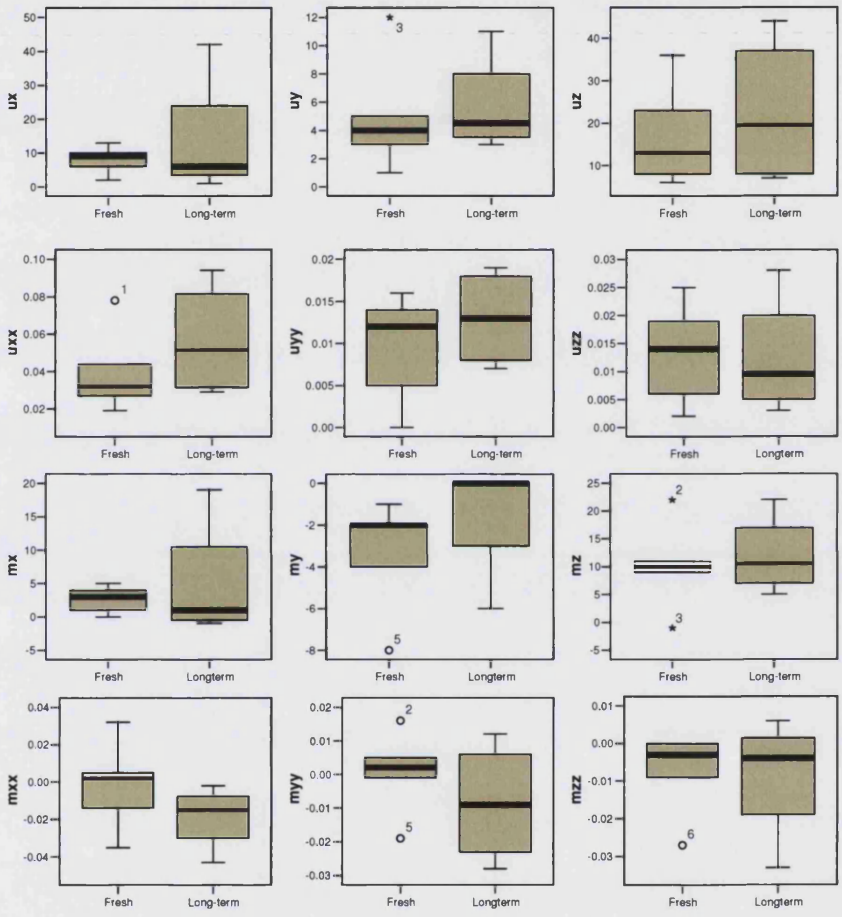

SLS Distal

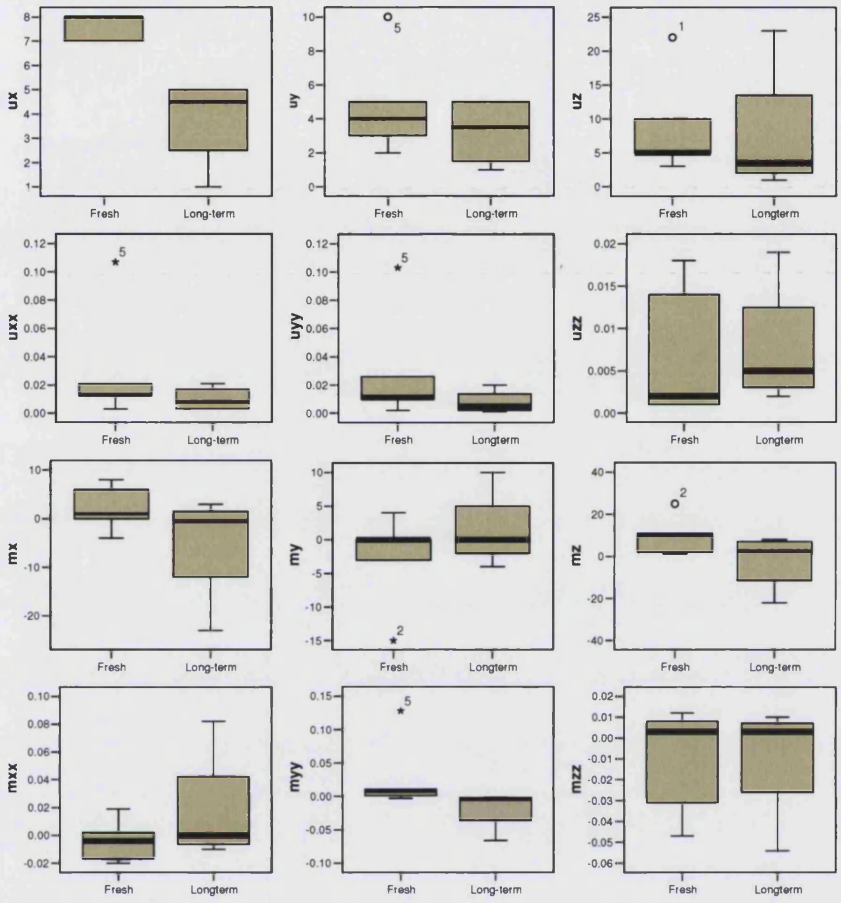

SC Proximal

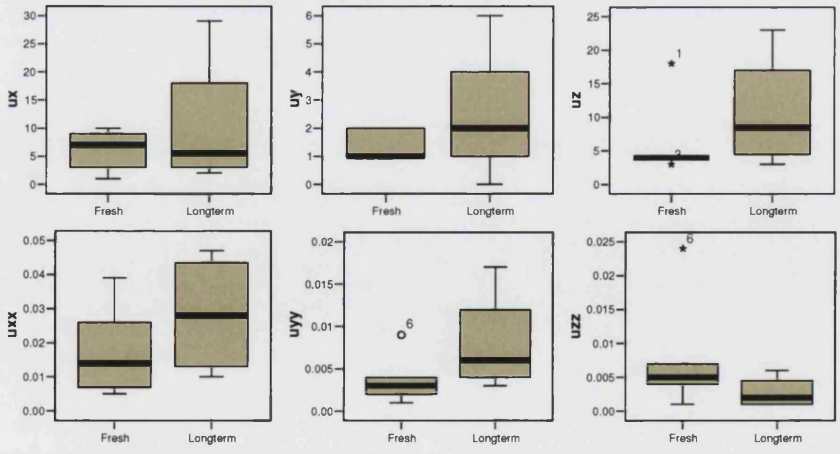

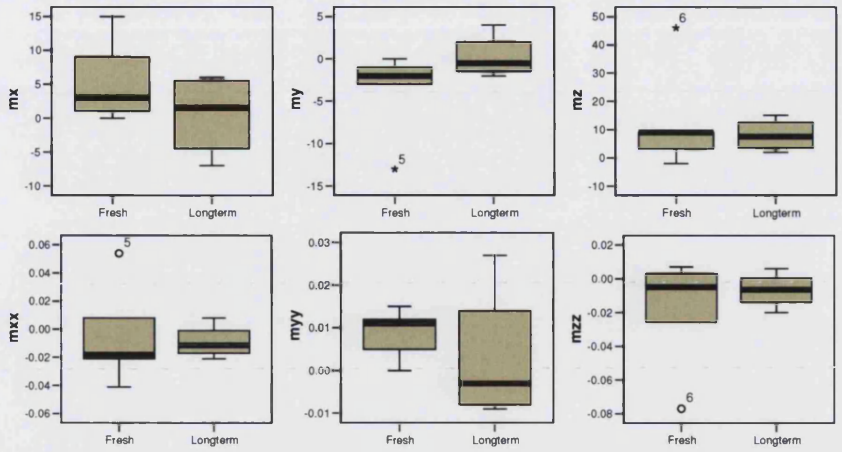
mx
my
mz
mxx
myy
mzz
Fresh
Longterm

SC Distal

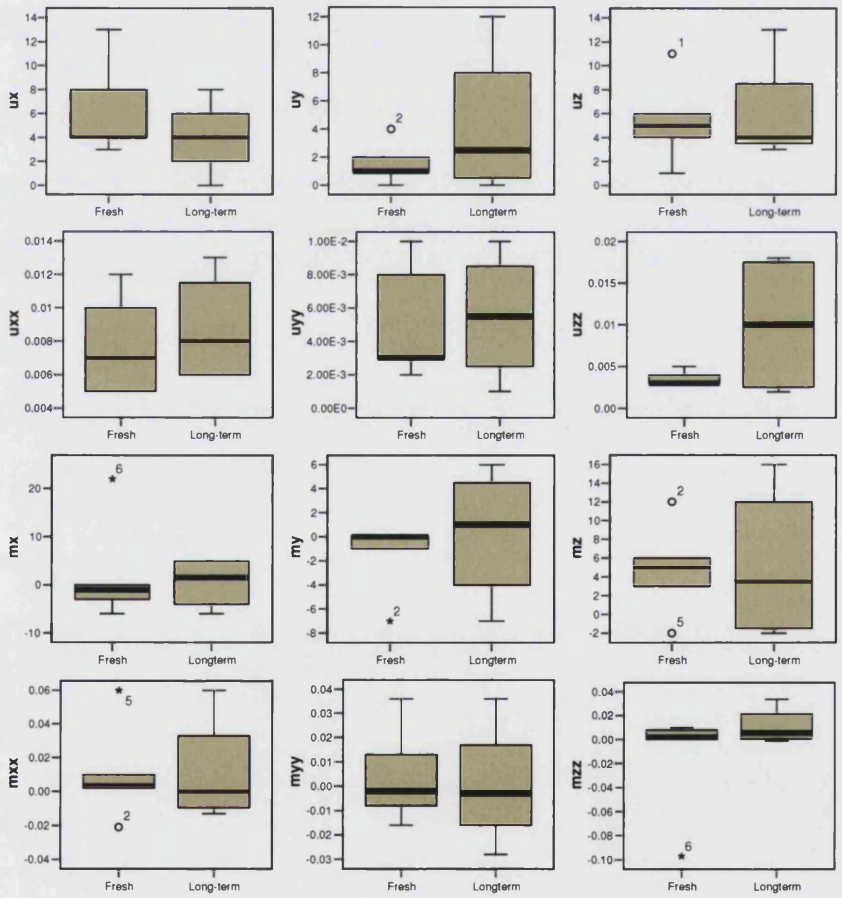
ux
uy
uz
uxx
uyy
uzz
mx
my
mz
mxx
myy
mzz
Fresh
Long-term
Longterm

Appendix V

ux=micromotion along x
uy= micromotion along y
uz= micromotion along z
uxx= micromotion about x
uyy= micromotion about y
uzz= micromotion about z

mx=migration along x
my= migration along y
mz= migration along z
mxx= migration about x
myy= migration about y
mzz= migration about z

Results Cadaveric v Composite

SLS Proximal

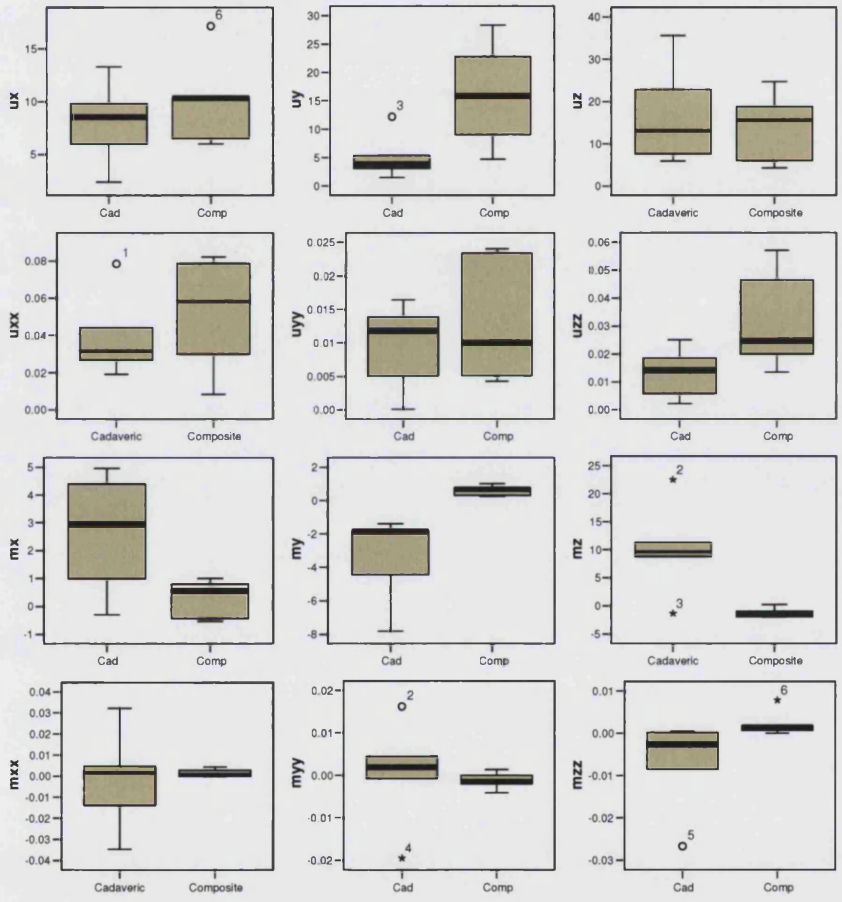

SLS Distal

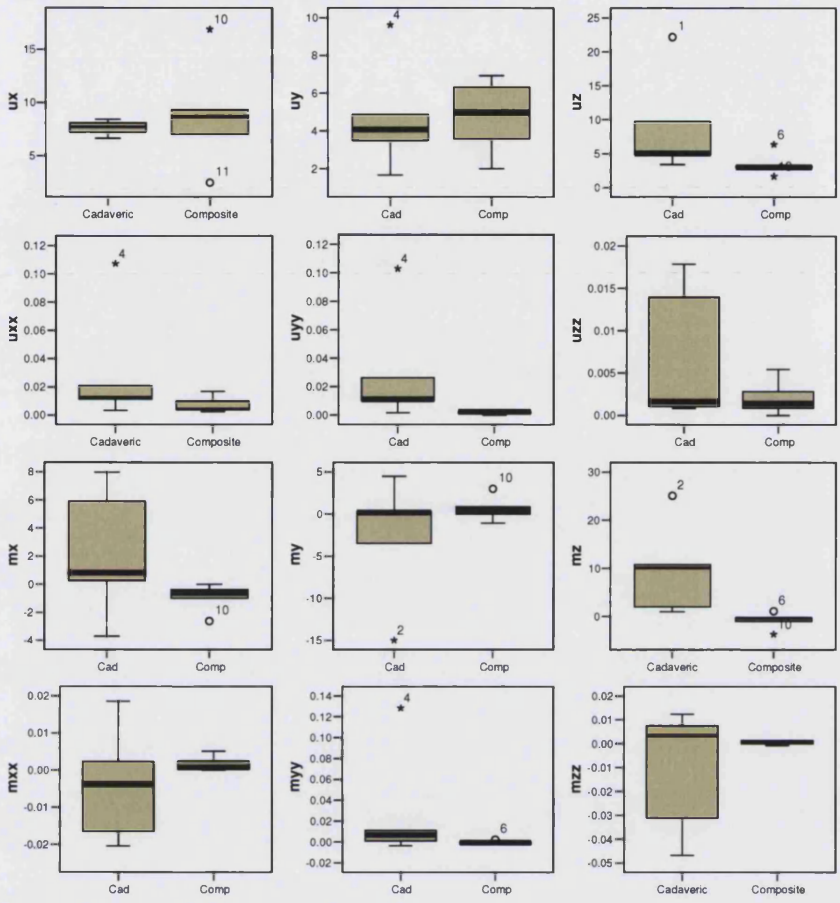

SC Proximal

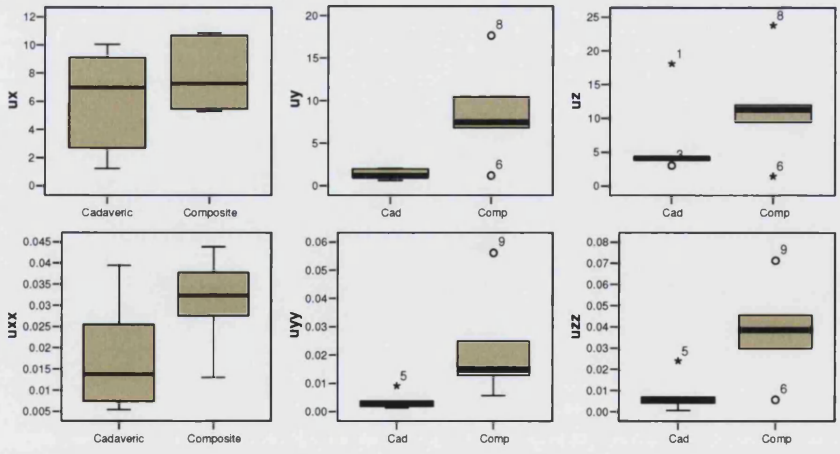

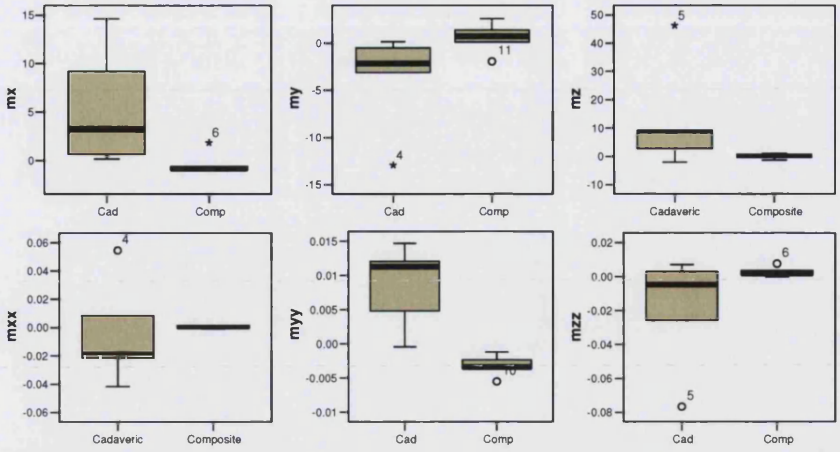
mx
my
mz
mxx
myy
mzz
Cad
Comp
Cadaveric
Composite

SC Distal

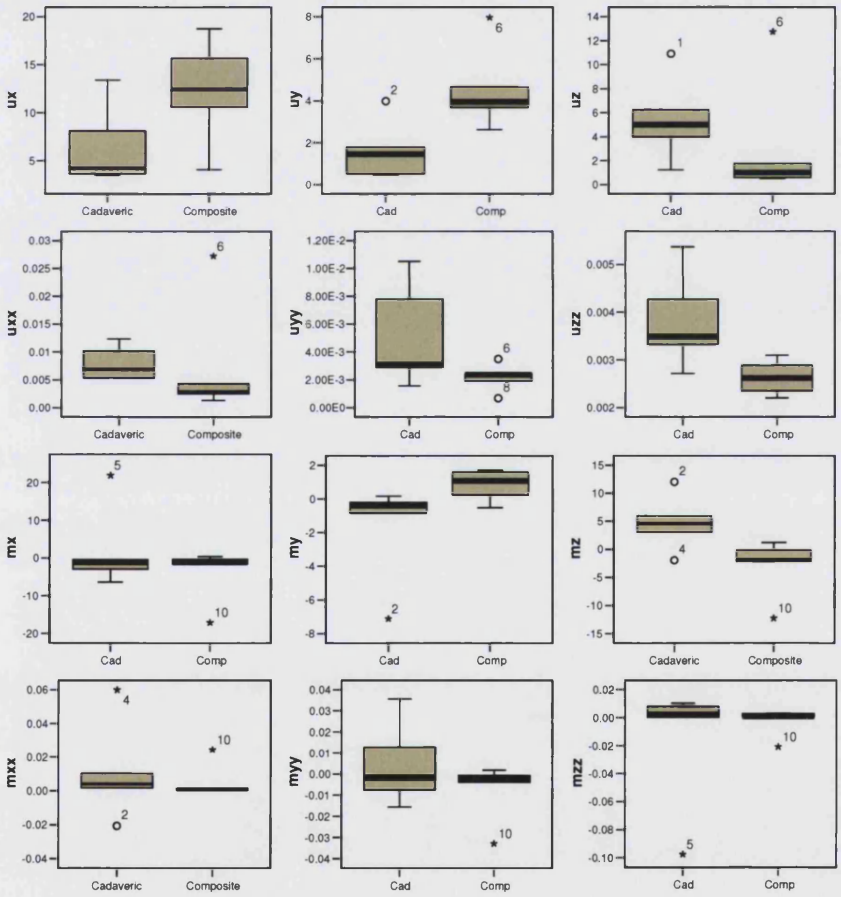
ux
uy
uz
uxx
uyy
uzz
mx
my
mz
mxx
myy
mzz
Cad
Comp
Cadaveric
Composite

Appendix VI

Results – Calculations of femoral head force during loading regimes

Load on Implant in Single Leg Stance

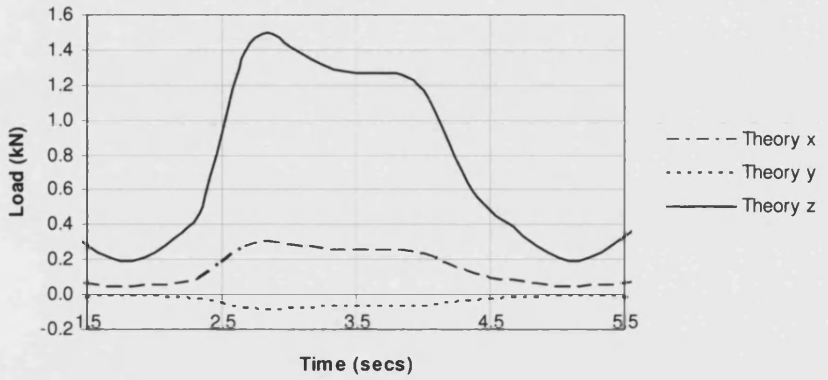

Load on Implant in Heel Strike

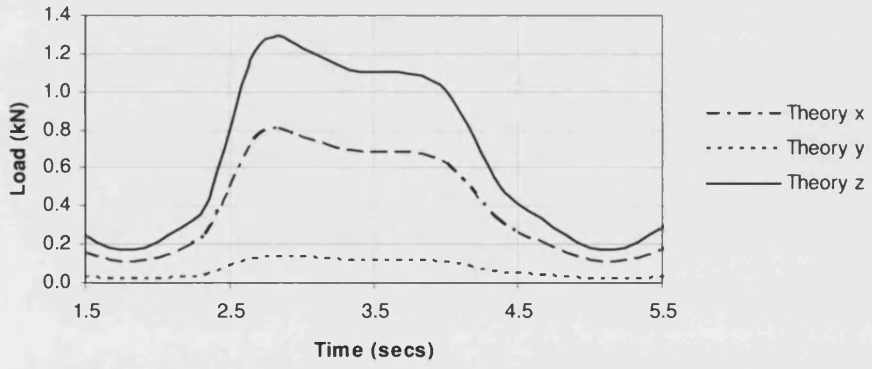

Load on Implant inToe Off

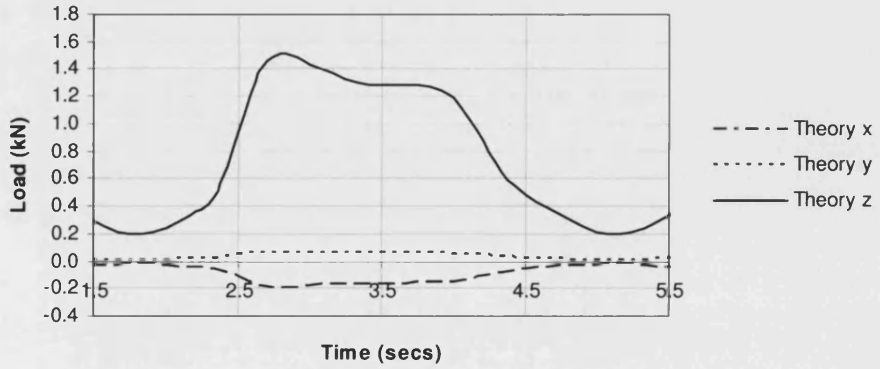

Load on Implant in Initial Stance

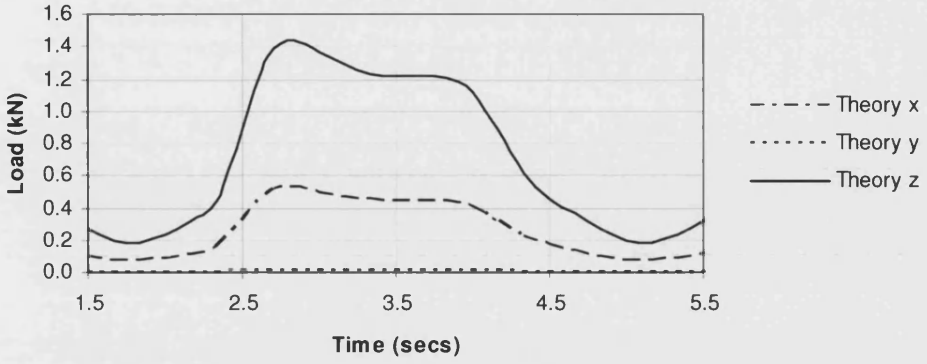

Load on Implant in Dynamic

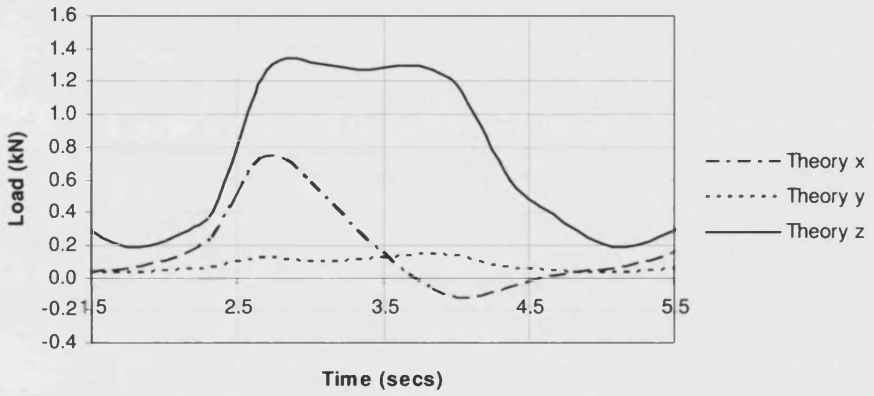

Load on Implant in Dynamic One Sided Run

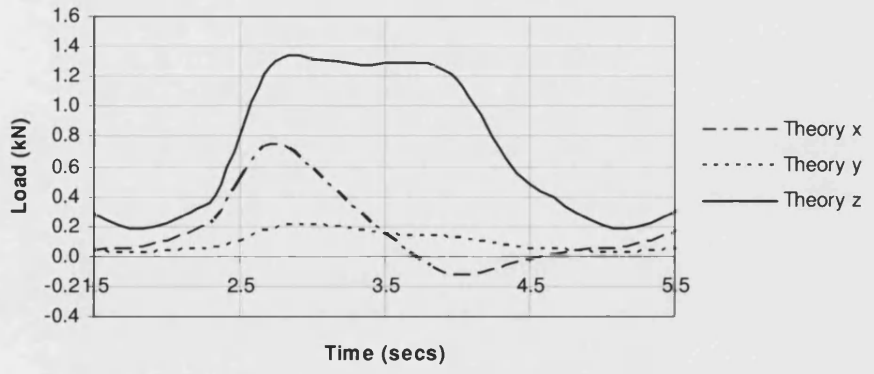

Appendix VII

Results from Dynamic testing

1 = Single leg stance
2 = Heel Strike
3 = Toe off
4 = Initial Stance
5 = Dynamic
6 = Dynamic one sided

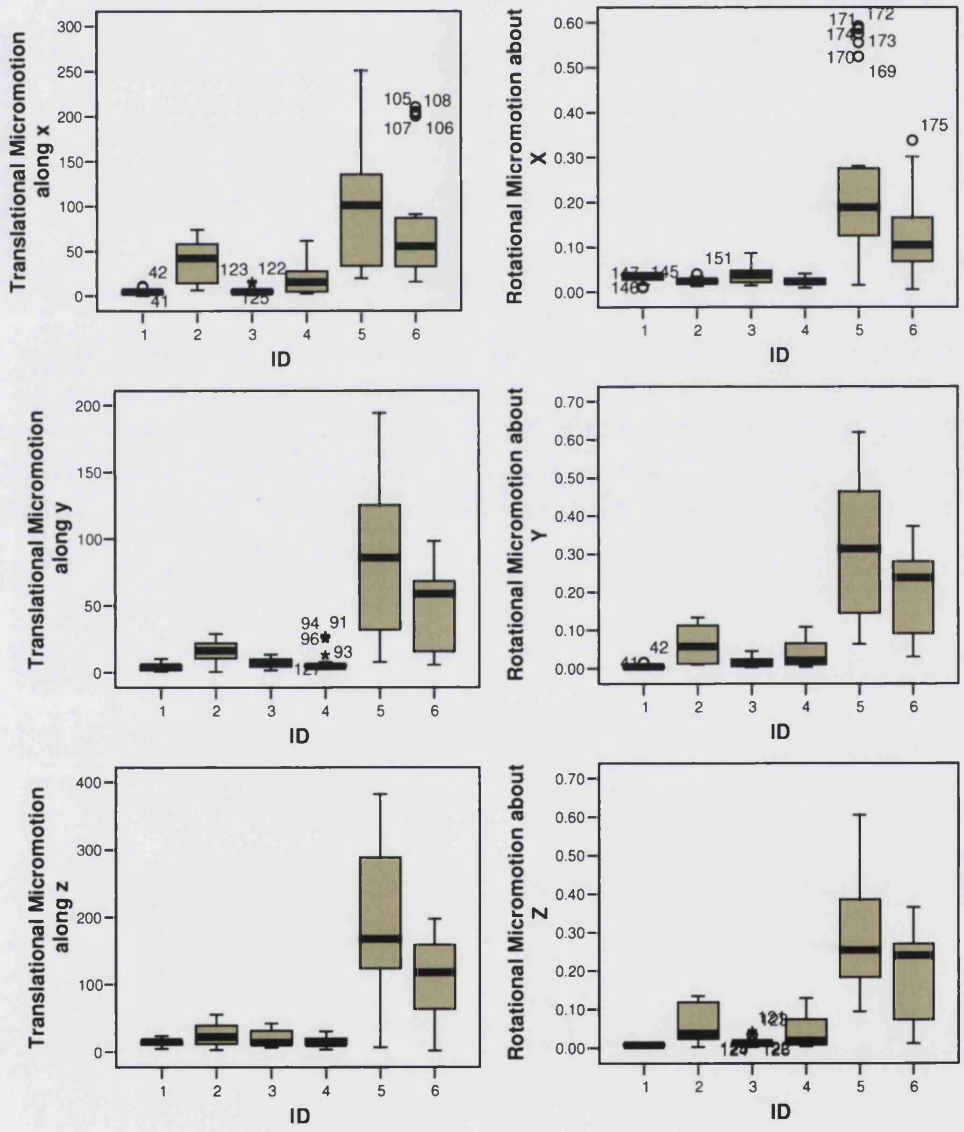

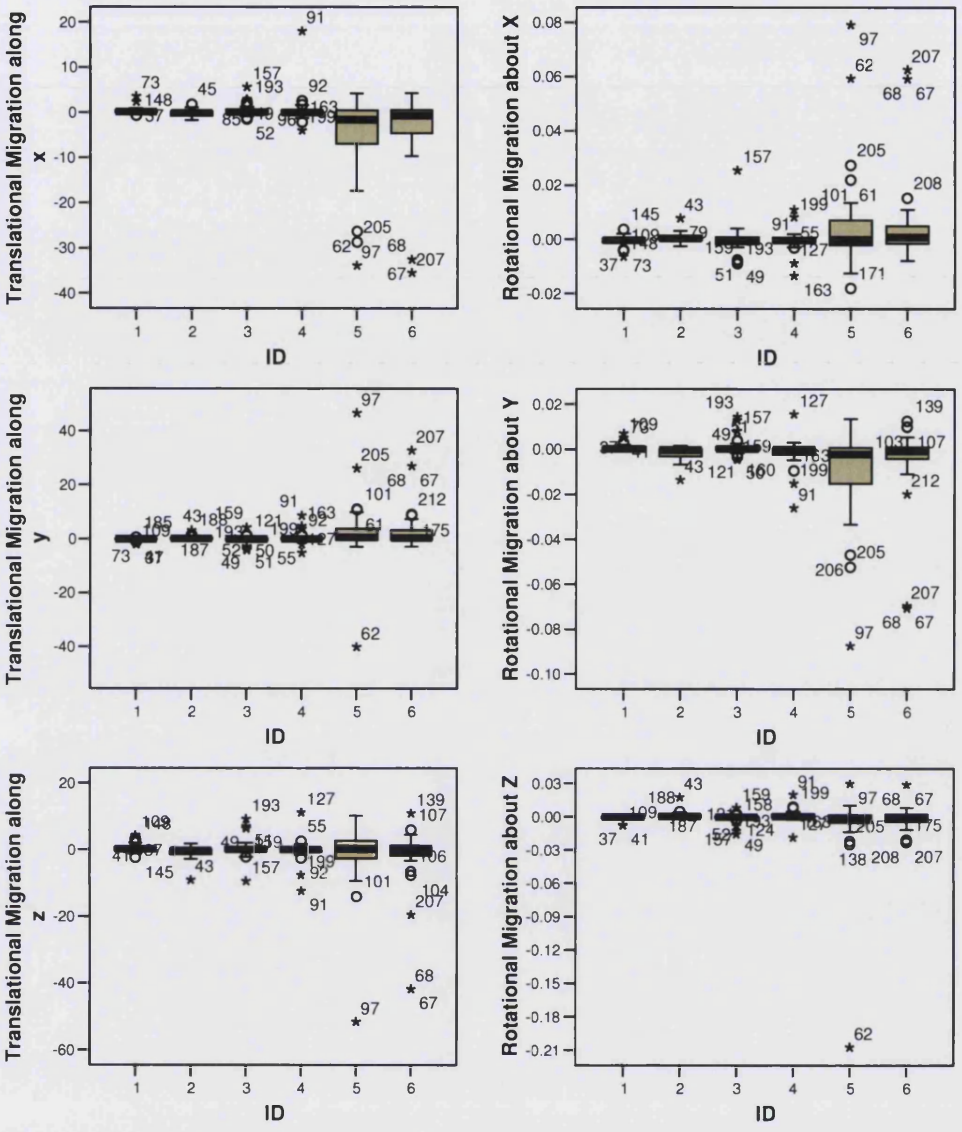
Translational Migration along x
Rotational Migration about X
Translational Migration along y
Rotational Migration about Y
Translational Migration along z
Rotational Migration about Z
ID

Distal

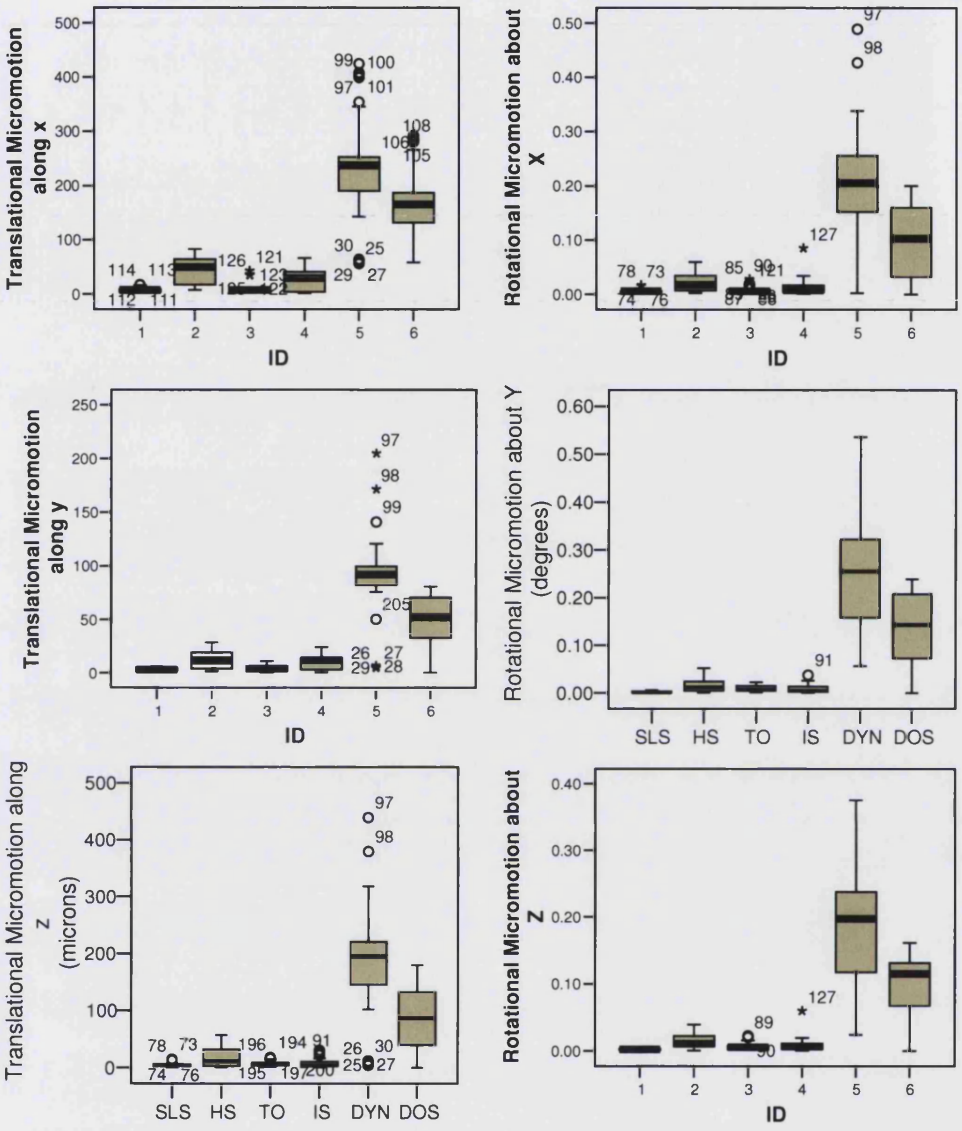
Translational Micromotion along x
Rotational Micromotion about X
Translational Micromotion along y
Rotational Micromotion about Y (degrees)
Translational Micromotion along Z (microns)
Rotational Micromotion about Z
ID
SLS HS TO IS DYN DOS

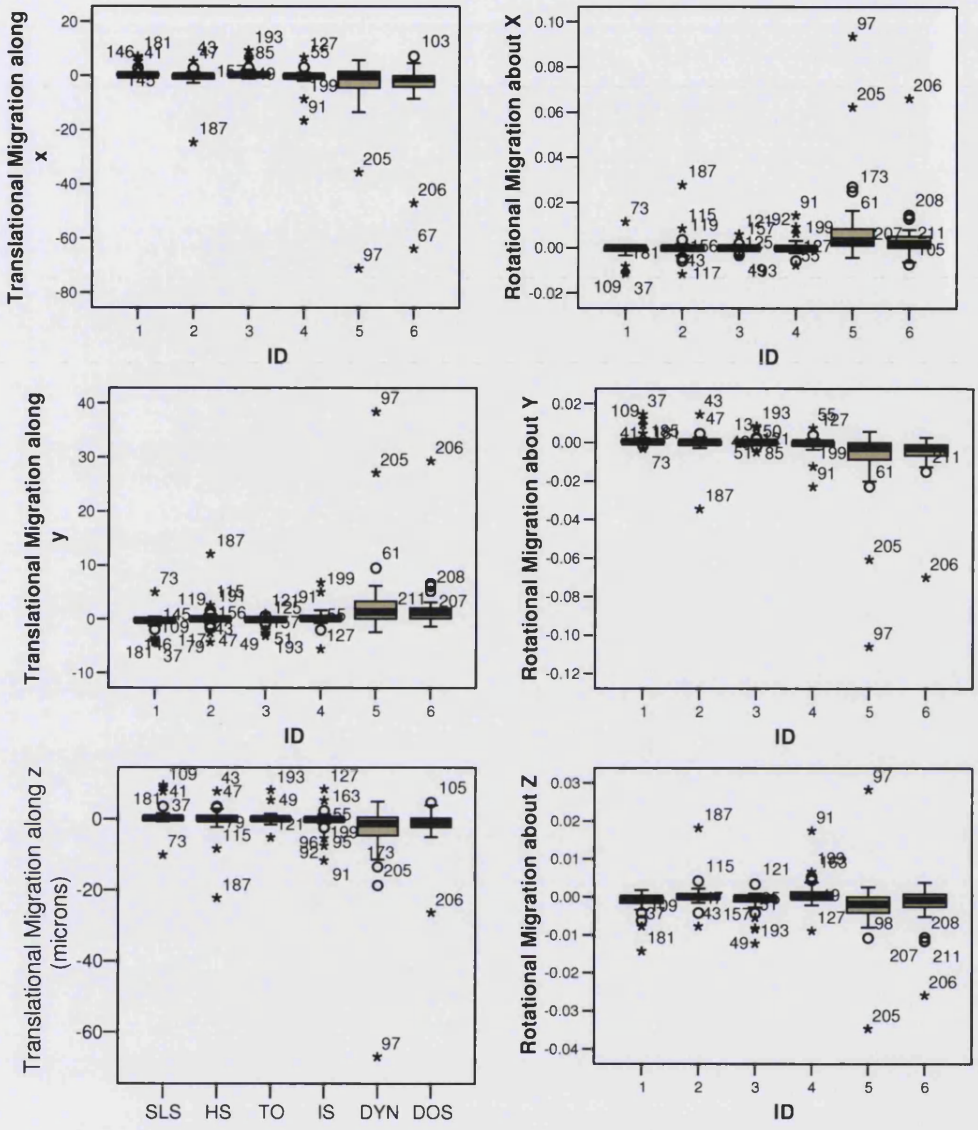
Translational Migration along x
Rotational Migration about X
Translational Migration along y
Rotational Migration about Y
Translational Migration along z (microns)
Rotational Migration about Z
ID
SLS
HS
TO
IS
DYN
DOS

Appendix VIII

Results Load Level

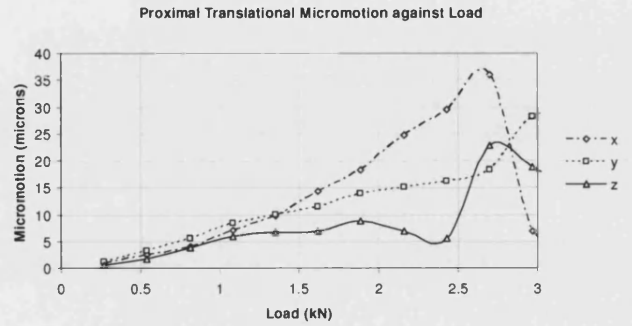

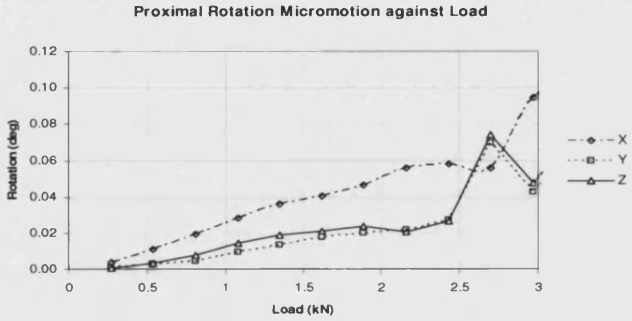

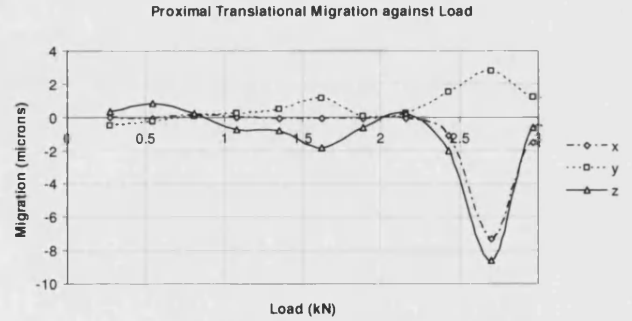

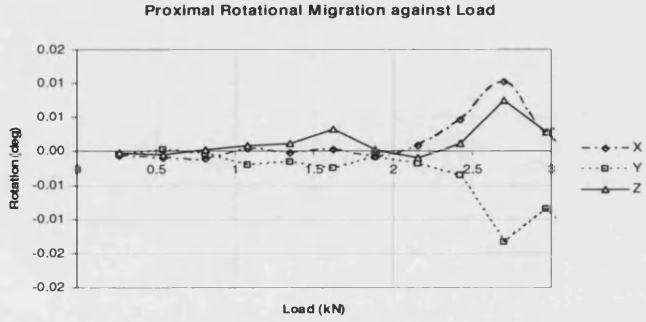

Distal Translational Micromotion against Load

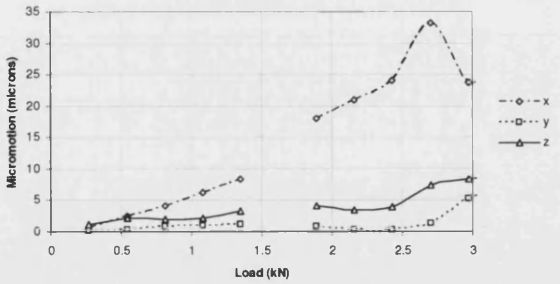

Distal Rotational Micromotion against Load

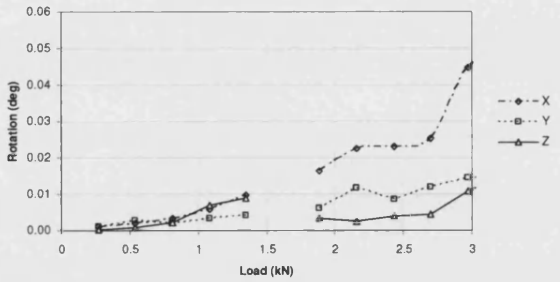

Distal Translational Migration against Load

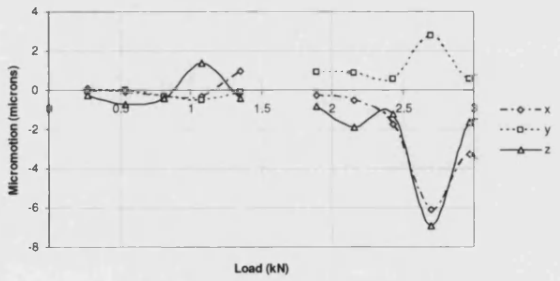

Distal Rotational Migration against Load

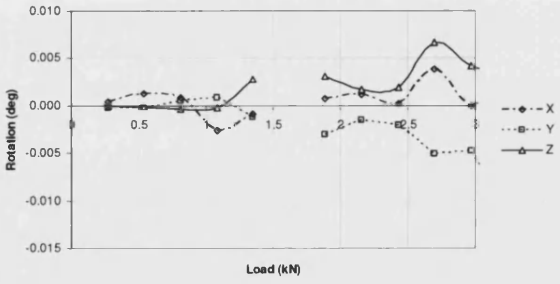

Appendix IX

Force on head and motion

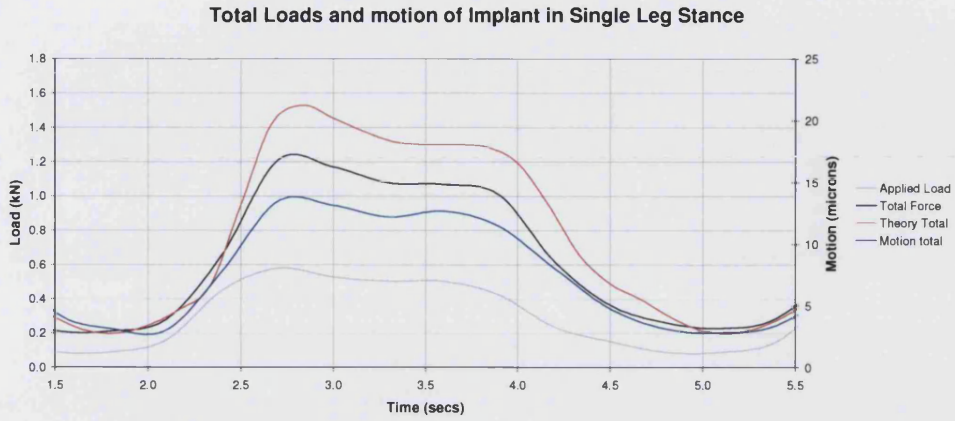

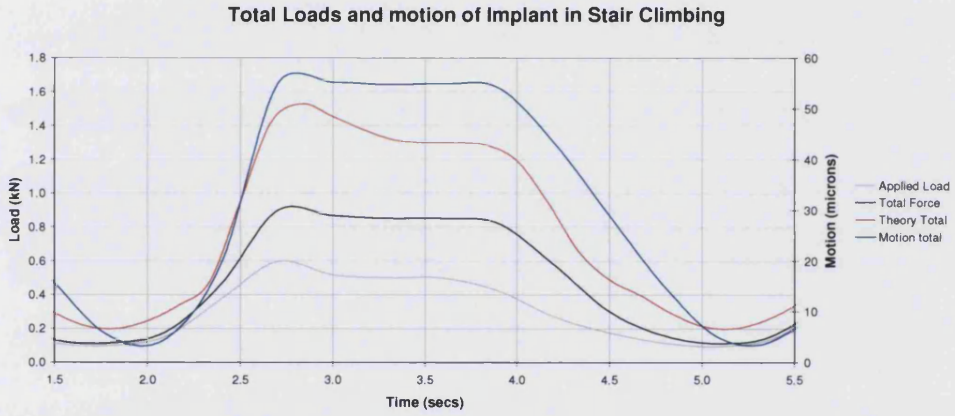

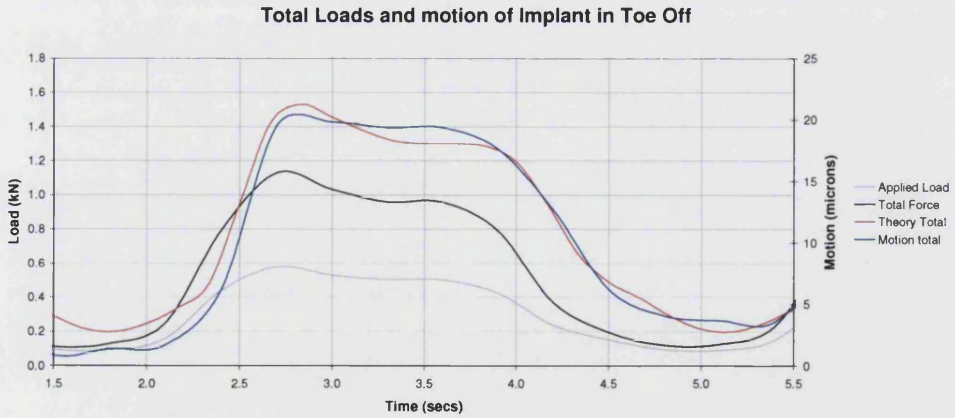

Total Loads and motion of Implant in Initial Stance

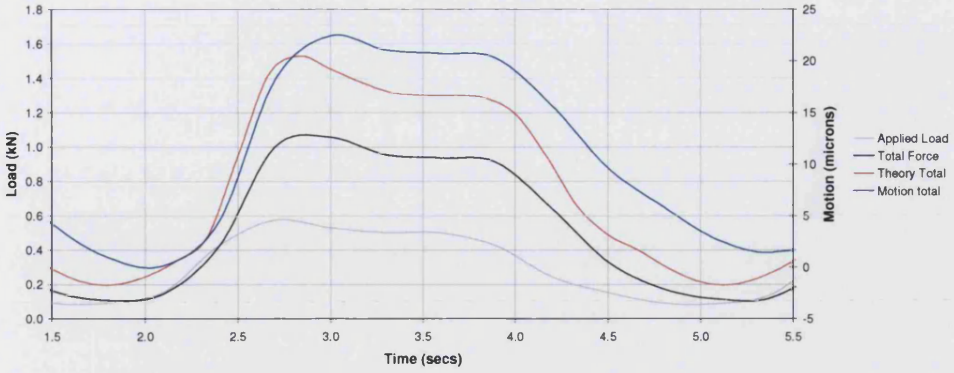

Total Loads and motion of Implant in Dynamic

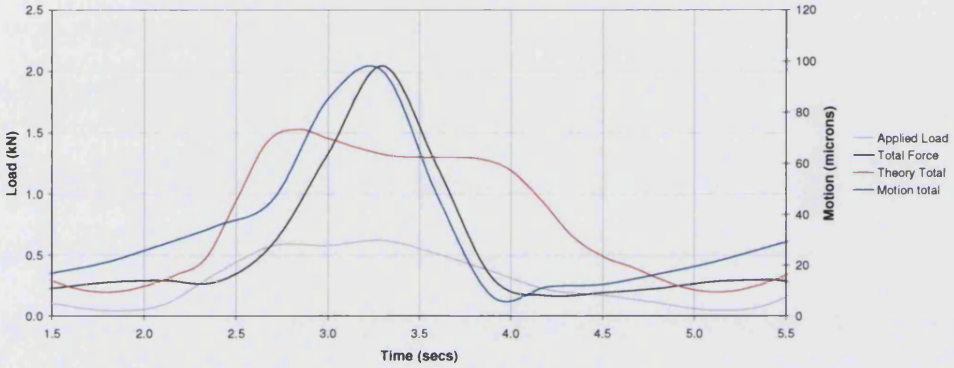

Total Loads and motion of Implant in Dynamic (one side)

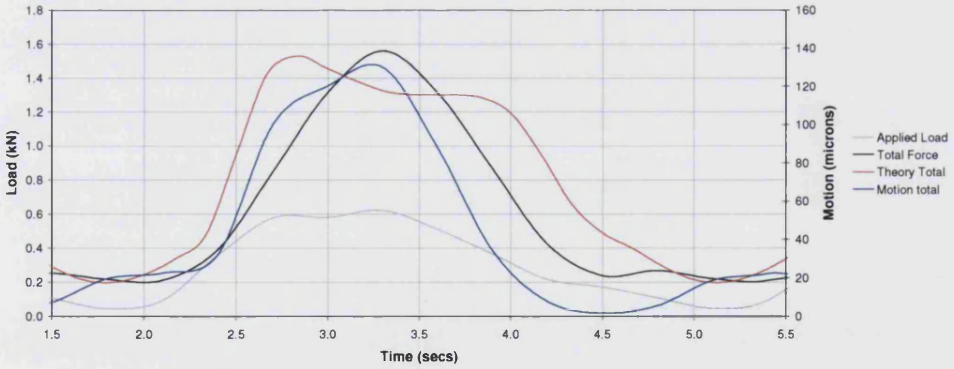

Appendix X

Programs

MATLAB Routine for converting data captured from motion transducers into micromotion and migration

```
% hipcon3.m
% Routine to convert LVDT output voltages into
        translation and rotation
% of hip stem.
% Input is read from space delimited ASCII file
        "volt#.dat", where # represents
% the experimental run number.
% The input file expected format:
% Eight columns and n rows, where n=sample
        frequency*time
% The column entries are:
% Load displacement; Applied load; vdy; vby; vbz;
        vdz; vcz; vbx
% Required units are:
% um;    N;          v;  v;  v;  v;  v;  v
% where the last six represent output voltages from
        each LVDT e.g. vbz=output
% from LVDT montitoring z axis displacement of
        target ball B.

% Interrogates user for:
% 1)  |AE| (distance from centre of target frame to
        stem axis in y direction)
%     This distance must be adjusted to give correct
        alignment each time the
%     target frame is fixed to the stem.
% 2)  Run number i.e. the "#" from "volt#.dat"
% 3)  The input sampling frequency that will be used
        to calculate the time (JH 13/02/01).
% 4)  The run number results against which to plot the
        current results

% Sends micromotion data to output file
        "motion#.dat":
% Format is 9 columns x n rows:
% Column entries are:
% time;  load disp; load;      trx;      try;      trz;
                    rox;      roy;      roz
% Units are:
% s;um;  N;         um;       um;       um;
                    deg;      deg;      deg

% Variables:
% geo = Conversion matrix (6 x 6)
% r = Distance between target balls and centre of
        frame
% m = LVDT calibration factor = .0001, the LVDT
        calibration offset = 0
% ifile = name of input data file
% ofile = name of output data file
% n = Number of rows of <ifile>
% voltin = matrix into which <ifile> is loaded
% def = matrix containing LVDT deflections
% radeg = factor to convert from radians to degrees
        (180/pi)

%*************************************************************
%
%Clear current figure
clear;
clf;
count = 0;

for mm=1:100
clc;
   count =count + 1;

% Ask user to input target geometry if desired
change=input('Alter Geometry? (y/n) ','s');
   if change=='y'
      array(mm,1) = 1;
   elseif change=='n'
      array(mm,1) = 0;
   end

% Ask user to enter filename:
disp(' ');
fnum=input('volt data file number? ');


%Ask user to enter frequency of sampling:
disp (' ');
freq=input('Frequency of sampling? ');
%

array(mm,2)=fnum;
array(mm,3)=freq;
clc;
ch=input('input another file (y/n)?','s');
      if ch=='y'
         continue;
      elseif ch=='n'
         break;
      end
end



clc;
disp('processing....')
for mm = 1:count
clear voltin; clf;




r = 0.03;
m = 1;
c = 0;
radeg = 180/pi;


% Set LVDT calibration factor
m=.0001;



   if array(mm,1) == 0
      change = 'n';
   elseif array(mm,1) == 1
      change = 'y';
   end

if (change=='y')

  ea=input('Target geometry:  EA? (mm) ')/1000;
  eb=input('Target geometry:  EB? (mm) ')/1000;
  ec=input('Target geometry:  EC? (mm) ')/1000;
  ed=input('Target geometry:  ED? (mm) ')/1000;

else
```

```
 ea=0.03;
 eb=0.03;
 ec=0.03;
 ed=0.03;

end


fnum=array(mm,2);
ifile=strcat('experiment',int2str(fnum),'.txt');
voltin=load(ifile);

freq=array(mm,3);


%Find the number of measurements taken n:
n=size(voltin,1);
%
%Need to add column with time data:
for i=1:n,;
   time(i,1)=(i-1)/freq;
end;
%
volts(:,2:9)=voltin(:,1:8);
volts(:,1)=time(:,1);

% Transpose data using " ' ":
u = volts';
% Only rows 4 through 9 contain LVDT data:
co=u(4:9,:);


%Re-order rows to allow for D. SIRKETT LVDT
        labelling (MODIFICATION J.HODEY
        16/02/01)
v(4:5,:)=co(4:5,:);
v(1,:)=co(6,:);
v(2,:)=co(3,:);
v(3,:)=co(2,:);
v(6,:)=co(1,:);

% LVDT output voltages vbz, vcz, vdz are in opposite
        sense to co-ordinate axes.
% So need to invert sense of vbz, vcz,  vdz (i.e. rows
        3,4 and 5 of "v"):
v(3:5,:)=-v(3:5,:);


% Use calibration equation to convert voltages to
        deflection in metres:
def = v(:,:)*m;


geo = [0 1 0 0 0 -r;
0 1 0 0 0 r;
0 0 1 r -r 0;
0 0 1 r r 0;
0 0 1 2*r 0 0;
1 0 0 0 0 -r];

% overwrite "r,-r" entries with factors that allow for
        unequal geometry:
geo(1,6)=-sqrt(ea^2+ed^2)*cos(atan(ea/ed));
geo(2,6)=+sqrt(ea^2+eb^2)*cos(atan(ea/eb));
geo(3,4)=+ea;
geo(3,5)=-eb;
geo(4,4)=+ea;
geo(4,5)=+ed;
geo(5,4)=ea+ec;
geo(6,6)=-sqrt(ea^2+eb^2)*cos(atan(eb/ea));

% Perform inverse matrix operation on each column
        of deflection matrix
% to obtain micromotion translation and rotation
        matrix:

inverse = inv(geo);

for i=1:n,;
  micro(:,i) = inverse*def(:,i);
end;

% convert first three rows from metres to micrometres
        translation:
micro(1:3,:)=1e6*micro(1:3,:);
% Convert last three rows from radians to degrees
        rotation:
micro(4:6,:)=radeg*micro(4:6,:);

% Send data to output file:

% Transpose micromotion matrix for correct format:
b=micro';
% a gets dumped into the output file:
% columns 4 to 9 contain trans and rot data:
a(:,4:9)=b(:,1:6);
% column 1 contains time (from input file):
a(:,1)=volts(:,1);
% columns 2 and 3 contain load disp. and load
        respectively  (from input file):
a(:,2:3)=volts(:,2:3);

%Modify output to account for system being munted
        upside down (JH 19/03/01)
%x=-x, z=-z, X=-X, Z=-Z
a(:,4)=-a(:,4);
a(:,6:7)=-a(:,6:7);
a(:,9)=-a(:,9);

%
% Modified to output to tab delimited text file. J
        HODEY (13/03/01)
A=a';
ofile=strcat('motion',int2str(fnum),'.txt');
fid=fopen(ofile,'w');
fprintf(fid,'%12.8f\t %12.8f\t %12.8f\t %12.8f\t %12.8f\t
        %12.8f\t %12.8f\t %12.8f\t %12.8f\n' ,A);
fclose(fid);

disp(' ');
msg = 'Micromotion calculated and written to text
        datafile: ';
disp(msg)
disp(ofile)




%%%%%%%%%%%%%%%%%%%%%%%%%%%
%yank.m
%matlab routine to work out migration and
        micromotion of stems
%runs after hipcon3.m
%prints pretty pictures as well!
%%%%%%%%%%%%%%%%%%%%%%%%%%%
%Sabina 09/01/02
%%%%%%%%%%%%%%%%%%%%%%%%%%%
%ask user which file they want to analyse
%filenumber=input('Which file number do you want to
        analise? ');
inputfile=strcat('motion',int2str(fnum),'.txt');


%clear previous picture (if any)
clf;

%clear buffer
clear time displacement applied_load x y z X Y Z;

%load data from inputfile and create data vectors
```

```
%remember that in motionXX.txt data is organised in
        columns as follows:
%time(s), actuator displacement(um), load (N), x(um),
        y(um), z(um), X(deg), Y(deg), Z(deg)
%
%convert displacement of actuator in mm all the rest
        stays the same as motionXX.txt
datain=load(inputfile);

time=datain(:,1);
displacement=datain(:,2)/1000;
applied_load=datain(:,3);
x=datain(:,4);
y=datain(:,5);
z=datain(:,6);
X=datain(:,7);
Y=datain(:,8);
Z=datain(:,9);


[k]=subplot(2,3,1);
plot (time, x, 'k')
grid on

[k]=subplot(2,3,2);
plot (time, y, 'k')
grid on

[k]=subplot(2,3,3);
plot (time, z, 'k')
grid on

[k]=subplot(2,3,4);
plot (time, X, 'k')
grid on

[k]=subplot(2,3,5);
plot (time, Y, 'k')
grid on

[k]=subplot(2,3,6);
plot (time, Z, 'k')
grid on

outputfile=strcat('motion',int2str(fnum),'.jpeg');

print('-djpeg',outputfile)


%%%%%%%%%%%%%%%%%%%%%%%%%%%
%fourier.m
%matlab routine to work out amplitude of micromotion
%and overall migration of stems runs after hipcon3.m
%prints pretty pictures as well!
%%%%%%%%%%%%%%%%%%%%%%%%%%%
%Sabina 05/03/02
%%%%%%%%%%%%%%%%%%%%%%%%%%%
clear datain;

%ask user which file they want to analyse
%filenumber=input('Which motion file number do you
        want to analise? ');
inputfile1=strcat('motion',int2str(fnum),'.txt');

%clear previous picture
clf;

%clear buffer
clear ti xi yi zi Xi Yi Zi ts x y z X Y Z SIZE;
clear N bin mmotion_x mmotion_y mmotion_z
        mmotion_X mmotion_Y mmotion_Z;
clear x_fft y_fft z_fft X_fft Y_fft Z_fft;

%load data from inputfile and apply filter
%only data between 15 and 135 s from start of
%experiment will be analysed

datain=load(inputfile1);

ti=datain(:,1);
xi=datain(:,4);
yi=datain(:,5);
zi=datain(:,6);
Xi=datain(:,7);
Yi=datain(:,8);
Zi=datain(:,9);

filter_o=strcat('filter',int2str(fnum),'.txt');
filter_id=fopen(filter_o,'w');

k=751   ;
while (ti(k)<135)
   k=k+1;
   f=[ti(k), xi(k), yi(k), zi(k), Xi(k), Yi(k), Zi(k)];
   fprintf(filter_id,'%12.8f %12.8f %12.8f %12.8f
        %12.8f %12.8f %12.8f\n', f);
end

fclose(filter_id);

%load filtered data into appropriat vectors and
%perform fft

finputfile=strcat('filter',int2str(fnum),'.txt');
filterin=load(finputfile);

ts=filterin(:,1);
x=filterin(:,2);
y=filterin(:,3);
z=filterin(:,4);
X=filterin(:,5);
Y=filterin(:,6);
Z=filterin(:,7);

%size of vectors
SIZE=size(ts);
N=SIZE(1);

%frequency and bins
b=1:N;
fs=50;
%fft each vector and work out magnitude of
        micromotion ampl_*

x_fft=fft(x);
x_pwr=x_fft.*conj(x_fft)/N;

y_fft=fft(y);
y_pwr=y_fft.*conj(y_fft)/N;

z_fft=fft(z);
z_pwr=z_fft.*conj(z_fft)/N;

X_fft=fft(X);
X_pwr=X_fft.*conj(X_fft)/N;

Y_fft=fft(Y);
Y_pwr=Y_fft.*conj(Y_fft)/N;

Z_fft=fft(Z);
Z_pwr=Z_fft.*conj(Z_fft)/N;
%
%bin of interest (0.3Hz)
bin=1+((N*0.3)/fs);

%amplitudes at 0.3 HZ
mmotion_x=sqrt(4*x_pwr(bin)/N)*2;
mmotion_y=sqrt(4*y_pwr(bin)/N)*2;
mmotion_z=sqrt(4*z_pwr(bin)/N)*2;
mmotion_X=sqrt(4*X_pwr(bin)/N)*2;
```

```
mmotion_Y=sqrt(4*Y_pwr(bin)/N)*2;
mmotion_Z=sqrt(4*Z_pwr(bin)/N)*2;

% % write data to file called mmotion#.txt

outputfile1=strcat('micro',int2str(fnum),'.txt');
fid=fopen(outputfile1,'w');
fprintf(fid,'%12.8f\t %12.8f\t %12.8f\t %12.8f\t %12.8f\t
        %12.8f\t' ,mmotion_x, mmotion_y,
        mmotion_z, mmotion_X, mmotion_Y,
        mmotion_Z);
fclose(fid);

disp(' ');
msg = 'Micromotion amplitudes calculated and written
        to text datafile: ';
disp(msg)
disp(outputfile1)

%need to quantify migration fit data with second order
        poly

poly_coeff_x=polyfit(ts,x,2);
poly_x=polyval(poly_coeff_x,ts);
ampli_x=polyval(poly_coeff_x,135)-
        polyval(poly_coeff_x,15);

poly_coeff_y=polyfit(ts,y,2);
poly_y=polyval(poly_coeff_y,ts);
ampli_y=polyval(poly_coeff_y,135)-
        polyval(poly_coeff_y,15);

poly_coeff_z=polyfit(ts,z,2);
poly_z=polyval(poly_coeff_z,ts);
ampli_z=polyval(poly_coeff_z,135)-
        polyval(poly_coeff_z,15);

poly_coeff_X=polyfit(ts,X,2);
poly_X=polyval(poly_coeff_X,ts);
ampli_X=polyval(poly_coeff_X,135)-
        polyval(poly_coeff_X,15);

poly_coeff_Y=polyfit(ts,Y,2);
poly_Y=polyval(poly_coeff_Y,ts);
ampli_Y=polyval(poly_coeff_Y,135)-
        polyval(poly_coeff_Y,15);

poly_coeff_Z=polyfit(ts,Z,2);
poly_Z=polyval(poly_coeff_Z,ts);
ampli_Z=polyval(poly_coeff_Z,135)-
        polyval(poly_coeff_Z,15);

moutputfile=strcat('migration',int2str(fnum),'.txt');
fid_m=fopen(moutputfile,'w');
fprintf(fid_m,'%12.8f\t %12.8f\t %12.8f\t %12.8f\t
        %12.8f\t %12.8f\t' ,ampli_x, ampli_y,
        ampli_z, ampli_X, ampli_Y, ampli_Z);
fclose(fid_m);

disp(' ');
msg = 'Micromotion amplitudes calculated and written
        to text datafile: ';
disp(msg)
disp(moutputfile)

%%%%%%%%%%%%%%%%%%%%%%%%%%%
%plot the lot!!!
%%%%%%%%%%%%%%%%%%%%%%%%%%%

[k]=subplot(2,3,1);
plot (ts, x, 'k', ts, poly_x, 'ow')
axis tight
%xlabel('time (s)')
ylabel('disp (um)')
title('x movement')
grid on

[k]=subplot(2,3,2);
plot (ts, y, 'k', ts, poly_y, 'ow')
axis tight
xlabel('time (s)')
%ylabel('disp (um)')
title('y movement')
grid on

[k]=subplot(2,3,3);
plot (ts, z, 'k', ts, poly_z, 'ow')
axis tight
% xlabel('time (s)')
% ylabel('disp (um)')
title('z movement')
grid on

[k]=subplot(2,3,4);
plot (ts, X, 'k', ts, poly_X, 'ow')
axis tight
%xlabel('time (s)')
ylabel('rot (deg)')
title('X rotation')
grid on

[k]=subplot(2,3,5);
plot (ts, Y, 'k', ts, poly_Y, 'ow')
axis tight
xlabel('time (s)')
%ylabel('rot (deg)')
title('Y rotation')
grid on

[k]=subplot(2,3,6);
plot (ts, Z, 'k', ts, poly_Z, 'ow')
axis tight
% xlabel('time (s)')
% ylabel('rot (deg)')
title('Z rotation')
grid on

picturefile=strcat('plot',int2str(fnum),'.jpg');

print('-djpeg',picturefile)

end
```